Influencing Rotational and Translational Motion in Stimuli-Responsive Hydrogen-Bonded [2]Rotaxanes

By

Giovanni Bottari

Degree of Doctor of Philosophy

Department of Chemistry

University of Edinburgh

February 2003

Table of Contents

Abstract

The controlled translocation of submolecular units is seen as an important requirement for the future development of "machines" which function through mechanical motion at the molecular level. Mechanically-interlocked molecules, *i.e.* catenanes and rotaxanes, are ideal candidates for application as components for molecular devices due to the inherent restrictions in the degrees of freedom presented in their architectures. Hydrogen bond-directed assembly offers powerful strategies for the synthesis of such structures on a scale where practical applications become a realistic area for study. This thesis focuses on (i) the use of hydrogen bonding interactions in the synthesis of structurally different fumaramide template-containing [2]rotaxanes, (ii) the control of the rotational and translational motion in stimuli-responsive [2]rotaxanes and (iii) the control of a physical property, such as elliptical polarization, in a stimuli-responsive two-station [2]rotaxane. The stimuli required to promote the submolecular motion are light and heat.

Declaration

The scientific work described in this Thesis was carried out in the Department of Chemistry at University of Warwick between January 2000 and September 2001 and in the Department of Chemistry at University of Edinburgh between September 2001 and January 2003. Unless otherwise stated, it is the work of the author and has not been submitted in whole or in support of an application for another degree or qualification of this or any other University or institute of learning.

Signed

Date...... 04.02.2003 ......

Attended Lectures and Meetings

1. NMR Spectroscopy and Mass Spectrometry Courses, October 2000, University of Warwick.

2. RSC lectures, University of Warwick.

3. Organic Research Seminars, University of Edinburgh.

4. 4th European Network on Benzylic Amide Catenanes (ENBAC) TMR network Meeting, 31st August-3rd September 2000, La Londe des Maures, France [talk: "Asymmetry is Beautiful: New Candidates Towards the Control of the Intramolecular Motions"].

5. 5th Design of Rotaxane-based Unconventional Materials (DRUM) TMR network Meeting, 5th-8th April 2001, Riezlern, Austria [talk: "A New Type of Molecular Shuttle: Photo- and Chemically- Induced Positional Isomerism in an "Abacus-like" [2]Rotaxane"].

6. 1st Mechanically Interlocked Polymer Architectures, (MIPA) TMR network Meeting, 7th-10th June 2001, Baja Sardinia, Italy. [talk: "A Light Switchable Hydrogen-bonded Molecular Shuttle: An Example of Abacus-type Movement at the Molecular Level"].

7. 26th International Symposium on Macrocyclic Chemistry (ISMC 2001), 15th-21st July 2001, Fukuoka, Japan.

8. Royal Society of Chemistry Scottish Regional Perkin Meeting, 19th December 2001, University of Glasgow, Scotland (UK). [poster: "Large Amplitude Stimuli-induced Motion in a Hydrogen-bonded [2]Rotaxane"].

Acknowledgements

List of Abbreviations

DMSO dimethylsulphoxide

DMF *N,N'*-dimethylformamide

THF tetrahydrofuran

TFA trifluoroacetic acid

EDCI·HCl = 1-(3-dimethylaminopropyl)-3-ethyl-carbodiimide hydrochloride

4-DMAP 4-dimethylaminopyridine

Et Ethyl

Me Methyl

NMR Nuclear Magnetic Resonance

ppm part per million

mins minutes

δ chemical shift

COSY COrrelation SpectroscopY

NOESY Nuclear Overhauser Enhancement SpectroscopY

HMQC Heteronuclear Multiple-Quantum Correlation

HMBC Heteronuclear Multiple-Bond Correlation

E trans isomer

Z cis isomer

m.p. melting point

TLC Thin Layer Chromatography

FAB Fast Atom Bombardment

rt room temperature

CD Circular Dichroism

mL millilitres

g grams

HRMS High Resolution Mass Spectrometry

Calcd. calculated

VT Variable Temperature

SPT-IR Spin Polarisation Transfert by Selective Inversion Recovery

ΔG° Gibbs energy

General Remarks of Experimental Data

All the melting points (m.p.) were determined using a Electrotermal 9100 melting point apparatus and are uncorrected. ^1H (400 MHz) and ^{13}C (100 MHz) NMR spectra were recorded on a Bruker DPX 400 MHz spectrometer using dilute solution in $CDCl_3$, CD_2Cl_2, d_6-DMSO, $C_2D_2Cl_4$ without any internal reference and referenced to the residual solvent signal as internal standard ($CHCl_3$ at $\delta_H = 7.27$, s; $\delta_C = 77.0$, t; $CDHCl_2$ at $\delta_H = 5.32$, t; $\delta_C = 53.5$, m; d_5-DMSO at $\delta_H = 2.54$, m; $\delta_C = 40.5$, m; C_2DHCl_4 at $\delta_H = 5.96$, s; $\delta_C = 78.0$, t) and the chemical shifts are reported in part per million (ppm) from low to high field. All the ^1H and ^{13}C NMR spectra were recorded at 298K unless otherwise stated. The FIDs were processed by the software WinNMR and where it was necessary the FIDs were treated with different kind of apodization functions. ^1H NMR are reported as follows: br = broad, s = singlet, d = doublet, dd = doublet of doublets, t = triplet, dt doublet of triplets, q = quartet, m = multiplet, $^2J(H,H)$ = geminal coupling constant, $^3J(H,H)$ = vicinal coupling constant, $^4J(H,H)$ = dihedral coupling constant. ^{13}C NMR are reported as follows: ArC (ipso) = quaternary aromatic, ArCH = non quaternary aromatic. H-H COSY, HMQC, HMBC, NOESY 2D were also recorded for some compounds to enable more detailed assignement of ^1H and ^{13}C signals. Rotaxanes and their respective threads have been named using IUPAC/ACD software. Column chromatography was carried out using Kiesegel C60 (Merck) as stationary phase. TLC detection was performed on silica gel plates (0.25 mm thick, 60 F254, Merck, Germany). The TLC plates were observed under UV light or stained with iodine vapours, or spotted used different developing solutions as 8% sulphuric acid, 0.1N $KMnO_4$ or 0.2% ninhydrin in EtOH and successively heated using an heatgun. Mass spectrometry and HRMS analyses were performed by the University of Warwick and University of Edinburgh mass spectrometry service using fast atom bombardment (FAB) from m-nitrobenzyl alcohol matrix unless otherwise stated. Elemental analyses were performed by the University of Warwick and University of Edinburgh elemental analysis service. The CD measurements were recorded in the range 235-320 nm on a JASCO J-810 spectropolarimeter at 0.1 mM substrate concentration with a path length of 0.1 cm. The path length allowed the reproducible measurements of the CD spectra even in $CHCl_3$ in the range 235-320 nm, despite the strong absorbance of the solvent at these

wavelengths. Photo-isomerizations were carried out in quartz vessels using a multilamp photoreactor model MLU18 manufactured by Photochemical Reactors Ltd, Reading UK. Reagents and anhydrous solvents used for the reactions were purchased from Aldrich and were in general used without further purification. Isophthaloyl dichloride was routinely recrystallized from hexane and *para*-xylylenediamine was distilled under reduced pressure. Anhydrous chloroform used for the rotaxane formation reactions was stabilized with amylenes.

Layout of this Thesis

The work presented in this thesis describes (i) the synthesis of rotaxanes by using hydrogen bonding and (ii) the control of motion of their submolecular components. A brief review of the literature is given in chapter one describing the background to controlled motion at the molecular level, from rotational motion in trypticene groups to the translational motion in molecular shuttles.

The remainder of the thesis discusses my own experiments in this area – sometimes in collaboration with colleagues - and is presented in the form of five chapters that are actually articles that have either already been published, are in press or have been prepared for submission to a peer-reviewed journal. No attempt has been made to rewrite the work out of context, instead the contributions of others are gratefully acknowledged at the start of each chapter. For the benefit of the reader - and the flow of the story - a brief synopsis is included before each chapter to set the scene, outline the ideas behind the work and the approach that was taken. I hope that the reader will forgive me for the small amount of repetition that stems from this approach!

Giovanni Bottari February 2003

I dedicate this Thesis to my parents Teresa and Nicola,

to all my relatives and to my "bedda" Andrea

for their support throughout these years,

making me realise how lucky I am

to have them in my life!

My biggest Thanks

Molecular Machines:

The Beginning of a Revolution

"Fatti non foste a viver come bruti,
ma per seguir virtute e canoscenza"
Dante Alighieri
Inferno, Canto XXVI, vv 119-120

"Ye were not made to live like unto brutes,
but for pursuit of virtue and of knowledge"

1.1 From Macroscopic to Artificial Molecular-Level Machines

Since their first appearance, lost in the midst of time, macroscopic machines have significantly changed and continue to deeply influence the face of our society. Nowadays in fact we use machines, designed to perform a diverse range of tasks, in such an extensive way that our society would be inconceivable without them.

A new "revolution" is now taking place extending the concept of macroscopic machines down to the molecular level and opening new interesting fields of research found within the broad topic of nanoscience.

The first time the possibility of constructing artificial molecular-level machines was contemplated was in 1959 by the Nobel Laureate Richard Feynman during the annual meeting of the American Physical Society in his historical address: "There is Plenty of Room at the Bottom".[1] Here are some prophetic sentences from this lecture:

> *What would be the utility of such machines? Who knows? I cannot see exactly what should happen, but I can hardly doubt that when we have some control of the arrangement of things on a molecular scale we will get an enormously greater range of possible properties that substances can have, and of the different things we can do.*

This new approach requires a fine manipulation of molecules, the smallest entities with defined shape and property present in Nature, therefore a prominent role is assigned to the chemists. Their ability and creativity, particularly in the last two decades, has made it possible to create molecules of high complexity and in sufficient yields to allow studies of properties, making it possible to apply such a systems to everyday life.

1.1.1 Main Features of Artificial Molecular-Level Machines

A molecular-level machine can be defined as an assembly of a discrete number of molecular components designed to perform mechanical-like movements (output) as a consequence of appropriate external stimulus (input).[2] The main features of such a machine are i) the kind of energy by which it is powered, ii) the type of movement performed, iii) the manner in which the motion can be monitored and controlled and iv) the function performed by the machine.

As pointed out by Feynman more than 40 years ago, such a machine should be powered by "cold" chemical reactions because of the impossibility of an internal combustion engine of molecular size. Moreover the reactions must be reversible so that the work performed by the machine can be cycled more than once. Examples of such reactions are isomerisation of double bonds, acid-base reactions, redox processes and complexation-decomplexation equilibria such as forming and breaking of hydrogen bonds. The use of chemical reagents as "fuel" for such machines would result in accumulation of by-products and ultimately could compromise a proper functioning of the machine itself, whereas photochemically or electrochemically reactions are instead ideal being in general fast and relatively clean processes. As a result of the external input applied a change in the relative position of some of the constitutive parts of the molecular level machine is achieved. The movement can then be monitored by following changes in some of the physical properties of the molecular species. Finally the functions that can be performed as consequence of the submolecular motion of some of the machine components are, to a large extent, still unpredictable and unexplored.

The dynamic of these machines is strictly dependent upon the shape and the spatial arrangement of the molecular components. Two distinct categories of molecular level machines can be envisaged, by analogy with their macroscopic counterparts: i) systems with rotating moving parts and ii) systems with translating moving parts.

## 1.2 Molecular Level Devices with Covalently-Connected Rotating Parts

1.2.1 Molecular propellers and gears

Historically, molecular species consisting of two or three aryl rings covalently connected to a central atom, are considered the first examples of molecules presenting internally restricted motion reported in the literature (**1** and **2**).[3] A combination of NMR spectroscopy and *X*-ray crystallography provided evidence that the aromatic rings are tilted in the same direction relative to the reference plane in an arrangement similar to the blades of a propeller. Even though there are no restrictions to the *independent* rotation of each of the aromatic units, this process is energetically disfavoured compared to the *concerted* rotation of the aryl rings.

$Z=CH_2, NH$
$Z'=CH, N$

1   **2**
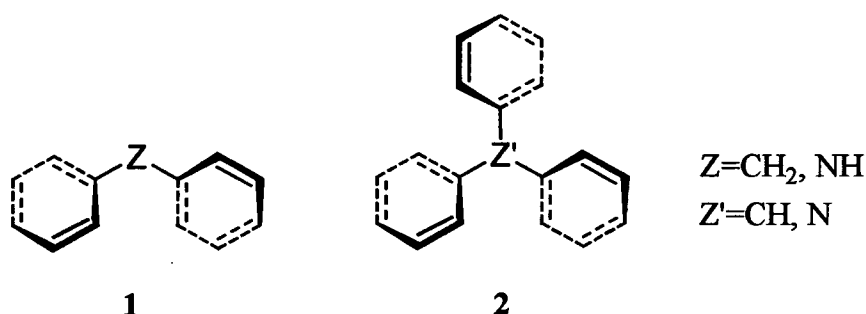
The concept of the interdependent motion of aryl units in molecular propellers has been exploited in the design of a new class of molecules presenting restricted internal motion, the molecular "bevel gears". These molecules present two or more tightly intermeshed rotating units arranged in such way that the rotation of these groups are mutually dependent.

An example of this phenomenon is **3**, which consists of two bridged triptycene groups in which the rotational movement of one of the units induces the concerted motion of the second one as the two units are interdigitated.[4] A combination of ^1H and ^{13}C NMR spectroscopy quantified the energy barrier of the "gear rotation" of the triptycyl unit as 8 kcal mol^{-1}, whereas molecular modelling showed a much higher value, 30-40 kcal mol^{-1} for the uncorrelated rotation of the tridentate unit, referred as a "gear slippage".

3   **4**
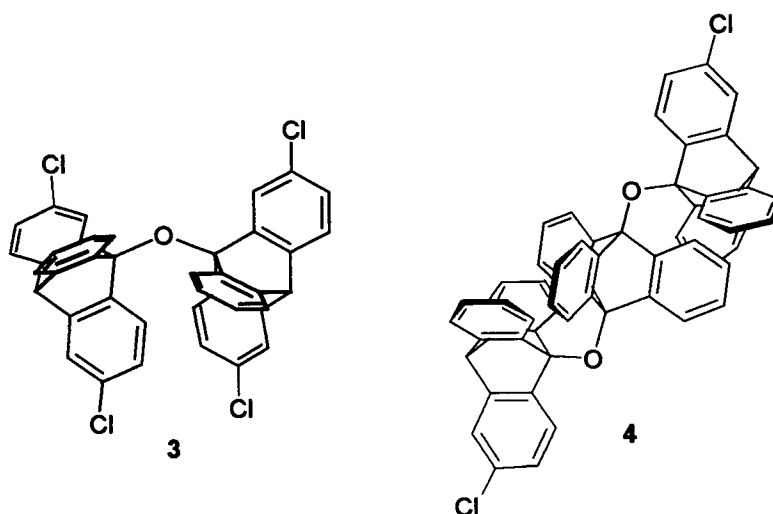
The concept of a double connected bevel gear has been implemented by the synthesis of 4, which consists of three triptycil units.[5] In this system the rotation of the two external non-directly connected triptycyl groups is mutually influenced and the concerted rotational motion made possible by the presence of a third central-bridging triptycyl group.[6]

1.2.2 Controlled Chemical Rotors

In the molecular rotors mentioned so far the interdependent rotational motion of the triptycyl units is powered by the thermal energy of the system and thus uncontrolled. Kelly and co-workers attempted to overcome this limitation by synthesising a "molecular brake".[7] The molecule 5 is a triptycyl derivative covalently connected to a chelating 2,2'-bipyridine unit (Scheme 1.1). The rapid rotation around the carbon-carbon bond connecting the two units is demonstrated by the presence in the ^{1}H NMR at 30 °C of four distinct signals for the aromatic protons of the triptycyl unit (*brake off*).

**5 (brake off)**   **6 (brake on)**
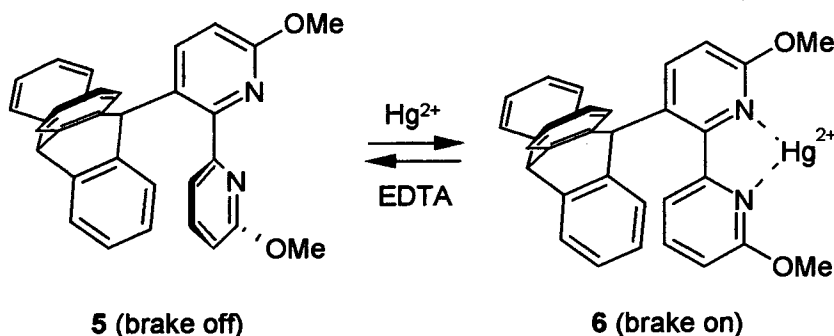
Scheme 1.1 The molecular brake is controlled through the complexation-decomplexation of the bipyridine unit. The brake is turned *on* by addition of Hg^{2+} (6) and sequentially turned *off* upon addition of EDTA (5).

Treatment of **5** with Hg^{2+} affords a new molecular species **6** where the metal cation is coordinated to the two pyridine nitrogens. This chelation aligns the two bipyridyl units hence slowing the rotation of the triptycyl unit as confirmed by the loss in the degeneration of some of its aromatic protons at –30 °C (*brake on*). At 30 °C however the protons of the triptycene coalesce in a broad signal indicating that the steric hindrance of the pyridyl group is not sufficient to stop the spontaneous rotation of the trypticene and slipping of the brake is occurring. The original demetallated species **5** can be restored by adding EDTA to **6** proving the reversibility of the system.

1.2.3 Towards Unidirectional Molecular Motors

In order to generate a chemical rotor that exhibits unidirectional motion, the design of the molecular brake **5** was modified. The 2,2'-bipyridine group was replaced by an [4]helicene unit functionalised with a hydroxypropyl group whereas the triptycyl unit was functionalised with an amine, to obtain the molecular rotor **7** (Scheme 1.2). [8]
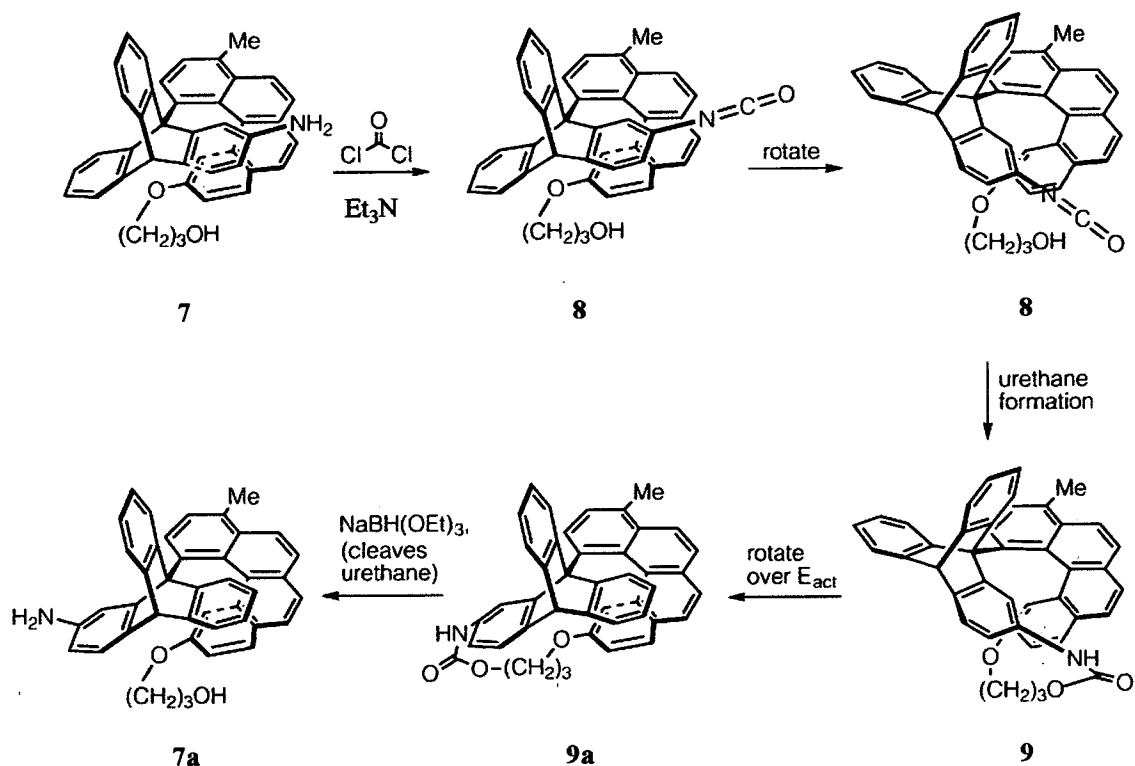
Scheme 1.2 Sequence of the 120° unidirectional rotation of a chemically powered rotor 7.

Treatment of 7 with $COCl_2$ and Et_3N gives the isocyanate 8 which once formed can react intramolecularly with the hydroxyalkyl group of the helicene affording the urethane 9 in a highly strained conformation. Compound 9 then rotates around the single bond connecting the helicene to the triptycyl unit forming the isomer 9a and thus releasing the strain. Finally cleavage of the urethane with H_2O affords the compound 7a in a conformation which is different from its isomer 7. This new conformation is obtained as result of a unidirectional 120° rotation promoted by the formation and breaking of a covalent bond.

1.2.4 Light- and Temperature- Driven Unidirectional Molecular Rotor

Feringa and co-workers reported the first example of molecular motor displaying repetitive and controlled 360° unidirectional motion around an alkene bond in response

to photonic and thermal stimuli (Scheme 1.3).[9] The system is constituted by two tetrahydrophenanthrene units covalently connected by a carbon-carbon double bond.[10] Each of the two helical groups, due to steric reasons, can adopt a right-handed (P) or a left-handed (M) helicity, distorting the expected planarity imposed by the double bond. The four step rotation is achieved by an initial irradiation at $\lambda \geq 280$ nm at –55 °C of (P,P)-*trans*-**10** to obtain the (M,M)-*cis*-**10** isomer.
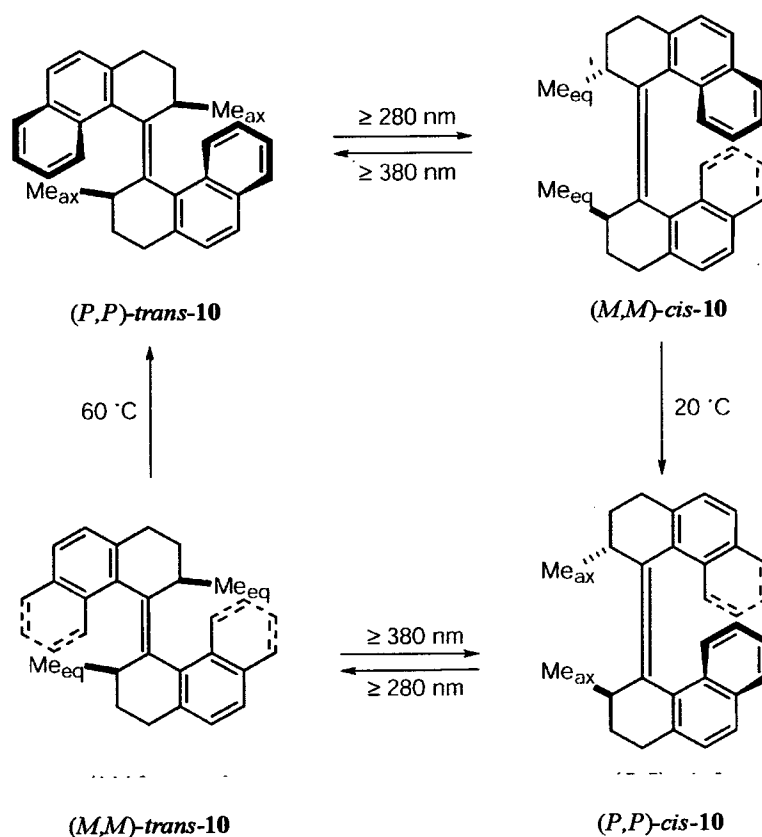

Scheme 1.3 The 360° unidirectional rotation is achieved in a four-step process involving alternative isomerisation of double bond and thermal interconversion of helicity.

Interconversion of helicity, while maintaining the Z configuration, is achieved by heating the solution of (M,M)-*cis*-**10** at 20 °C generating the thermodynamically more stable (P,P)-*cis*-**10** isomer bearing the two methylene groups in a less sterically demanding axial position. A further 180° rotation is obtained by $Z \rightarrow E$ isomerisation at $\lambda \geq 280$ nm to afford (M,M)-*trans*-**10** whose helicity can be inverted by heating the

solution at 60 °C to obtain the original (*P,P*)-*trans*-**10** isomer, the most thermodynamically stable of the all four isomers of the cycle, where the methylene substituents are, once again, adopting a more stable equatorial orientation. The overall process can be monitored by following the changes in the absorption intensity of circular polarised light at 217 nm. The correct functioning of the system depends crucially on the control of the temperature, in fact by irradiating the compound (*P,P*)-*trans*-**10** at 60 °C all the four species are obtained at once without control.

Control over the speed of the unidirectional rotation in molecular rotors has been achieved by synthesising a series of overcrowded alkenes, **11-19**.[11] The phenomenon is exploited by changing the nature of the heteroatoms X and Y thereby modifying the energy barrier of the helical inversion, the rate-determining step of the unidirectional rotation. The speed of the thermal inversion of helicity changes by a factor of 400 from **17** to **16**.
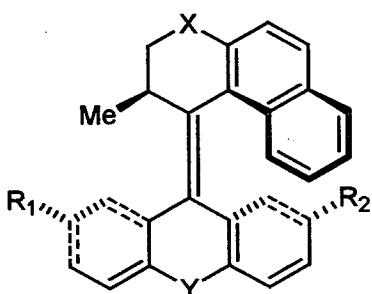
11, X=S, Y= S, R_1=OMe, R_2=H
12, X=S, Y= S, R_1=H, R_2=OMe
13, X=S, Y= S, R_1=H, R_2=H
14, X=S, Y= S, R_1=OMe, R_2=OMe
15, X=S, Y= O, R_1=H, R_2=H
16, X=S, Y= C(CH$_3$)$_2$, R_1=H, R_2=H
17, X=CH$_2$, Y= S, R_1=H, R_2=H
18, X=CH$_2$, Y= C(CH$_3$)$_2$, R_1=H, R_2=H
19, X=CH$_2$, Y= CHCH, R_1=H, R_2=H

The construction of stimuli-responsive molecular species that could lead to changes in some of the macroscopic properties of a system is one of the major endeavours in contemporary science. Recently, Feringa and co-workers demonstrated that if the molecular rotor (*P,P*)-*trans*-**10** is doped into a nematic liquid crystal film and irradiated at λ ≥ 280 nm, the demonstrated unidirectional rotation of the molecular rotor induces a

rearrangement of the mesogenic molecules which leads to a gradual change in the colour of the doped film from purple to red after only 80 seconds of irradiation (Figure 1.1).[12] The colour of the mesogenic film can be finely tuned by changing parameters such as irradiation time, wavelength used or light intensity.
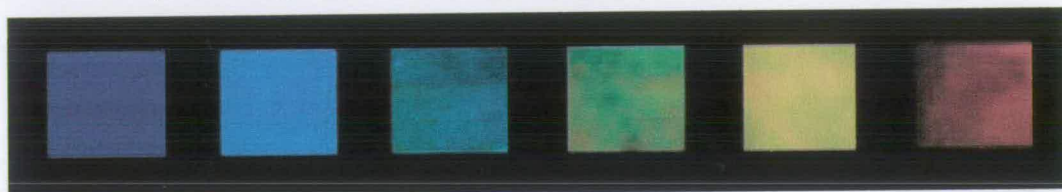

Figure 1.1 Colors of a molecular rotor doped liquid crystal phase, starting from pure *(P,P)-trans-***10** (far left) upon irradiation at λ >280 nm at room temperature, until an irradiation time of 80 s (far right)

1.3 Molecular Level Devices with Noncovalently-Connected Translating Parts

1.3.1 Catenanes and rotaxanes

Catenanes and rotaxanes, molecules consisting of mechanically interlocked, non-covalently connected components, are ideal candidates for use, as molecular devices where translational movement is required (Figure 1.2).[13]

[2]catenane   [2]rotaxane
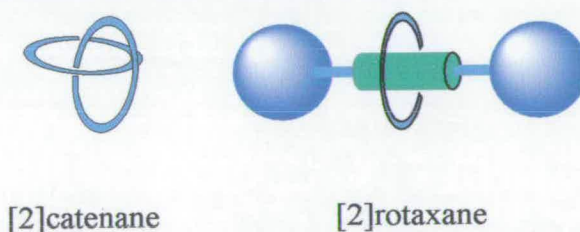
Figure 1.2 Cartoon representing the topology of a [2]catenane and a [2]rotaxane

A catenane, from the Latin *catena*, meaning chain, is a molecular species formed by two, or more, interlocked macrocycles which can be separated only by breaking one or more covalent bonds. Instead a rotaxane, from the Latin *rota* and *axis* meaning respectively wheel and axle, consists of a macrocycle threaded onto a linear molecule

(thread) which bears two bulky groups (stoppers) at its extremities preventing the slippage of the macrocyclic unit. A rotaxane without "stoppers" is referred to as a pseudo-rotaxane. A prefix number in square bracket is usually present for such molecules indicating the number of the interlocked components.

1.3.2 Early synthetic approaches in the synthesis of [2]rotaxanes

The first synthesis of a [2]rotaxane, **20**, was reported by Harrison and Harrison in 1967.[14] The synthesis was performed using a statistical approach based on the random threading of a linear dialcohol onto a 30-membered ring. The obtained pseudo-rotaxane was then "stoppered" by reaction with an excess of a bulky acid chloride resulting in the formation of the [2]rotaxane in 6% yield after repeating the reaction 70 times (Scheme 1.4).
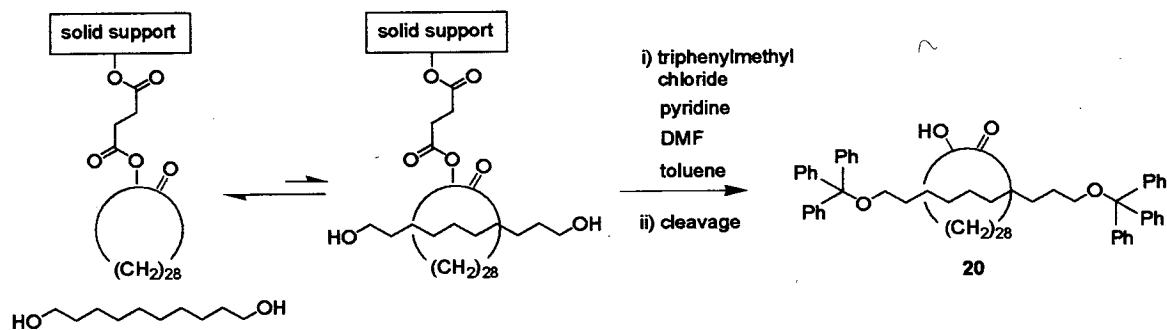
Scheme 1.4 Synthesis of the first rotaxane, **20**, obtained in a 6% yield by a statistical method repeated 70 times

Shortly after, Schill and co-workers reported another synthetic methodology consisting of the synthesis of a rotaxane precursor species, **21**, followed by selective cleavage of covalent bonds to afford the desired interlocked molecule **22** (Scheme 1.5).[15] This later methodology however left unsolved the major and limiting problem in the synthesis of such interlocked molecules: the extremely poor yields.
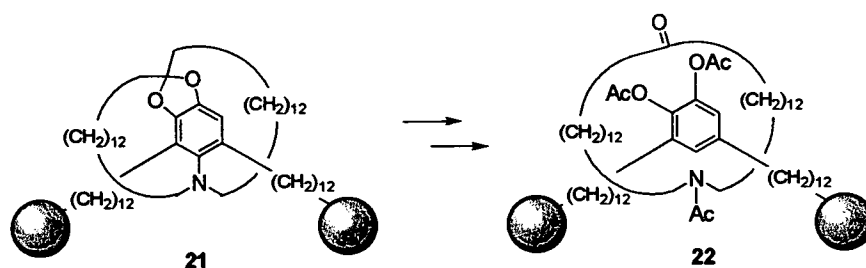
Scheme 1.5 Synthesis of the first rotaxane, **22**, obtained by "covalently"directed synthesis

1.3.3 Supramolecular chemistry assistance in the synthesis of [2]rotaxanes

The advent of "supramolecular assistance" represented the real breakthrough in the synthesis of interlocked species.[16] A variety of attractive, non-covalent interactions (metal-ligand, π donor-π acceptor, hydrophobic and/or hydrogen bonding) have been exploited in the last few decades, in so-called template directed synthesis. The supramolecular interactions are required in order to organise the precursor components of the interlocked molecule prior the interlocking.

To this point three distinct strategies have been developed for the synthesis of rotaxanes (Figure 1.3): i) the "slippage"[17] where a macrocyclic unit passes over the stoppers of a thread, usually at elevated temperatures, ii) the "threading"[18] where the equilibrium-dependent formation of a pseudo-rotaxane is trapped by a "capping" reaction with two bulky stoppers preventing the macrocycle from unthreading, and iii) the "clipping"[19] where the rotaxane is obtained by the closure of an acyclic unit templated around a "stoppered" thread.
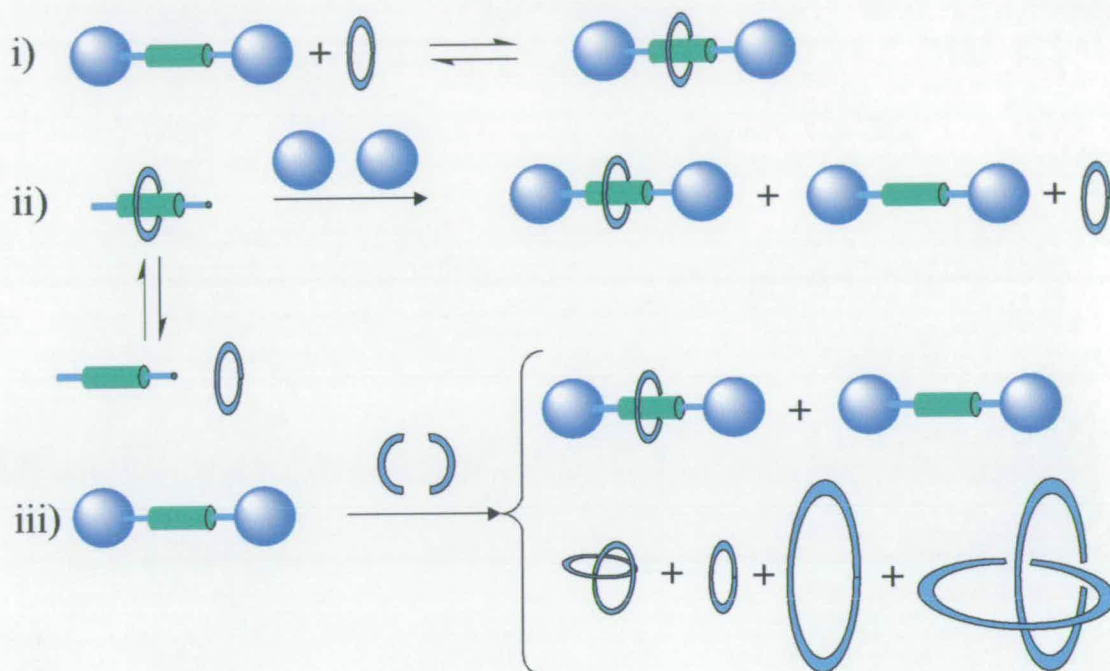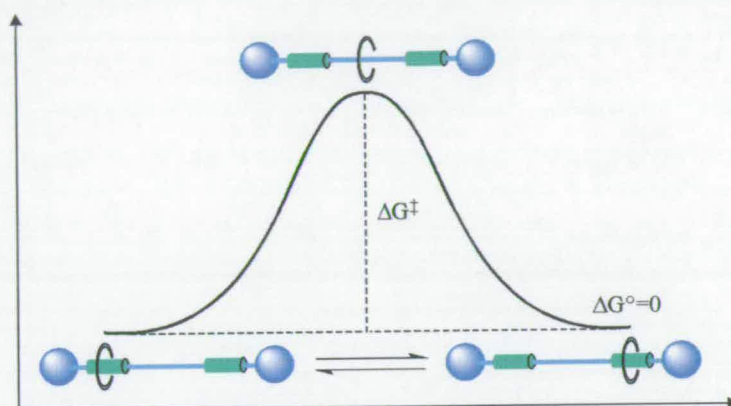
Figure 1.3 Cartoon representing the three different synthetic strategies to obtain rotaxanes. In the last case the formation of the desidered rotaxane is accompanied by the production of other species such as macrocycles and catenanes
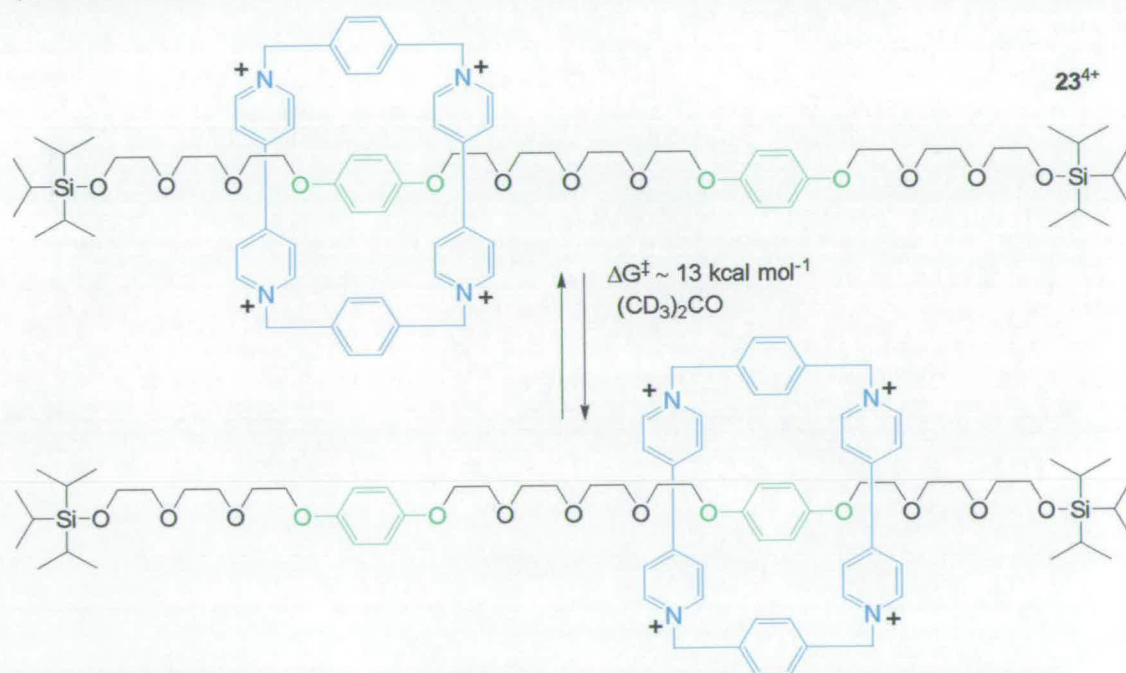
1.3.4 Rotaxanes as molecular shuttles

Rotaxanes are ideal candidates to exploit translational movements at the molecular level due to their unique mechanically interlocked architectures. A "shuttling" movement of the macrocycle along the dumbbell-shape component is realised if more than one binding site for the macrocyclic ring is present on the thread. The binding sites, called *stations*, must present accessible free activation energy barriers between them and be located far enough apart so that the shuttling movement can be well distinguished from any other internal motion governed by conformational rearrangements. A [2]rotaxane containing two degenerate and well-separated stations on its thread can be considered as the simplest example to study the shuttling phenomenon (Figure 1.4).
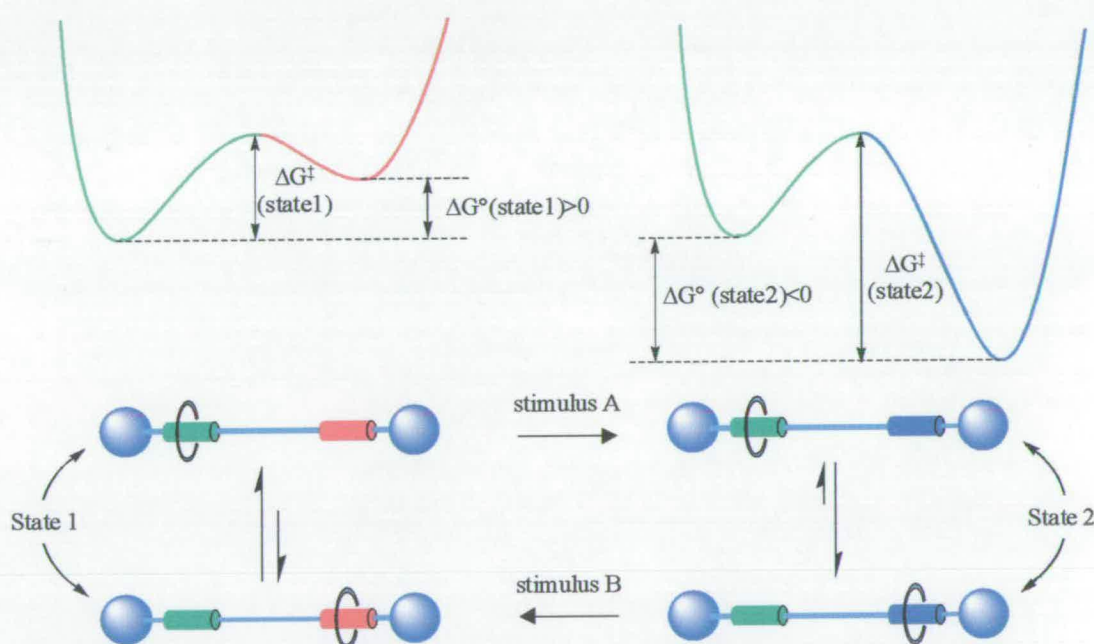
Figure 1.4 A cartoon representing the shuttling movement in a two degenerate stations-containing [2]rotaxane and the associate potential energy profile.

In such a system the macrocycle shuttles back and forward between the two isoenergetic, and thus equally occupied, stations. The first example of molecular shuttling in a rotaxane architecture was reported by Stoddart and co-workers in 1991 (Scheme 1.6).[20]

Scheme 1.6 The first molecular shuttle. The cyclophane unit moves back and forth between two isoenergetic stations

The rotaxane **23**[4+] consists of a π-electron poor tetracationic cyclophane mechanically interlocked onto a linear thread containing two isoenergetic π-electron rich hydroquinone stations separated by a polyether spacer. Since the two stations are identical, the macrocyclic unit has no preference for either of the two sites and shuttles between them with a $k = 2360$ s^{-1} in $(CD_3)_2CO$ at 34 °C measured by ^1H NMR spectroscopy. The motion of the macrocycle is powered by the molecular tumbling of the medium which provides the energy required to overcome the free activation energy barrier between the two stations so that two "co-conformations"[21] are obtained. This molecular shuttle does not perform any work because the $\Delta G°$ of the system is zero.

In order to have a stimuli-responsive [2]rotaxane the two binding sites on the thread must be different so that the $\Delta G°$ between the two stations is not zero (Figure 1.5).


Figure 1.5 A cartoon representing a rotaxane as a molecular machine, showing the work cycle together with the associated potential energy curves for the two different states.

In such a rotaxane the macrocycle sits preferentially over the station that provides the best stabilisation energy (*i.e.* state 1, station green). An appropriate external stimulus applied, can then increase the binding affinity of the macrocycle for the initial less favourite station (as in the cartoon of Figure 1.5) or destabilise the binding affinity of the macrocycle for the initial favourite station. This ultimately results in the shuttling of the macrocycle over to the initial unfavoured station (*i.e.* state 2, blue station) that now provides the best stabilisation energy. Applying a second stimulus restores the original state and closes the cycle. All the stimuli-responsive molecular machines based on rotaxane architectures reported in literature work along these principles;[22] the only difference lies on the nature of the stimuli applied.

1.3.5 Chemically and electrochemically switchable molecular shuttles

Stoddart and co-workers have reported in 1994 the first example of stimuli-responsive rotaxane, 24^{4+} (Scheme 1.7).[23] This rotaxane consists of a π-electron poor tetracationic cyclophane macrocycle mechanically interlocked onto a thread containing two stations with different π-donor abilities, namely a benzidine and a biphenyl station. At −44 °C in CD_3CN the benzidine station has a greater π-electron donor ability than the biphenol station therefore the π-electron poor macrocyclic unit spends 84% of its time over it.
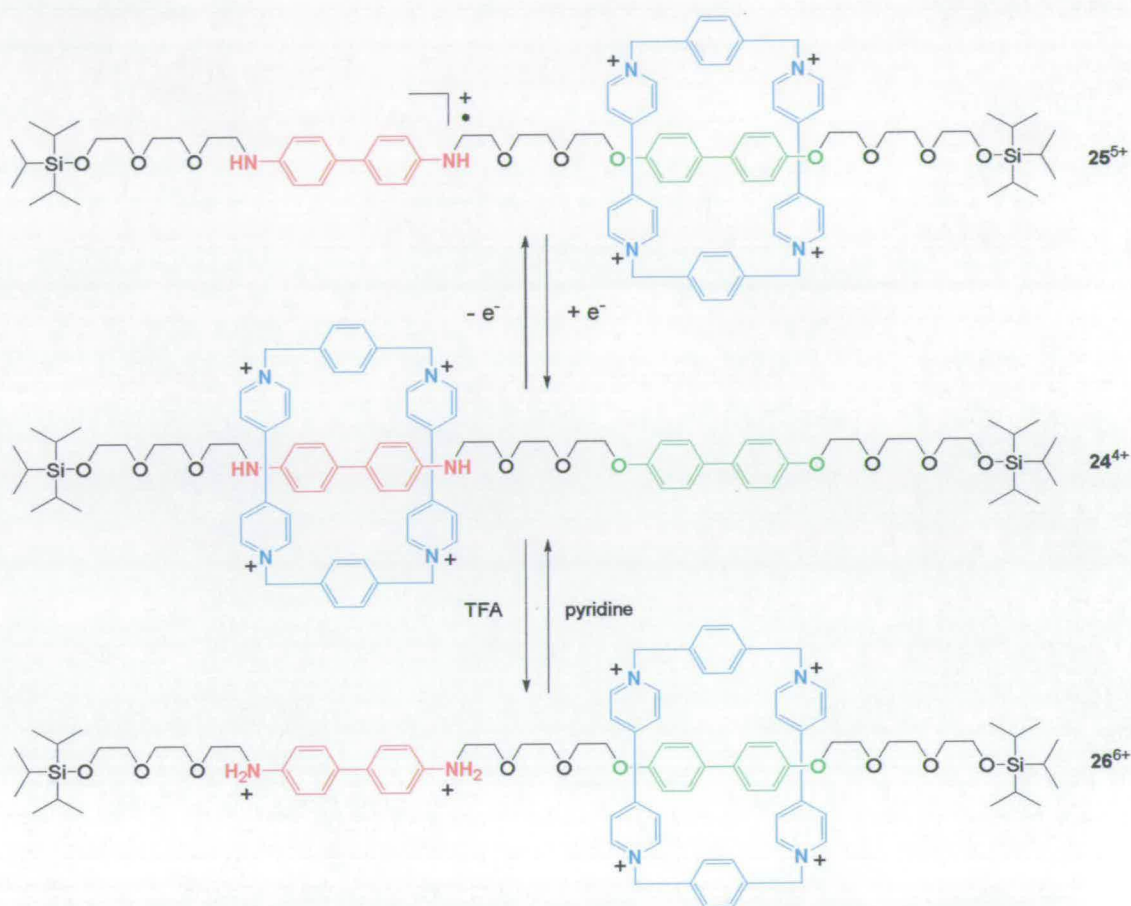
Scheme 1.7 The shuttling process of the tetracationic cyclophane macrocycle along the thread in 24^{4+} can be achieved both electrochemically (25^{5+}) or chemically (26^{6+})

An electrochemical stimulus oxidises the neutral benzidine unit to a monocationic radical ($24^{4+} \rightarrow 25^{5+}$), and the resulting repulsion of charges, induces the cyclophane unit to move from the station where it was residing to the biphenol station which now provides the best stabilisation energy. Evidence of this molecular dynamic is obtained by analysing the cyclic voltammetric (CV) response of 24^{4+} and model compounds containing benzidine units. The shuttling process is reversible and cyclable therefore the original species 24^{4+} can be re-obtained by reducing 25^{5+} restoring the original equilibrium. The electrochemically-responsive tetracationic rotaxane 24^{4+} can also be switched by using a chemical stimulus. The macrocyclic cyclophane moves from the

17

preferred benzidine station in 24^{4+} to the biphenol unit in 26^{6+} upon double protonation of the diamine unit. The shuttling movement can be reversed by deprotonation of the di-cationic amine upon addition of pyridine to 26^{6+} to afford the original species 24^{4+}.

Sauvage and co-workers took a different approach to produce an electrochemically-powered shuttling movement by synthesising the metal-containing two-station rotaxane 27^+ (Scheme 1.8).[24]
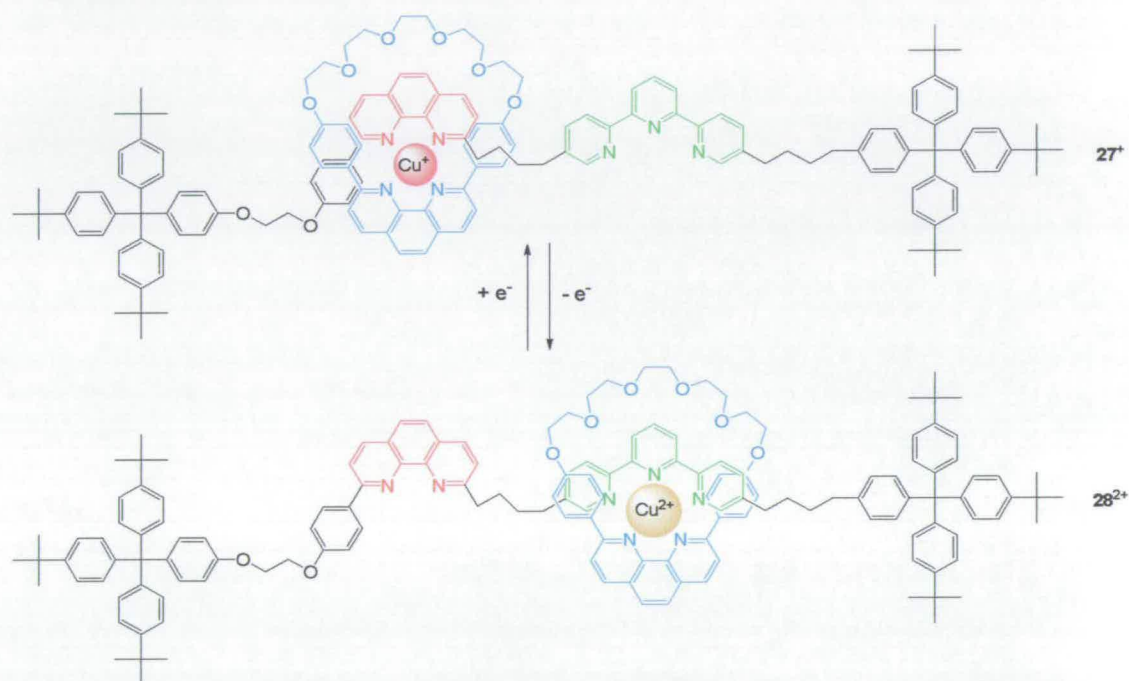

Scheme 1.8 An electrochemically switchable molecular shuttle based upon oxidation-reduction of copper metal ions

The shuttling movement lies on the different coordination geometry adopted by a mono- and di- cationic copper species. The rotaxane consists of a macrocycle containing a bidentate, 1,10 phenanthroline ligand, which is also present on the thread as one of the binding stations. The second binding site on the thread is a terdentate terpyridine ligand. In 27^+ the copper(I) cation species adopts a low coordinate, tetrahedral geometry coordinating to the two bidentate phenantroline ligands of both thread and macrocycle. The shuttling of the macrocycle is promoted by the oxidation of Cu$^+$ to Cu^{2+} to obtain

28^{2+}. The preference of Cu^{2+} for a high coordination geometry causes the macrocycle to "glide" along the thread around the terpyridine station where the copper(II) can adopt a more stable, trigonal, pentacoordinating arrangement. Cyclic voltammetry measurements proved that the motion of the macrocycle after the oxidation of Cu^{+} to Cu^{2+} is slow (hours). The oxidation process is reversible and reduction of Cu^{2+} to Cu^{+} drives the macrocycle back to the phenantroline station so that the cycle can be repeated again.

1.3.6 Solvent-switchable molecular shuttles

In 1997 Leigh and co-workers prepared *via* hydrogen bond-directed synthesis, a series of rotaxanes, **29-31**, displaying translational motion of the macrocycle along the dumbbell-shape component in response to a change in the nature of the solvent (Scheme 1.9).[25]

CHCl$_3$ DMSO

29, X=(CH$_2$)$_2$

30, X=(CH$_2$)$_{10}$

31, X=S
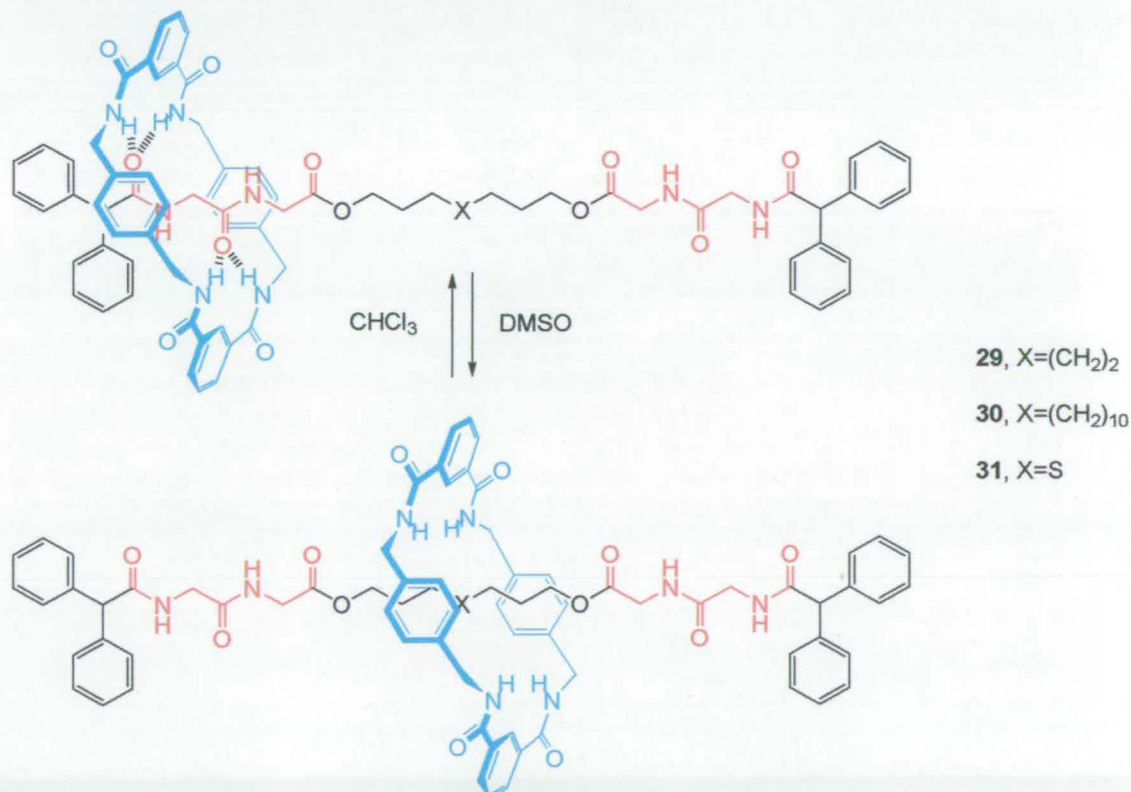
Scheme 1.9 Example of solvent switchable molecular shuttles

The molecular shuttles are composed of a benzylic tetra-amide macrocycle mechanically interlocked onto threads containing two degenerate templating glycyl-glycine peptide stations separated by different lipophilic alkyl chains. At room temperature in a non-hydrogen bonding disrupting solvent such as $CDCl_3$ the macrocycle shuttles between the two isoenergetic peptidic stations and the rates of shuttling determined by variable temperature ^1H NMR experiments. The shuttling movement occurs through the disruption of the hydrogen bonding interactions, which are the driving force for the formation of the rotaxane between the macrocyclic unit and the templating dipeptide station. Changes in the polarity of the solvent mediate the shuttling process, e.g. addition of 5% CD_3OD to a deuterochloroform solution of **31** increases the shuttling rate by more that 100 orders of magnitude at 25 °C. In response to a major change in the polarity of the environment of the rotaxane, from the apolar $CDCl_3$ to the polar, hydrogen bonding disrupting solvent d_6-DMSO, the macrocycle stops shuttling between the stations and resides exclusively over the lipophilic chain as proved by ^1H NMR spectroscopy.

1.3.7 Photochemically switchable molecular shuttles

A limiting factor to the long-term functioning of chemically-driven molecular machines is the build up of waste products as each cycle is repeated.

Alternatively the use of a photonic stimulus is a potentially clean and reversible way to generate translational motion of the macrocycle in rotaxane architectures.

The [2]rotaxane **E-32**$^{4+}$ comprises a toroidal-shape α-cyclodextrin, locked onto a tetracationic thread containing a *trans*-azobiphenoxy moiety (Scheme 1.10).[26]
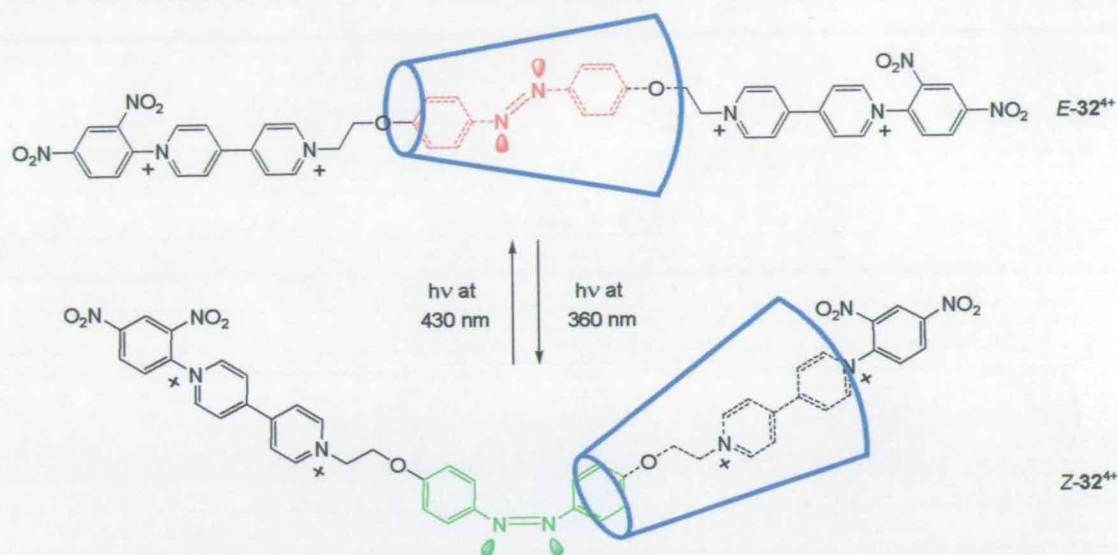
Scheme 1.10 Photochemically-driven shuttling movement of an α-cyclodextrin in an azobenzene-containing thread through reversible *E/Z* photoisomerisation

^{1}H NMR spectra comparison of the [2]rotaxane and its "free" acyclic component in D$_2$O at 30 °C shows two sets of resonances for the alkene protons of the azobenzene in the unlocked thread, which are split into four separate resonances in the rotaxane due to the presence of the macrocycle with its toroidal shape over the azobiphenoxy recognition site. Irradiation of *E*-32^{4+} at 360 nm for 15 minutes causes *E*→*Z* interconversion of the azobenzene unit and the formation of *Z*-32^{4+} in 67% yield. The interconversion causes the macrocycle to move from the sterically demanding *cis*-azobenzene station to the end of the thread. The original rotaxane *E*-32^{4+} can be re-obtained by isomerising *Z*-32^{4+} at 430 nm.

Recently an example of unidirectional shuttling in an α-cyclodextrin-containing [2]rotaxane has been reported by Anderson and co-workers (*E*-**33**, Scheme 1.11).[27] The translational movement of the macrocycle is based on the reversible *E/Z* photochemical isomerisation of a stilbene unit incorporated on the thread. Isomerisation at 340 nm of *E*-**33** to the *cis* isomer *Z*-**33** induces the macrocycle to move from the stilbene station in a unidirectional shuttling movement and brings the major rim of the α-cyclodextrin close

to one of the thread stoppers, as confirmed by NOE investigation. The co-conformer bearing the macrocycle over the other end of the thread is not observed. The $E \rightarrow Z$ isomerisation process can be reversed by irradiating Z-**33** at 265 nm to reform E-**33**.

E-**33**   Z-**33**
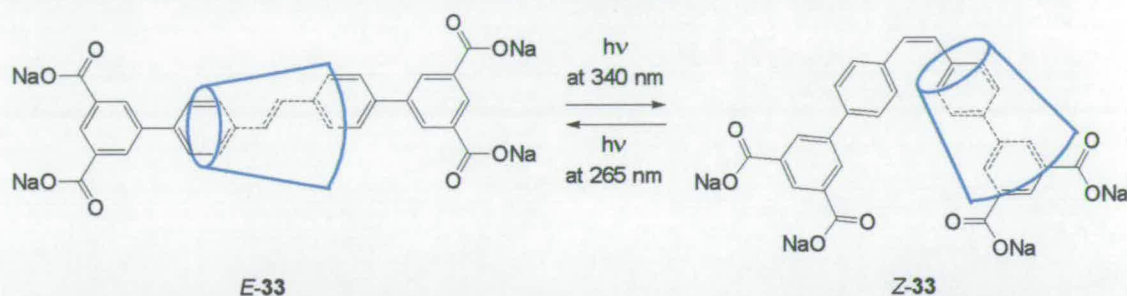
Scheme 1.11 Unidirectional translational motion of an α-cyclodextrin macrocycle along a stilbene-containing thread obtained through reversible E/Z photoisomerisation

Leigh and co-workers recently reported an interesting example of photochemically-driven molecular shuttle. The system consists of a benzylic tetra-amide macrocycle threaded onto a linear component featuring two potential stations: a succinic diamide unit on one side and a naphthalamide unit on the other side of the thread, both separated by a C_{12} lipophilic chain (**34**, Scheme 1.12)[28].
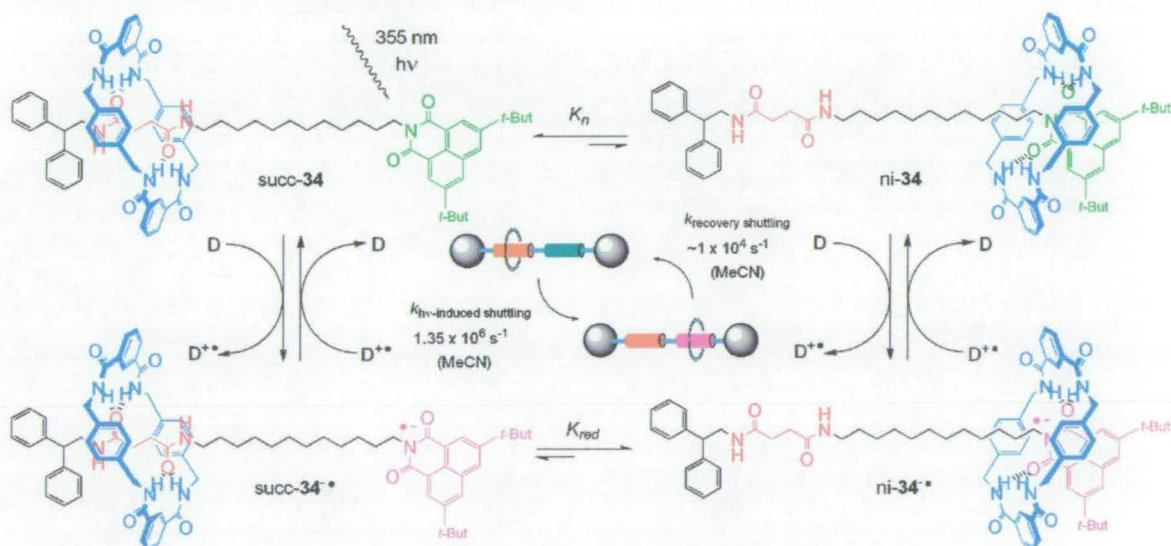

Scheme 1.12 Cycle of a photoresponsive, hydrogen bond assembled, molecular shuttle

In the neutral state of this rotaxane, as confirmed by ^{1}H NMR spectroscopy, the tetra-amide macrocycle is preferentially positioned over the succinic template as the naphtalamide unit has poor hydrogen bond accepting ability (succ-**34** co-conformer). A laser pulse at 355 nm in conjunction with an electron donor D (DABCO, 1,4-diazabicyclo[2.2.2]octane, 1-10 mM) is used to photoreduce the naphthalamide unit. In its reduced state the radical naphthalamide anion is a better hydrogen bond acceptor for the macrocycle, inducing the ring to shuttle, ni-**34**⁻. Analysis of the transient changes in the optical absorption spectrum of succ-**34** after the laser pulse proves that the submolecular movement is fast (~1 µs) compared to the previous molecular shuttles where it was on the time scale of minutes to hours. Charge recombination of the radical naphthalamide anion with the donor radical cation D⁺ occurs over a slow timeframe (~100 µs), after which the macrocycle shuttles back to the succinic station to afford succ-**34** and the cycle is ready to be repeated again. This molecular shuttle is reminiscent of a piston functioning through a power stroke (the laser pulse) and a recovery stroke (charge recombination). The molecular "machine" if cycled by a laser at the frequency of its recovery stroke (10^4 s⁻¹) can produce ~10^{-15} W of mechanical power per molecule.

1.3.8 From molecular shuttles to a molecular muscle

Sauvage and co-workers have recently reported the first example of a linear rotaxane-like dimer **35**²⁺ capable of contracting and stretching under the action of a chemical stimulus, in a manner reminiscent of a skeletal muscle (Scheme 1.13).[29] The movement of the "molecular muscle" is powered by the different coordination geometry adopted by the copper (I) and zinc (II) cations. The molecule **35**²⁺ was initially synthesised in its extended conformation with two copper (I) cations coordinating to two phenanthroline units each. Demetalation of **35**²⁺ using KCN followed by treatment with zinc (II) produces **36**⁴⁺, where contraction occurs in response to the new coordination requirements of the two zinc (II) cations each coordinating a phenanthroline and a

terpyridine unit. The original stretched conformation could be obtained again by subjecting 36^{4+} to $Cu(CH_3CN)_4 \cdot PF_6$.
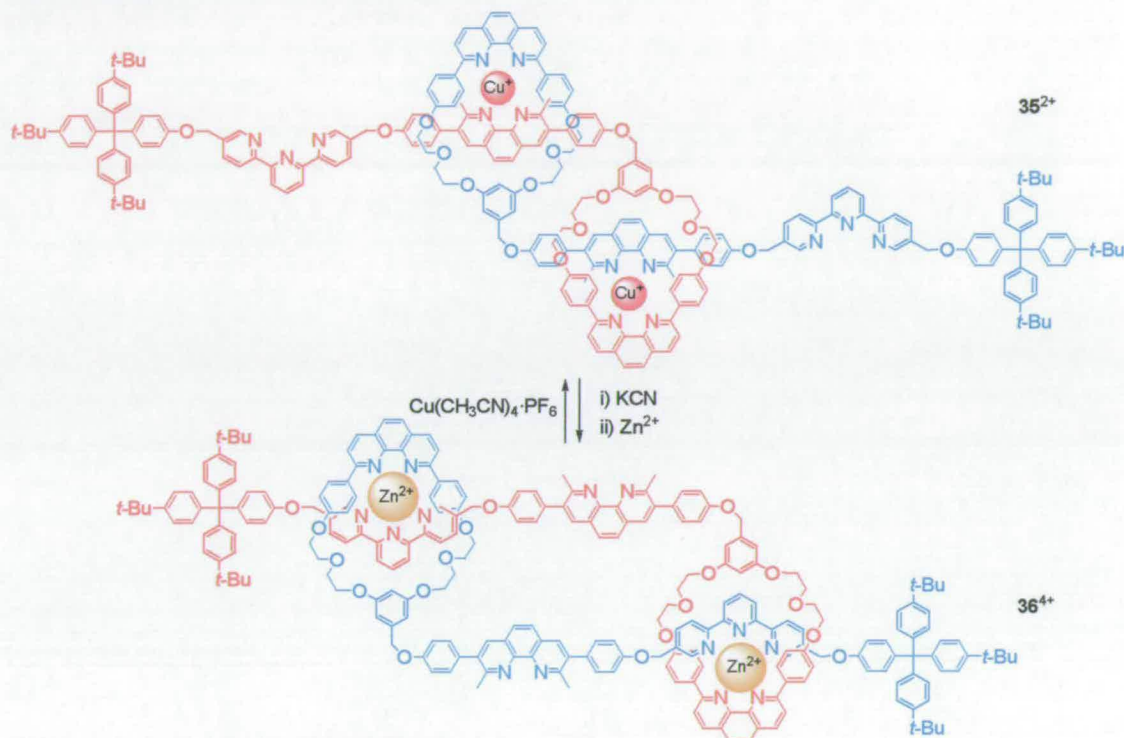
Scheme 1.13 Reversible chemically induced motion in an interlocked molecule between its extended (35^{2+}) and contracted (36^{4+}) conformation

1.3.9 Reflections

Interlocked molecules in general, and rotaxanes in particular, present interesting features for possible applications as constitutive components of macroscopic devices.

The realisation of sophisticated artificial molecular systems that mimic the functioning of macroscopic machines has rapidly grown in the last years thanks to our increasing comprehension of some of the basic concepts operating at the molecular level. However, many challenges and obstacles remain, beginning from the incompatibility between the solution media in which the majority of the systems so far reported have been studied and their possible behaviour in the solid phase in which practical applications of such molecular architectures are likely to first find application.

Chemists throughout the world, in collaboration with physicists, material scientists, biologists and engineers, are actively researching in an interdisciplinary "playground" in order to effectively reduce the gap between the macroscopic and the molecular "world" finally realising Feynman's vision.

1.4 Preamble to the Thesis

In 1995 Leigh and co-workers reported the serendipitous discovery of benzylic amide catenanes by hydrogen bond-directed synthesis.[30] This template strategy has been subsequently adapted towards the assembly of benzylic amide macrocycles around linear components to give rotaxanes.[31]

The general mechanism leading to this class of rotaxanes involves a five-component "clipping" reaction of the macrocycle precursors around the thread template (Scheme 1.14).
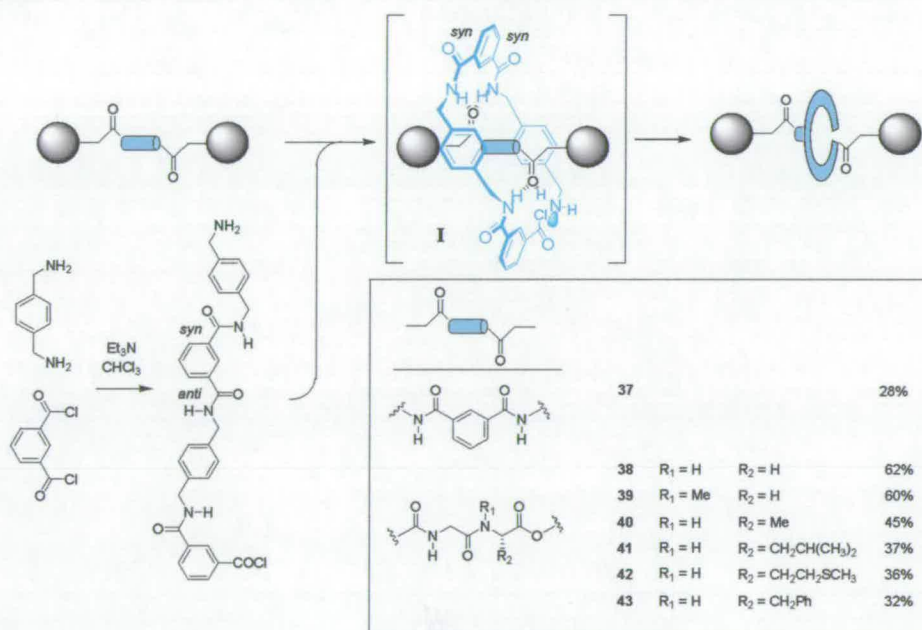
Scheme 1.14 Hydrogen bond-directed synthesis of a series of benzylic amide macrocycle-containing [2]rotaxanes through a five-component "clipping" reaction.

25

This route to mechanically interlocked architectures allowed the preparation of a whole series of rotaxanes (37-43), the yields ranging from 28% using an isophthalamide template (37) to 62% with a glycylglycine-containing thread (38).

Although the dipeptide motif is clearly a good template for the benzylic amide macrocycle system, the thread template possesses several internal degrees of freedom that are lost in the key supramolecular complex I of Scheme 1.14, including torsional freedom around the three backbone bonds (Scheme 1.15a).
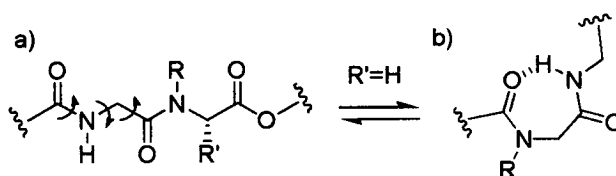
Scheme 1.15 The free dipeptide template can present a) rotation movements around the glycyl backbone and b) formation of seven-membered ring intramolecular hydrogen bonds.

Furthermore the peptide template can adopt a conformation leading to the formation of seven-membered ring intramolecular hydrogen bonds in the non-polar solvents used for promoting the rotaxane formation (Scheme 1.15b).

It seems likely, therefore, that the unfavorable requirements of breaking intramolecular hydrogen bonds and/or the loss in entropy in going from a flexible thread to the much stricter conformational and co-conformational requirements of the supramolecular transition state could be overcome more efficiently by preorganising the hydrogen bonding sites of the thread in a spatial arrangement already suited for templating benzylic amide macrocycle formation.

Introducing rigidity in the template backbone through the use of a fumaric diamide unit afforded the rotaxane **44** in an astonishing 97% yield, a "world record" yield for a [2]rotaxane synthesis (Scheme 1.16).[32] The success of the fumaramide template can be attributed to the spatial arrangement of the co-operative hydrogen bonding sites on the thread kept by the *E*-alkene double bond in a fixed position at an ideal distance apart to

template the formation of the benzylic amide macrocycle through the formation of intercomponent hydrogen bonds.

44	X, Y = NH	97%
45	X = O, Y = NH	35%
46	X, Y = O	3%
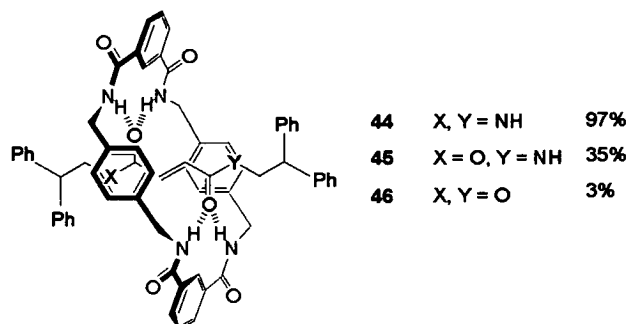
Scheme 1.15 Fumaramide-containing [2]rotaxanes

Remarkably enough the high preorganisation offered by the template is so effective that even if one or both the amides of the thread are substituted for much weaker hydrogen bond acceptor groups as esters still the formation of the rotaxane is observed (**45** and **46**).

This thesis describes the synthesis of stimuli-responsive fumaramide-based rotaxanes and the study of their interesting dynamic properties. In chapter two the synthesis, the solid state determination and the photochemical behaviour of a family of structurally different fumaramide-based rotaxanes is reported, once again confirming the remarkable ability of the fumaramide unit as template for the formation of benzylic amide macrocycles. The remaining four chapters exploit the possibility to influence some of the dynamic properties present in fumaramide-based rotaxane architectures. From the control of the rotation in fumaramide-based rotaxanes through *E/Z* isomerisation (chapter three) to the synthesis of a family of stimuli-responsive molecular shuttles (chapter four). The last two chapters report about the realisation of the first entropy-driven, temperature-dependent molecular shuttle (chapter five) and the possibility of control a physical property such as the CD absorption of a dipeptide rotaxane through controlled submolecular motion of the ring (chapter six).

1.5 References

1. R. P. Feynman, *Saturday. Rev.* **1960**, *43*, 47-54

2. For a review about artificial molecular machines see: a) V. Balzani, A. Credi, F. M. Raymo, J. F. Stoddart, *Angew. Chem. Int. Ed. Engl.* **2000**, *39*, 3348-3391 and references therein. b) J.-P. Sauvage *Molecular Machines and Motors*; Ed. Struct. Bonding (Berlin) **2001**, *99*.

3. For examples of two- and three- blades propellers see: a) D. Gust, K. Mislow, *J. Am. Chem. Soc.* **1973**, *95*, 1535-1547. b) P. Finocchiaro, D. Gust, K. Mislow, *J. Am. Chem. Soc.* **1974**, *96*, 3198-3205. c) P. Finocchiaro, D. Gust, K. Mislow, *Top. Curr. Chem.* **1974**, 47, 1-28. d) R. Glaser, J. F. Blount, K. Mislow, *J. Am. Chem. Soc.* **1980**, *102*, 277-278. e) S. E. Biali, D. A. Nugiel, Z. Rappoport, *J. Am. Chem. Soc.* **1989**, *111*, 846-847.

4. K. Mislow, *Acc. Chem. Res.* **1976**, *9*, 26-33.

5. H. Iwamura, *J. Mol. Struct.* **1985**, *126*, 401-412.

6. For other example of molecular bevel gears see: a) W. D. Hounshell, C. A. Johnson, A. Guenzi, F. Cozzi, K. Mislow, *Proc. Natl. Acad. Sci. USA* **1980**, *77*, 6961-6973. b) F. Cozzi, A. Guenzi, C. A. Johnson, K. Mislow, W. D. Hounshell, J. F. Blount, *J. Am. Chem. Soc.* **1981**, *103*, 957-960. c) C. A. Johnson, A. Guenzi, K. Mislow, *J. Am. Chem. Soc.* **1981**, *103*, 6240-6244. d) N. Koga, Y. Kawada, H. Iwamura, *J. Am. Chem. Soc.* **1983**, *105*, 5498-5502 e) Y. Kawada, H. Iwamura, *J. Am. Chem. Soc.* **1981**, *103*, 958-962. f) H. Iwamura, T. Ito, H. Ito, K. Toriumi, Y. Kawada, E. Osawa, T. Fujiyoshi, C. Jaime, *J. Am. Chem. Soc.* **1984**, *106*, 4712-4721.

7. T. R. Kelly, K. V. Bowyer, K. V. Bhaskar, A. Bebbington, A. Garcia, F. Lang, M. H. Kim, M. P. Jette, *J. Am. Chem. Soc.* **1994**, *116*, 3657-3658.

8. a) T. R. Kelly, H. De Silva, R. A. Silva, *Nature*, **1998**, *401*, 150-152. b) T. R. Kelly, H. De Silva, R. A. Silva, S. Jasmina, Y. J. Zhao, *J. Am. Chem. Soc.* **2000**,

122, 6935-6949.

9.   N. Koumura, R. W. J. Zijlstra, R. A. van Delden, N. Harada, B. L. Feringa, *Nature*, **1999**, *401*, 152-155.

10. N. Harada, N. Koumura, B. L. Feringa, *J. Am. Chem. Soc.* **1997**, *119*, 7256-7264.

11. N. Koumura, E. M. Geertema, M. B. van Gelder, A. Meetsma, B. L. Feringa, *J. Am. Chem. Soc.* **2002**, *124*, 5037-5051.

12. R. A. van Delden, N. Koumura, N. Harada, B. L. Feringa, *Proc. Natl. Acad. Sci. USA* **2002**, *99*, 4945-4949.

13. For books and reviews about interlocked molecules see: a) G. Schill, *Catenanes, Rotaxanes and Knots*, Academic Press, New York, **1971**. b) D. B. Amabilino, J. F. Stoddart, *Chem. Rev.* **1995**, *95*, 2725-2828. c) J.-P. Sauvage, C. O. Dietrich-Buchecker, *Molecular Catenanes, Rotaxanes and Knots*, Ed. Wiley-VCH, Weinheim, **1999**.

14. I. T. Harrison, S. J. Harrison, *J. Am. Chem. Soc.* **1967**, *89*, 5723-5725.

15. G. Schill, H. Zollenkopf, *Liebig. Ann. Chem.* **1979**, *721*, 53-74.

16. For a book about supramolecular chemistry see: J.-M. Lehn, *Supramolecular Chemistry: Concepts and Perspectives*, Wiley-VCH, Weinheim, **1995**.

17. For examples of rotaxanes synthesised by "slippage" methodology see: a) P. R. Ashton, M. Belohradskym, D. Philp, J. F. Stoddart, *J. Chem. Soc. Chem. Commun.* **1993**, *16*, 1269-1274. b) M. Händel, M. Plevoets, S. Gestermann, F. Vögtle, *Angew. Chem. Int. Ed. Engl.* **1997**, *368*, 1199-1200.

18. For examples of rotaxanes synthesised by "threading" methodology see: a) C. Wu, P. R. Lecavallier, Y. X. Shen, H. W. Gibson, *Chem. Mater.* **1991**, *3*, 569-572. b) P. L. Anelli, P. R. Ashton, R. Ballardini, V. Balzani, M. Delgado, M. T. Gandolfi, T. T. Goodnow, A. E. Kaifer, D. Philp, M. Pietraszkiewicz, L. Prodi, M. V. Reddington, A. M. Z. Slawin, N. Spencer, J. F. Stoddart, C. Vincent, D. J. Williams, *J. Am. Chem. Soc.* **1992**, *114*, 193-218. c) A. G. Kolchinski, D. H. Bush,

N. W. Alcook, *J. Chem. Soc. Chem. Commun.* **1995**, 1289-1290.

19. For an example of rotaxane synthesised by "clipping" methodology see: D. Philp, J. F. Stoddart, *Synlett* **1991**, 445-458.

20. P. L. Anelli, N. Spencer, J. F. Stoddart, *J. Am. Chem. Soc.* **1991**, *113*, 5131-5133.

21. The term "co-conformation" is used to designate the different three-dimensional spatial arrangements of a) the constituent parts (for example host and guest) in supramolecular systems and of b) the components of interlocked molecular systems, see: M. C. T. Fyfe, P. T. Glink, S. Menzer, J. F. Stoddart, A. J. P. White, D. J. Williams, *Angew. Chem. Int. Ed. Engl.* **1997**, *36*, 2068-2070.

22. a) M. Gomez-Lopez, J. A. Prece, J. F. Stoddart, *Nanotechnology* **1996**, *7*, 183-192. b) P. L. Anelli, M. Asakawa, P. R. Ashton, R. A. Bissell, G. Clavier, R. Gorski, A. E. Kaifer, S. J. Langford, G. Mattersteig, S. Menzer, D. Philp, A. M. Z. Slawin, N. Spencer, J. F. Stoddart, M. S. Tolley, D. J. Williams. *Chem. Eur. J.*, **1997**, *3*, 1113-1135. c) V. Balzani, M. Gomez-Lopez, J. F. Stoddart, Acc. Chem. Res. **1998**, *31*, 405-414.

23. R. A. Bissell, E. Córdova, A. E. Kaifer, J. F. Stoddart, *Nature*, **1994**, *369*, 133-137.

24. a) P. Gaviña, J.- P. Sauvage, *Tetrahedron Lett.* **1997**, *38*, 3521-3524. b) N. Armaroli, V. Balzani, J.-P. Collin, P. Gaviña, J.- P. Sauvage, B. Ventura, *J. Am. Chem. Soc.* **1999**, *121*, 4397-4408.

25. D. A. Leigh, A. Murphy, J. P. Smart, A. M. Z. Slawin, *Angew. Chem. Int. Ed. Engl.* **1997**, *119*, 7605-7606.

26. H. Murakami, A. Kawabuchi, K, Kotoo, M. Kunitake, N. Nakashima, *J. Am. Chem. Soc.* **1997**, *119*, 7605-7606.

27. C. A. Stainer, S. J. Alderman, T. D. W. Claridge, H. L. Anderson, *Angew. Chem. Int. Ed. Engl.* **2002**, *41*, 1769-1772.

28. A. M. Brouwer, C. Frochot, F. G. Gatti, D. A. Leigh, L. Mottier, F. Paolucci, S. Roffia, G. W. H. Wurpel, *Science*, **2001**, *291*, 2124-2128.

29. a) M. C. Jiménez, C. O. Dietrich-Buchecker, J.-P. Sauvage, *Angew. Chem. Int. Ed. Engl.* **2000**, *39*, 3284-3287. b) J. P. Collin, C. O. Dietrich-Buchecker, P. Gaviña, M. C. Jiménez, J.-P. Sauvage, *Acc. Chem. Res.* **2001**, *34*, 477-487.

30. a) A. G. Johnston, D. A. Leigh, R. J. Pritchard, M. D. Deegan, *Angew. Chem. Int. Ed. Engl.* **1995**, *34*, 1209-1212. b) A. G. Johnston, D. A. Leigh, L.Nezhat, J. Smart, M. D. Deegan, *Angew. Chem. Int. Ed. Engl.* **1995**, *34*, 1212-1216.

31. a) A. G. Johnston, D. A. Leigh, A. Murphy, J. Smart, M. D. Deegan, *J. Am. Chem. Soc.* **1996**, *118*, 10662-10663. b) D. A. Leigh, A. Murphy, J. Smart, A. M. Z. Slawin, *Angew. Chem. Int. Ed. Engl.* **1997**, *36*, 728-732, c) A. S. Lane, D. A. Leigh, A. Murphy, *J. Am. Chem. Soc.* **1997**, *119*, 11092-11093.

32. F. G. Gatti, D. A. Leigh, S. Nepogodiev, A. M. Z. Slawin, S. J. Teat, J. K. Y. Wong, *J. Am. Chem. Soc.* **2001**, *121*, 5983-5989.

Synthesis of Fumaramide-Based Hydrogen Bonded [2]Rotaxanes

Prepared for submission to Journal of American Chemical Society as:

"Synthesis, Solid State Structure and Photochemical Behaviour of Structurally Diverse Fumaramide Template-Containing [2]Rotaxanes"

Bottari, G.; Gatti, F. G.; Leigh, D. A.; Wilson, A.; Wong, J. K. W.

Chapter Two- Synopsis

In this chapter the ability of fumaramide-containing threads to template the formation of structurally diverse benzylic amide macrocycles, ultimately leading to [2]rotaxanes, has been exploited (Scheme 1).
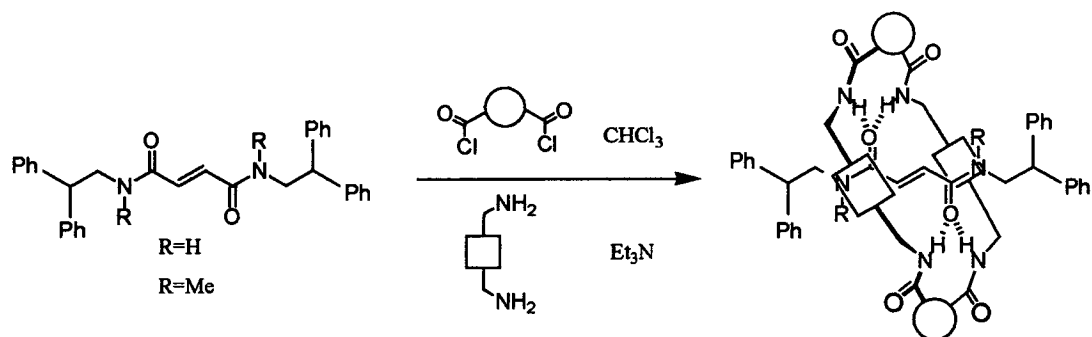
Scheme 1 *General scheme of the hydrogen bonded-directed synthesis of [2]rotaxanes by reaction of fumaramide-containing threads with different substituted diamines and acid dichlorides.*

The interlocked species are formed via a five-component "clipping" reaction in which an acyclic macrocycle precursor, formed by the condensation of acid dichlorides and diamines, templates around the fumaric diamide unit through the formation of hydrogen bonding interactions. The threads proved to be tolerant towards significant variations in the nature of the reagents, giving in one case a rotaxane in an amazing 97% yield! The remarkable template ability of the threads towards benzylic amide macrocycles can be attributed to the rigidity offered by the double bond, which holds the fumaramide carbonyls, excellent hydrogen bonding accepting groups, in a fixed transoid arrangement, at an ideal distance to template the formation of the ring. X-ray crystal structures were obtained for the all [2]rotaxanes synthesised providing some insight into the intra- and inter- molecular hydrogen bonding interactions between the mechanically interlocked components. Irradiation at 254 nm in CH_2Cl_2 of some of the fumaramide-containing rotaxanes afforded the maleamide rotaxane isomers, otherwise inaccessible via direct synthesis, due to the cisoid arrangement adopted by the maleamide carbonyl units, which are not suitable as templates for the formation of the benzylic macrocycles. The isomerisation process has been proved to be reversible by using a thermal stimulus as amply demonstrated in the following chapters.

2.1 Introduction

Through supramolecular chemistry,[1] the utilisation of non-covalent interactions has made possible the synthesis of interlocked molecules, such as rotaxanes,[2] in high yields. The formation of hydrogen bonding interactions between rotaxane precursor species in solution can be exploited in order to induce preorganisation of the rotaxane components prior to the interlocking.[3] Being able to prepare non-trivial molecules in high yields allows to readily study the interesting structural and dynamic properties of such molecules. The fumaramide-based thread *E*-1 has been shown to template, in non-hydrogen bonding disrupting solvents, the formation of the benzylic amide macrocycle, affording rotaxane *E*-2, in an astonishing 97% yield (Scheme 2.1).[4]
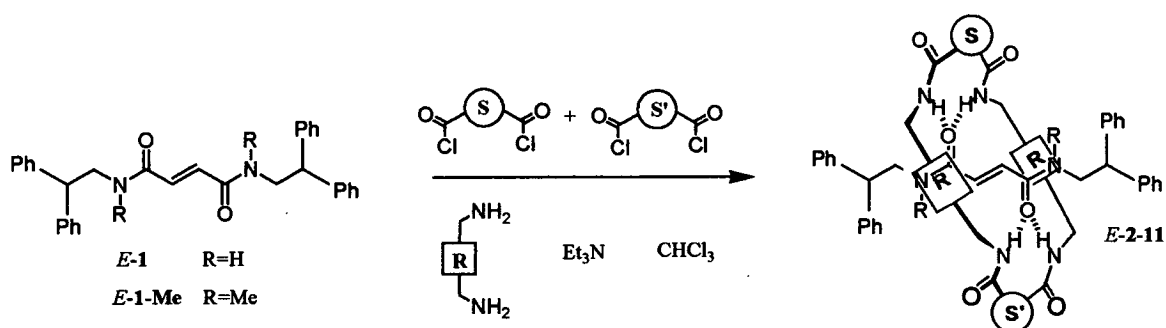
Scheme 2.1. Preparation of the [2]rotaxanes *E*-2-11 (Table 2.1) *via* a five-molecule condensation reaction.
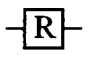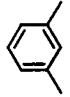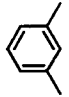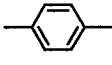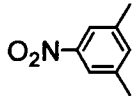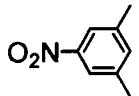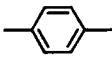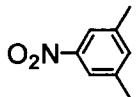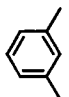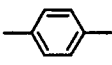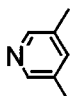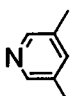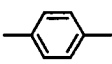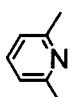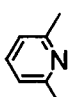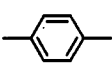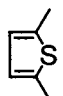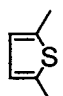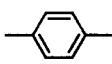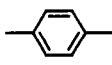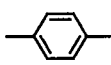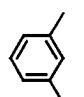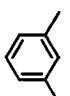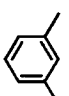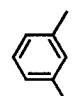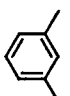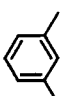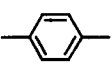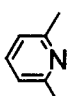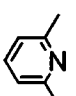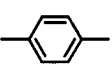
The interlocked species *E*-2 is formed *via* a five-component "clipping" reaction in which an acyclic macrocycle precursor is templated around the fumaric diamide unit. The "world record" yield for a synthesis of rotaxane can be attributed to the rigidity offered by the double bond, which holds the fumaramide carbonyls, excellent hydrogen bonding accepting groups, in a fixed *transoid* arrangement, at an ideal distance to template formation of the benzylic amide macrocycle. Due to this high preorganisation the fumaramide unit templates the acyclic macrocycle precursor and successive macrocyclisation affords the mechanically interlocked molecule *E*-2. The preorganisation offered by the templating unit on the thread is so remarkable that when

one or even both of the amide groups are substituted for esters (poor hydrogen bond acceptor groups), the formation of hydrogen bonded assembled rotaxanes still takes place. The fact that the rotaxane forming reaction occurs is even more surprising if one considers the high concentrations of amines, amides and halide ions in solution, all significantly stronger alternative hydrogen bonding acceptors than esters![5]

2.2 Results and discussion

The synthesis, solid state structure and photochemical behaviour of a family of structurally diverse fumaric-based [2]rotaxanes, *E*-2-11, has been studied (Table 2.1). Variation in both the aromatic dicarbonyl dichloride compound [(1,3- dicarbonyl phenyl (*E*-2), 1,4-dicarbonyl phenyl (*E*-8), nitro substituted phenyl (*E*-3-4), thiophenes (*E*-7), pyridines (*E*-5-6)] and the benzylic spacer [(1,4-phenylene (*E*-2-7) and 1,3-phenylene (*E*-8-9)] were tolerated by the fumaramide template giving, in all cases, the expected [2]rotaxane. Even *N*-alkylation of *E*-1 to afford the dimethylated fumaramide thread *E*-1-Me still gave an efficient template for the benzylic amide macrocycle (*E*-10-11).

The [2]rotaxanes listed in Table 2.1 were all prepared by simultaneous dropwise addition of commercially available or readily accessible dicarboxylic acid dichlorides and diamines to "stoppered" fumaric-based threads (*E*-1 or *E*-12) in the presence of Et_3N in a non-polar, non hydrogen bonding disrupting solvent such as $CHCl_3$. After 1 hour the resulting suspensions were filtered and the filtrates concentrated in volume and purified by column chromatography to yield the unconsumed threads, [2]catenanes and the desired [2]rotaxanes. *X*-ray crystal structures were obtained for the all [2]rotaxanes synthesised providing some insight into the intra- and inter- molecular hydrogen bonding interactions between the mechanically interlocked components.

S	S'	R	N—R	[2]Rotaxane	A	B
			NH	*E*-2	97%	45% (*Z*-2)
			NH	*E*-3	65%	32%* (*Z*-3)
			NH	*E*-4	27%	54% (*Z*-4)
			NH	*E*-5	42%	decompose
			NH	*E*-6	37%	51% (*Z*-6)
			NH	*E*-7	30%	
			NH	*E*-8	30%	
			NH	*E*-9	3%	
			NMe	*E*-10	33%	47% (*Z*-10)
			NMe	*E*-11	27%	

A=Yield of the rotaxane-forming reaction; B=Yield of the photochemical isomerisation of the *E*-rotaxane to its corresponding *Z*-isomer (* = calculated by ^{1}H NMR)

Table 2.1. Products and yields of (A) the fumaric-containing rotaxanes and (B) their photochemical isomerisation to their maleamide-containing isomers

Solid state structures of *E*-**2** from crystals grown in hydrogen bonding disruptive solvents (*i.e.* DMF and DMSO, Figure 2.1a and 2.1b respectively) show remarkable similarity, having the region comprising the macrocycle and the fumaric unit virtually superimposable. The macrocycle adopts in both structures a perfect chair-like conformation with its four amide hydrogens forming double bifurcated, intramolecular hydrogen bonds orthogonal to the lone pairs of the fumaramide carbonyl groups. Two more hydrogen bonds are formed between the two fumaramide hydrogens of the thread and the carbonyl units of the solvent molecules (either DMSO or DMF).
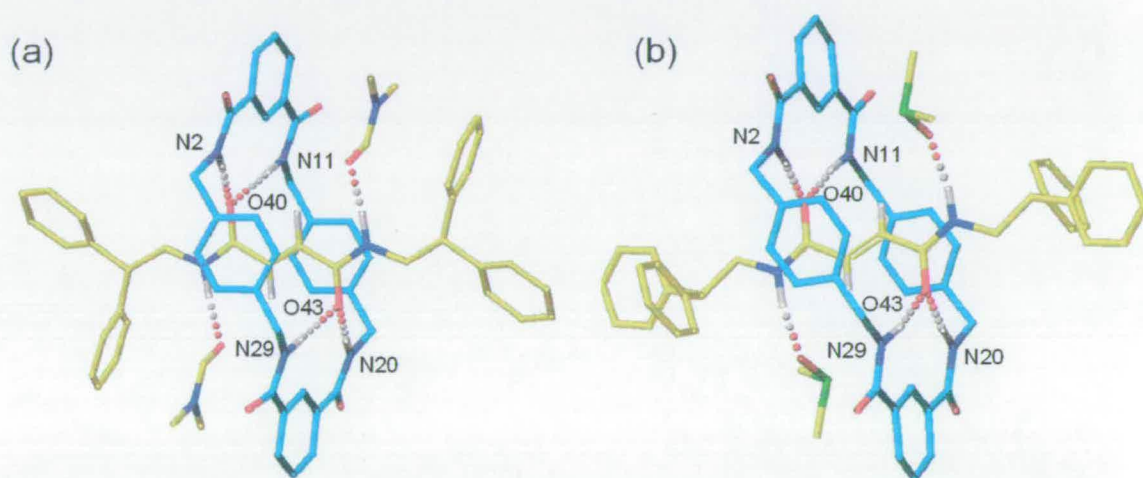
Figure 2.1. *X*-ray crystal structures of the fumaramide-based [2]rotaxane *E*-**2** (a) crystallised from DMF and (b) crystallised from DMSO. The carbon atoms of the macrocycles are shown in blue, carbon atoms of the threads in yellow, oxygen atoms in red, sulphur atoms in light green and nitrogen atoms in dark blue. The amide and alkene hydrogen atoms are shown in white while all others are removed for clarity. Intramolecular hydrogen bond distances (Å) are the following: (a) O40-HN2/O43-HN20 = 1.98, O40-HN11/O43-HN29 = 2.06; (b) O40-HN2/O43-HN20 = 2.09, O40-HN11/O43-HN29 = 1.89.

By crystallising *E*-**2** from a solvent with a poor hydrogen bonding acceptor ability such as CH$_3$CN, a different crystal lattice is observed in the solid state structure of *E*-**2** (Figure 2.2a). In this example, the number of intramolecular, intercomponent hydrogen bonds has decreased from the maximum four possible (as observed in DMSO and DMF) to two. The loss in the number of intramolecular hydrogen bonds is compensated for by

the formation of two sets of bifurcated, intermolecular hydrogen bonds as revealed by the crystal packing (Figure 2.2b).
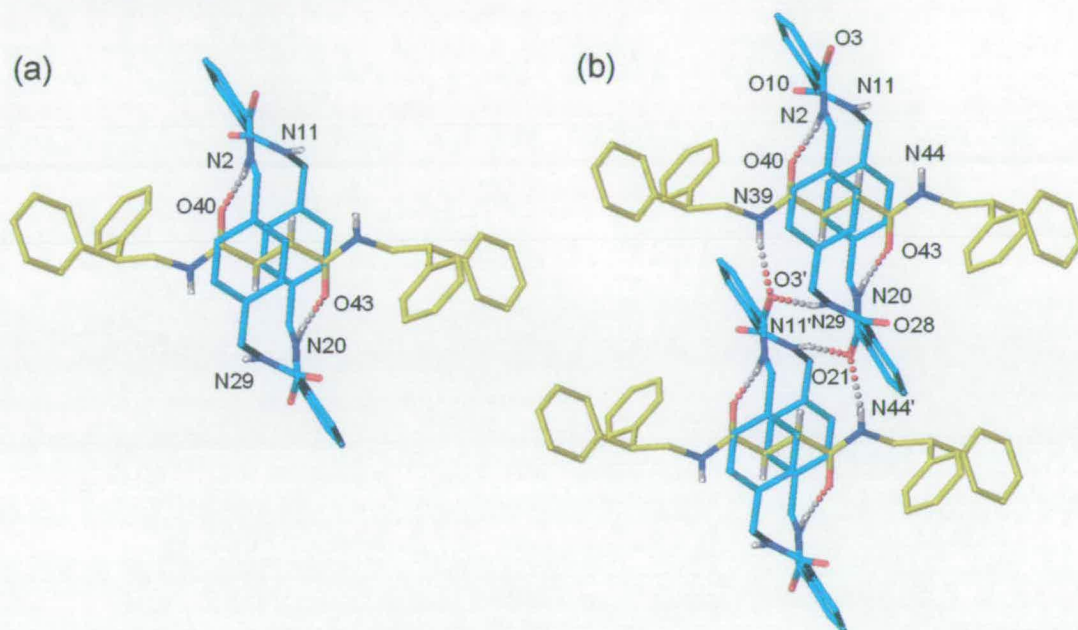
Figure 2.2. *X*-ray crystal structures of the fumaramide-based [2]rotaxanes *E*-**2** crystallised from CH$_3$CN (a) as single crystal and (b) in its crystal packing. The carbon atoms of the macrocycles are shown in blue, carbon atoms of the threads in yellow, oxygen atoms in red, sulphur atoms in light green and nitrogen atoms in dark blue. The amide and alkene hydrogen atoms are shown in white while all others are removed for clarity. Intramolecular hydrogen bond distances (Å) are the following: O40-HN2/O43-HN20 = 1.99. Intermolecular hydrogen bond distances (Å) are the following: O21-HN11'/O3'-HN29 = 2.16, O21-HN44'/O3'-HN39 = 2.14.

This new arrangement adopted by the rotaxane in the solid state allows all the six amide hydrogens to act as hydrogen bond donors at the price of distorting the chair-conformation of the macrocycle seen in the previous structures.

The dinitro rotaxane *E*-**3** was obtained in 65% yield. The crystal structures of *E*-**3** and the unsubstituted rotaxane *E*-**2**, both from DMF, present similar hydrogen bonding patterns with the dinitro substituted macrocycle in *E*-**3** adopting a twisted conformation (Figure 2.3a).

The truly remarkable ability of the fumaramide unit to template benzylic amide macrocycles allowed to exploit the synthesis of an unsymmetrical macrocycle-

containing rotaxane through a statistical reaction. The [2]rotaxane *E*-**4** containing a mononitro-substituted benzylic amide macrocycle was synthesised in 27% yield by simultaneous addition of 10 equivalents of *para*-xylylene diamine and 5 equivalents each of isophthaloyl acid dichloride and 5-nitro isophthaloyl acid dichloride to a solution of *E*-**1**.
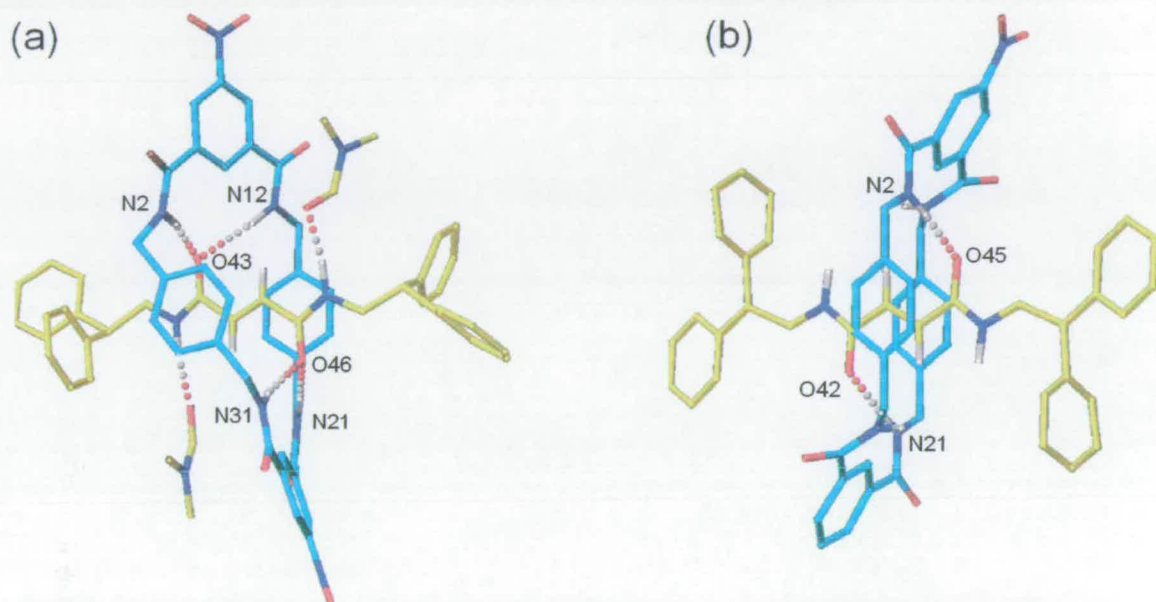
Figure 2.3. *X*-ray crystal structures of the fumaramide-based [2]rotaxanes (a) *E*-**3** and (b) *E*-**4**, both crystallised from DMF. The carbon atoms of the macrocycles are shown in blue, carbon atoms of the threads in yellow, oxygen atoms in red, sulphur atoms in light green and nitrogen atoms in dark blue. The amide and alkene hydrogen atoms are shown in white while all others are removed for clarity. Intramolecular hydrogen bond distances (Å) are the following: (a) O43-HN2 = 1.91, O43-HN12 = 2.15, O46-HN21 = 2.13, O46-HN31 = 2.01; (b) O45-HN2/O42-HN21 = 1.97.

The desired rotaxane *E*-**4** was separated from the other statistical products, *E*-**2** and *E*-**3**, by column chromatography. The ^{1}H NMR (400 MHz, 298K) spectra of *E*-**1** and *E*-**4** in d_6-DMSO shows the influence upon interlocking in the chemical shift of the thread protons (Figure 2.4). The tight fitting nature of the interlocked macrocycle provoke, with its xylylene aromatic units, the shielding of the encapsulated region of the thread, in particular the *E*-alkene protons, "core" of the fumaramide templating unit. Solid state structure of *E*-**4** from crystals grown in DMF shows the macrocycle adopting a stretched

conformation forming only two intramolecular hydrogen bonds with the carbonyl units of the thread (Figure 2.3b).
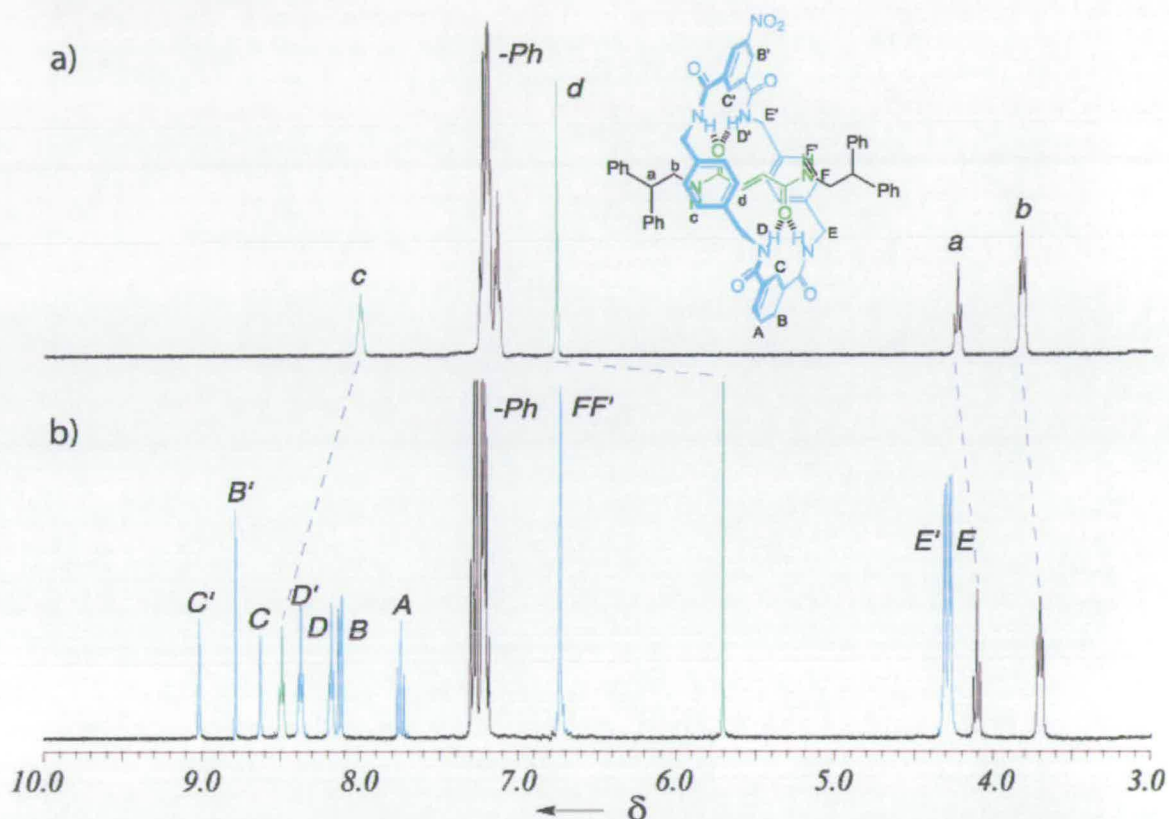
Figure 2.4. 400 MHz ^{1}H NMR spectra of (a) thread *E*-1 and (b) rotaxane *E*-4 in d_6-DMSO at 298K.

The pyridine macrocycle-containing rotaxanes *E*-5 and *E*-6 were obtained in a 42% and 37% yield respectively. Solid state structures obtained from crystals of *E*-5 and *E*-6 both grown in DMSO show how the different position of the pyridine nitrogen in the two macrocyclic units results in a different hydrogen bonding motif between the two isomers (Figure 2.5a and 2.5b). In rotaxane *E*-5 the interlocked components form two sets of bifurcated, intramolecular hydrogen bonds, resembling the hydrogen bonding motif already seen in the structure of *E*-2 from the same solvent. Rotaxane *E*–6 shows a different hydrogen bonding motif where beside the two sets of intercomponent, bifurcated hydrogen bonds, two more sets of intracomponent, bifurcated hydrogen bonds

are observed between the amide hydrogens of the macrocycle and the pyridine nitrogens that act, with their electron lone pairs, as hydrogen bond acceptor groups.
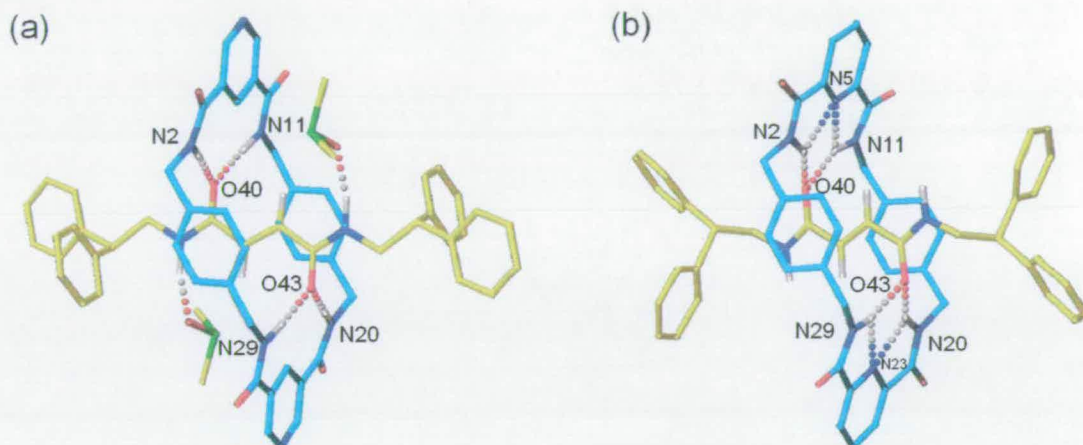
Figure 2.5. *X*-ray crystal structures of the pyridine macrocycle-containing [2]rotaxanes (a) *E*-**5** and (b) *E*-**6**, both crystallised from DMSO. The carbon atoms of the macrocycles are shown in blue, carbon atoms of the threads in yellow, oxygen atoms in red, sulphur atoms in light green and nitrogen atoms in dark blue. The amide and alkene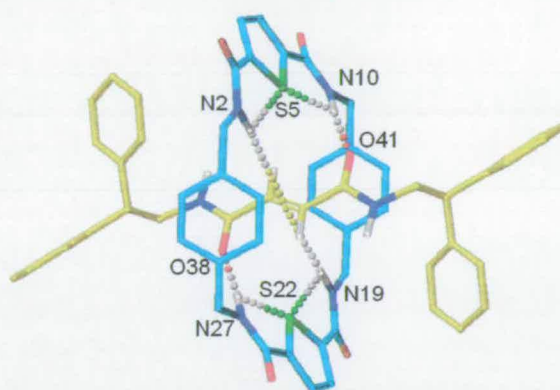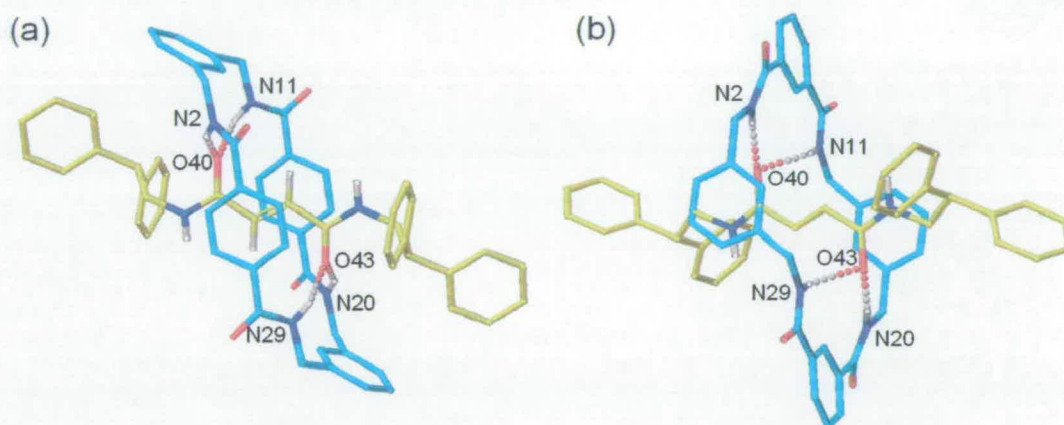 hydrogen atoms are shown in white while all others are removed for clarity. Intramolecular hydrogen bond distances (Å) are the following: (a) O40-HN2/O43-HN20 = 2.09, O40-HN11/O43-HN29 = 1.89; (b) O40-HN2 = 1.92, O40-HN11 = 1.97, O43-HN29 = 1.93, O43-HN20 = 1.90, N5-HN2 = 2.27, N5-HN11 = 2.25, N23-HN29 = 2.21, N23-HN20 = 2.19.

The remarkable macrocycle-templating ability of the fumaramide unit was once again confirmed in the formation of the sulphur-containing rotaxane *E*-**7** in 30% yield. The solid state structure of *E*-**7** from crystals grown in DMSO shows the sulphur atoms of the macrocycle involved in the formation of two sets of intracomponent, bifurcated hydrogen bonds with the four amide hydrogens of the macrocycle, similar to the pyridine nitrogens in *E*-**6** (Figure 2.6). Moreover two intercomponent hydrogen bonds are formed between two macrocycle amide hydrogens and the divergent carbonyls of the fumaric unit on one side and between the remaining two amide hydrogens of the macrocycle and the π-cloud of the alkene double bond on the other. The "inverted" benzylic amide macrocycle-containing rotaxane *E*-**8**, isomer of *E*-**2**, was obtained in 30% yield. Solid state structure of *E*-**8** from crystals grown in MeOH (Figure 2.7a)

shows, with its two sets of bifurcated intramolecular hydrogen bonds, a hydrogen bonding motif already seen for its isomer *E*-**2**, although the conformation adopted by the macrocycles in the two rotaxanes is remarkably different.

Figure 2.6. *X*-ray structures of fumaramide-based thiophene rotaxanes *E*-**7** crystallised from MeOH. The carbon atoms of the macrocycles are shown in blue, carbon atoms of the threads in yellow, oxygen atoms in red, sulphur atoms in light green and nitrogen atoms in dark blue. The amide and alkene hydrogen atoms are shown in white while all others are removed for clarity. Intramolecular hydrogen bond distances (Å) are the following: (a) O41-HN10/O38-HN27 = 1.89, S5-HN10/S22-HN27 = 2.56, S5-HN2/S22-HN19 = 2.51, HN2-π alkene/HN19-π alkene = 3.41.

(a)   (b)

Figure 2.7. *X*-ray structures of fumaramide-based rotaxanes (a) *E*-**8** crystallised from MeOH and (b) *E*-**9** crystallised from EtOH. The carbon atoms of the macrocycles are shown in blue, carbon atoms of the threads in yellow, oxygen atoms in red, sulphur atoms in light green and nitrogen atoms in dark blue. The amide and alkene hydrogen atoms are shown in white while all others are removed for clarity. Intramolecular hydrogen bond distances (Å) are the following: (a) O40-HN2/O43-HN20 = 2.17, O40-HN11/O43-HN29 = 2.34; (b) O40-HN2/O43-HN20 = 2.12, O40-HN11/O43-HN29 = 2.31.

By comparing the crystal structures of *E*-**8** and *E*-**2** it is possible to notice that the cavity presented by the two structurally different isomeric macrocycles is considerably tighter in case of *E*-**8** due to a different positioning of the macrocyclic amides. Since the transition state of the rotaxane-forming reaction is similar in structure to the final rotaxane,[6] this could explain the lowering in the yield of the rotaxane forming reaction observed going from *E*-**2** to its isomer *E*-**8**, presenting this last one a higher activation energy for macrocyclisation.

A drastic variation in the geometry of the rotaxane benzylic amide macrocycle was realised by subjecting the fumaramide-based thread *E*-**1** to the simultaneous addition of 1,3-substituted acid dichloride and *meta*-xylylenediamine in presence of Et_3N obtaining the rotaxane *E*-**9** in a 3% yield. While at first sight this yield may appear low compared to the previous example, that the rotaxane-forming reaction proceeds at all is remarkable, considering the crystal structure of *E*-**9** (Figure 2.7b). Rotaxanes *E*-**1-8** each bear 26-membered benzylic amide macrocycles, whereas *E*-**9** contains a smaller 24-membered macrocycle. This smaller macrocycle adopts a distorted high-energy conformation although still able to form two sets of bifurcated hydrogen bonds between amide hydrogens of the macrocycle and carbonyl units of the thread. As already seen for *E*-**8**, even for *E*-**9** the restricted cavity offered by the macrocycle to the fumaramide template ultimately results in a lower yield of the interlocked molecule formation.

A modification in the fumaramide motif (from the secondary fumaric amides of *E*-**1** to the tertiary *N*-methylated fumaric amides of *E*-**1-Me**) has also been exploited in rotaxane-forming reactions. The rotaxanes *E*-**10** and *E*-**11** containing a *N*-methylated fumaramide template unit were both synthesised from *E*-**1-Me** in 33% and 27% yield respectively. Solid state crystal structures of both *E*-**10** and *E*-**11** (Figure 2.8a and 2.8b) show remarkable similarity in the hydrogen bonding patterns with their respective unmethylated rotaxane analogues *E*-**2** and *E*-**6**.

Somewhat remarkably however, given the tight encapsulated binding site and that only the *trans*-olefin has hydrogen bonding sites complementary to the benzylic macrocycle

geometry, irradiation at 254 nm of some of the E-rotaxanes[7] in CH_2Cl_2 resulted in the conversion of the fumaramide rotaxanes into their corresponding Z-rotaxane isomers (except in the case of E-**5**) in 32-54% yield.
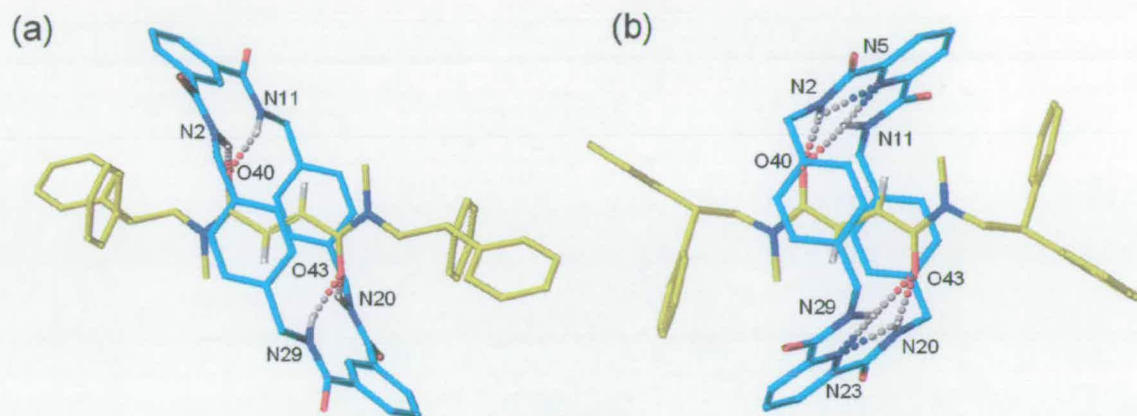
Figure 2.8. X-ray crystal structures of the N-methylated fumaramide rotaxanes (a) E-**10** and (b) E-**11**. The carbon atoms of the macrocycles are shown in blue, carbon atoms of the threads in yellow, oxygen atoms in red and nitrogen atoms in dark blue. The amide and alkene hydrogen atoms are shown in white while all others are removed for clarity. Intramolecular hydrogen bond distances (Å) are the following: (a) O40-HN2/O43-HN20 = 2.22, O40-HN11/O43-HN29 = 1.94; (b) O40-HN2/O43-HN20 = 2.10, O40-HN11/O43-HN29 = 2.17, N5-HN2/N23-HN20 = 2.24, N5-HN11/N23-HN29 = 2.23.

It is worth noticing that the photochemical isomerisation of the E-rotaxanes is the only possible way to obtain the Z-rotaxanes otherwise unobtainable *via* hydrogen bonded templated synthesis of the maleamide isomer of E-**1**, a consequence of the mis-matching between the carbonyl groups in the Z-thread and the amide hydrogens of the benzylic macrocycle. The ^{1}H NMR spectra in CD_2Cl_2 of Z-**3**, product of the photoisomerisation of E-**3**, and its uninterlocked maleamide-containing linear component are shown in Figure 2.9 as example. As already seen for E-**3**, the presence of the macrocycle in Z-**3** causes a considerable upfield shift in the chemical shift of the encapsulated region, affecting mainly the Z-alkene protons. The Z-rotaxanes can be converted once again in their E-isomers by using a thermal stimulus to provoke the maleamide→fumaramide interconversion, as described in the following chapters.
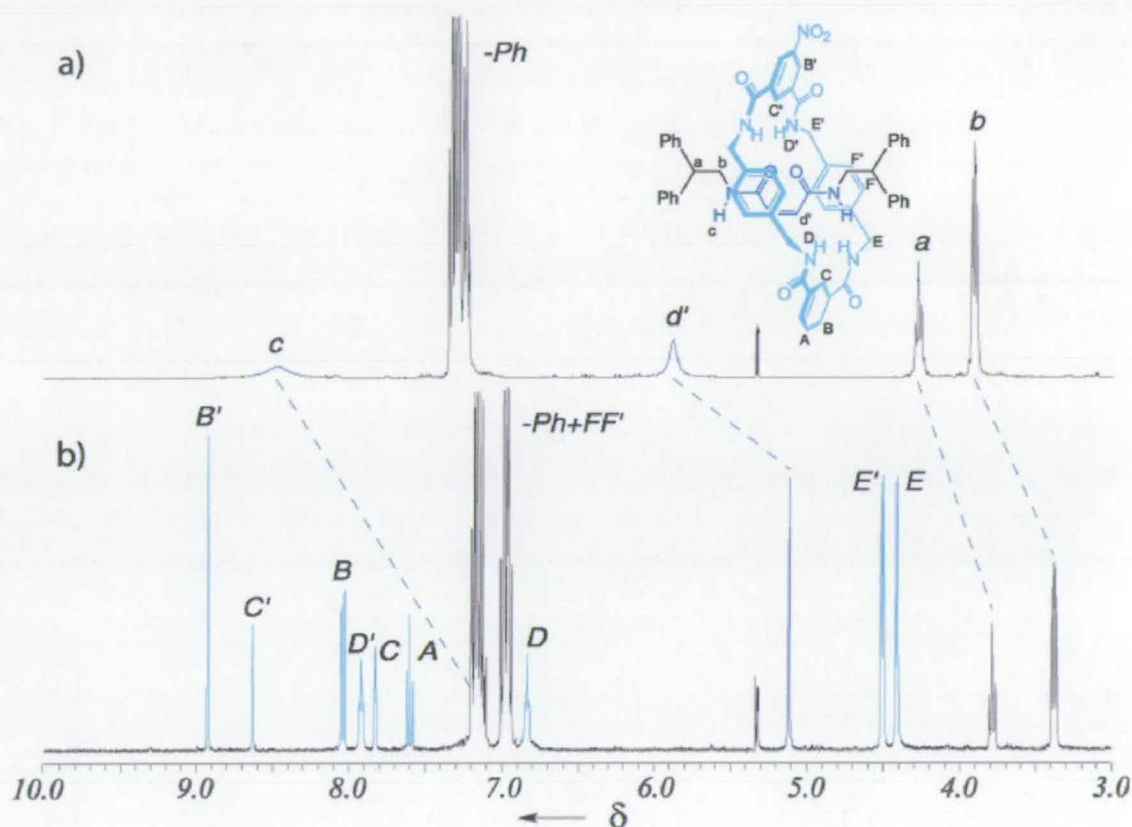
Figure 2.9. 400 MHz ^{1}H NMR spectra of (a) uninterlocked maleamide-containing thread and (b) rotaxane Z-**3** in CD$_2$Cl$_2$ at 298K.

2.3 Conclusions

In this chapter the remarkable ability of fumaramide units as templates in the synthesis of structurally different benzylic amide macrocycles-containing [2]rotaxanes has been shown. The formation in solution of intercomponent hydrogen bonds between thread and macrocycle precursor, driving force for the rotaxane-forming reaction, is partially maintained in the solid state as confirmed from the X-ray crystal structures obtained for all of the hydrogen bonded rotaxanes synthesised. The presence in the E-rotaxanes of a photoisomerisable fumaramide unit allowed us to use a photonic stimulus to afford the respective maleamide rotaxane isomers. The consequences of the isomerisation over the dynamic properties of rotaxanes will be discussed in the next chapters.

45

2.4 Experimental Section

### 2.4.1 General Method for the Preparation of Benzylic Amide Macrocycle Containing Fumaramide [2]Rotaxanes.

The thread (*E*-1 or *E*-1-Me) (0.5 mmol) was dissolved in $CHCl_3$ (100 mL) (in the case of *E*-1 9.5/0.5 $CHCl_3/CH_3CN$) and stirred vigorously whilst solutions of the diamine (5 mmol) and Et_3N (10 mmol) in $CHCl_3$ (40 mL) and the acid dichloride (5 mmol) in $CHCl_3$ (40 mL) were simultaneously added over a period of 2 h using motor-driven syringe pumps. After a further 1 h the resulting suspension was filtered and concentrated under reduced pressure.

2.4.2 General Method for the Photoisomerization of Fumaramide [2]Rotaxanes.

The *E*-rotaxane (0.10 mmol) was dissolved in CH_2Cl_2 (20 mL) [except for solubility reasons *E*-2, $MeOH/CH_2Cl_2$ (1/9)] in a quartz vessel. The solutions were directly irradiated at 254 nm using a multilamp photoreactor model MLU18 manufactured by Photochemical Reactors Ltd, Reading UK. The progress of photoisomerization was monitored by TLC (silica gel, $CHCl_3/EtOAc$ 4/1) or ^1H NMR. The different photostationary states were reached in a range of times not exceeding 30 mins after which the reaction mixture was concentrated under reduced pressure to afford crude product. Because the photoisomerisation process produces few byproducts it could be recycled more times.

***N,N'–bis* (2,2–diphenyl-ethyl)- (*E*)-butendiamide, *E*-1**
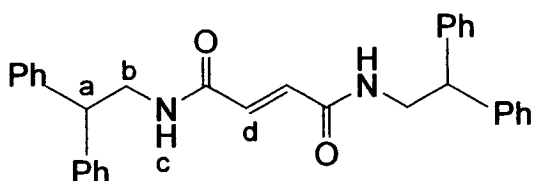
To a stirred solution of 2,2-diphenylethylamine (0.493 g, 2.50 mmol) and Et$_3$N (0.252g, 2.50 mmol) in CH$_2$Cl$_2$ (20 mL) at 0 °C was added dropwise a solution of fumaryl dichloride (0.191 g, 1.25 mmol) in CH$_2$Cl$_2$. After 3 h the solution was washed with 1N HCl (2 x 20 mL), 1N NaOH (2 x 20 mL) and H$_2$O (1 x 20 mL). The organic layer was dried over anhydrous MgSO$_4$, filtered and the solvent removed under reduced pressure to obtain a solid that was recrystallized from CH$_2$Cl$_2$ to afford colourless needles (*E*-1, 1.150 g, 97 %). m.p. 252-253 °C. ^{1}H NMR (400 MHz, CDCl$_3$): δ = 7.36-7.28 (m, 8H, ArC*H*), 7.26-7.20 (m, 12H, ArC*H*), 6.66 (s, 2H, C*H*$_d$), 5.66 (br t, ^3J(H,H) = 5.8 Hz, 2H, N*H*$_c$), 4.20 (t, ^3J(H,H) = 7.8 Hz, 2H, C*H*$_a$) and 3.98 (dd, ^3J(H,H) = 7.8 Hz, ^3J(H,H) = 5.8 Hz, 4H, C*H*$_b$); ^{13}C NMR (100 MHz, d_6-DMSO): δ = 163.7 (*C*O), 142.7 (Ar*C* (ipso)), 132.5 (*C*H$_d$), 128.4 (Ar*C*H (meta)), 127.8 (Ar*C*H (ortho)), 126.3 (Ar*C*H (para)), 49.9 (*C*H$_a$) and 43.3 (*C*H$_b$); HRMS (FAB) Calcd. for C$_{32}$H$_{31}$N$_2$O$_2$ [M+H]$^+$ 475.23855. Found 475.23799.

***N,N'*- Dimethyl-*bis*(2,2-diphenyl-ethyl)- *(E)*-butendiamide, *E*-1-Me**
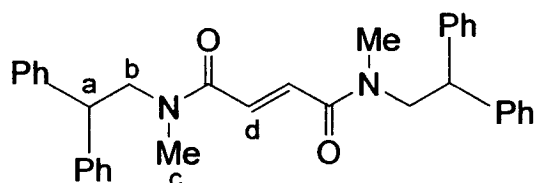
To a stirred solution kept under inert atmosphere of *E*-1 (1 g, 2.10 mmol) in dry THF (20mL) was added at 0 °C under nitrogen NaH (0.2 g, 60% dispersion in oil, excess) portion-wise. After the effervescence had subsided, methyl iodide (0.3 mL, excess) was

added in one portion. The reaction was allowed to warm to rt and stirred for 16 h, then H$_2$O (20 mL) and ammonia solution (10 mL) added drop-wise to quench the reaction. Most of the solvent was removed under reduced pressure, and the remainder partitioned between H$_2$O and CH$_2$Cl$_2$ (3 x 20 mL). The organic extracts were washed with 1N NaOH (20 mL) and dried over anhydrous MgSO$_4$. The filtered solution was concentrated under reduced pressure to give an oil that slowly solidified. Recrystallization from CH$_2$Cl$_2$/diisopropyl ether afforded colorless needles (*E*-**1-Me**, 0.876 g, 83%). m.p. 134-136 °C; ^{1}H NMR (400 MHz, C$_2$D$_2$Cl$_4$ at 363K): δ = 7.34-7.19 (m, 20H, ArC*H*), 6.99 (s, 2H, C*H*$_d$), 4.37 (t, ^3J(H,H) = 8.0 Hz, 2H, C*H*$_a$), 4.04 (d, ^3J(H,H) = 8.0 Hz, 4H, C*H*$_b$) and 2.79 (s, 6H, C*H*$_c$); ^{13}C NMR (100 MHz, C$_2$D$_2$Cl$_4$ at 400K): δ = 166.7 (*C*O), 143.0 (Ar*C* (ipso)), 132.1 (*C*H$_d$), 129.7 (Ar*C*H (meta)), 128.9 (Ar*C*H (ortho)), 127.2 (Ar*C*H (para)), 55.5 (*C*H$_a$), 51.0 (*C*H$_b$) and 37.5 (*C*H$_c$); MS (FAB, *m*NBA): *m/z* = 502 [(M+H)$^+$]; Anal. Calcd. for C$_{34}$H$_{34}$N$_2$O$_2$: C 81.24, H 6.82, N 5.57. Found: C 81.61, H 6.68, N 5.43. HRMS (FAB) Calcd. for C$_{34}$H$_{35}$N$_2$O$_2$ [M+H]$^+$ 503.26985. Found 503.27004.

[2](1,7,14,20-Tetraaza-2,6,15,19-tetraoxo-3,5,9,12,16,18,22,25-tetrabenzocyclohexacosane)-(*N,N'–bis* (2,2–diphenyl-ethyl)-(*E*)-butendiamide)-rotaxane, *E*-2
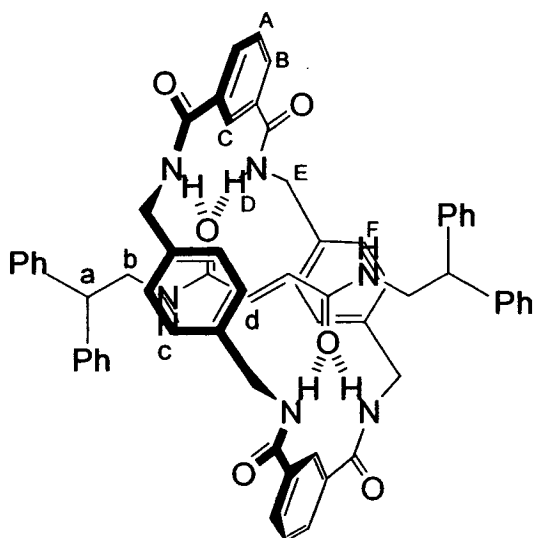
Rotaxane *E*-2 was obtained using the general procedure for the preparation of benzylic amide macrocycle containing [2]rotaxane from thread *E*-1 (0.237 g) using as diamine the *p*-xylylenediamine (0.681 g) and as acid dichloride the isophthaloyl dichloride (1.015 g). The crude was purified by trituration of the solid in CH_2Cl_2 (to remove the polar impuries- catenane, macrocycles, $Et_3HN^+Cl^-$, etc), and subsequently the rotaxane separated from the unreacted thread through trituration in hot toluene. Rotaxane *E*-2 was recrystallized from DMF (*E*-2, 0.488 g, 97%). m.p. 355-356 °C (DMF/H_2O); ^1H NMR (400 MHz, CDCl$_3$): δ = 8.40 (br t, 2H, $^4J(H_C,H_B)$ = 1.8 Hz, ArCH_C), 8.21 (dd, 4H, $^3J(H_B,H_A)$ = 7.8 Hz, $^4J(H_B,H_C)$ = 1.8 Hz, ArCH_B), 7.66 (t, 2H, $^3J(H_A,H_B)$ = 7.8 Hz, ArCH_A), 7.43 (br t, 4H, $^3J(H,H)$ = 5.3 Hz, NH_D), 7.32-7.20 (m, 12H, ArCH (meta and para thread)), 7.14 (d, 8H, $^3J(H,H)$ = 6.8 Hz, ArCH (ortho thread)), 6.74 (s, 8H, ArCH_F), 5.99 (br t, 2H, $^3J(H,H)$ = 5.8 Hz, NH_c), 5.44 (s, 2H, CH_d), 4.40 (d, 8H, $^3J(H,H)$ = 5.3 Hz, CH_E), 4.10 (t, 2H, $^3J(H,H)$ = 7.8 Hz, CH_a) and 3.70 (dd, 4H, $^3J(H,H)$ = 7.8 Hz, $^3J(H,H)$ = 5.8 Hz, CH_b); ^{13}C NMR (100 MHz, d_6-DMSO): δ = 166.1 (*C*O thread), 165.7 (*C*O macrocycle), 143.0 (Ar*C* (ipso thread)), 136.7 (Ar*C*-CH$_2$NH), 134.6 (Ar*C*-CO-), 131.1(*C*H$_B$), 129.6 (*C*H$_d$), 129.4 (*C*H$_A$), 128.9 (*C*H$_F$), 128.8 (Ar*C*H (meta thread), 128.1 (Ar*C*H (ortho thread)), 126.9 (Ar*C*H (para thread)), 125.7 (*C*H$_C$), 50.3 (*C*H$_a$), 44.0 (*C*H$_b$)

and 43.6 (CH_E); HRMS (FAB) Calcd. for $C_{64}H_{59}N_6O_6$ [M+H]$^+$ 1007.44961. Found 1007.44972.

[2](1,9,16,24-Tetraaza-2,8,17,23-tetraoxo-5,20-dinitro-3,7,11,14,18,22,26,29-tetrabenzocyclohexacosane))-(*N*,*N'*-*bis*(2,2–diphenyl-ethyl)-(*E*)-butendiamide)-rotaxane, *E*-3
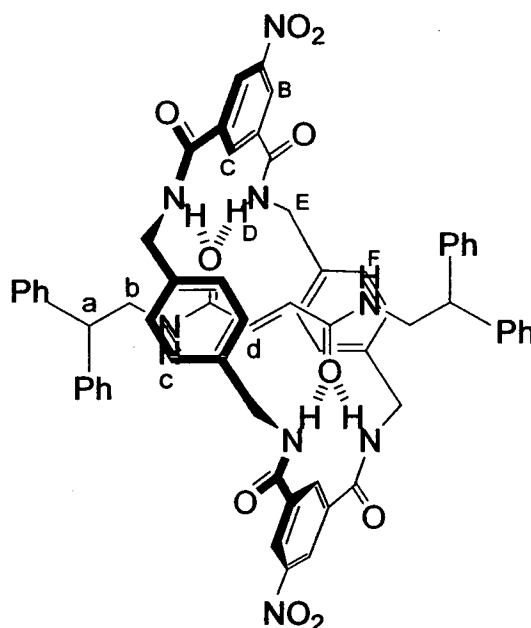
Rotaxane *E*-3 was obtained using the general procedure for the preparation of benzylic amide macrocycle containing [2]rotaxane from thread *E*-1 (0.237 g) using as diamine the *p*-xylylenediamine (0.681 g) and as acid dichloride 5-nitroisophthaloyl dichloride (1.240 g). The crude obtained was purified by column chromatography on silica gel using a gradient of CH_2Cl_2/EtOAc as eluent to obtain the desired compound as a colourless powder (*E*-3, 0.357 g, 65%). m.p. 324 °C; ^{1}H NMR (400 MHz, d_6-DMSO): δ = 8.96 (s, 2H, ArCH_C), 8.76 (s, 4H, ArCH_B), 8.41 (br t, 4H, NH_D), 7.28-7.14 (m, 22H, ArCH + NH_c), 6.75 (s, 8H, ArCH_F), 5.71 (s, 2H, CH_d), 4.30 (d, 8H, ^3J(H$_E$,H$_D$) = 4.8 Hz, CH_E),

4.02 (t, 2H, $^3J(H_a,H_b)$ = 7.3 Hz, CH_a), 3.66 (br dt, 4H, CH_b); ^{13}C NMR (100 MHz, d_6-DMSO) δ 167.0, 165.5, 150.2, 144.4, 137.9, 137.7, 132.6, 131.3, 130.4, 130.3, 129.4, 128.3, 126.8, 51.7, 45.3, 45.1; HRMS (FAB) Calcd. for $C_{64}H_{57}N_8O_{10}$ [M+H]$^+$ 1097.41977. Found 1097.41991.
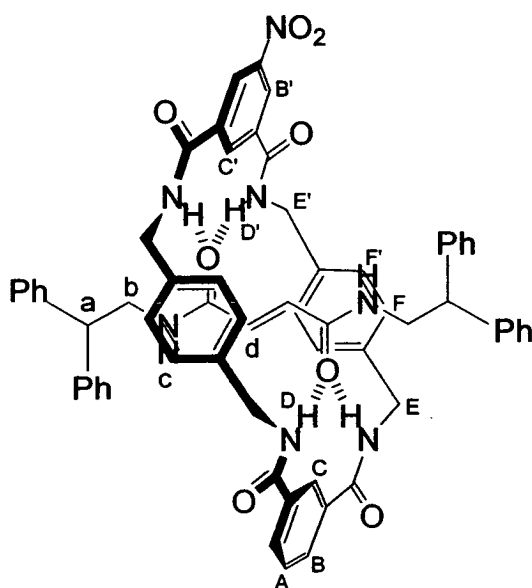
[2](1,9,16,22-Tetraaza-2,8,17,21-tetraoxo-5-nitro-3,7,11,14,18,20,24,27-tetrabenzocyclohexacosane))-(*N,N'*–*bis*(2,2–diphenyl-ethyl)-(*E*)-butendiamide)-rotaxane, *E*-4

Rotaxane *E*-4 was obtained using the general procedure for the preparation of benzylic amide macrocycle containing [2]rotaxane from thread *E*-1 (0.237 g) using as diamine the *p*-xylylenediamine (0.681 g) and as acid dichloride isophthaloyl dichloride (0.507 g, 2.5 mmol) and 5-nitroisophthaloyl dichloride (0.620 g, 2.5 mmol). The crude obtained was purified by column chromatography on silica gel using a gradient of CH$_2$Cl$_2$/EtOAc as eluent to obtain the desired compound as a colourless powder (*E*-4, 0.142 g, 27%). m.p. 318 °C; ^{1}H NMR (400 MHz, d_6-DMSO) δ 9.00 (s, 1H, $^4J(H_{C'},H_{B'})$ = 1.5 Hz, ArC$H_{C'}$), 8.79 (t, 2H, $^4J(H_{B'},H_{C'})$ = 1.5 Hz, ArC$H_{B'}$), 8.63 (s, 1H, $^4J(H_C,H_B)$ = 1.5 Hz, ArCH_C), 8.49 (t, 2H, $^3J(H_c,H_b)$ = 5.6 Hz, NH_c), 8.38 (t, 2H, $^3J(H_{D'},H_{E'})$ = 5.0 Hz, N$H_{D'}$), 8.18 (t,

2H, ^3J(H$_D$,H$_E$) = 4.9 Hz, NH_D), 8.12 (2H, d, ^4J(H$_B$,H$_C$) = 1.5 Hz, ^3J(H$_B$,H$_A$) = 7.8 Hz, ArCH_B), 7.74 (t, 1H, ^3J(H$_A$,H$_B$) = 7.8 Hz, ArCH_A), 7.30-7.15 (m, 20H, ArCH), 6.73 (s, 8H, ArC$H_{F \, and \, F'}$), 5.70 (s, 2H, CH_d), 4.30 (d, 4H, ^3J(H$_{E'}$,H$_{D'}$) = 5.0 Hz, C$H_{E'}$), 4.27 (d, 4H, ^3J(H$_E$,H$_D$) = 5.0 Hz, CH$_E$), 4.10 (t, 2H, ^3J(H$_a$,H$_b$) = 7.7 Hz, CH_a), 3.69 (dd, 4H, ^3J(H$_b$,H$_a$) = 7.7 Hz, ^3J(H$_b$,H$_c$) = 5.6 Hz, CH_b); ^{13}C NMR (100 MHz, d_6-DMSO) δ 166.2 (CO), 165.6 (CO), 164.1 (CO), 142.9, 136.9, 136.3, 134.6, 131.1, 129.8, 129.5, 128.9, 128.8, 128.1, 126.9, 125.6, 125.4, 50.3 (CH_a), 44.0, 43.8, 43.6; HRMS (FAB) Calcd. for C$_{64}$H$_{58}$N$_7$O$_8$ [M+H]$^+$ 1052.43469. Found 1052.43498.
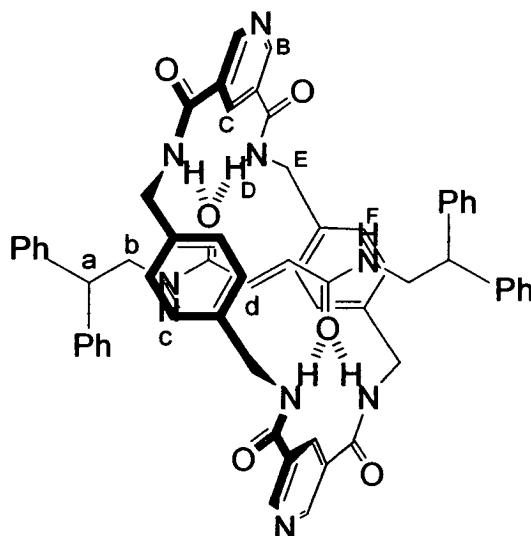
[2](1,5,9,16,20,24-Hexaaza-2,8,17,23-tetraoxo-3,7,11,14,18,22,26,29-tetrabenzocyclohexacosane))-(*N,N'–bis*(2,2–diphenyl-ethyl)-(*E*)-butendiamide)-rotaxane, *E*-5

Rotaxane *E*-5 was obtained using the general procedure for the preparation of benzylic amide macrocycle containing [2]rotaxane from thread *E*-1 (0.237 g) using as diamine the *p*-xylylenediamine (0.681 g) and as acid dichloride 3,5 pyridyl acid dichloride (1.020 g). The crude obtained was purified by column chromatography on silica gel using a

gradient of CH$_2$Cl$_2$/EtOAc as eluent to obtain the desired compound as a colourless powder (*E*-5, 0.211 g, 42%). m.p. 320 °C decomp.; ^{1}H NMR (400 MHz, CDCl$_3$): δ = 9.23 (s, 4H, ArCH_B), 8.85 (s, 2H, ArCH_C), 8.11 (br t, 2H, NH_c), 7.78 (br t, 4H, NH_D), 7.32-7.06 (m, 20H, ArCH), 6.64 (s, 8H, ArCH_F), 5.48 (s, 2H, CH_d), 4.27 (s, 8H, CH_E), 4.05 (t, 2H, ^3J(H,H) = 7.3 Hz, CH_a), 3.67 (br dd, 4H, CH_b); ^{13}C NMR (100 MHz, CDCl$_3$) δ 167.4 (*C*O), 166.9 (*C*O), 153.4, 143.3 (Ar*C* (ipso)), 138.0 (Ar*C* (ipso)), 134.9, 131.4, 130.7, 130.5, 129.4, 128.8, 52.1 (*C*H$_a$), 46.2(*C*H$_b$), 45.7 (*C*H$_E$); HRMS (FAB) Calcd. for C$_{62}$H$_{57}$N$_8$O$_6$ [M+H]$^+$ 1009.44011. Found 1009.44075.

[2](1,4,7,14,17,20-Hexaaza-2,6,15,19-tetraoxo-3,5,9,12,16,18,22,25-tetrabenzocyclohexacosane))-(*N*,*N*'–*bis*(2,2–diphenyl-ethyl)-   (*E*)-butendiamide)-rotaxane, *E*-6
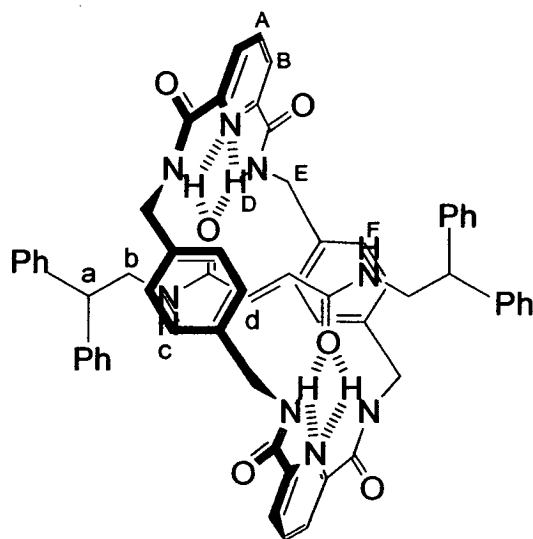
Rotaxane *E*-6 was obtained using the general procedure for the preparation of benzylic amide macrocycle containing [2]rotaxane from thread *E*-1 (0.237 g) using as diamine the *p*-xylylenediamine (0.681 g) and as acid dichloride 2,6 pyridyl acid dichloride (1.020 g). The crude obtained was purified by column chromatography on silica gel using a

gradient of CH_2Cl_2/EtOAc as eluent to obtain the desired compound as a colourless powder (E-6, 0.187 g, 37%). m.p. 330 °C decomp.; ^1H NMR (400 MHz, $CDCl_3$): δ = 9.63 (t, 4H, ^3J(H,H) = 6.1 Hz, NH_D), 8.41 (d, 4H, ^3J(H,H) = 7.6 Hz, ArCH_B), 8.12 (t, 2H, ^3J(H,H) = 7.6 Hz, ArCH_A), 7.29-7.11 (m, 22H, ArCH and NH_c), 6.48 (s, 8H, ArCH_F), 5.00 (s, 2H, CH_d), 4.90-4.18 (br, 8H, CH_E), 4.16 (t, 2H, ^3J(H,H) = 7.8 Hz, CH_a), 4.16 (br dd, 4H, CH_b); ^{13}C NMR (100 MHz, $CDCl_3$) δ 165.4 (CO), 164.0 (CO), 149.1 (ArC (ipso)), 141.7 (ArC (ipso)), 139.0 (CH_A), 137.5 (ArC (ipso)), 128.9, 128.3 (CH_F), 127.7, 127.4 (CH_d), 127.2, 125.1 (CH_B), 50.3 (CH_a), 44.7 (CH_E), 44.5 (CH_b); HRMS (FAB) Calcd. for $C_{62}H_{57}N_8O_6$ [M+H]$^+$ 1009.44011. Found 1009.44013.

[2](1,8,14,21-Tetraaza-2,7,15,20-tetraoxo-3,6,10,12,16,19,23,25-tetrabenzocyclohexacosane))-(*N,N'*–*bis*(2,2–diphenyl-ethyl)-(*E*)-butendiamide)-rotaxane, *E*-8
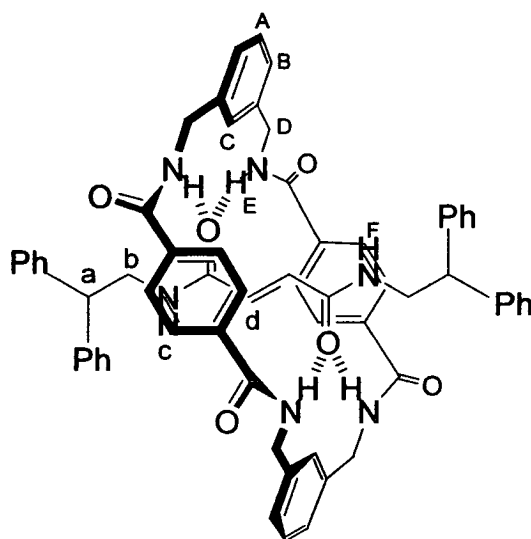

Rotaxane E-8 was obtained using the general procedure for the preparation of benzylic amide macrocycle containing [2]rotaxane from thread E-1 (0.237 g) using as diamine *m*-xylylenediamine (0.681 g) and as acid dichloride terephthaloyl dichloride (1.015). The

filtrate was then washed with HCl (0.2M, 100 mL) and Na_2CO_3 solution (100 mL). The organic layer was then dried over $MgSO_4$ and the solvent removed *in vacuo* to leave a cream solid. The rotaxane was isolated by column chromatography on silica gel (2% $MeOH/CH_2Cl_2$) (*E*-**8**, 0.151 g, 30 %). m.p. 329.9-331.9°C; ^1H NMR (400 MHz, d_6-DMSO): δ = 8.35 (t, 2H, $^3J(H,H)$ = 6.5 Hz, NH_c), 8.00 (t, 4H, $^3J(H,H)$ = 5.5 Hz, NH_E), 7.74 (s, 2H, ArCH_C), 7.31 (22H, m, ArCH), 7.19 (t, 4H, $^3J(H,H)$ = 7.5 Hz, ArCH), 6.80 (8H, s, ArCH_F), 4.85 (s, 2H, CH_d), 4.58 (d, 8H, $^3J(H,H)$ = 5.5 Hz, CH_D), 4.21 (t, 2H, $^3J(H,H)$ = 6.5 Hz, CH_a), 3.77 (dd, 4H, $^3J(H,H)$ = 6.5 Hz, CH_b); ^{13}C NMR (100 MHz, d_6-DMSO): δ = 167.6 (*C*O), 165.3 (*C*O), 143.2 (Ar*C* (ipso)), 139.5 (Ar*C* (ipso)), 138.2 (Ar*C* (ipso)), 132.1 (*C*H_d), 132.0 (Ar*C*H), 128.9 (Ar*C*H), 128.8 (Ar*C*H), 126.9 (Ar*C*H), 126.7, (Ar*C*H), 126.5 (Ar*C*H), 125.4 (Ar*C*H), 50.8 (*C*H), 44.0 (*C*H$_2$), 43.4 (*C*H$_2$); MS (FAB): m/z = 1007 [M+H]$^+$; Anal. Calcd. for $C_{64}H_{58}O_6N_6$: C 76.32, H, 5.80, N, 8.34. Found C 75.96, H 5.83, N 8.19.
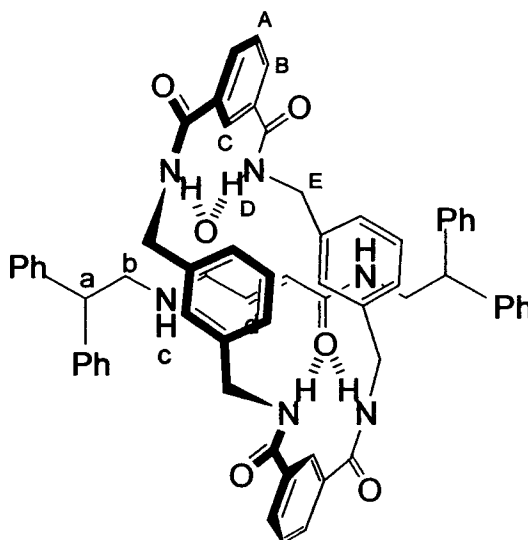
[2](1,7,13,19-Tetraaza-2,6,14,18-tetraoxo-3,5,9,11,15,17,21,23-tetrabenzocyclohexacosane))-(*N,N'–bis*(2,2–diphenyl-ethyl)-(*E*)-butendiamide)-rotaxane, *E*-9

Rotaxane *E*-**9** was obtained using the general procedure for the preparation of benzylic amide macrocycle containing [2]rotaxane from thread *E*-**1** (0.237 g) using as diamine *m*-xylylenediamine (0.681 g) and as acid dichloride isophthaloyl dichloride (1.015 g). The filtrate was then washed with HCl (0.2M, 100 mL) and saturated Na$_2$CO$_3$ solution (100 mL). The organic layer was then dried Mg$_2$SO$_4$ and the solvent removed *in vacuo* to leave a cream solid. The rotaxane was isolated by column chromatography on silica gel (2% MeOH/CH$_2$Cl$_2$) (*E*-**9**, 0.015 g, 3%). m.p. 332.2-334.2°C; ^{1}H NMR (400 MHz, *d$_6$*-DMSO): δ = 8.52 (br s, 2H, ArC*H*$_C$), 8.29 (t, 4H, *J* = 5.0 Hz, N*H*$_D$), 8.03 (d, 4H, ^{3}*J*(H,H) = 8.0 Hz, ArC*H*$_B$), 7.69 (t, 2H, ^{3}*J*(H,H) = 8.0 Hz, ArC*H*$_A$), 7.28 (m, 14H, ArC*H* + CHCH$_2$N*H*), 7.19 (m, 8H, ArC*H*), 6.79 (m, 4H, ArC*H*), 6.68 (m, 4H, ArC*H*), 6.08 (s, 2H, C*H*$_d$), 4.06 (d, 8H, ^{3}*J*(H,H) = 5.5 Hz, C*H*$_E$), 3.75 (t, 4H, ^{3}*J*(H,H) = 7.0 Hz, C*H*$_b$), 3.67 (t, 2H, ^{3}*J*(H,H) = 7.0 Hz, C*H*$_a$); ^{13}C NMR (100 MHz, *d$_6$*-DMSO): δ = 166.1 (*C*O), 166.0 (*C*O), 142.7 (Ar*C* (ipso)), 137.9 (Ar*C* (ipso)), 134.8 (Ar*C* (ipso)), 131.6 (*C*H$_d$), 130.5 (Ar*C*H), 128.6 (Ar*C*H), 128.5 (Ar*C*H), 128.4 (Ar*C*H), 128.2 (Ar*C*H), 127.8 (Ar*C*H), 127.7, (Ar*C*H), 126.9 (Ar*C*H), 126.6 (Ar*C*H), 50.0 (*C*H), 43.5 (*C*H$_2$), 42.5 (*C*H$_2$); MS (FAB): *m/z* = 1007 [M+H]$^+$; Anal. Calcd. for C$_{64}$H$_{58}$O$_6$N$_6$: C 76.32, H 5.80, N 8.34. Found C 76.51, H 5.64, N 8.16.

[2](1,7,14,20-Tetraaza-2,6,15,19-tetraoxo-3,5,9,12,16,18,22,25-tetrabenzocyclohexacosane)-(*N*,*N'*-(dimethyl)-*bis*{2',2'-diphenylethyl}-(*E*)-butendiamide)-rotaxane, *E*-10
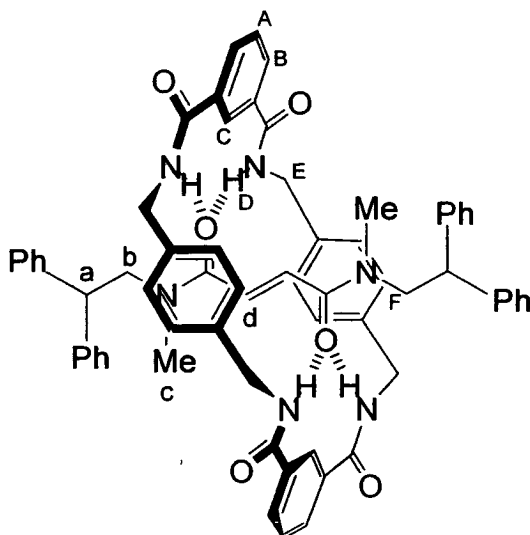
(*E*-10, 0.170 g, 33%). m.p. 320-323°C; ^{1}H NMR (400 MHz, d_6-DMSO at 403K): δ = 8.51 (br s, 2H, ArCH_C), 8.09 (dd, 4H, ^3J(H,H) = 7.8 Hz, ArCH_B), 7.78 (br t, 4H, NH_D), 7.60 (t, 2H, ^3J(H,H) = 7.8 Hz, ArCH_A), 7.35-7.11 (m, 20H, ArCH), 6.96 (s, 8H, ArCH_F), 5.92 (br s, 2H, CH_d), 4.40 (br d, 8H, ^3J(H,H) = 5.4 Hz, CH_E), 4.26 (br t, 2H, CH_a), 3.91 (br d, 4H, CH_b), 2.41 (s, 6H, CH_c); ^{13}C NMR (100 MHz, CDCl$_3$): δ = 166.9-166.0, 142.9, 138.9, 134.9, 129.3-127.6, 125.1, 53.9-53.1, 49.8, 44.6-44.1, 36.3-36.1; FAB-MS (*m*NBA matrix): *m/z* = 1036 [(M+H)$^+$]; Anal. Calcd for C$_{66}$H$_{62}$N$_6$O$_6$: C 76.57, H 6.04, N 8.12. Found: C 76.88, H 6.20, N 8.30; HRMS (FAB) Calcd. for C$_{66}$H$_{63}$N$_6$O$_6$ [M+H]$^+$ 1035.48091. Found 1035.48124.

N,N'–bis (2,2–diphenyl-ethyl)-(*Z*)-butendiamide, *Z*-1
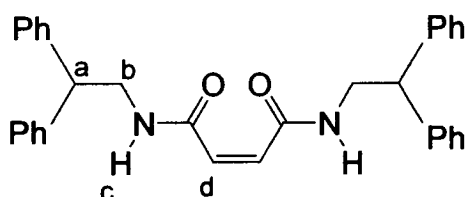
Compound *Z*-1 was obtained using the general method for the photoisomerization of fumaramide [2]rotaxanes from thread *E*-1 (0.047 g). The compound was isolated by column chromatography on silica gel (2% MeOH/CH$_2$Cl$_2$) (*Z*-1, 0.027 g, 56%). m.p. 86-87 °C; ^{1}H NMR (400 MHz, CD$_2$Cl$_2$) δ 8.14 (br s, 2H, N*H*$_c$), 7.41-7.22 (m, 20H, ArC*H*), 5.92 (br s, 2H, C*H*$_d$), 4.21 (t, 2H, ^3J(H$_A$, H$_B$) = 7.7 Hz, ArC*H*$_a$), 3.93 (dd, 4H, ^3J(H$_b$,H$_a$) = 7.7 Hz, ^3J(H$_b$,H$_c$) = 6.0 Hz, ArC*H*$_b$); ^{13}C NMR (100 MHz, CD$_2$Cl$_2$) δ 164.7 (*C*O), 141.8 (Ar*C* (ipso)), 130.6 (*C*H$_d$), 128.9 (Ar*C*H (meta)), 128.5 (Ar*C*H (ortho)), 126.8 (Ar*C*H (para)), 50.2 (*C*H$_a$), 44.2 (*C*H$_b$); HRMS (FAB) Calcd. for C$_{32}$H$_{31}$N$_2$O$_2$ [M+H]$^+$ 475.23855. Found 475.23879.

.

[2](1,7,14,20-Tetraaza-2,6,15,19-tetraoxo-3,5,9,12,16,18,22,25-tetrabenzocyclohexacosane))-(*N,N'–bis*(2,2–diphenyl-ethyl)-(*Z*)-butendiamide)-rotaxane, *Z*-2

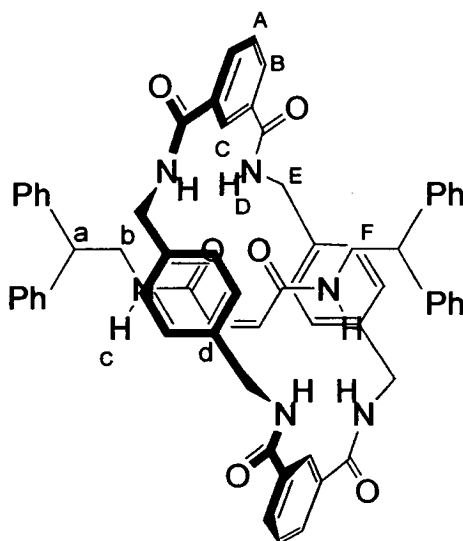Rotaxane Z-**2** was obtained using the general procedure for the photoisomerisation of fumaramide [2]rotaxanes from rotaxane E-**2** (0.100 g) and the crude obtained subjected to column chromatography on silica gel (CH$_2$Cl$_2$/EtOAc) to obtain a colourless solid (Z-**2**, 0.045 g, 45%). m.p. >300 °C (decompose); ^{1}H NMR (400 MHz, CDCl$_3$): δ = 8.22 (d, 4H, ^3J(H,H) = 7.8, ArCH$_B$), 8.13 (s, 2H, ArCH$_C$), 7.73 (t, 4H, ^3J(H,H) = 5.4 Hz, NH$_D$), 7.62 (t, 2H, ^3J(H,H) = 7.8 Hz, ArCH$_A$), 7.27-7.11 (m, 18H, ArCH (ortho and meta thread) and NH$_c$), 6.98 (d, 4H, ^3J(H,H) = 7.5 Hz, ArCH (para thread)), 6.83 (s, 8H, ArCH$_F$), 5.11 (s, 2H, CH$_d$), 4.38 (d, 8H, ^3J(H,H) = 5.4 Hz, CH$_E$), 3.87 (t, 2H, ^3J(H,H) = 7.8 Hz, CH$_a$) and 3.41 (dd, 4H, ^3J(H,H) = 7.8 Hz, ^3J(H,H) = 5.7 Hz, CH$_b$); ^{13}C NMR (100 MHz, CDCl$_3$): δ = 166.8 (CO macrocycle), 165.5 (CO thread), 141.8 (ArC ipso thread), 137.4 (ArC ipso), 134.3 (ArC-CO ipso), 131.9 (CH$_B$), 131.2 (CH$_d$), 129.9 (CH$_A$), 129.3 (ArCH$_F$), 129.2 (ArCH (meta thread)), 128.5 (ArCH (ortho thread)), 127.5 (ArCH (para thread)), 124.8 (CH$_C$), 50.32 (CH$_a$), 44.9 (CH$_b$) and 44.8 (CH$_E$); MS (FAB, mNBA): m/z=1029 [(M+Na)$^+$]. Anal. Calcd. for C$_{64}$H$_{58}$N$_6$O$_6$: C 76.32, H 5.80, N 8.34. Found: C 76.39, H 5.91, N 8.19.

[2](1,9,16,22-Tetraaza-2,8,17,21-tetraoxo-5-nitro-3,7,11,14,18,20,24,27-tetrabenzocyclohexacosane))-(N,N'-bis(2,2–diphenyl-ethyl)-(Z)-butendiamide)-rotaxane, Z-4
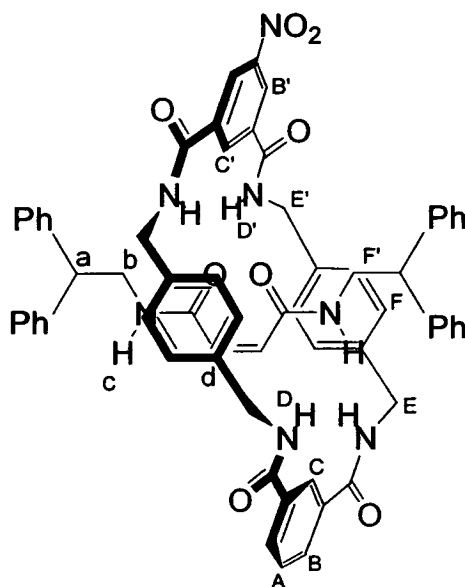
Rotaxane _Z_-**4** was obtained using the general procedure for the photoisomerisation of fumaramide [2]rotaxanes from rotaxane _E_-**4** (0.105 g) and the crude obtained subjected to column chromatography on silica gel (CH$_2$Cl$_2$/EtOAc) to obtain a colourless solid (_Z_-**4**, 0.057 g, 54%). m.p. 281 °C; ^{1}H NMR (400 MHz, CD$_2$Cl$_2$) δ 8.91 (d, 2H, ^4J(H$_{B'}$,H$_{C'}$) = 1.3 Hz, ArC_H_$_{B'}$), 8.62 (t, 1H, ^4J(H$_{C'}$, H$_{B'}$) = 1.3 Hz, ArC_H_$_{C'}$), 8.03 (dd, 2H, ^4J(H$_B$,H$_C$) = 1.8 Hz, ^3J(H$_B$,H$_A$) = 7.8 Hz, ArC_H_$_B$), 7.90 (t, 2H, ^3J(H$_{D'}$,H$_{E'}$) = 4.8 Hz, N_H_$_{D'}$), 7.91 (d, 1H, ^4J(H$_C$,H$_B$) = 1.8 Hz, ArC_H_$_C$), 7.59 (t, 1H, ^3J(H$_A$,H$_B$) = 7.8 Hz, ArC_H_$_A$), 7.20-7.06 (m, 13H, ArC_H_ (ortho and para thread) and ArC_H_$_C$), 7.00-6.91 (m, 16H, ArC_H_ (meta thread), ArC_H_$_F$ and ArC_H_$_{F'}$), 6.82 (t, 2H, ^3J(H$_D$,H$_E$) = 5.5 Hz, N_H_$_D$), 5.10 (s, 2H, C_H_$_d$), 4.49 (d, 4H, ^3J(H$_{E'}$,H$_{D'}$) = 5.0 Hz, C_H_$_{E'}$), 4.40 49 (d, 4H, ^3J(H$_E$,H$_D$) = 5.5 Hz, C_H_$_E$), 3.77 (t, 2H, ^3J(H$_a$,H$_b$) = 7.9 Hz, C_H_$_a$), 3.36 (dd, 4H, ^3J(H$_b$,H$_a$) = 7.9 Hz, ^3J(H$_b$,H$_c$) = 5.8 Hz, C_H_$_b$); ^{13}C NMR (100 MHz, CD$_2$Cl$_2$) δ 167.0 (_C_O-NH$_D$ macrocycle), 166.0 (_C_O thread), 164.7 (_C_O-NH$_{D'}$ macrocycle), 142.5 (Ar_C_ (ipso)), 138.2 (Ar_C_-CH$_{E'}$), 137.7 (Ar_C_-CH$_E$), 136.9 (Ar_C_-CO-NH$_{D'}$), 135.0 (Ar_C_-CO-NH$_D$), 131.4, 130.3, 130.2, 130.1, 129.6, 129.5, 128.3, 127.7, 126.9, 50.9 (_C_H$_a$), 45.3 (_C_H$_{E'}$), 45.2 (_C_H$_E$), 44.8 (_C_H$_b$); HRMS (FAB) Calcd. for C$_{64}$H$_{58}$N$_7$O$_8$ [M+H]$^+$ 1052.43469. Found 1052.43528.

[2] (1,4,7,14,17,20-Hexaaza-2,6,15,19-tetraoxo-3,5,9,12,16,18,22,25-tetrabenzocyclohexacosane)-(*N,N'*–*bis* (2,2–diphenyl-ethyl)-(*Z*)-butendiamide)-rotaxane, *Z*-6
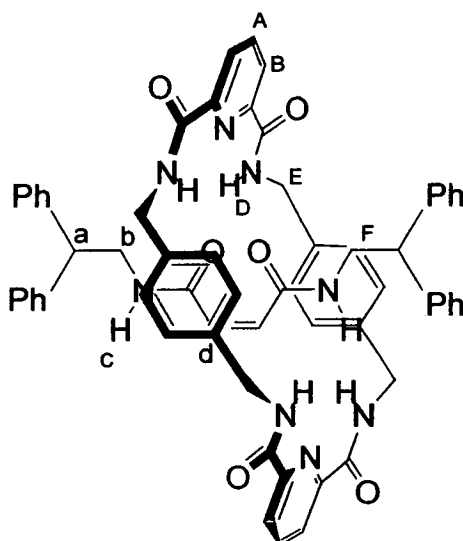

Rotaxane *Z*-6 was obtained using the general procedure for the photoisomerisation of fumaramide [2]rotaxanes from rotaxane *E*-6 (0.101 g) and the crude obtained subjected to column chromatography on silica gel (CH$_2$Cl$_2$/EtOAc) to obtain a colourless solid (*Z*-6, 0.051 g, 51%); ^{1}H NMR (400 MHz, CDCl$_3$) δ 9.18 (t, 4H, ^3J(H,H) = 5.8 Hz, N*H*$_D$), 8.89 (br s, 2H, N*H*$_c$), 8.50 (t, 4H, ^3J(H,H) = 7.9 Hz, ArC*H*$_B$), 8.14 (t, 2H, ^3J(H,H) = 7.9 Hz, ArC*H*$_A$), 7.14-7.09 (m, 12H, ArC*H*), 6.96-6.91 (m, 8H, ArC*H*), 6.70 (s, 8H, ArC*H*$_F$), 5.49 (s, 2H, C*H*$_d$), 4.50 (br d, 8H, ^3J(H,H) = 5.8 Hz, C*H*$_E$), 3.87 (t, 2H, ^3J(H,H) = 7.3 Hz, C*H*$_b$); ^{13}C NMR (100 MHz, CDCl$_3$) δ 165.4 (*C*O), 163.7 (*C*O), 149.6 (Ar*C* (ipso)), 141.5 (Ar*C* (ipso)), 138.9 (*C*H$_d$), 136.8 (Ar*C* (ipso)), 129.1, 128.9, 127.2, 127.1, 125.8, 50.2 (*C*H$_a$), 45.3, 43.5; HRMS (FAB) Calcd. C$_{62}$H$_{57}$N$_8$O$_6$ [M+H]$^+$ 1009.44011. Found 1009.44018.

[2](1,7,14,20-Tetraaza-2,6,15,19-tetraoxo-3,5,9,12,16,18,22,25-tetrabenzocyclohexacosane)-(*N*,*N*'-(dimethyl)-*bis*{2',2'-diphenylethyl}-(*Z*)-butendiamide)-rotaxane, *Z*-10
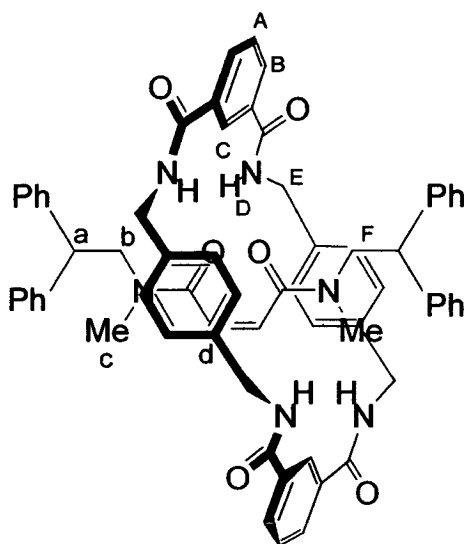
Rotaxane *Z*-10 was obtained using the general procedure for the photoisomerisation of fumaramide [2]rotaxanes from rotaxane *E*-10 (0.103 g) and the crude obtained subjected to column chromatography on silica gel (CH$_2$Cl$_2$/EtOAc) to obtain a colourless solid (*Z*-10, 0.049 g, 47%). m.p. > 300 °C (decompose); ^{1}H NMR (400 MHz, C$_2$D$_2$Cl$_4$ at 403K): δ = 8.13 (dd, 4H, ^3J(H,H) = 7.8 Hz, ArC*H*$_B$), 7.91 (br s, 2H, ArC*H*$_C$), 7.63 (t, 2H, ^3J(H,H) = 7.8 Hz, ArC*H*$_A$), 7.35-7.11 (m, 24H, ArC*H* + N*H*$_D$), 6.98 (s, 8H, ArC*H*$_F$), 4.92 (br s, 2H, C*H*$_d$), 4.40 (br d, 8H, ^3J(H,H) = 5.4 Hz, C*H*$_E$), 4.07 (b t, 2H, C*H*$_a$), 3.51 (br d, 4H, C*H*$_b$), 2.21 (s, 6H, C*H*$_c$); ^{13}C NMR (100 MHz, CDCl$_3$): δ = 166.9-166.0, 142.9, 138.2, 134.9, 129.3-127.6, 125.1, 53.9-53.1, 49.8, 44.6-44.1, 36.3-36.1; FAB-MS (*m*NBA matrix): *m/z*=1036 [(M+H)$^+$]; Anal. Calcd. for C$_{66}$H$_{62}$N$_6$O$_6$: C 76.57, H 6.04, N 8.12. Found: C 76.98, H 6.30, N 8.23.

2.5 References

1. J.-M. Lehn, *Supramolecular Chemistry: Concepts and Perspectives*, Wiley-VCH, Weinheim, **1995**.

2. For reviews on rotaxanes see: a) D. B. Amabilino, J. F. Stoddart, *Chem. Rev.* **1995**, *95*, 2725-2828. b) J.-P. Sauvage, C. O. Dietrich-Buchecker, *Molecular Catenanes, Rotaxanes and Knots*, Ed. Wiley-VCH, Weinheim, **1999**.

3. a) F. Vögtle, T. Dunnwald, T. Schmidt, *Acc. Chem. Res.* **1996**, *29*, 451-460. b) P. R. Ashton, P. T. Glink, J. F. Stoddart, P. A. Tasker, J. P. White, D. J. Williams, *Chem. Eur. J.* **1996**, *118*, 11333-11334. c) A. G. Johnston, D. A. Leigh, A. Murphy, J. P. Smart, M. D. Deegan, *J. Am. Chem. Soc.* **1996**, *118*, 10662-10663. d) D. A. Leigh, A. Murphy, J. P. Smart, A. M. Z. Slawin, *Angew. Chem. Int. Ed. Engl.* **1997**, *36*, 728-732.

4. F. G. Gatti, D. A. Leigh, S. A. Nepogodiev, A. M. Z. Slawin, S. J. Teat, J. K. Y. Wong, *J. Am. Chem. Soc.* **2001**, *123*, 5983-5989.

5. K. Kavallieratos, S. R. de Gala, D. J. Austin, R. H. Crabtree, *J. Am. Chem. Soc.* **1997**, *119*, 2325-2326.

6. G. Brancato, F. Coutrot, D. A. Leigh, A. Murphy, J. K. Y. Wong, F. Zerbetto, *Proc. Natl. Acad. Sci. USA* **2002**, *99*, 4967-4971.

7   F. G. Gatti, S. León, J. K. Y. Wong, G. Bottari, A. Altieri, M. A. Farran Morales, S. J. Teat, C. Frochot, D. A. Leigh, A. M. Brouwer, F. Zerbetto, *Proc. Natl. Acad. Sci. USA* **2003**, *100*, 10-14.

Control of the Rotational Motion in Hydrogen Bonded [2]Rotaxanes

In chapter two the remarkable templating ability of fumaramide-based threads in the formation of structurally-diverse benzylic amide macrocycle-containing [2]rotaxanes has been demonstrated. Photochemical isomerisation of the E-rotaxanes afforded the corresponding Z-isomers. In the following chapters we will focus our attention on possibility to control some of the dynamic processes present in rotaxane architectures.

In this chapter control over the rate of pirouetting of the macrocycle around the thread in tetra-amide benzylic macrocycle-containing [2]rotaxanes is achieved through E/Z isomerisation. The isomerisation process is reversible and driven by photonic and thermal stimuli, bringing about changes in the rate of the pirouetting of more than six orders of magnitude.

A series of fumaramide-based rotaxanes were synthesised and converted in their respective, thermodynamically unfavoured, Z isomers by using light (Scheme 1).

E-1	R^1= R^2= CH$_2$CO$_2$CH$_2$Ph	Z-1
E-2	R^1= Me, R^2= CH$_2$CHPh$_2$	Z-2
E-3	R^1= H, R^2= CH$_2$CHPh$_2$	Z-3

hυ 254 nm
Δ

E-4	R^1= R^2= CH$_2$CO$_2$CH$_2$Ph	Z-4
E-5	R^1= Me, R^2= CH$_2$CHPh$_2$	Z-5
E-6	R^1= H, R^2= CH$_2$CHPh$_2$	Z-6
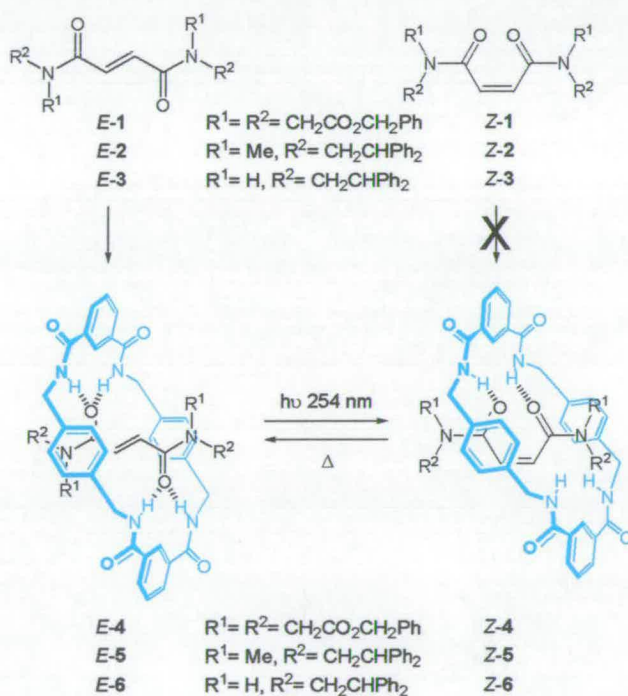
Scheme 1 *The [2]rotaxanes E-4-6 were synthesised from the corresponding threads (E-1-3) and converted in their respective Z-isomers (Z-4-5) by using a photonic stimulus. The isomerisation process can be reversed by applying a thermal stimulus affording the original E-rotaxanes.*

The change in geometry accompanied with the isomerisation process alters the strength of the intercomponent hydrogen bond interactions between the macrocycle and the thread and consequentially the rotational dynamic of the macrocyclic unit. A thermal stimulus is then used to reverse the photoisomerisation process to give back the thermodynamically more stable E isomers.

Variable temperature ^1H NMR spectroscopy experiments were used to determine the energies barrier for the pirouetting process of the macrocycle for E-4 and Z-4 giving spinning rates of ~1 s^{-1} and ~1.2 x 10^6 s^{-1} respectively. Energies barrier for the circumrotation of the macrocycle for E-4 and Z-4 were also calculated by computational simulations using MM3 forcefield and the TINKER program giving results in excellent agreements with the experimental values.

3.1 Introduction

Large amplitude internal rotations which resemble to some extent processes found in authentic machinery have recently inspired analogic molecular versions of gears[1], turnstiles[2], brakes[3], ratchets[4,5], rotors[6] and unidirectional spinning motors[7-10], and are an inherent characteristic of many catenanes and rotaxanes[11-13]. Establishing methods for controlling aspects of such movements is a prerequisite for the development of artificial devices that function through rotary motion at the molecular level.[†]   In this regard, we recently reported the unexpected discovery that the rate of rotation of the interlocked components of benzylic amide macrocycle-containing nitrone and fumaramide [2]rotaxanes can be slowed ("dampened") by 2-3 orders of magnitude by applying a modest ($\sim 1 Vcm^{-1}$) external oscillating electric field[14]. Here we demonstrate that the rate of rotation of the interlocked components of the olefin-based rotaxanes can also be accelerated - by more than *six* orders of magnitude – using another broadly useful stimulus, light.

[†] Speculation over the possible utility of submolecular rotation in synthetic molecular structures ranges from 'gearing' systems, where controlled motion in one part of a molecule brings about changes in conformation in another (*e.g.* to generate catalysts with rotating binding sites, *cf.* F_1-ATPase *etc*), to systems which rotate functional groups on surfaces, or in the bulk, to bring about changes in local or macroscopic characteristics(11,23). Indeed, for wonderful examples of the use of submolecular rotational motion to bring about property changes in materials see (24) and (25).   Examples of specifically controlling the frequency of large amplitude internal rotary motions include the redox-mediated acceleration/deceleration of the spinning of porphyrin ligands in cerium and zirconium sandwich complexes(26), the environment-dependant rate of circumrotation in hydrogen bonded [2]catenanes(27), and the electrochemically-induced pirouetting of a macrocycle in a rotaxane(28).

3.2 Results and Discussion

Fumaramide threads template the assembly of benzylic amide macrocycles around them to form rotaxanes in high yields[15]. This cheap and simple preparative procedure (suitable threads are prepared in a single step from fumaryl chloride and a bulky primary or secondary amine) is particularly efficient because the *trans*-olefin fixes the two hydrogen bond-accepting groups of the thread in an arrangement which is complementary to the geometry of the hydrogen bond-donating sites of the forming macrocycle. However, the feature of the fumaramide unit that makes it such an effective template also provides an opportunity to enforce a geometrical change in the thread *after* rotaxane formation, thus altering the nature and strength of the interactions between the interlocked components. Isomerization of the olefin from *E*- to *Z*- must necessarily disrupt the near-ideal hydrogen bonding motif between macrocycle and thread and therefore also change any internal dynamics governed by those interactions.

To test this idea, the photochemical isomerization of three fumaramide-based threads (*E*-1-3) and rotaxanes (*E*-4-6) was investigated. The synthesis of rotaxanes *E*-4 and *E*-6 has previously been described[15] and *E*-5 was prepared in analogous fashion from the corresponding thread, *E*-2, isophthaloyl dichloride and *p*-xylylene diamine (Scheme 3.1).[‡] Under the same reaction conditions the *cis*-olefin (maleamide) threads, *Z*-1-3, did not give detectable quantities of the corresponding *Z*-rotaxanes.

E-1	R^1= R^2= CH$_2$CO$_2$CH$_2$Ph	*Z*-1
E-2	R^1= Me, R^2= CH$_2$CHPh$_2$	*Z*-2
E-3	R^1= H, R^2= CH$_2$CHPh$_2$	*Z*-3

hυ 254 nm

Δ

E-4	R^1= R^2= CH$_2$CO$_2$CH$_2$Ph	*Z*-4
E-5	R^1= Me, R^2= CH$_2$CHPh$_2$	*Z*-5
E-6	R^1= H, R^2= CH$_2$CHPh$_2$	*Z*-6
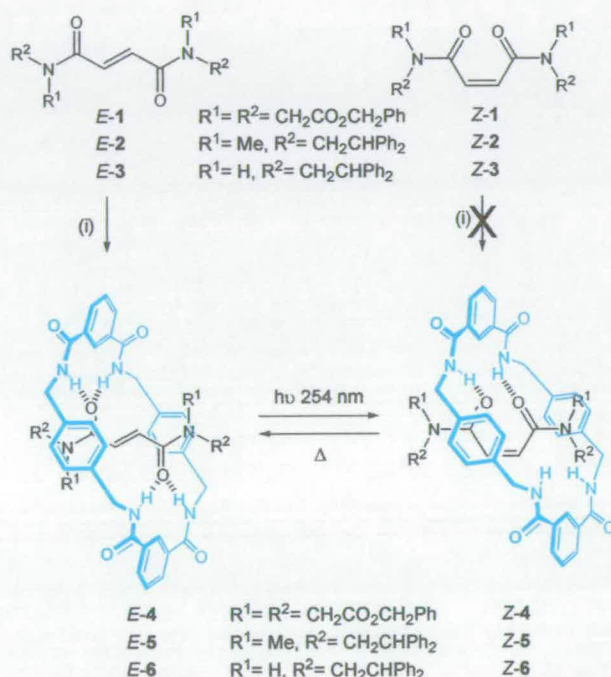
Scheme 3.1. Synthesis of [2]rotaxanes *E*/*Z*-4-6. (i) 4 equivs. isophthaloyl dichloride, 4 equivs. *p*-xylylene diamine, Et$_3$N, 4 h, high dilution; CHCl$_3$ for *E*-4 (67%) and *E*-5 (33%), 1/9 MeCN/CHCl$_3$ for *E*-6 (97%). Direct irradiation (254 nm, 30 min.) of a solution of an *E*-rotaxane (0.1 M, RT, CH$_2$Cl$_2$ [1:9 MeOH/CHCl$_3$ for *E*-6]) yields the "accelerated" *Z*-isomer (45-50% single experiment; >90% from 4 successive cycles). Heating a 0.02 M solution of a *Z*-rotaxane at 400K reforms the "dampened" *E*-isomer (*E*-6: C$_2$D$_2$Cl$_4$, 7 days, 84% or d_6-DMSO, 4 days, 100%).

[‡] The modest yield (33%) of *E*-5 is probably a consequence of the {*E*,*E*}- and/or {*E*,*Z*}- tertiary amide rotamers being sterically mismatched with the forming macrocycle. Interestingly, a small amount (2%) of rotaxane *E*-6, presumably arising from *p*-xylylene diamine-catalyzed isomerization of the thread, was isolated from the reaction of pristine *Z*-3, again exemplifying the extraordinary efficiency of the *E*-3 template for rotaxane formation.

Single crystals suitable for investigation by *X*-ray crystallography were obtained for each of the three *E*-rotaxanes. In each case the solid-state structure shows two sets of bifurcated hydrogen bonds between the amide groups of the macrocycle and the carbonyl groups of the fumaramide system[15]. The crystal structure of *E*-5 is typical (Fig. 3.1), and shows the macrocycle in a chair conformation forming short, close-to-linear, hydrogen bonds orthogonal to the lone pairs of the fumaramide carbonyl groups. Of the three different tertiary amide rotamers present in solution (as observed by NMR) only the {*ZZ*}amide rotamer of *E*-5 is found in the crystal.
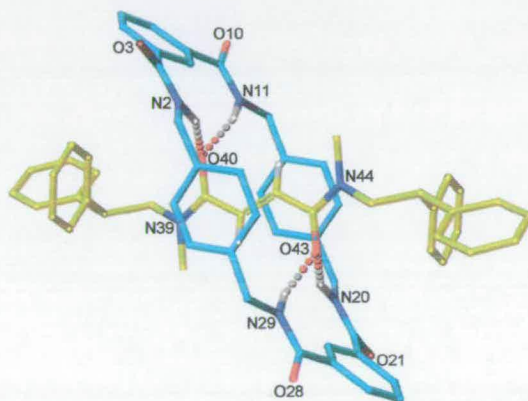
Figure 3.1. *X*-Ray crystal structure of [2]rotaxane *E*-5 (for clarity carbon atoms of the macrocycle are shown in blue and the carbon atoms of the thread in yellow; oxygen atoms are depicted in red, nitrogen atoms dark blue and selected hydrogen atoms white). Intramolecular hydrogen bond distances (Å): O40–HN2/O43–HN20 = 2.22, O40–HN11/O43–HN29 = 1.94.

All three fumaramide threads *E*-1-3 and rotaxanes *E*-4-6 smoothly undergo photoisomerization[16,17] (254 nm; 0.1 M solution in CH_2Cl_2 or, for solubility reasons in the case of *E*-6, 1:9 $MeOH/CHCl_3$; 30 min.) to the corresponding maleamide (*Z*-olefin) systems. The yields for the rotaxanes, 45-50%, are remarkably good considering the confined cavity that the molecular rearrangement has to occur in and that the intercomponent hydrogen bonding between the thread and macrocycle is complementary to the positions of the amide groups only in the *E*-olefin. Unanticipated enhanced solubility of the *Z*-rotaxanes in nonpolar solvents allowed the separation of the *E/Z*

photochemical reaction mixtures into the individual isomers by simple trituration (PhMe/CH$_2$Cl$_2$, 1:1). The photoisomerization reaction produces few byproducts so E-rotaxanes recovered in this way could be recycled leading to >90% overall conversion to the Z-isomer from a series of irradiation experiments.

The ^{1}H NMR spectra of each pair of E- and Z-olefin rotaxanes gives insight regarding their structure and relative dynamic properties in nonpolar solvents. The trends are similar in all cases but the clearest information is provided by E/Z-**4**.*
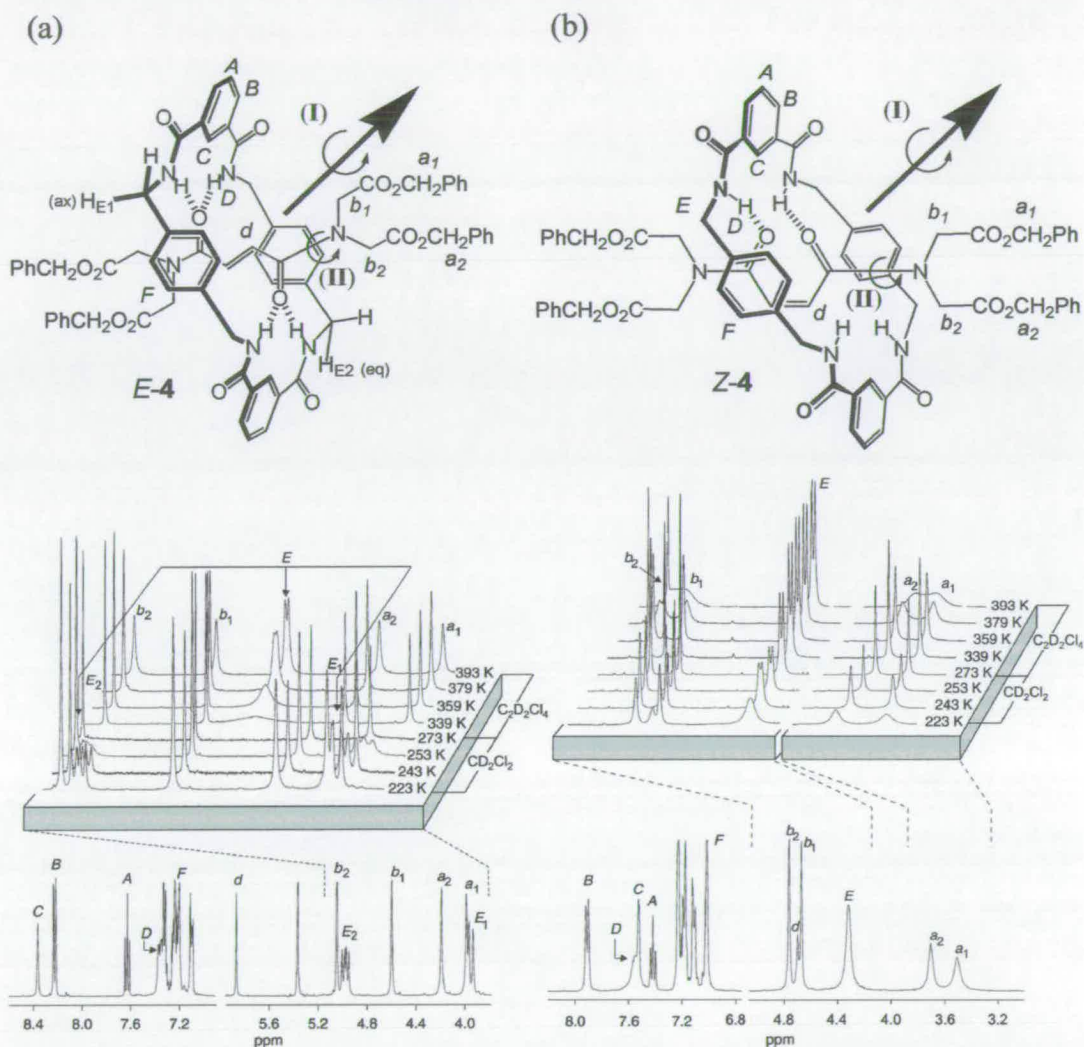
The variable temperature ^{1}H NMR spectra of E-**4** and Z-**4** in CD$_2$Cl$_2$ (223-273K) and C$_2$D$_2$Cl$_4$ (339-393K) are shown in Fig. 3.2 (the wide temperature range involved meant different non-hydrogen bond-disrupting solvents were required to monitor the dynamic processes at high and low temperatures). Pirouetting, a 180° rotation of the macrocycle about the axis of the arrow plus formal chair-chair flip of the macrocycle, is the simplest process that must occur in order to translate the equatorial macrocycle methylene protons, H_{E2}, onto the axial, H_{E1}, sites. In the fumaramide system the H_E protons coalesce at 273K and are fully resolved into the H_{E1} and H_{E2} resonances at 223K (Fig. 3.2a). The coupling constants confirm the axial and equatorial assignments of H_{E1} and H_{E2}. Spin polarization transfer by selective inversion recovery (SPT-SIR) experiments provided a direct measure of the rate of the exchange process I (*i.e.* half circumrotation of the macrocycle) at 298K corresponding to an energy barrier $\Delta G^{\ddagger}$= 13.4±0.1 kcal mol^{-1} which extrapolates to a rate of macrocycle rotation of ~1 s^{-1} at 223K[15].

In contrast, the macrocycle methylene protons (H_E) in Z-**4** remain sharp and well resolved throughout this temperature range and only begin to broaden significantly at

---

* The spectra of Z-**6** are complicated because intracomponent hydrogen bonding of the maleamide group desymmetrizes the rotaxane (the macrocycle methylene groups appear as an ABX system because the two faces of the macrocycle experience different environments). Similarly, the temperature-dependent equilibrium between the populations of the different amide rotamers present in the methylated rotaxanes E/Z-**5** makes their study nontrivial, whereas the symmetrical tertiary amides means E/Z-**4** suffers no such complication. For a discussion of the effect of the different strengths of intercomponent hydrogen bonding in E-**4** and Z-**4** on the dynamics of amide rotamerization see the Experimental Section.

223K (Fig. 3.2b); remarkably, the broadening of H_E in Z-**4** at 223K is comparable to that in E-**4** at 359K – a 136° temperature difference between the two rotaxane isomers!

(a)   (b)

Figure 3.2. Variable temperature ^{1}H NMR spectra (400 MHz) of (a) E-**4** and (b) Z-**4** in CD_2Cl_2 at 223K (main traces) and 223-273K (stackplot expansions) and $C_2D_2Cl_4$ 339-393K (stackplot expansions). Lettering corresponds to selected non-equivalent proton environments. A 180° rotation of the macrocycle about the axis of the arrow, plus chair-chair flipping of the macrocycle, translates the H_{E_2} (equatorial) protons onto the H_{E_1} (axial) sites. The NMR spectra in (a) reveal slow pirouetting of the macrocycle about the thread in E-**4**, (H_{E_1} and H_{E_2} coalesce at 273K, $\Delta G^{\ddagger}=13.4\pm0.1$ kcal mol^{-1}; process I) and slow rotation of the thread tertiary amide bonds (H_{a_1} and H_{a_2}/H_{b_1} and H_{b_2} fully resolved even at 393K, $\Delta G^{\ddagger}=21.1\pm0.1$ kcal mol^{-1}; process II). The NMR spectra in (b) show that process I is much lower in energy for Z-**4** ($\Delta G^{\ddagger}=6.8\pm0.8$ kcal mol^{-1}) than E-**4** and that process II is also more facile (H_{a_1} and H_{a_2}/H_{b_1} and H_{b_2} broadening at higher temperatures, $\Delta G^{\ddagger}=20.0\pm0.1$ kcal mol^{-1})(30).

Exchange is so fast in Z-**4** that it is not possible to resolve the signals and prove unequivocally by experiment that the process responsible for the broadening at this temperature is, in fact, macrocycle pirouetting (it could be occurring at even lower temperatures). However, making the assumption (*vide infra*) that this is the process responsible for broadening, line shape analysis gives an energy barrier of 6.8 ±0.8 kcal mol^{-1}, *i.e.* a macrocycle spinning rate $> 1.2 \times 10^6$ s^{-1} at 223K.

Remarkably, it was possible to obtain an *X*-ray crystal structure of one of the rotaxanes with a 'switched off' recognition motif. Small crystals of Z-**5** suitable for investigation using a synchrotron source were grown from slow evaporation of a saturated solution in CHCl$_3$/MeOH. In contrast to the crystal structure of *E*-**5**, two of the three tertiary amide rotamers, *i.e.* {*ZE*} and {*EE*} rotamers are present in the unit cell of Z-**5** (Fig. 3.3a and 3.3b, respectively).
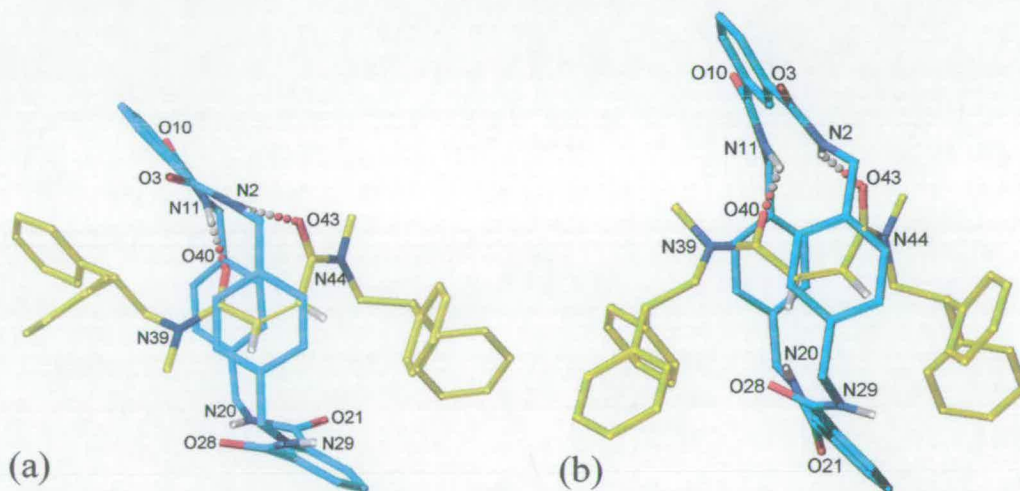
Figure 3.3. *X*-ray crystal structures of (a) {*ZE*} and (b) {*EE*} rotamers of *N,N'*-dimethylmaleamide [2]rotaxane Z-**5**. Intramolecular hydrogen bond distances (Å): (a) O40-HN11 = 2.08, O43-HN2 = 2.05; (b) O40-HN11 = 1.76, O43-HN2 = 2.08.

Both forms are consistent with the dramatic increase in the rate of rotation in solution for the *cis*-rotaxanes observed experimentally by ^{1}H NMR spectroscopy; the consequence of isomerizing the double bond is that the amide groups of the thread are held in positions such that they can hydrogen bond to only one of the two isophthalamide groups of the

macrocycle. It is interesting to note that the energy barrier for the *trans*-rotaxane with four intercomponent hydrogen bonds (13.4 kcal mol^{-1}) is almost exactly twice the value for the *cis*-rotaxane with two intercomponent hydrogen bonds (~6.8 kcal mol^{-1}).

In order to obtain a more detailed understanding of the dynamic properties of these systems and, in particular, to confirm that the low energy dynamic process measured by NMR in the maleamide rotaxane was circumrotation, we carried out simulations of the dynamic processes present in both *E*- and *Z*-**4**.

Using a computational procedure which employs the MM3 forcefield[18] and the TINKER program[19], and has previously proved successful in describing the circumrotation pathway in catenanes[20], macrocycle pirouetting in rotaxanes[13] and other properties in mechanically-interlocked molecules[21,22], it was possible to locate the saddle points for macrocycle circumrotation in *E*-**4** and *Z*-**4**. Fig. 3.4 shows the transition states, the arrows indicating the initial motion that the macrocycle would undergo away from the saddle point (arrows showing the movement of the thread are not shown for clarity).
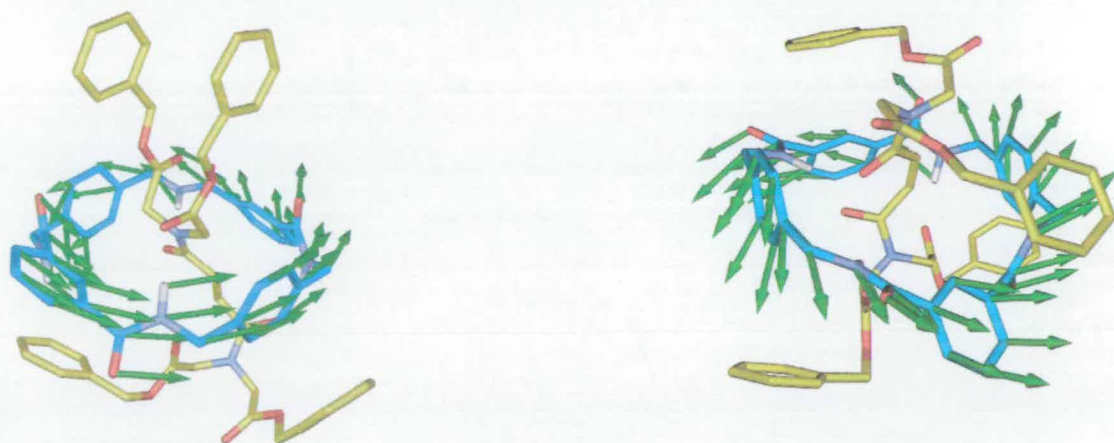
Figure 3.4. Calculated transition-state structures for the macrocycle ring motions for rotaxanes (a) *Z*-**4** and (b) *E*-**4**. Green arrows represent the corresponding atomic motion vectors connecting the transition states to their minima.

The calculated activation energies (13.51 kcal mol^{-1} for *E*-**4** and 6.53 kcal mol^{-1} for *Z*-**4**) compare well with the NMR determined ΔG's of 13.4±0.1 and 6.8±0.8 kcal mol^{-1},

respectively, and thus confirm that macrocycle pirouetting is probably a major contributor to the broadening of resonances observed in the low temperature NMR spectra of Z-4. The good agreement of calculations and experiments also allows one to take a closer look at the contributions of various kinds of interactions to the dynamic process of pirouetting. Table 3.1 shows the different energy contributions to the E-4 and Z-4 minima and transition states. Interestingly, from the calculations the ~7 kcal mol^{-1} difference between the activation barriers of circumrotation in the two molecules can be ascribed to contributions from *all* the energy components, not just H-bonding.

	E_v	$E_{H-bonding}$	$E_{\pi-stacking}$	E_{vdW}
E-4^a	29.18	-20.14	-15.36	-24.91
E-4^b	33.09	-13.75	-12.65	-24.40
	(3.91)	(6.39)	(2.71)	(0.51)
Z-4^a	38.11	-16.84	-14.89	-30.97
Z-4^b	44.66	-15.99	-16.73	-29.99
	(6.55)	(0.85)	(-1.84)	(0.98)

(a) energy minimum   (b) transition state energy

Table 3.1. Molecular energy contributions (kcal mol^{-1}) divided into four components: (i) a valence term, E_v, which includes stretchings and in-plane and out-of-plane bendings, (ii) a hydrogen bond contribution, $E_{H-bonding}$, (iii) π-π stacking energy, $E_{\pi-stacking}$, and (iv) the remaining van der Waals components, E_{vdW}. The energy differences between the minima and the transition states are given in parentheses.

Preliminary studies show that it is possible to reverse the photo-isomerization process thermally. Heating each of Z-4-6 ($C_2D_2Cl_4$ or d_6-DMSO, 400K, 4-7 days) resulted in re-conversion to the more thermodynamically stable E-rotaxanes in good-to-excellent (80-100%) yields. Other simple *cis-trans* olefin interconversion reactions are currently being investigated.[*]

---

[*] Attempts to grow crystals of Z-6 resulted in significant yields of crystalline E-6 although no E-6 could be detected at any stage in solution! It appears that the growing crystal surface of E-6 is able to catalyse the *cis-trans* isomerization process. Such a phenomenon is not unprecedented (29).

3.3 Conclusions

The post-assembly photoconversion of a precise hydrogen bonding, rotaxane-forming, template to a motif that does not template the formation of mechanical bonds is unprecedented. The resulting mis-match in recognition sites between macrocycle and thread dramatically reduces the energy barrier to macrocycle pirouetting in the rotaxane. Such control could be useful for the future construction of synthetic molecular machines that utilize large amplitude internal rotary motions.

3.4 Experimental Section

Preparation of thread *(E)-N,N'*- dimethyl-*bis*(2,2-diphenylethyl)-butendiamide (*E*-2).
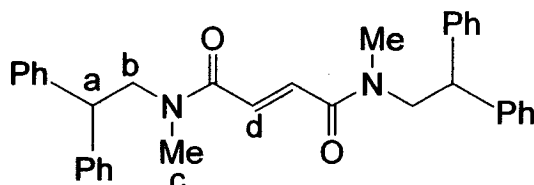
To a stirred ice-cooled solution of *bis*-(2,2-diphenylethyl) fumaramide (1g, 2.10 mmol) in dry THF (20 mL) under nitrogen was added NaH (0.2 g, 60% dispersion in oil, excess) portion-wise under nitrogen. After the effervescence had subsided, methyl iodide (0.3 mL, excess) was added in one portion. The reaction was allowed to warm to room temperature and stirred overnight and water (20 mL) and ammonia solution (10 mL) added drop-wise to quench the reaction. Most of the solvent was removed under reduced pressure, and the remainder partitioned between water and CH_2Cl_2 (3 x 20 mL). The organic extracts were washed with sodium hydroxide (1N, 20 mL) and dried over anhydrous magnesium sulfate. The filtered solution was concentrated under reduced pressure to give an oil that slowly solidified. Recrystallization from CH_2Cl_2/diisopropyl ether afforded colorless needles (*E*-2, 0.87g, 83%); m.p. 134-136°C; ^1H NMR (400 MHz, $C_2D_2Cl_4$ at 363K): δ = 7.34-7.19 (m, 20H, ArCH), 6.99 (s, 2H, CH_d), 4.37 (t, ^3J(H,H) = 8.8 Hz, 2H, CH_a), 4.04 (d, ^3J(H,H) = 8.8 Hz, 4H, CH_b), 2.79 (s, 6H, CH_c); ^{13}C NMR (100 MHz, $C_2D_2Cl_4$ at 393K): δ = 166.7, 143.0, 132.1, 129.7, 128.9, 127.2, 55.5, 51.0, 37.5; MS (FAB, mNBA): *m/z* = 502 [(M+H)$^+$]; Anal. Calcd. for $C_{34}H_{34}N_2O_2$: C 81.24, H 6.82, N 5.57. Found: C 81.61, H 6.68, N 5.43.

3.4.1 General Method for the Preparation of Benzylic Amide Macrocycle Fumaramide [2]Rotaxanes.

The threads *E*-1-3 (1.00 mmol) and Et_3N (2.1 mL, 15.7 mmol) were dissolved in $CHCl_3$ (100 mL) or, in the case of *E*-3, 1/9 $CH_3CN/CHCl_3$, and stirred vigorously whilst

solutions of the diamine (1.09 g, 4 equivs.) in CHCl₃ (45 mL) and the acid chloride (1.62 g, 4 equivs.) in CHCl₃ (45 mL) were simultaneously added over a period of 2 hours using motor-driven syringe pumps. After a further two hours the resulting suspension was filtered and concentrated under reduced pressure. The rotaxanes _E_-**4** and _E_-**5** were purified by trituration of the respective solids in CH₂Cl₂ (to remove the polar impurities - catenane, macrocycles, Et₃HN⁺Cl⁻ etc), and subsequently separating the rotaxane from unreacted thread through trituration in hot toluene. Rotaxane _E_-**6** was obtained by spontaneous crystallization from the reaction mixture as previously described.[15]

Selected data for ([2](1,7,14,20-tetraaza-2,6,15,19-tetraoxo-3,5,9,12,16,18,22,25-tetrabenzocyclohexacosane)-((_E_)-_N_,_N'_-(dimethyl)-_bis_{2',2'-diphenylethyl}-butendiamide)-rotaxane (_E_-5):
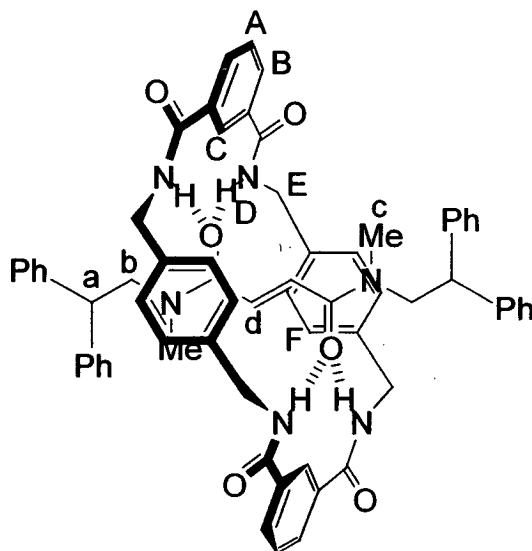
(_E_-**5**, 0.34 g, 33%); m.p. 320-323°C; ¹H NMR (400 MHz, d_6-DMSO at 403K): δ = 8.51 (br s, 2H, ArCH_C), 8.09 (dd, ^3J(H,H) = 7.8 Hz, 4H, ArCH_B), 7.78 (br t, 4H, NH_D), 7.60 (t, ^3J(H,H) = 7.8 Hz, 2H, ArCH_A), 7.35-7.11 (m, 20H, ArCH), 6.96 (s, 8H, ArCH_F), 5.92 (br s, 2H, CH_d), 4.40 (br d, ^3J(H,H) = 5.4 Hz, 8H, CH_E), 4.26 (br t, 2H, CH_a), 3.91 (br d,

4H, CH_b), 2.41 (s, 6H, CH_c); ^{13}C NMR (100 MHz, CDCl$_3$): δ = 166.9-166.0, 142.9, 138.9, 134.9, 129.3-127.6, 125.1, 53.9-53.1, 49.8, 44.6-44.1, 36.3-36.1; FAB-MS (mNBA matrix): m/z = 1036 [(M+H)$^+$]; Anal. Calcd. for C$_{66}$H$_{62}$N$_6$O$_6$: C 76.57, H 6.04, N 8.12. Found: C 76.88, H 6.20, N 8.30.

### 3.4.2   General Method for the Photoisomerization of Fumaramide [2]Rotaxanes.

The rotaxanes E-4-6 (0.60 g) were dissolved in CH$_2$Cl$_2$ [except for solubility reasons E-6, MeOH/CHCl$_3$ (1/9)] in a quartz vessel. The solutions were directly irradiated at 254 nm using a multilamp photoreactor model MLU18 manufactured by Photochemical Reactors Ltd, Reading UK. The progress of photoisomerization was monitored by TLC (silica, CHCl$_3$/EtOAc 4/1) or ^{1}H NMR.   The different photostationary states were reached in a range of times not exceeding 30 mins after which the reaction mixture was concentrated under reduced pressure to afford the crude products (Z-4-6).   The unconverted *trans* isomers were isolated by triturating the solids with PhMe/CH$_2$Cl$_2$ (1:1, ~20 mL) and, because the photoisomerization process produces few byproducts, could be recycled eventually leading to >90% conversion of each rotaxane to the corresponding *cis*-isomer. The solutions were then passed through a pad of silica (CHCl$_3$/EtOAc 4:1) to afford the *cis* isomers E-4-6 in 50, 47 and 45% yields, respectively, from a single photoisomerization experiment.

Selected data for [2](1,7,14,20-tetraaza-2,6,15,19-tetraoxo-3,5,9,12,16,18,22,25-tetrabenzocyclohexacosane)-benzyl-2-[[2-(benzyloxy)-2-oxoethyl]((Z)-5-(bis[2-(benzyloxy)-2-oxoethyl]amino})2,5-dioxo-3-pentenyl)amino]acetate-rotaxane (Z-4):
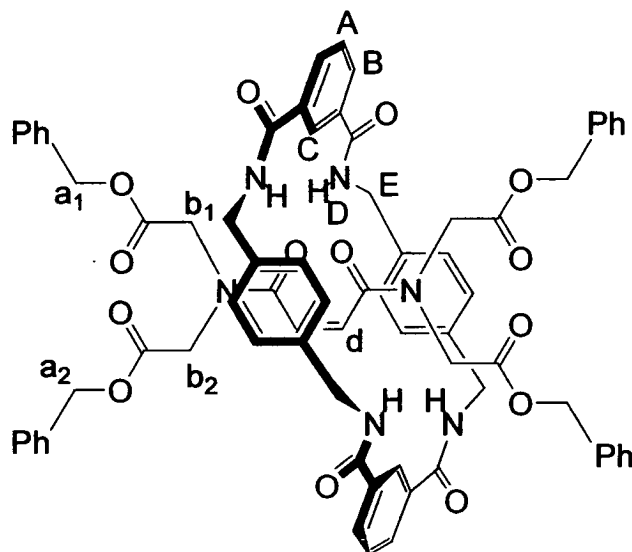
(Z-4, 0.3 g, 50%); m.p. 243-244°C; ^{1}H NMR (400 MHz, CD$_2$Cl$_2$): δ = 8.92 (dd, ^4J(H,H) = 1.7 Hz, ^3J(H,H) = 7.8 Hz, 4H, ArCH$_B$), 7.60 (t, ^4J(H,H) = 1.7 Hz, 2H, ArCH$_C$), 7.40 (t, ^3J(H,H) = 7.8 Hz, 2H, ArCH$_A$), 7.30 (t, ^3J(H,H) = 5.1 Hz, 4H, NH$_D$), 7.23-7.11 (m, 20H, ArCH), 7.03 (s, 8H, ArCH$_F$), 4.89 (s, 4H, CH$_{b2}$), 4.83 (s, 2H, CH$_d$), 4.78 (s, 4H, CH$_{b1}$), 4.36 (d, ^3J(H,H) = 5.1 Hz, 8H, CH$_E$), 3.63 (s, 4H, CH$_{a2}$), 3.58 (s, 4H, CH$_{a1}$); ^{13}C NMR (100 MHz, CDCl$_3$): δ = 168.4, 167.6, 166.6, 166.2, 137.3, 135.9, 134.5, 134.4, 132.5, 129.9-128.6, 123.4, 68.8, 68.3, 50.9, 50.6; LSIMS, m/z = 1239 [(M+H)$^+$], 1262 [(M+Na)$^+$]. Anal. Calcd. for C$_{72}$H$_{66}$N$_6$O$_{14}$: C 69.78, H 5.37, N 6.78. Found: C 69.56, H 5.32, N.6.68.

Selected data for ([2](1,7,14,20-tetraaza-2,6,15,19-tetraoxo-,5,9,12,16,18,22,25-tetrabenzocyclohexacosane)-((Z)-N,N'-(dimethyl)-bis{2',2'-diphenylethyl}-butendiamide)-rotaxane (Z-5):
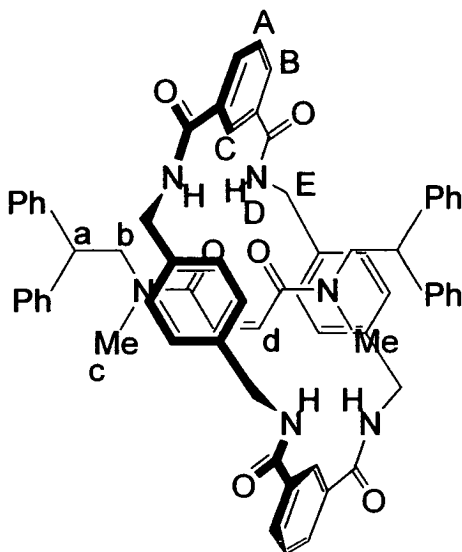
(Z-5, 0.28 g, 47%); m.p. > 300 °C (decompose); ^{1}H NMR (400 MHz, C$_2$D$_2$Cl$_4$ at 403K): δ = 8.13 (dd, ^3J(H,H) = 7.8 Hz, 4H, ArCH$_B$), 7.91 (br s, 2H, ArCH$_C$), 7.63 (t, ^3J(H,H) = 7.8 Hz, 2H, ArCH$_A$), 7.35-7.11 (m, 24H, ArCH + NH$_D$), 6.98 (s, 8H, ArCH$_F$), 4.92 (br s, 2H, CH$_d$), 4.40 (br d, ^3J(H,H) = 5.4 Hz, 8H, CH$_E$), 4.07 (b t, 2H, CH$_a$), 3.51 (br d, 4H, CH$_b$), 2.21 (s, 6H, CH$_c$); ^{13}C NMR (100 MHz, CDCl$_3$): δ = 166.9-166.0, 142.9, 138.2, 134.9, 129.3-127.6, 125.1, 53.9-53.1, 49.8, 44.6-44.1, 36.3-36.1; FAB-MS (mNBA matrix): m/z = 1036 [(M+H)$^+$]; Anal. Calcd. for C$_{66}$H$_{62}$N$_6$O$_6$: C 76.57, H 6.04, N 8.12. Found: C 76.98, H 6.30, N 8.23.

Selected data for ([2](1,7,14,20-tetraaza-2,6,15,19-tetraoxo-3,5,9,12,16,18,22,25-tetrabenzocyclohexacosane)-((Z)-N,N'-(dimethyl)-bis{2',2'-diphenylethyl}-butendiamide)-rotaxane (Z-6):
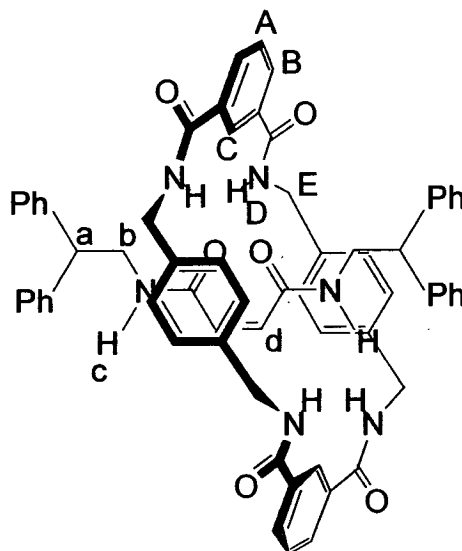
(Z-6, 0.27 g, 45%); m.p. >300 °C (decompose); ^{1}H NMR (400 MHz, CDCl$_3$) δ = 8.22 (d, ^3J(H,H) = 7.8 Hz, 4H, ArCH$_B$), 8.13 (s, 2H, ArCH$_C$), 7.73 (t, ^3J(H,H) = 5.4 Hz, 4H, NH$_D$), 7.62 (t, ^3J(H,H) = 7.8 Hz, 2H, ArCH$_A$), 7.27-7.11 (m, 18H, ArCH + NH$_c$), 6.98 (d, ^3J(H,H) = 7.5 Hz, 4H, ArCH), 6.83 (s, 8H, ArCH$_F$), 5.11 (s, 2H, CH$_d$), 4.38 (d, ^3J(H,H) = 5.4 Hz, 8H, CH$_E$), 3.87 (t, 2H, CH$_a$), 3.41 (d, 4H, CH$_b$); ^{13}C NMR (100 MHz, CDCl$_3$): δ = 166.8, 165.5, 141.8, 137.4, 134.3, 131.9, 131.2, 129.9, 129.3, 129.2, 128.0, 127.5, 124.8, 50.3, 44.9, 44.8; MS (FAB, mNBA): m/z = 1029 [(M+Na)$^+$]. Anal. Calcd. for C$_{64}$H$_{58}$N$_6$O$_6$: C 76.32, H 5.80, N 8.34. Found: C 76.39, H 5.91, N 8.19.

3.4.3 X-Ray Crystallographic Structure Determinations:

E-5: C$_{64}$H$_{58}$N$_6$O$_6$, M=1039.22, crystal size 0.18×0.04×0.02 mm, triclinic P-1, a=13.4337(13), b=16.2778(16), c=29.964(3) Å, α=75.716(2), β=87.934(2), γ= 71.880(2) °, V=6028.9(10) Å^3, Z=4, ρcalcd=1.145 Mg m^{-3}; synchrotron radiation (CLRC Daresbury Laboratory Station 9.8, silicon monochromator, λ=0.69290 Å), μ=0.107 mm$^-$

[1], T=150(2)K. 23260 data (12003 unique, R_{int}=0.0466, 1.73<θ<20.00°), were collected on a Siemens SMART CCD diffractometer using narrow frames (0.3° in ω), and were corrected semi-empirically for absorption and incident beam decay (transmission 0.20-1.00). The structure was solved with SIR97 (Altomare A., Burla M.C., Camalli M., Cascarano G.L., Giacovazzo C., Guagliardi A., Moliterni A.G.G., Polidori G., Spagna R. *J. Appl. Cryst.* **32**, 115-119 (1999)) and refined by full-matrix least-squares on F^2 values of all data (G.M.Sheldrick, SHELXTL manual, Siemens Analytical X-ray Instruments, Madison WI, USA, 1994, version 5) to give $wR=\{\Sigma[w(F_O^2-F_C^2)^2]/\Sigma[w(F_O^2)^2]\}^{1/2}$=0.2771, conventional R=0.0952 for F values of 12003 reflections with $F_O^2>2\sigma(F_O^2)$, S=1.050 for 1480 parameters. Residual electron density extremes were 1.093 and −0.420 Å^{-3}.

Z-**5**: $C_{66}H_{62}N_6O_6$, M=1035.22, crystal size 0.30×0.14×0.08 mm, monoclinic, P2$_1$/c, a=10.5696(3), b=27.7157(9), c=10.7503(3) Å, β=115.2530(10), V=2848.27(15) Å^3, Z=2, ρ_{calcd}=1.207 Mg m^{-3}; MoK$_a$ radiation (graphite monochromator, λ=0.71073 Å), μ=0.078 mm^{-1}, T=293(2) K. 13437 data (4049 unique, R_{int}=0.1701, 1.47<θ<23.29°), were collected on a Siemens SMART CCD diffractometer using narrow frames (0.3° in ω), and were corrected semi-empirically for absorption and incident beam decay (transmission 0.20-1.00). The structure was solved by direct methods and refined by full-matrix least-squares on F^2 values of all data (G.M.Sheldrick, SHELXTL manual, Siemens Analytical X-ray Instruments, Madison WI, USA, 1994, version 5) to give $wR=\{\Sigma[w(F_O^2-F_C^2)^2]/\Sigma[w(F_O^2)^2]\}^{1/2}$=0.2136, conventional R=0.0811 for F values of 4049 reflections with $F_O^2>2\sigma(F_O^2)$, S=0.754 for 361 parameters. Residual electron density extremes were 0.355 and -0.337 Å^{-3}. Amide hydrogen atoms were refined isotropically subject to a distance constraint N-H = 0.98 Å, with the remainder constrained; anisotropic displacement parameters were used for all non-hydrogen atoms. Crystallographic data for E-**5** and Z-**5** (excluding structure factors) have been deposited with the Cambridge Crystallographic Data Centre as supplementary publication numbers

CCDC-149672 and 149673 (*E*-5 and *Z*-5). Copies of the data can be obtained free of charge on application to The Director, CCDC, 12 Union Road, Cambridge CB2 1EZ, UK (fax: +44-1223-336-033; e-mail: teched@chemcrys.cam.ac.uk).

3.4.4 The Effect of Olefin Stereochemistry on Amide Bond Rotamerization in *E/Z*-4.

The energy barrier for amide bond rotamerization in tertiary amide rotaxanes increases if intercomponent hydrogen bonding occurs to stabilise the $R_2N^+=C-O^-$ resonance contribution of the tertiary amide group [W. Clegg, C. Gimenez-Saiz, D. A. Leigh, A. Murphy, A. M. Z. Slawin, S. J. Teat, *J. Am. Chem. Soc.*, **1999**, *121*, 4124-4129]. In Fig. 2a, slow amide bond rotamerization is responsible for the magnetically distinct environments observed for H_{a_1} and H_{a_2} (and H_{b_1}/H_{b_2}). Even though the coalescence temperature for their interconversion cannot be reached in $C_2D_2Cl_4$, their exchange rate can be measured directly by SPT-SIR and gives an energy barrier of 21.1 kcal mol^{-1} at 383K (*cf.* 17.2 kcal mol^{-1} at 383K for rotamerization in the *trans* thread, obtained by ^{1}H line shape analysis). In contrast, it is clear from the broadening of the H_{a_1}/H_{a_2} resonances in Fig. 2b that the same process is occurring with a lower energy barrier in the *cis*-rotaxane. Indeed, ^{13}C line shape analysis (^{1}H line shape analysis was not possible because the diastereotopic methylene protons in the *cis* thread are accidentally isochronous) experiments give the energy barrier of 20.0 kcal mol^{-1} for *Z*-4 at 383K (*cf.* 17.4 kcal mol^{-1} at 383K for rotamerization of the *cis* thread).

3.5 References

1. H. Iwamura, K. Mislow, *Acc. Chem. Res.* **1988**, *21*, 175-182.

2. T. C. Bedard, J. S. Moore, *J. Am. Chem. Soc.* **1995**, *117*, 10662-10671.

3. T. R. Kelly, M. C. Bowyer, K. V. Bhaskar, D. Bebbington, A. Garcia, F. Lang, M. H. Kim, M. P. Jette, *J. Am. Chem. Soc.* **1994**, *116*, 3657-3658.

4. T. R. Kelly, I. Tellitu, J. P. Sestelo, *Angew. Chem. Int. Ed. Engl.* **1997**, *36*, 1866-1868.

5. T. R. Kelly, J. P. Sestelo, I. Tellitu, *J. Org. Chem.* **1998**, *63*, 3655-3665.

6. A. M. Schoevaars, W. Kruizinga, R. W. J. Zijlstra, N. Veldman, A. L. Spek, B. L. Feringa, *J. Org. Chem.* **1997**, *62*, 4943-4948.

7. T. R. Kelly, H. De Silva, R. A. Silva, *Nature* **1999**, *401*, 150-152.

8. N. Koumura, R. W. J. Zijlstra, R. A. van Delden, N. Harada, B. L. Feringa, *Nature* **1999**, *401*, 152-155.

9. T. R. Kelly, R. A. Silva, H. De Silva, S. Jasmin, Y. Zhao, *J. Am. Chem. Soc.* **2000**, *122*, 6935-6949.

10. N. L. Koumura, E. M. Geertsema, M. B. van Gelder, A. Meetsma, B. L. Feringa, *J. Am. Chem. Soc.* **2002**, *124*, 5037-5051.

11. V. Balzani, A. Credi, F. M. Raymo, J. F. Stoddart, *Angew. Chem. Int. Ed.* **2000**, *39*, 3348-3391.

12. Special issue on *Molecular Machines Acc. Chem. Res.* **2001**, *34*, 409-522.

13. *Molecular Machines and Motors.* Structure and Bonding, Vol. 99, ed. by J.-P. Sauvage (Springer, Berlin 2001).

14. V. Bermudez, N. Capron, T. Gase, F. G. Gatti, F. Kajzar, D. A. Leigh, F. Zerbetto, S. Zhang, *Nature* **2000**, *406*, 608-611.

15. F. G. Gatti, D. A. Leigh, S. A. Nepogodiev, A. M. Z. Slawin, S. J. Teat, J. K. Y.Wong, *J. Am. Chem. Soc.* **2001**, *123*, 5983-5989.

16.   G. Campari, M. Fagnoni, M. Mella, A. Albini, *Tetrahedron Asym.* **2000**, *11*, 1891-1906.

17.   L. Frkanec, M. Jokic, J. Makarevic, K. Wolsperger, M. Zinic, *J. Am. Chem. Soc.* **2002**, *124*, 9716-9717.

18.   N. L. Allinger, Y. H. Yuh, J.-H. Lii, *J. Am. Chem. Soc.* **1989**, *111*, 8551-8556.

19.   M. J. Dudek, J. Ponder, *J. Comput. Chem.* **1995**, *16*, 791-816.

20.   M. S. Deleuze, D. A. Leigh, F. Zerbetto, *J. Am. Chem. Soc.* **1999**, *121*, 2364-2379.

21.   F. Biscarini, M. Cavallini, D. A. Leigh, S. León, S. J. Teat, J. K. W. Wong, F. Zerbetto, *J. Am. Chem. Soc.* **2002**, *124*, 225-233.

22.   C.-A. Fustin, D. A. Leigh, P. Rudolf, D. Timpel, F. Zerbetto, *ChemPhysChem* **2000**, *1*, 97-100.

23.   J. Vacek J. Michl, *New J. Chem.* **1997**, *21*, 1259-1268.

24.   R. A. van Delden, N. Koumura, N. Harada, B. L. Feringa, *Proc. Natl. Acad. Sci. USA* **2002**, *99*, 4945-4949.

25.   C. P. Collier, G. Mattersteig, E. W. Wong, Y. Luo, K. Beverly, J. Sampaio, F. M. Raymo, J. F. Stoddart, J. R. Heath, *Science* **2000**, *289*, 1172-1175.

26.   K. Tashiro, K. Konishi, T. Aida, *J. Am. Chem. Soc.* **2000**, *122*, 7921-7926.

27.   D. A. Leigh, A. Murphy, J. P. Smart, M. S. Deleuze, F. Zerbetto, *J. Am. Chem. Soc.* **1998**, *120*, 6458-6467.

28.   L. Raehm, J.-M. Kern, J.-P. Sauvage, *Chem. Eur. J.* **1999**, *5*, 3310-3317.

29.   S. Chatterjee, V. R. Pedireddi, C. N. R. Rao, *Tetrahedron Lett.* **1998**, *39*, 2843-2846.

30.   W. Clegg, C. Gimenez-Saiz, D. A. Leigh, A. Murphy, A. M. Z. Slawin, S. J. Teat, *J. Am. Chem. Soc.* **1999**, *121*, 4124-4129.

Control of the Translational Motion in Hydrogen Bonded [2]Rotaxanes

Accepted for publication in Angewandte Chemie as:

"Remarkable Positional Discrimination in Bistable, Light and Heat-Switchable,

Hydrogen Bonded Molecular Shuttles"

Altieri, A.; Bottari, G.; Dehez, F.; Leigh, D. A.; Wong, J. K. Y.; Zerbetto, F.

*In chapter three it has been demonstrated how the rate of the pirouetting of the macrocycle around the thread in [2]rotaxanes can be controlled through reversible E/Z isomerisation.*

In this chapter we show the possibility to influence and control, by applying different stimuli, another dynamic property present in hydrogen-bonded rotaxane architectures: the translational motion (shuttling movement).

A series of two-station rotaxanes, E-1-3, were synthesised each containing on the thread a fumaramide station (green) that has been proved to be a photochemically isomerisable and a highly efficient templating unit (chapters two and three) and a non-photoreactive station (orange) (Scheme 1). ^{1}H NMR studies in CHCl$_3$ at room temperature showed unambiguously that in all the three E-rotaxanes the macrocycle sits preferentially over the fumaramide unit presenting a remarkable positional discrimination between the two well-separated stations as a consequence of the quite different binding affinity that it has for the two templating units.
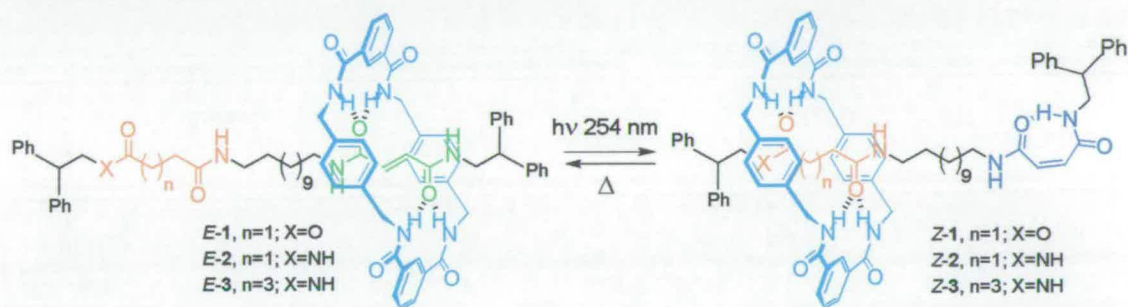

Scheme 1 *The positioning of the macrocycle along the thread can be controlled in response to photonic or thermal stimuli.*

A photonic stimulus is then used to isomerise the fumaramide group into the poor macrocycle-templating maleamide unit (blue) thus provoking the shuttling of the macrocycle over the initially poorly-binded, non-photoreactive, station that now offers the higher binding affinity for the ring as confirmed by ^{1}H NMR spectroscopy studies in CHCl$_3$ at room temperature of Z-1-3. The positional discrimination of the macrocycle between the two templating units present on the thread is extremely good for the rotaxanes Z-1-2, whereas for Z-3 is surprisingly poor even though the adipamide unit should be a much better template than the maleamide unit for the

benzylic amide macrocycle. A thermal stimulus is then used to reverse the photochemical isomerisation process converting the Z-rotaxanes in their respective E-isomers. Molecular modelling calculations of the rotaxanes E/Z-1-3 were also performed leading to results broadly in line with the experimental data, although they could not reproduce the anomalously poor binding of the adipamide station in Z-3.

4.1 Introduction

Stimuli-responsive molecular 'shuttles'[1-11] (*i.e.* mechanically interlocked molecules where a macrocycle can be translocated between different sites in response to an external signal) all operate through the same basic principle. The external stimulus does not induce directional motion of the macrocycle *per se*, rather it alters the equilibrium between different translational co-conformers by increasing the binding strength of the less populated station and/or destabilizing the initially preferred binding site. The motion of the components arises from the background thermal energy, the net result being a change in the position of the macrocycle through biased Brownian motion (Figure 4.1).
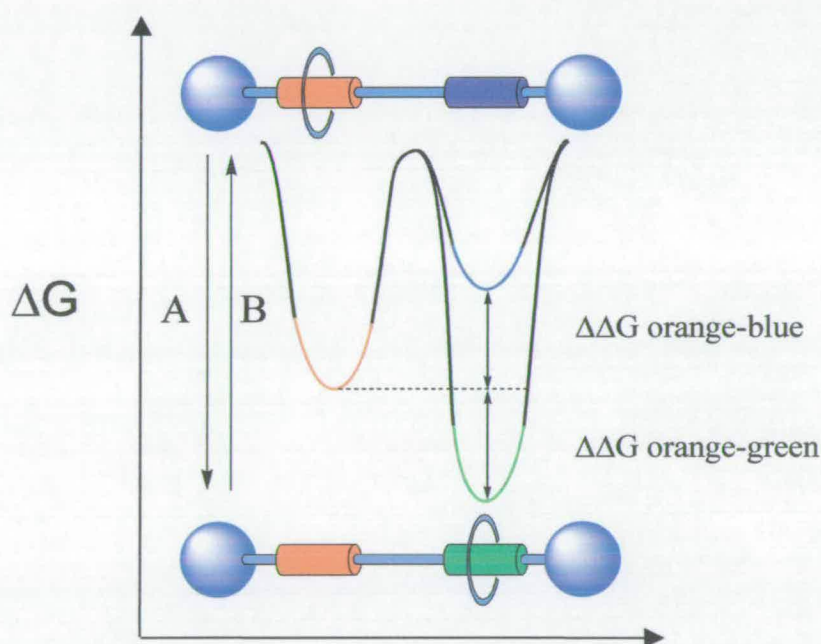

Figure 4.1. Macrocycle translation in a stimuli-responsive molecular shuttle. Stimulus A induces a blue-to-green transformation, stimulus B a green-to-blue transformation. The equilibrium distribution of the macrocycle between two stations is determined by the difference in their binding energies ($\Delta\Delta G_{orange-blue}$, $\Delta\Delta G_{orange-green}$) and the temperature.

4.2 Results and Discussion

Given this mode of action, a major problem in trying to design photo-active shuttles that could function as practical components for molecular machinery is finding ways of generating sufficiently large, long lived, binding energy differences between pairs of positional isomers.[2-10] A Boltzmann distribution at 298K requires a $\Delta\Delta G$ between translational co-conformers of ~2 kcal mol^{-1} for 95% occupancy of one station. Achieving such discrimination in <u>two</u> states to form a positionally bistable shuttle (*i.e.* both $\Delta\Delta G_{orange-blue}$ and $\Delta\Delta G_{orange-green} \geq 2$ kcal mol^{-1}) by modifying only intrinsically weak, non-covalent binding modes thus presents a significant challenge. The problem has previously been overcome in part by using photochemistry to block the position of the macrocycle in what are essentially 'one station' rotaxanes.[5,10] In these systems the macrocycle is only able to sit on an azobenzene[5] or stilbene unit[10] in the *E*- diastereomer of the rotaxane and must reside elsewhere in the *Z*-form. Unfortunately, the integrity of macrocycle positioning in such systems is likely to be limited unless the thread is very short. Here we describe photo- and thermally-responsive shuttles (**1-3**) where the macrocycle moves over a relatively large distance (~1.5 nm) between two discrete stations with remarkable positional integrity (even at room temperature), despite the fact that the discrimination between the binding sites is caused only by 'matched' and 'mis-matched' hydrogen bonding motifs. Each translational form is stable until a new stimulus is applied.

The basis for the new shuttles lies in the photochemical and thermal interconversion of fumaramide and maleamide groups.[12] The *trans*-olefin *bis*-amide acts as an excellent template for the formation of benzylic amide macrocycle-based rotaxanes (*e.g E*-**4**, Figure 4.2) because the amide carbonyl groups of the thread are rigidly held in positions that fit the hydrogen bond-donating sites of the forming macrocycle (an arrangement maintained even in crystals of *E*-**4** obtained from DMSO, Figure 4.2a).[13] Irradiation of fumaramide rotaxanes at 254 nm[14] produces the corresponding *cis*- (maleamide)

rotaxane in which the maximum number of intercomponent hydrogen bonds changes from four to two (Figure 4.2b), considerably reducing the strength of binding[15] between macrocycle and thread. By incorporating a second binding site into the thread we reasoned it might be possible to generate photoinduced, thermally reversible, translation of the rotaxane components.
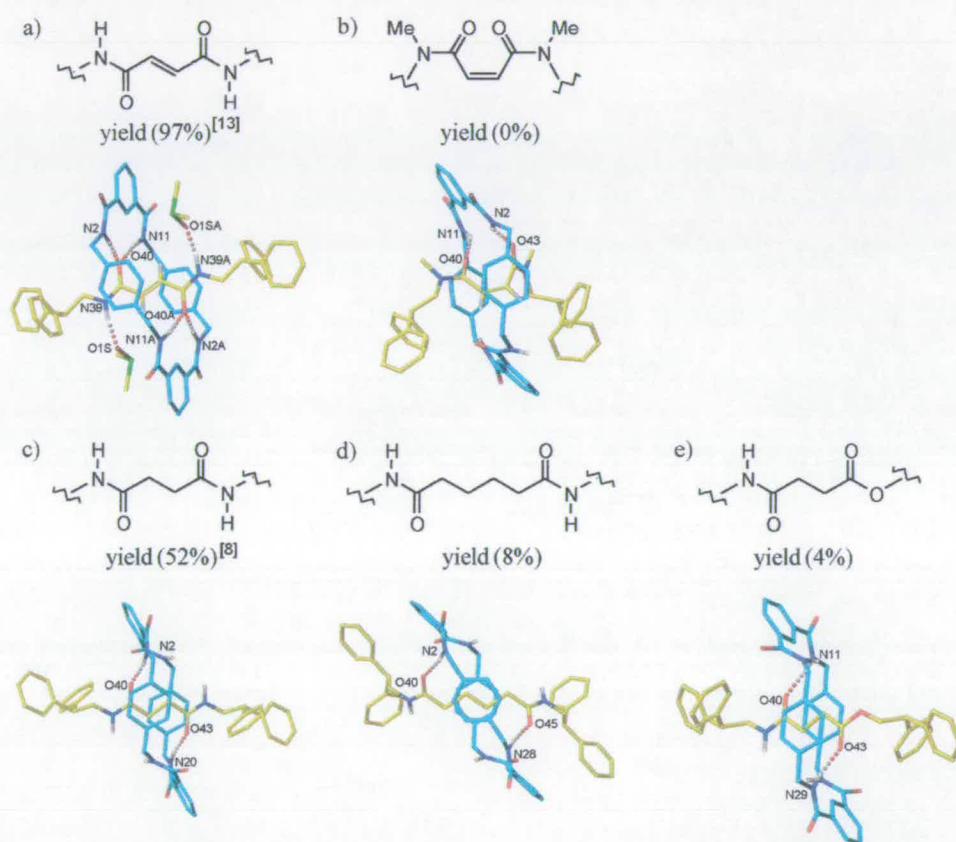
Figure 4.2. *X*-ray structures of model single binding site [2]rotaxanes showing hydrogen bonding characteristics of predicted (a) 'strong', (b) 'weak', and (c)-(e) 'intermediate strength' hydrogen bonding stations. (a) fumaramide rotaxane *E*-4 crystallized from DMSO; (b) *N,N*'-dimethyl derivative of the corresponding maleamide (*Z*) rotaxane; (c) succinamide analogue of *E*-4; (d) adipamide analogue of *E*-4; (e) succinic amide ester analogue of *E*-4. Intramolecular hydrogen bond distances and angles: (a) O40–HN2/O40A–HN2A 2.13 Å, 173.7°; O40–HN11/O40A–HN11A 1.89 Å, 169.3°; (b) O40–HN11 2.08 Å, 139.3°; O43–HN2 2.00 Å, 142.1°; (c) O40–HN2/O43–HN20 1.88 Å, 165.3°; (d) O40–HN2/O45–HN28 2.00 Å, 168.8°; (e) O40–HN11/O43–HN29 1.89 Å, 156.1°. For clarity the carbon atoms of the macrocycles are shown in blue and the carbon atoms of the threads in yellow; oxygen atoms are red, nitrogen atoms dark blue and selected hydrogen atoms white. In all cases the rotaxane 'stoppers' are -CH$_2$CHPh$_2$.

We prepared three different molecular shuttles (**1-3**, Scheme 4.1), each containing a fumaramide/maleamide site plus a non-photoactive second station of predicted intermediate macrocycle binding affinity.
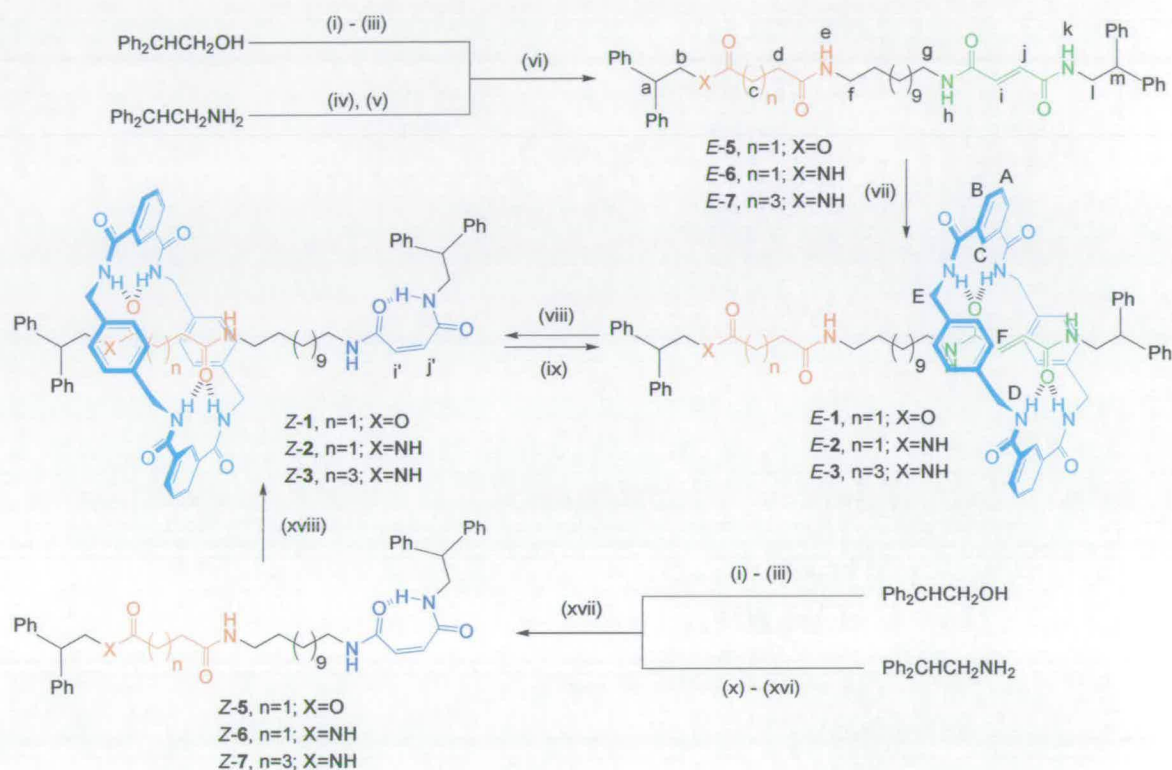

Scheme 4.1. Synthesis of bistable molecular shuttles **1-3**. (i) succinic anhydride, Et₃N, CH₂Cl₂, 90%. (ii) H₂N(CH₂)₁₂NHBoc, 4-dimethylaminopyridine (DMAP), 1-(3-dimethylaminopropyl)-3-ethyl-carbodiimide hydrochloride (EDCI.HCl), CH₂Cl₂, 68%. (iii) trifluoroacetic acid, CHCl₃, quantitative. (iv) fumaric acid monoethylester, DMAP, EDCI.HCl, CH₂Cl₂, 85%. (v) NaOH in H₂O, EtOH, 91%. (vi) DMAP, EDCI.HCl, DMF, *E*-**5**, 76%. (vii) isophthaloyl dichloride, *p*-xylylenediamine, Et₃N, CHCl₃, *E*-**1**, 57%. (viii) hv at 254 nm for 30 min., CH₂Cl₂, *Z*-**1**, 54%; *Z*-**2**, 48%; *Z*-**3**, 39%. (ix) C₂H₂Cl₄ at 120 °C for 7 days, *E*-**1**, 80%; *E*-**2**, 80%; or 1 day, *E*-**3**, 95%. (x) maleic anhydride, anhydrous THF, 75%. (xi) succinic anhydride, anhydrous THF, 95%. (xii) SOCl₂, 1,12 diaminododecane, CH₂Cl₂, 35%. (xiii) adipic acid monoethylester, DMAP, EDCI.HCl, CH₂Cl₂, 86%. (xiv) KOH in H₂O, EtOH, 95%. (xv) H₂N(CH₂)₁₂NHBoc, DMAP, EDCI.HCl, CHCl₃, 92%. (xvi) trifluoroacetic acid, CHCl₃, quantitative. (xvii) DMAP, EDCI.HCl, CHCl₃, *Z*-**5**, 70%; *Z*-**6**, 70%; *Z*-**7**, 70%; (xviii) isophthaloyl dichloride, *p*-xylylenediamine, Et₃N, CHCl₃, *Z*-**1**, 2%, *Z*-**2**, 40% and *Z*-**3**, 20%. Full experimental procedures can be found in the Experimental Section.

Since the transition state of the rotaxane-forming reaction is similar in structure to the final rotaxane,[16] it seemed likely that the macrocycle binding affinity of a given station should be related to its ability to template the formation of the rotaxane. Several factors are known to affect both template efficacy and the nature of the intercomponent hydrogen bonding interactions (NH⋯O=C distances, angles *etc*, Figure 4.2) including: the hydrogen bond basicity of the functional groups (*e.g.* amides are better than esters[13]), preorganisation (*e.g.* fumaramide is better than succinamide[17]) and distance between the binding sites (succinamide better than adipamide[18]).

Some features of the synthetic routes to **1-3** are worthy of note: Although *E*-**1** was prepared from the corresponding thread, *E*-**5**, in good yield the other *E*-threads were insufficiently soluble in non-hydrogen bond-disrupting solvents to be utilized in this way. Rotaxanes *Z*-**2** and *Z*-**3** were therefore prepared from the corresponding *Z*-threads and converted to the *E*-rotaxanes thermally (120 °C, 1-7 days, $C_2H_2Cl_4$, 80-95%). In fact, the *E*-isomers of each molecular shuttle could be converted to the *Z*-forms with light (*E*→*Z*, direct irradiation at 254 nm, CH_2Cl_2, 30 min, 39-54% or with catalytic benzophenone sensitizer at 350 nm, CH_2Cl_2, 5 min, 60-65%) and back again *via* heat or reversible Michael addition (catalytic ethylenediamine, 60 °C, 4 h, 75-85%).

Since the xylylene rings of the macrocycle shield encapsulated regions of the thread, the position of the macrocycle in $CDCl_3$ could be determined for each pair of rotaxane diastereomers by comparing the chemical shift of the protons in the rotaxane with those of the corresponding thread (or suitable model compounds in the case of *E*-**2** and *E*-**3**).[19] The spectra of *E*/*Z*-**1** and *E*/*Z*-**5** in $CDCl_3$ (400 MHz, 298K) are shown in Figures 3 and 4. The H_i and H_j protons of the fumaramide group are shielded in the rotaxane *E*-**1** compared to the thread *E*-**5** by 1.09 and 1.02 ppm, whereas the chemical shifts of the H_c and H_d protons of the succinic amide-ester group are similar in both compounds (Figure 4.3). In the maleamide isomer, the situation is completely reversed (Figure 4.4).
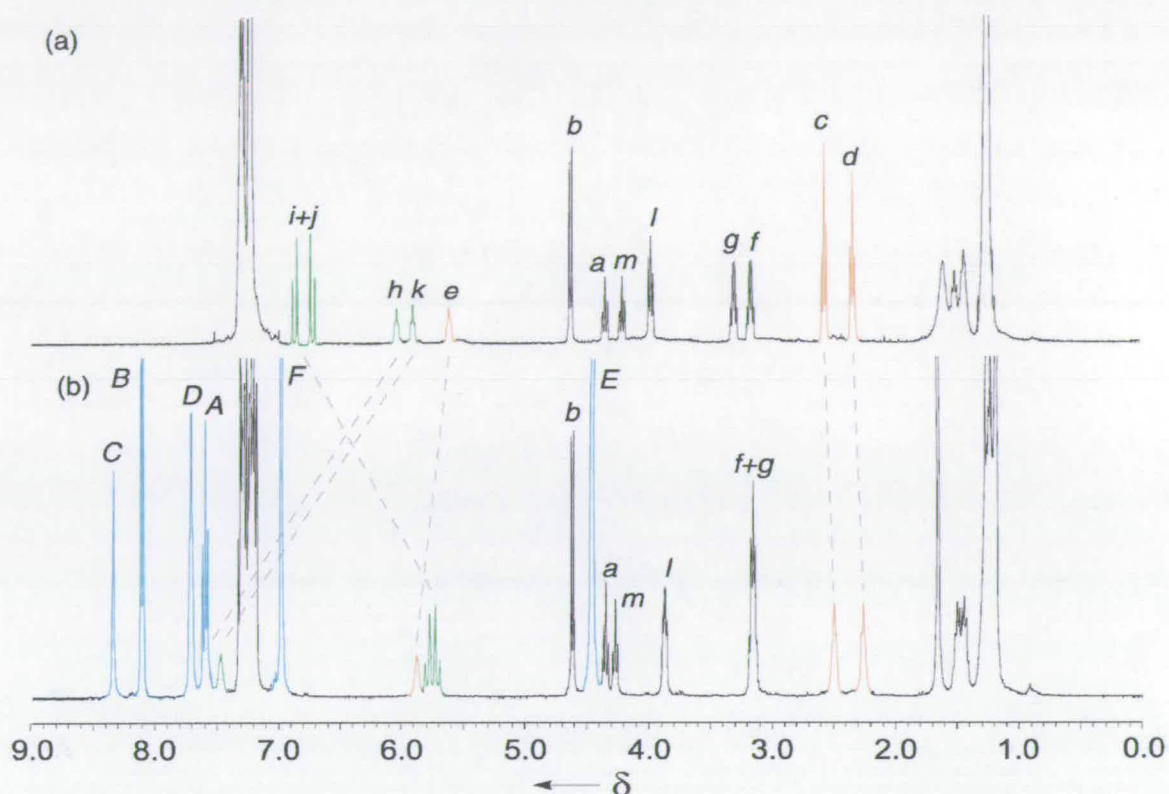
Figure 4.3. 400 MHz ^{1}H NMR spectra of (a) thread *E*-**5** and (b) rotaxane *E*-**1** in CDCl$_3$ at 298K. The assignments correspond to the lettering shown in Scheme 4.1.

The *Z*-olefin protons (H$_{i'}$ and H$_{j'}$) occur at almost identical chemical shifts in the rotaxane and thread, whereas the succinic amide-ester methylene groups (H$_c$ and H$_d$) are each shielded by >1.3 ppm in the rotaxane. A similar series of shifts occurs in the ^{1}H NMR spectra of the other molecular shuttle pairs. Thus, even at 298K, in each of *E*-**1**, *E*-**2** and *E*-**3** the occupancy of the fumaramide station is greater than 95% (the limit we can determine with reasonable confidence using this method). The occupancy of the alternative, non-photoactive station in the corresponding maleamide rotaxanes is similarly high for *Z*-**1** and *Z*-**2**. In *Z*-**3** the maleamide:adipamide occupancy ratio is reduced to ~15:85 (Figure 4.5), corresponding to a ΔΔG of ~1.1 kcal mol^{-1}.
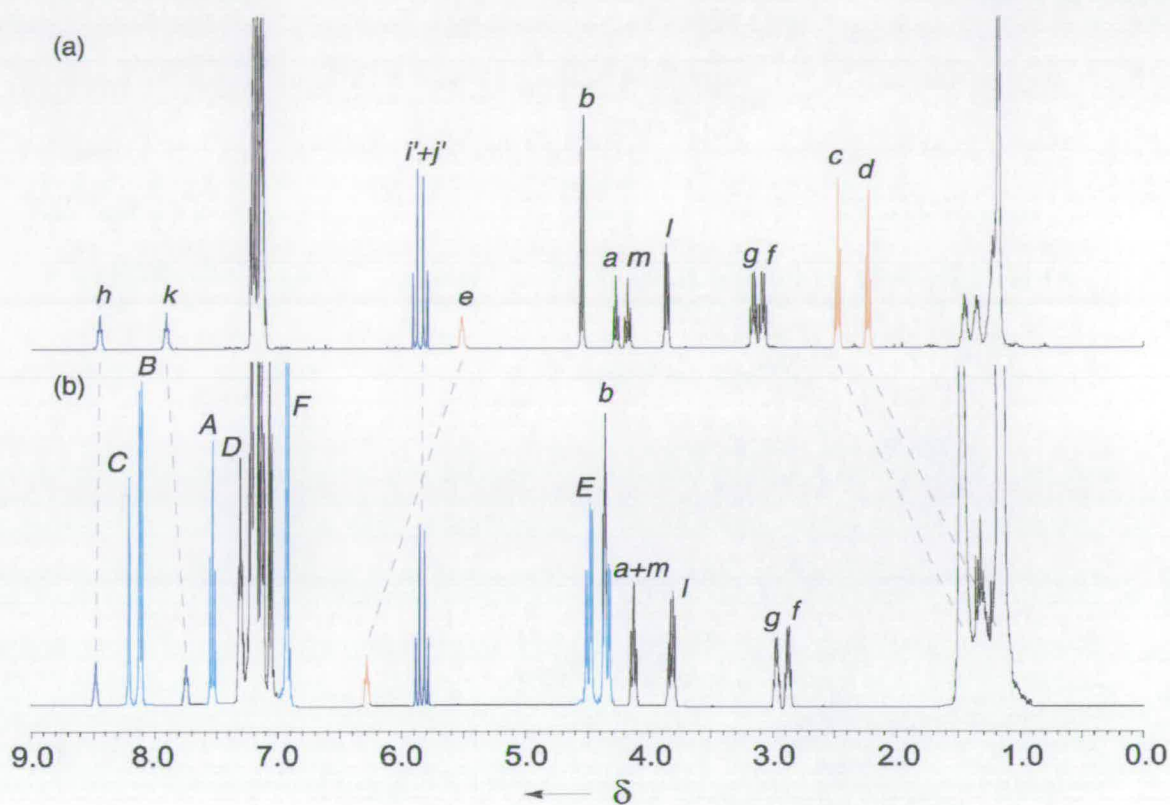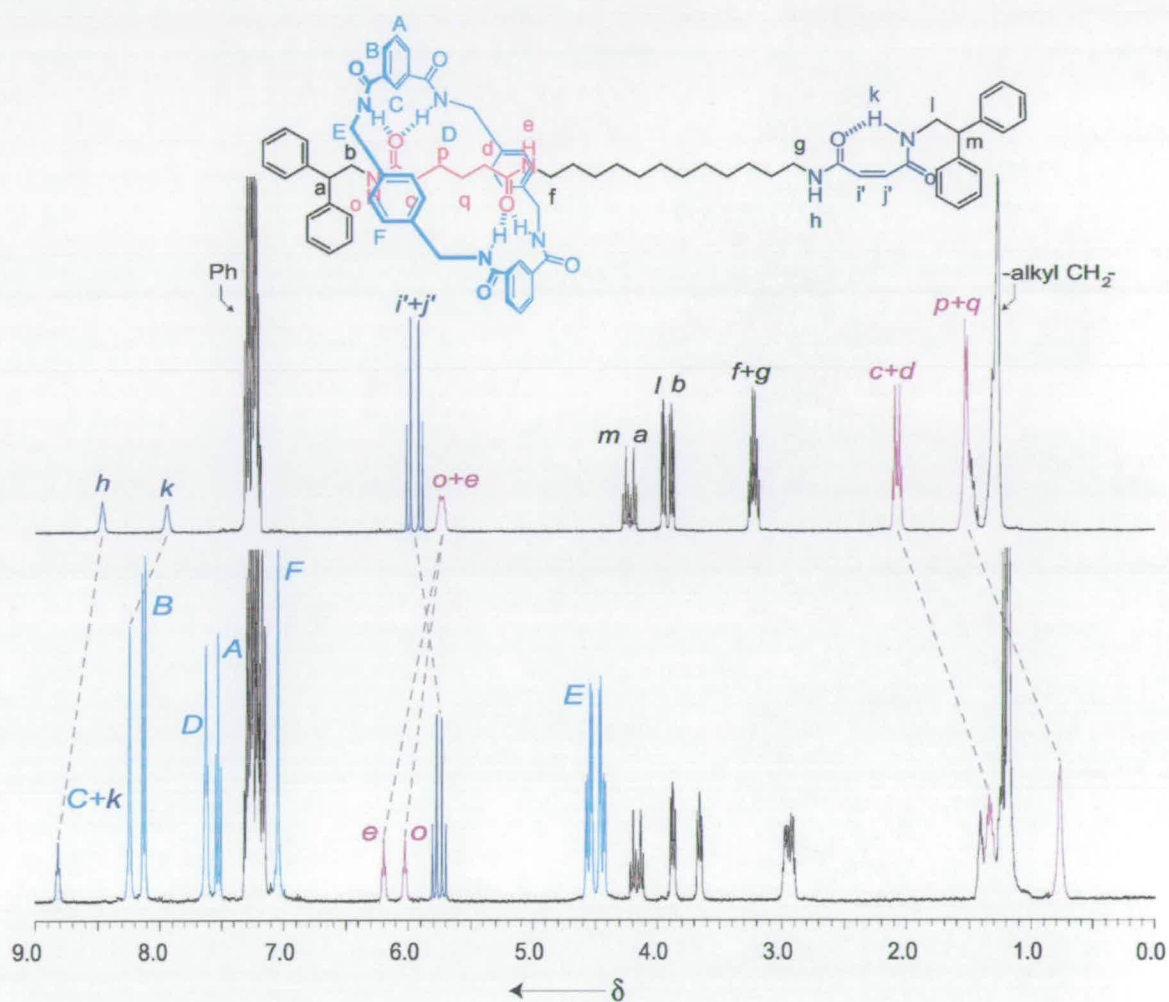
Figure 4.4. 400 MHz ^{1}H NMR spectra of (a) thread Z-**5** and (b) rotaxane Z-**1** in CDCl$_3$ at 298K.

It is interestingly to note that our predictions of the relative station binding affinities from rotaxane yield and hydrogen bond distances/angles are not completely accurate. Although the maleamide station is significantly populated in Z-**3** the same station does not compete at all with the succinic amide ester site in Z-**1** (Figure 4.4), even though the yields[20] and X-ray structure suggest the adipamide group should be the better station. Overall the discrimination for the macrocycle for the different stations is excellent and, at temperatures which require substantial energy differences to significantly bias the population distribution, somewhat remarkable (most notably between the fumaramide and succinamide stations in E-**2** which offer virtually identical hydrogen bonding surfaces to the macrocycle).

Figure 4.5. 400 MHz ^{1}H NMR spectra of (a) maleamide-adipamide thread *Z*-**7** and (b) rotaxane *Z*-**3** in CDCl$_3$ at 298K.

To probe this further, molecular modelling[16,17,21-24] was carried out by simulated annealing followed by geometrical optimization using the TINKER program with the MM3 forcefield. The difference in co-conformer stability for each pair of rotaxane diastereomers was calculated by comparing the energies (including zero point energies) of the occupied and unoccupied stations in each co-conformer to give:

$\Delta\Delta G$ 3.6 kcal mol^{-1} (fumaramide cf. succinic amide ester occupancy) in *E*-**1**;

$\Delta\Delta G$ 2.9 kcal mol^{-1} (succinic amide ester cf. maleamide occupancy) in *Z*-**1**;

$\Delta\Delta G$ 3.6 kcal mol^{-1} (fumaramide cf. succinamide occupancy) in *E*-**2**;

$\Delta\Delta G$ 3.0 kcal mol^{-1} (succinamide cf. maleamide occupancy) in *Z*-**2**;

$\Delta\Delta G$ 3.9 kcal mol^{-1} (fumaramide cf. adipamide occupancy) in *E*-**3**;

$\Delta\Delta G$ 3.1 kcal mol^{-1} (adipamide cf. maleamide occupancy) in *Z*-**3**.

Whilst in each case there is probably overbinding as a result of solvation and folding not being included in the model, the calculations are broadly in line with the experimental results (*i.e.* $\Delta\Delta G$'s ≥ 2 kcal mol^{-1}), although at this level they do not reproduce the anomalously poor binding of the adipamide station in *Z*-**3**.[20] However, the calculations do offer a simple explanation for why the positional discrimination is so good in these rotaxane systems: when it's not occupied, each station – except fumaramide – can intramolecularly hydrogen bond to itself and so the positional isomer which has that station occupied has at least one hydrogen bond less than the positional isomer with the fumaramide station occupied (Figure 4.6).
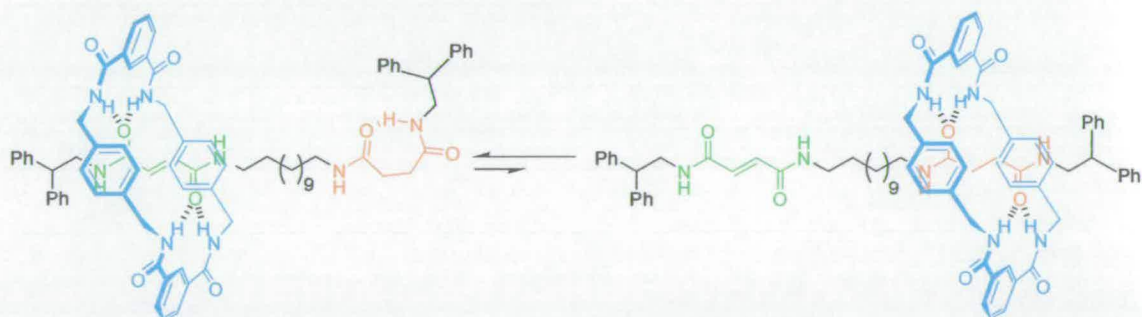
Figure 4.6. Translational isomerism in fumaramide-succinamide shuttle *E*-**2**. Positional discrimination is excellent (>95:5 at 298K in CDCl$_3$) even though the fumaramide and succinamide stations present nearly identical surfaces to the macrocycle.

The use of 'self-binding' to compensate for the lack of station occupancy could prove a useful concept for driving submolecular motion in molecular machines that rely only on weak, noncovalent, interactions.

4.3 Experimental Section

4.3.1 General Procedure for the Preparation of Benzylic Amide Macrocycle-Containing [2]Rotaxanes and Shuttles

The thread (1 equiv.) and Et_3N (24 equiv.) in anhydrous $CHCl_3$ [or for *E*-4 and *E*-1, $CH_3CN/CHCl_3$ (1/9)] (100 mL) were stirred vigorously whilst solutions of *para*-xylylene diamine (12 equiv.) in anhydrous $CHCl_3$ (40 mL) and isophthaloyl dichloride (12 equiv.) in anhydrous $CHCl_3$ (40 mL) were simultaneously added over a period of 2 h using motor-driven syringe pumps. After a further 2 h the resulting suspension was filtered and the solvent removed under reduced pressure. The resulting solid was subjected to column chromatography (silica gel) to yield unconsumed thread, [2]rotaxane, [2]catenane and, in some cases, [3]rotaxane.

4.3.2 General Procedure for the Photoisomerization of Fumaramide Derivatives:

The fumaramide derivative (0.05 mmol) was dissolved in CH_2Cl_2 (30 mL) [except for solubility reasons *E*-4 and *E*-2, $MeOH/CHCl_3$ (1/9)] in a quartz vessel. The solution was directly irradiated at 254 nm using a multilamp photo-reactor. The progress of the photoisomerization was monitored by TLC [$CHCl_3/EtOAc$ (4/1)] or ^1H NMR. Different photostationary states were reached in a range of times not exceeding 30 min, after which the reaction mixture was concentrated under reduced pressure to afford the crude product.

4.3.3 General Procedure for the Thermal-Isomerization of Maleamide Derivatives:

The maleamide derivative (0.02 mmol) was dissolved in $C_2D_2Cl_4$ or d_6-DMSO (30 mL) and heated at 400K for 4-7 days, resulting in the conversion to the more thermodynamically stable fumaramide derivative in good-to-excellent (80-95%) yields as indicated by ^1H NMR.

[2]-(1,7,14,20-Tetraaza-2,6,15,19-tetraoxo-3,5,9,12,16,18,22,25 –

tetrabenzocyclohexacosane)-((*E*)-*N*-{12-[3-(2,2-diphenylethylcarbamoyl)-

acryloylamino]-dodecyl}-succinamic acid 2,2-diphenylethyl ester)-rotaxane, *E*-1.
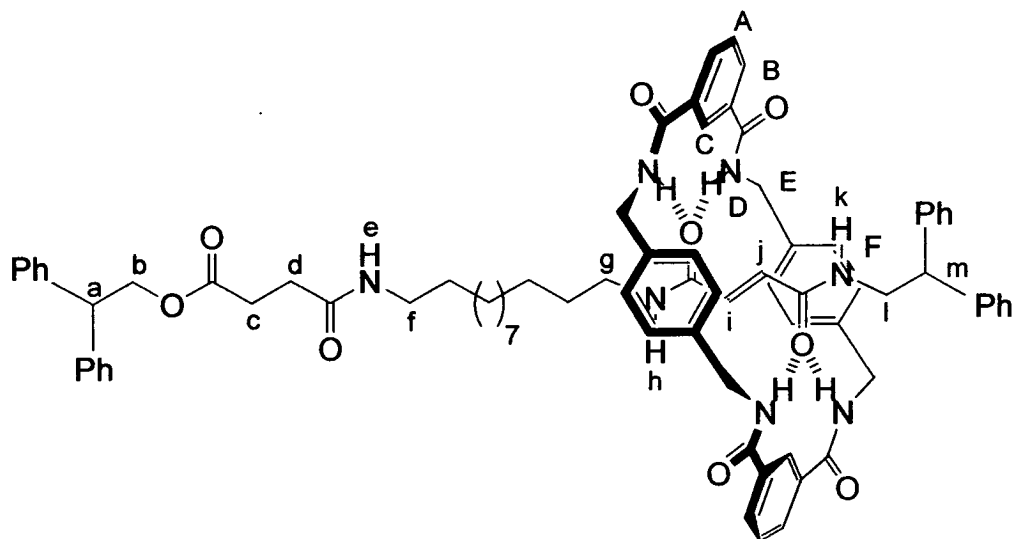

Rotaxane *E*-1 has been made using the general procedure for the preparation of benzylic amide macrocycle containing [2]rotaxane from the thread *E*-5 (0.19 g, 0.25 mmol). The crude material was subjected to column cromatography on silica gel using a gradient of CH_2Cl_2 to CH_2Cl_2/EtOAc (80/20) as eluent to obtain the desired compound as a colourless powder (*E*-1, 0.19 g, 57%).

Rotaxane *E*-1 has been also obtained using the general procedure for the thermal-isomerization from rotaxane *Z*-1 (70% in $C_2H_2Cl_4$). m.p. 186-187 °C. ^{1}H NMR (400 MHz, $CDCl_3$,): δ = 8.31 (br t, $^4J(H_C,H_B)$ = 1.2 Hz, 2H, ArCH_C), 8.08 (dd, $^4J(H_B,H_C)$ = 1.2 Hz, $^3J(H_B,H_A)$ = 7.8 Hz, 4H, ArCH_B), 7.68 (br t, $^3J(H,H)$ = 5.4 Hz, 4H, NH_D), 7.60 (br t, $^3J(H,H)$ = 5.7 Hz, 1H, NH_h), 7.56 (t, $^3J(H_A,H_B)$ = 7.8 Hz, 2H, ArCH_A), 7.45 (br t, $^3J(H,H)$ = 5.7 Hz, 1H, NH_k), 7.31-7.14 (m, 20H, ArCH), 6.95 (s, 8H, ArCH_F), 5.86 (br t, $^3J(H,H)$ = 5.7 Hz, 1H, NH_e); 5.77 (d, $^3J(H,H)$ = 14.8 Hz, 1H, CH_i or CH_j), 5.69 (d, $^3J(H,H)$ = 14.8 Hz, 1H, CH_i or CH_j), 4.59 (d, $^3J(H,H)$ = 7.7 Hz, 2H, CH_b), 4.42 (br d,

^3J(H,H) = 5.4 Hz, 8H, CH_E), 4.32 (t, ^3J(H,H) = 7.7 Hz, 1H, CH_a), 4.24 (t, ^3J(H,H) = 8.0 Hz, 1H, CH_m), 3.84 (dd, ^3J(H,H) = 8.0 Hz, ^3J(H,H) = 5.7 Hz, 2H, CH_l), 3.17-3.07 (m, 4H, CH_f and CH_g), 2.47 (br t, ^3J(H,H) = 7.0 Hz, 2H, CH_c), 2.23 (br t, ^3J(H,H) = 7.0 Hz, 2H, CH_d), 1.51-1.36 (m, 4H, -CH_2-CH$_f$ and -CH_2-CH$_g$) and 1.31-1.10 (m, 16H, CH_2 (alkyl chain)); ^{13}C NMR (100 MHz, CDCl$_3$,): δ = 173.0 (CH$_c$-CO-O), 171.3 (CH$_d$-CO-NH), 166.6 (CO macrocycle), 165.5 (CO fumaric), 165.2 (CO fumaric), 141.4 (ArC-CH (ipso thread)), 141.0 (ArC-CH (ipso thread)), 137.0 (ArC-CH$_E$), 134.6 (ArC-CO), 131.3 (CH$_B$), 130.3 (CH$_i$ or CH$_j$), 129.8 (CH$_i$ or CH$_j$), 129.1 (ArCH$_A$), 129.0 (ArCH$_F$), 128.9 (ArCH (meta thread), 128.6 (ArCH (meta thread), 128.2 (ArCH (ortho thread), 127.8 (ArCH (ortho thread), 127.2 (ArCH (para thread), 126.8 (ArCH (para thread), 124.5 (ArCH$_C$), 67.0 (CH$_b$), 50.3 (CH$_a$), 49.8 (CH$_m$), 44.8 (CH$_l$), 44.2 (CH$_E$), 40.1 (CH$_f$ or CH$_g$), 39.6 (CH$_f$ or CH$_g$), 30.8 (-CH$_2$-), 29.6 (-CH$_2$-), 29.5 (-CH$_2$-), 29.3 (-CH$_2$-), 29.1 (-CH$_2$-), 26.9 (-CH$_2$-) and 26.8 (-CH$_2$-); ^{1}H NMR (400 MHz, d_6-DMSO): δ = 8.59 (br t, ^3J(H,H) = 5.7 Hz, 1H, NH_h), 8.53 (br t, ^3J(H,H) = 5.6 Hz, 4H, NH_D), 8.41 (s, 2H, ArCH_C), 8.26 (br t, ^3J(H,H) = 5.8 Hz, 1H, NH_k), 8.03 (d, ^3J(H$_B$,H$_A$) = 7.6 Hz, 4H, ArCH_B), 7.64 (t, ^3J(H$_A$,H$_B$) = 7.6 Hz, 3H, ArCH_A and NH_e), 7.36-7.28 (m, 16H, ArCH), 7.26-7.19 (m, 4H, ArCH), 6.99 (s, 8H, ArCH_F), 6.27 (s, 2H, CH_i and CH_j), 4.56 (d, ^3J(H,H) = 7.6 Hz, 2H, CH_b), 4.40-4.29 (br m, 9H, CH_E and CH_a), 4.22 (t, ^3J(H,H) = 7.5 Hz, 1H, CH_m), 3.81 (dd, ^3J(H,H) = 7.5 Hz, ^3J(H,H) = 5.8 Hz, 2H, CH_l), 2.87-2.77 (m, 4H, CH_f and CH_g), 2.32 (br t, ^3J(H,H) = 6.8 Hz, 2H, CH_c), 2.20 (br t, ^3J(H,H) = 7.0 Hz, 2H, CH_d), 1.19-1.11 (m, 4H, -CH_2-CH$_f$ and -CH_2-CH$_g$) and 0.99-0.87 (m, 16H, CH_2 (alkyl chain)); MS (FAB): m/z = 1290 [(M+H)$^+$]; Anal. Calcd. for C$_{80}$H$_{87}$N$_7$O$_9$: C 74.45, H 6.79, N 7.60. Found: C 74.53, H 6.92, N 7.66.

[2]-(1,7,14,20-Tetraaza-2,6,15,19-tetraoxo-3,5,9,12,16,18,22,25-tetrabenzocyclohexacosane)-((*E*)-but-2-enedioic acid 2,2-diphenylethylamide {12-[3-(2,2-diphenylethylcarbamoyl)-propionylamino]-dodecyl}-amide)-rotaxane, *E*-2.
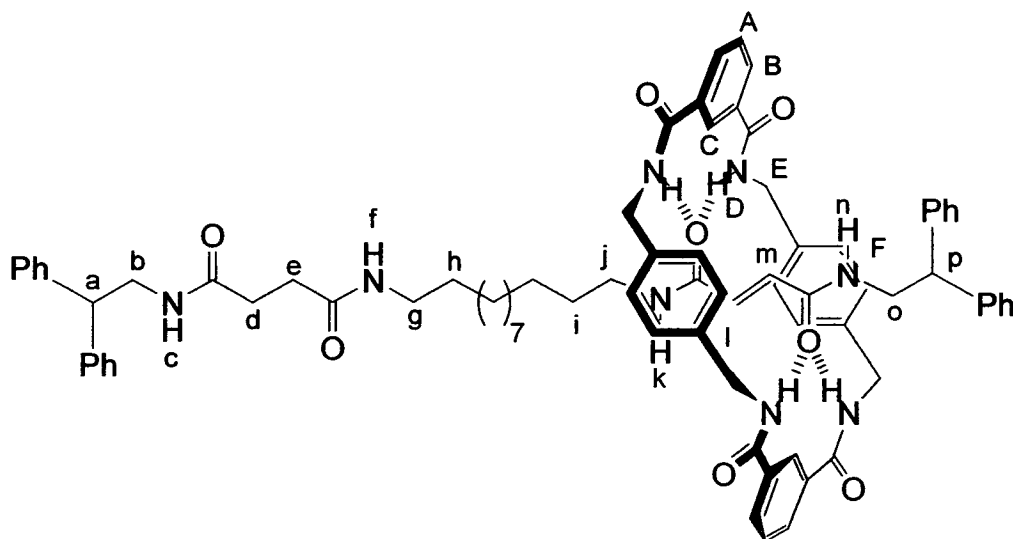

Rotaxane *E*-2 was obtained using the general procedure for the thermal-isomerization from rotaxane *Z*-2 (80% in $C_2D_2Cl_4$, isolated by preparative TLC).

m.p. 186-187°C; ^{1}H NMR (400 MHz, CDCl$_3$, 320K): δ = 8.39 (br t, $^4J(H_C,H_B)$ = 1.2 Hz, 2H, ArCH_C), 8.11 (dd, $^4J(H_B,H_C)$ = 1.2 Hz, $^3J(H_B,H_A)$ = 7.6 Hz, 4H, ArCH_B), 7.63 (br t, $^3J(H,H)$ = 5.4 Hz, 4H, NH_D), 7.71 (t, $^3J(H_A,H_B)$ = 7.6 Hz, 2H, ArCH_A), 7.30-7.14 (m, 21H, ArCH (thread) and NH_k), 6.93 (s, 8H, ArCH_F), 6.86 (br t, $^3J(H,H)$ = 5.7 Hz, 1H, NH_n), 6.27 (br t, $^3J(H,H)$ = 5.7 Hz, 1H, NH_f), 6.13 (br t, $^3J(H,H)$ = 5.7 Hz, 1H, NH_c), 5.89 (d, $^3J(H,H)$ = 15.1 Hz, 1H, CH_l or CH_m), 5.72 (d, $^3J(H,H)$ = 15.1 Hz, 1H, CH_l or CH_m), 4.42 (br d, $^3J(H,H)$ = 5.4 Hz, 8H, CH_E), 4.20 (t, $^3J(H,H)$ = 7.8 Hz, 1H, CH_p or CH_a), 4.15 (t, $^3J(H,H)$ = 7.7 Hz, 1H, CH_p or CH_a), 3.85-3.78 (m, 4H, CH_b and CH_o), 3.14-3.06 (m, 4H, CH_g and CH_j), 2.08 (br s, 4H, CH_d and CH_e), 1.50-1.39 (m, 4H, CH_h and CH_i) and 1.30-1.15 (m, 16H, -CH_2- (alkyl chain)); ^{13}C NMR (100 MHz, CDCl$_3$) δ 172.4 (*C*O succinic), 172.2 (*C*O succinic), 166.7 (*C*O macrocycle), 165.6 (*C*O fumaric),

165.3 (*C*O fumaric), 141.9 (Ar*C*-CH- (ipso, thread)), 141.6 (Ar*C*-CH (ipso, thread)), 136.9 (Ar*C*-CH$_E$), 133.6 (Ar*C*-CO), 131.3 (*C*H$_B$), 130.7 (*C*H$_l$ or *C*H$_m$), 128.9 (*C*H$_l$ or *C*H$_m$), 129.1 (Ar*C*H$_F$), 129.0 (*C*H$_A$), 128.9 (Ar*C*H (meta thread)), 128.7 (Ar*C*H (meta thread)), 127.9 (Ar*C*H (ortho thread)), 127.8 (Ar*C*H (ortho thread)), 127.1 (Ar*C*H (para thread), 126.8 (Ar*C*H (para thread), 124.6 (*C*H$_C$), 50.5 (*C*H$_p$ or *C*H$_a$), 50.4 (*C*H$_a$ or *C*H$_p$), 44.8 (*C*H$_b$ or *C*H$_o$), 44.2 (*C*H$_E$), 43.9 (*C*H$_b$ or *C*H$_o$), 40.0 (*C*H$_g$ or *C*H$_j$), 39.6 (*C*H$_g$ or *C*H$_j$), 31.8 (-*C*H$_2$-), 31.7 (-*C*H$_2$-), 29.7 (-*C*H$_2$-), 29.4 (-*C*H$_2$-), 29.3 (-*C*H$_2$-), 29.2 (-*C*H$_2$-), 29.1 (-*C*H$_2$-), 29.0 (-*C*H$_2$-), 26.9 (-*C*H$_2$-) and 26.7 (-*C*H$_2$-); MS(FAB): *m/z* = 1289 [(M+H)$^+$]; Anal. Calcd. for C$_{80}$H$_{88}$N$_8$O$_8$: C 74.51, H 6.88, N 8.69. Found: C 74.62, H 7.01, N 7.12.

(*E*)-*N*-{12-[3-(2,2-Diphenylethylcarbamoyl)acryloylamino]-dodecyl}-succinamic acid 2,2-diphenylethyl ester, *E*-5.
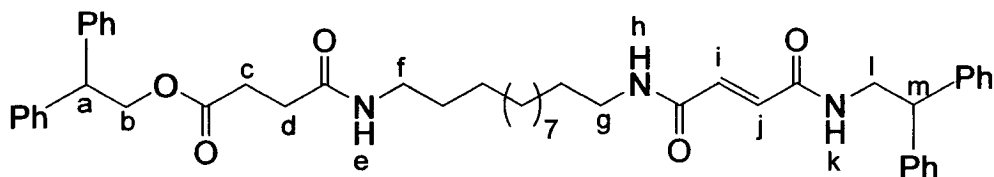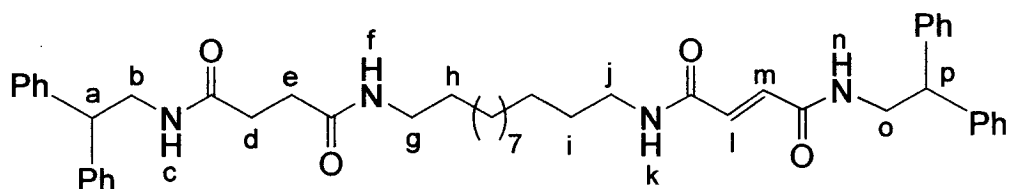

To a stirred solution of **S10** (0.52 g, 0.89 mmol) in anydrous CHCl$_3$ (30 mL) was added TFA (5 mL) and the solution allowed to stir for 2 h. The solution was reduced in volume and the excess of TFA removed *in vacuo* over 16 h. The resulting oil was taken up in anydrous DMF (40 mL) and **S12** (0.36 g, 1.21 mmol), 4-DMAP (0.20 g, 1.65 mmol) and EDCI·HCl (0.42 g, 2.17 mmol) added in order under argon at 0°C whilst stirring. After 16 h the solution was reduced in volume and the resulting oil taken up with CHCl$_3$ and washed with 0.5N HCl (3 x 100 mL). The organic layer was dried over anhydrous MgSO$_4$, filtered and the filtrate reduced in volume to obtain a compound that was

purified by column cromatography (CH_2Cl_2/EtOAc) to obtain the desidered compound as a colourless solid (*E*-**5**, 0.51 g, 76%).

Compound *E*-**5** has been also obtained using the general procedure for the thermal-isomerization from thread *Z*-**5** (75% in $C_2D_2Cl_4$). m.p. 151-152 °C; ^{1}H NMR (400 MHz, CDCl$_3$): δ = 7.34-7.18 (m, 20H, ArC*H*), 6.86 (d, ^3J(H,H) = 14.8 Hz, 1H, C*H*$_i$ or C*H*$_j$), 6.71 (d, ^3J(H,H) = 14.8 Hz, 1H, C*H*$_i$ or C*H*$_j$), 6.05 (br t, ^3J(H,H) = 5.7 Hz, 1H, N*H*$_h$), 5.91 (br t, ^3J(H,H) = 5.7 Hz, 1H, N*H*$_k$), 5.59 (br t, ^3J(H,H) = 5.7 Hz, 1H, N*H*$_e$), 4.64 (d, ^3J(H,H) = 7.7 Hz, 2H, C*H*$_b$), 4.34 (t, ^3J(H,H) = 7.7 Hz, 1H, C*H*$_a$), 4.21 (t, ^3J(H,H) = 8.0 Hz, 1H, C*H*$_m$), 3.98 (dd, ^3J(H,H) = 8.0 Hz, ^3J(H,H) = 5.7 Hz, 2H, C*H*$_l$), 3.30 (td, ^3J(H,H) = 7.0 Hz, ^3J(H,H) = 5.7 Hz, 2H, C*H*$_g$), 3.17 (td, ^3J(H,H) = 7.0 Hz, ^3J(H,H) = 5.7 Hz, 2H, C*H*$_f$), 2.58 (t, ^3J(H,H) = 7.0 Hz, 2H, C*H*$_c$), 2.34 (t, ^3J(H,H) = 7.0 Hz, 2H, C*H*$_d$), 1.55-1.38 (m, 4H, -C*H*$_2$-CH$_f$ and -C*H*$_2$-CH$_g$) and 1.34-1.17 (m, 16H, -C*H*$_2$- (alkyl chain)); ^{13}C NMR (100 MHz, CDCl$_3$): δ = 173.1 (*C*H$_c$-*C*O-O), 171.7 (-*C*O-NH$_e$), 165.2 (*C*O fumaric), 164.9 (*C*O fumaric), 141.8 (Ar*C*- (ipso)), 140.9 (Ar*C*- (ipso)), 132.8 (*C*H$_i$ or *C*H$_j$), 132.0 (*C*H$_i$ or *C*H$_j$), 128.5 (Ar*C*H (meta)), 128.4 (Ar*C*H (meta)), 128.0 (Ar*C*H (ortho)), 127.9 (Ar*C*H (ortho)), 126.7 (Ar*C*H (para)), 126.6 (Ar*C*H (para)), 66.9 (*C*H$_b$), 50.2 (*C*H$_m$ or *C*H$_a$), 49.7 (*C*H$_m$ or *C*H$_a$), 44.2 (*C*H$_l$), 39.7 (*C*H$_g$ or *C*H$_f$), 39.4 (*C*H$_g$ or *C*H$_f$), 30.6 (*C*H$_c$), 29.5 (*C*H$_d$), 29.3-29.0 (-*C*H$_2$-), 28.9 (-*C*H$_2$-) and 26.8 (-*C*H$_2$-); ^{1}H NMR (400 MHz, d_6-DMSO): δ = 8.51 (t, ^3J(H,H) = 5.9 Hz, 1H, N*H*$_h$), 8.39 (t, ^3J(H,H) = 5.6 Hz, 1H, N*H*$_k$), 7.82 (t, ^3J(H,H) = 5.8 Hz, 1H, N*H*$_e$), 7.36-7.28 (m, 16H, ArC*H*), 7.27-7.19 (m, 4H, ArC*H*), 6.81 (d, ^3J(H,H) = 14.9 Hz, 1H, C*H*$_i$ or C*H*$_j$), 6.76 (d, ^3J(H,H) = 14.9 Hz, 1H, C*H*$_i$ or C*H*$_j$), 4.61 (d, ^3J(H,H) = 7.6 Hz, 2H, C*H*$_b$), 4.35 (t, ^3J(H,H) = 7.6 Hz, 1H, C*H*$_a$), 4.25 (t, ^3J(H,H) = 7.8 Hz, 1H, C*H*$_m$), 3.84 (dd, ^3J(H,H) = 7.8 Hz, ^3J(H,H) = 5.6 Hz, 2H, C*H*$_l$), 3.12 (br dt, 2H, C*H*$_g$), 3.02 (br dt, 2H, C*H*$_f$), 2.41 (t, ^3J(H,H) = 7.1 Hz, 2H, C*H*$_c$), 2.28 (t, ^3J(H,H) = 7.1 Hz, 2H, C*H*$_d$), 1.44-1.34 (m, 4H, -C*H*$_2$-CH$_f$ and -CH$_2$-CH$_g$) and 1.30-1.17 (m, 16H, -C*H*$_2$- (alkyl chain)); MS (FAB): *m/z* = 758 [(M+H)$^+$]; Anal. Calcd. for $C_{48}H_{59}N_3O_5$: C 76.06, H 7.85, N 5.54. Found: C 76.21, H 8.08, N 5.49.

(E)-But-2-enedioic acid 2,2-diphenyl ethylamide{12-[3-(2,2-diphenylethylcarbamoyl)-propionylamino]-dodecyl}-amide, *E*-6.


To a stirred solution of **S12** (0.50 g, 1.69 mmol) in CH$_2$Cl$_2$ was added thionyl chloride (0.124 mL, 1.69 mmol). The solution was heated until complete dissolution of **S12** had occurred and the resulting solution was added dropwise to a solution of **S14** (0.81 g, 1.69 mmol) and Et$_3$N (0.17 g, 1.69 mmol) in CH$_2$Cl$_2$ at 0 °C and allowed to stir for 30 min. The solution was then filtered and the solid recrystallized from hot DMSO to give a colourless solid (*E*-**6**, 0.56 g, 44%). m.p. 213-214 °C; ^{1}H NMR (400 MHz, d_6-DMSO, 400K): δ = 8.12 (br t, ^3J(H,H) = 5.7 Hz, 1H, N*H*$_n$), 8.01 (br t, ^3J(H,H) = 5.7 Hz, 1H, N*H*$_k$), 7.52 (br t, ^3J(H,H) = 5.7 Hz, 1H, N*H*$_c$), 7.40 (br t, ^3J(H,H) = 5.7 Hz, 1H, N*H*$_f$), 7.32-7.15 (m, 20H ArC*H*), 6.76 (d, ^3J(H,H) = 15.3 Hz, 1H, C*H*$_l$ or C*H*$_m$), 6.71 (d, ^3J(H,H) = 15.3 Hz, 1H, C*H*$_l$ or C*H*$_m$), 4.26 (t, ^3J(H,H) = 8.0 Hz, 1H, C*H*$_p$), 4.20 (t, ^3J(H,H) = 8.0 Hz, 1H, C*H*$_a$), 3.82 (dd, ^3J(H,H) = 8.0 Hz, ^3J(H,H) = 5.7 Hz, 2H, C*H*$_o$), 3.70 (dd, ^3J(H,H) = 8.0 Hz, ^3J(H,H) = 5.7 Hz, 2H, C*H*$_b$), 3.12 (td, ^3J(H,H) = 7.0 Hz, ^3J(H,H) = 5.7 Hz, 2H, C*H*$_j$), 3.00 (td, ^3J(H,H) = 7.0 Hz, ^3J(H,H) = 5.7 Hz, 2H, C*H*$_g$), 2.22 (s, 4H, C*H*$_d$ and C*H*$_e$), 1.48-1.34 (m, 4H, C*H*$_h$ and C*H*$_i$) and 1.32-1.20 (br m, 16H, -C*H*$_2$- (alkyl chain)); ^{13}C NMR was not possible to be recorded for the low solubility of the compound; MS (FAB): m/z = 757 [(M+H)$^+$]; Anal. Calcd. for C$_{48}$H$_{60}$N$_4$O$_4$: C 76.16, H 7.99, N 7.40. Found: C 75.89, H 8.04, N 7.65.

(*E*)-Hexanedioic acid 2,2–diphenylethylamide{12-[3-(2,2-diphenylethylcarbamoyl)-acryloylamino]-dodecyl}-amide, *E*-7.
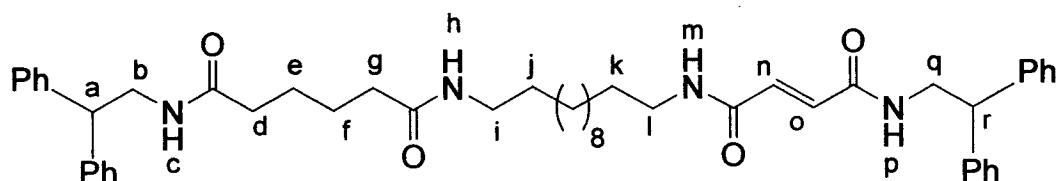
A solution of **S12** (0.053 g, 0.18 mmol), **S18** (0.1 g, 0.20 mmol) and 4-DMAP (0.02 g, 0.18 mmol) in CHCl$_3$ (10 mL) was stirred at 0 °C for 10 mins. EDCI·HCl (0.034 g, 0.18 mmol) was added and the reaction mixture allowed to stir for 16 h at rt. The reaction was diluted with CHCl$_3$ (10 mL) and the combined organic phase washed with 1N HCl (3 x 10 mL), saturated NaHCO$_3$ (3 x 10 mL) and brine (1 x 10 mL). The organic layer was dried over anhydrous MgSO$_4$, filtered and concentrated to give the product as a colourless solid (*E*-7, 69 mg, 45%). ^{1}H NMR (400 MHz, d_6-DMSO, 400K): δ = 8.47 (br t, 1H, NH_p), 8.34 (br t, 1H, NH_m), 7.82 (br t, 1H, NH_c), 7.69 (br t, 1H, NH_h), 7.31-7.19 (m, 20H, ArCH), 6.80 (d, ^3J(H,H) = 15.3 Hz, 1H, CH_n or CH_o), 6.73 (d, ^3J(H,H) = 15.3 Hz, 1H, CH_n or CH_o), 4.24 (t, ^3J(H,H) = 8.0 Hz, 1H, CH_r), 4.19 (t, ^3J(H,H) = 8.0 Hz, 1H, CH_a), 3.82 (dd, ^3J(H,H) = 8.0 Hz, ^3J(H,H) = 5.7 Hz, 2H, CH_q), 3.69 (dd, ^3J(H,H) = 8.0 Hz, ^3J(H,H) = 5.7 Hz, 2H, CH_b), 3.10 (td, ^3J(H,H) = 7.0 Hz, ^3J(H,H) = 5.7 Hz, 2H, CH_l), 3.01 (td, ^3J(H,H) = 7.0 Hz, ^3J(H,H) = 5.7 Hz, 2H, CH_i), 1.96 (m, 4H, CH_d and CH_g), 1.35 (m, 8H, CH_j, CH_k, CH_e and CH_f), 1.25 (m, 16H. CH_2 (alkyl chain)). ^{13}C NMR was not possible to be recorded for the low solubility of the compound. MS(FAB): *m/z* = 785 [(M+H)$^+$]; Anal. Calcd. for C$_{50}$H$_{64}$N$_4$O$_4$: C 76.50, H 8.22, N 7.14. Found: C 76.75, H 8.35, N 7.24.

[2]-(1,7,14,20-Tetraaza-2,6,15,19-tetraoxo-3,5,9,12,16,18,22,25-tetrabenzocyclohexacosane)-((Z)-N-{12-[3-(2,2-diphenylethylcarbamoyl)-acryloylamino]-dodecyl}-succinamic acid 2,2-diphenylethyl ester)-rotaxane, Z-1.
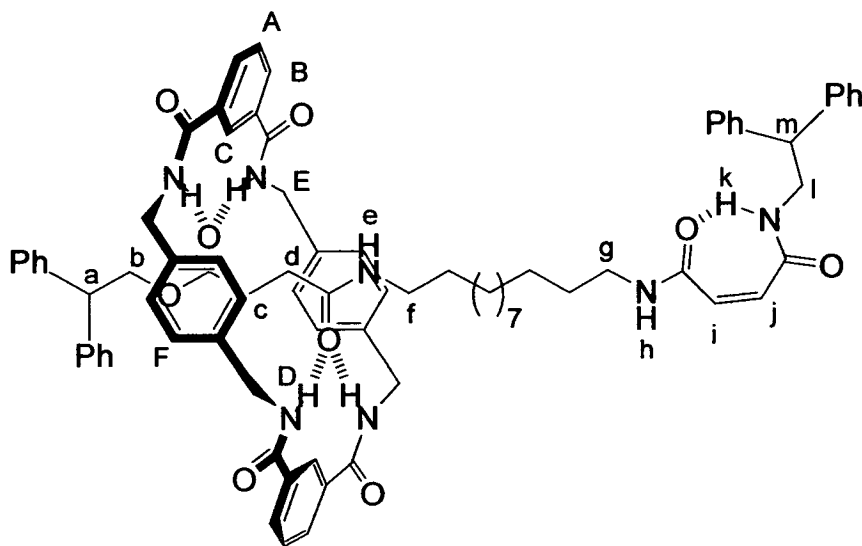
Rotaxane *Z*-1 was obtained using the general procedure for the photo-isomerization from rotaxane *E*-1. The crude was subjected to column chromatography using a solvent gradient of CH_2Cl_2 to CH_2Cl_2/EtOAc (70/30) to obtain the desired compound as a colourless solid (*Z*-1, 35 mg, 54%). m.p. 152-154 °C; ^{1}H NMR (400 MHz, CDCl$_3$): δ = 8.55 (br t, ^3J(H,H) = 5.7 Hz, 1H, NH_h), 8.28 (br t, ^4J(H$_C$,H$_B$) = 1.2 Hz, 2H, ArCH_C), 8.18 (dd, ^4J(H$_B$,H$_C$) = 1.2 Hz, ^3J(H$_B$,H$_A$) = 7.8 Hz, 4H, ArCH_B), 7.82 (br t, ^3J(H,H) = 5.7 Hz, 1H, NH_k), 7.60 (t, ^3J(H$_A$,H$_B$) = 7.8 Hz, 2H, ArCH_A), 7.38 (br dd, 4H, NH_D), 7.32-7.10 (m, 20H, ArCH), 7.00 (s, 8H, ArCH_F), 6.36 (t, ^3J(H,H) = 5.7 Hz, 1H, NH_e), 5.90 (d, ^3J(H,H) = 13.4 Hz , 1H, CH_i or CH_j), 5.82 (d, ^3J(H,H) = 13.4 Hz, 1H, CH_i or CH_j), 4.55 (dd, ^2J(H$_E$,H'$_E$) = 14.1 Hz, ^3J(H$_E$,H$_D$) = 5.8 Hz, 4H, CHH'$_E$), 4.44 (d, ^3J(H,H) = 7.7 Hz, 2H, CH_b), 4.40 (dd, ^2J(H$_E$,H'$_E$) = 14.1 Hz, ^3J(H'$_E$,H$_D$) = 5.0 Hz, 4H, CHH'_E), 4.20 (m, CH_a and CH_m), 3.88 (dd, ^3J(H,H) = 8.0 Hz, ^3J(H,H) = 5.7 Hz, 2H, CH_l), 3.04 (td, ^3J(H,H) = 7.0 Hz, ^3J(H,H) = 5.7 Hz, 2H, CH_g), 2.94 (td, ^3J(H,H) = 7.0 Hz, ^3J(H,H) = 5.7

Hz, 2H, CH_f), 1.47 (m, 2H, CH_c), 1.16 (m, 2H, CH_d),1.43-1.34 (m, 4H, CH_2-CH_f and CH_2-CH_g) and 1.30-1.13 (m, 18H, -CH_2- (alkyl chain)); ^{13}C NMR (100 MHz, CD$_2$Cl$_2$): δ = 174.7 (CH$_c$-CO-O), 172.6, (-CO-NH$_e$) 166.9 (CO macrocycle), 166.0 (CO maleic), 165.4 (CO maleic), 142.7 (ArC-CH- (ipso thread)), 141.9 (ArC-CH- (ipso thread)), 138.5 (ArC-CH$_E$), 135.0 (ArC-CO), 134.2 (CH$_i$ or CH$_j$), 132.1 (CH$_i$ or CH$_j$), 132.0 (ArCH$_B$), 130.0 (ArCH$_A$), 129.8 (ArCH$_F$), 129.5 (ArCH (meta thread)), 129.4 (ArCH (meta thread)), 128.8 (ArCH (ortho thread)), 128.6 (ArCH (ortho thread)), 127.8 (ArCH (para thread)), 127.6 (ArCH (para thread)), 124.8 (ArCH$_C$), 68.1 (CH$_b$), 51.2 (CH$_a$ or CH$_m$), 50.5 (CH$_a$ or CH$_m$), 44.9 (CH$_l$), 44.8 (CH$_E$), 40.7 (CH$_f$ or CH$_g$), 40.6 (CH$_f$ or CH$_g$), 30.2 (CH$_c$), 30.1 (CH$_d$), 29.9 (-CH$_2$-), 29.8-29.6 (-CH$_2$-), 29.5 (-CH$_2$-), 29.4 (-CH$_2$-), 27.5 (-CH$_2$-) and 27.3 (-CH$_2$-); MS (FAB): m/z = 1291 [(M+H)$^+$]; Anal. Calcd. for C$_{80}$H$_{87}$N$_7$O$_9$: C 74.45, H 6.79, N 7.60. Found: C 74.62, H 6.68, N 7.49.

[2]-(1,7,14,20-Tetraaza-2,6,15,19-tetraoxo-3,5,9,12,16,18,22,25-tetrabenzocyclohexacosane)-((Z)-but-2-enedioic acid 2,2-diphenylethylamide {12 -[3-(2,2-diphenylethylcarbamoyl)-propionylamino]-dodecyl}-amide)-rotaxane, Z-2.
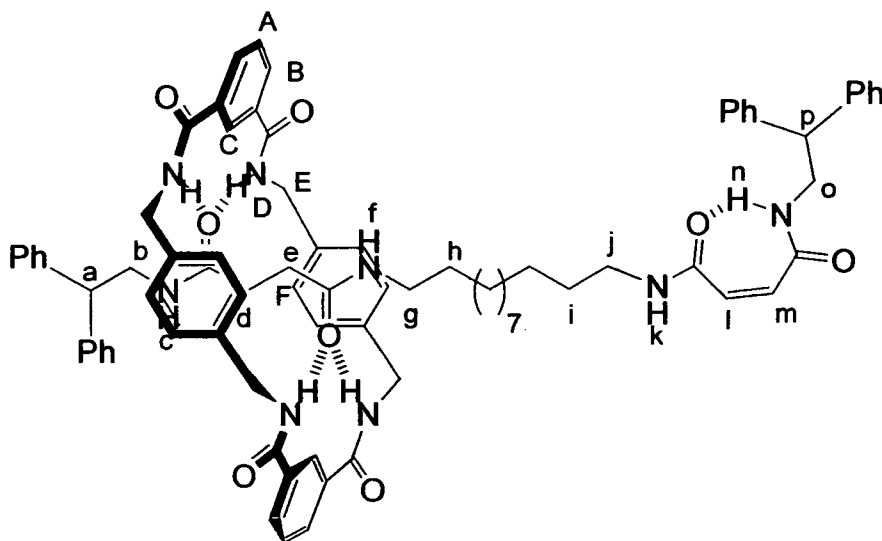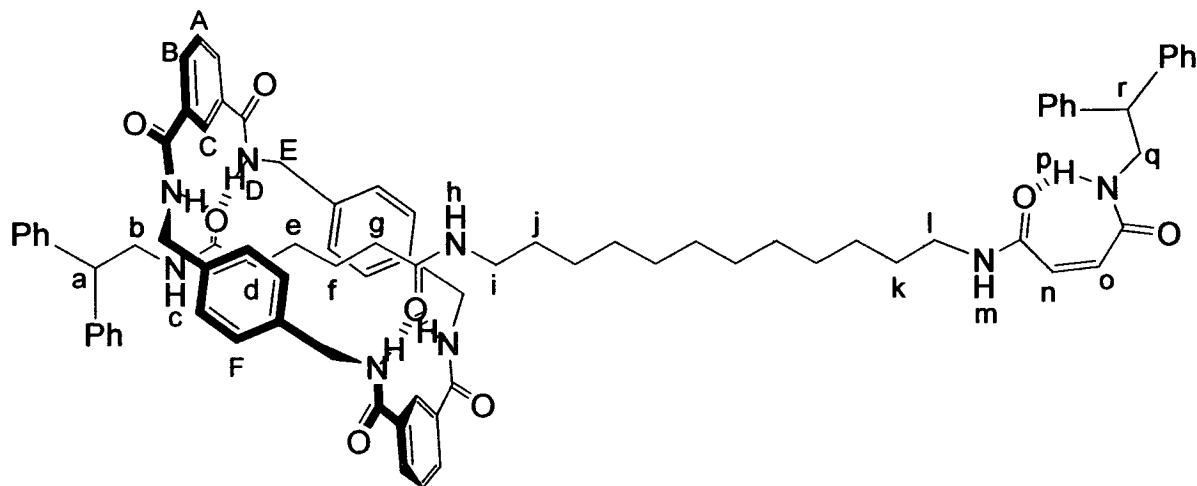
Rotaxane Z-2 was obtained using the general procedure for the preparation of the benzylic amide macrocycle containing [2]rotaxane from the thread Z-6 (0.50 g, 0.66 mmol). Column chromatography of the crude obtained using a solvent gradient of CHCl$_3$ to CHCl$_3$/MeOH (95/5) gave a colourless solid (Z-2, 0.34 g, 40%).

Rotaxane Z-2 was also obtained using the general procedure for the photo-isomerization from rotaxane E-2 (48% by ^{1}H NMR). m.p. 171-172 °C; ^{1}H NMR (400 MHz, CDCl$_3$): δ = 8.67 (br t, ^3J(H,H) = 5.7 Hz, 1H, NH$_k$), 8.31 (br t, ^4J(H$_C$,H$_B$) = 1.2 Hz, 2H, ArCH$_C$), 8.16 (br t, ^3J(H,H) = 5.7 Hz, 1H, NH$_n$), 8.14 (dd, ^4J(H$_B$,H$_C$) = 1.2 Hz, ^3J(H$_B$,H$_A$) = 7.8 Hz, 4H, ArCH$_B$), 7.67 (br t, ^3J(H,H) = 5.4 Hz, 4H, NH$_D$), 7.56 (t, ^3J(H$_A$,H$_B$) = 7.8 Hz, 2H, ArCH$_A$), 7.31-7.10 (m, 20H, ArCH (thread)), 7.02 (s, 8H, ArCH$_F$), 6.53 (br t, ^3J(H,H) = 5.7 Hz, 1H, NH$_f$), 6.15 (br t, ^3J(H,H) = 5.7 Hz, 1H, NH$_c$), 5.92 (d, ^3J(H,H) = 13.6 Hz, 1H, CH$_l$ or CH$_m$), 5.83 (d, ^3J(H,H) = 13.6 Hz, 1H, CH$_l$ or CH$_m$), 4.50 (dd, ^2J(H$_E$,H'$_E$) = 14.1 Hz, ^3J(H$_E$, H$_D$) = 5.4 Hz, 4H, CHH'$_E$), 4.43 (dd, ^2J(H$_E$,H'$_E$) = 14.1 Hz, ^3J(H'$_E$, H$_D$) = 5.4 Hz, 4H, CHH'$_E$), 4.23 (t, ^3J(H,H) = 8.0 Hz, 1H, CH$_p$), 4.06 (t, ^3J(H,H) = 8.0 Hz, 1H, CH$_a$), 3.90 (dd, ^3J(H,H) = 8.0 Hz, ^3J(H,H) = 5.7 Hz, 2H, CH$_o$), 3.67 (dd, ^3J(H,H) = 8.0 Hz, ^3J(H,H) = 5.7 Hz, 2H, CH$_b$), 3.15 (td, ^3J(H,H) = 7.0 Hz, ^3J(H,H) = 5.7 Hz, 2H, CH$_j$), 2.99 (td, ^3J(H,H) = 7.0 Hz, ^3J(H,H) = 5.7 Hz, 2H, CH$_g$), 1.48 (m, 2H, CH$_i$), 1.38 (m, 2H, CH$_h$), 1.33-1.16 (m, 16H, -CH$_2$- (alkyl chain)) and 1.07 (m, 4H, CH$_d$ and CH$_e$); ^{13}C NMR (100 MHz, CDCl$_3$): δ = 173.0 (CO succinic), 172.9 (CO succinic), 166.6 (CO macrocycle), 165.0 (CO maleic), 164.7 (CO maleic), 141.7 (ArC-CH (ipso thread)), 141.6 (ArC-CH (ipso thread)), 137.5 (ArC-CH$_E$), 133.8 (ArC-CO), 133.1 (CH$_l$ or CH$_m$), 131.5 (ArCH$_B$), 131.4 (CH$_l$ or CH$_m$), 129.2 (ArCH$_F$), 129.1 (ArCH$_A$), 128.8 (ArCH (meta thread)), 128.7 (ArCH (meta thread)), 127.9 (ArCH (ortho thread)), 127.8 (ArCH (ortho thread)), 127.1 (ArCH (para thread)), 126.8 (ArCH (para thread)), 124.0 (ArCH$_C$), 50.5 (CH$_p$), 50.3 (CH$_a$), 44.2 (CH$_o$), 44.1 (CH$_b$), 44.0 (CH$_E$), 39.7 (CH$_j$ and CH$_g$), 29.8 (CH$_d$ or CH$_e$), 29.4 (CH$_d$ or CH$_e$), 29.3 (-CH$_2$-), 29.2 (-CH$_2$-), 29.1 (-CH$_2$-), 29.0 (-CH$_2$-), 28.8 (-CH$_2$-) and 28.7 (-CH$_2$-); MS (FAB): m/z = 1289 [(M+H)$^+$]; Anal. Calcd. for C$_{80}$H$_{88}$N$_8$O$_8$: C 74.51, H 6.88, N 8.69. Found C 74.69, H 6.94, N 8.76.

[2]-(1,7,14,20-Tetraaza-2,6,15,19-tetraoxo-3,5,9,12,16,18,22,25-terabenzocyclohexacosane)-((Z)-hexanedioic acid (2,2-diphenylethyl)-amide{12-[3-(2,2–diphenylethylcarbamoyl)-acryloylamino]-dodecyl}-amide)-rotaxane, Z-3.

Rotaxane Z-3 has been made using the general procedure for the formation of the benzylic amide macrocycle containing [2]rotaxane from thread Z-7 (1.5 g, 1.9 mmol). Column chromatography of the crude product (silica gel, 3:97, MeOH/CHCl₃) gave the product as a colourless solid (Z-3, 0.5 g, 20 %). m.p. 115 °C; ^{1}H NMR (400 MHz, CDCl₃): δ = 8.82 (br t, ^3J(H,H) = 5.7 Hz, 1H, NH$_m$), 8.24 (br s, 3H, ArCH$_C$ and NH$_p$), 8.13 (dd, ^4J(H$_B$,H$_C$) = 1.5 Hz, ^3J(H$_B$,H$_A$) = 7.8 Hz, 4H, ArCH$_B$), 7.63 (t, ^3J(H,H) = 5.3 Hz, 4H, NH$_D$), 7.53 (t, ^3J(H$_A$,H$_B$) = 7.8 Hz, 2H, ArCH$_A$), 7.32-7.15 (m, 20H, ArCH), 7.05 (s, 8H, ArCH$_F$), 6.20 (br t, ^3J(H,H) = 5.6 Hz, 1H, NH$_h$), 6.03 (br t, ^3J(H,H) = 5.1 Hz, 1H, NH$_c$), 5.79 (d, ^3J(H,H) = 13.4 Hz, 1H, CH$_n$ or CH$_o$), 5.71 (d, ^3J(H,H) = 13.4 Hz, 1H, CH$_n$ or CH$_o$), 4.55 (dd, ^2J(H$_E$, H'$_E$) = 14.4 Hz, ^3J(H$_E$, H$_D$) = 5.3 Hz, 4H, CHH'$_E$), 4.45 (dd, ^2J(H$_E$, H'$_E$) = 14.4 Hz, ^3J(H'$_E$, H$_D$) = 5.3 Hz, 4H, CHH'$_E$), 4.19 (t, ^3J(H,H) = 7.8 Hz, 1H, CH$_r$), 4.13 (t, ^3J(H,H) = 7.8 Hz, 1H, CH$_a$), 3.87 (2d, ^3J(H,H) =7.8 Hz, 2H, CH$_q$), 3.66 (2d, ^3J(H,H) = 7.8 Hz, 2H, CH$_b$), 2.94 (m, 4H, CH$_i$ and CH$_j$), 1.41 (br m, 2H, -CH₂-, (alkyl chain)), 1.33 (br m, 4H, CH$_d$ and CH$_g$), 1.25-1.18 (m, 22H, -CH₂- (alkyl

chain)), 0.76 (br m, 4H, CH_d and CH_g); ^{13}C NMR (100 MHz, CDCl$_3$): δ = 173.4 (*CO* adipamide), 173.3 (*CO* adipamide), 166.4 (*CO* macrocycle), 165.4 (*CO* maleic), 164.6 (*CO* maleic), 142.1 (Ar*C*- (ipso thread)), 141.5 (Ar*C*- (ipso thread)), 137.6 (Ar*C*-CH$_E$), 133.9 (Ar*C*-CO-), 133.2 (*C*H$_n$ or *C*H$_o$), 131.9 (*C*H$_n$ or *C*H$_o$), 131.8 (Ar*C*H$_B$), 131.4 (Ar*C*H$_F$), 129.2 (Ar*C*H$_A$), 128.4 (Ar*C*H (meta thread)), 128.0 (Ar*C*H (ortho thread)), 126.91 (Ar*C*H (para thread)), 124.4 (*C*H$_c$), 50.7 (*C*H$_r$), 50.2 (*C*H$_a$), 44.4 (*C*H$_q$) , 44.3 (*C*H$_b$), 44.0 (*C*H$_E$), 40.1 (*C*H$_l$), 39.7 (*C*H$_i$), 35.5 (*C*H$_d$ or *C*H$_g$), 35.4 (*C*H$_d$ or *C*H$_g$), 29.4 (-*C*H$_2$-), 29.3 (-*C*H$_2$-), 29.2 (-*C*H$_2$-), 29.1 (-*C*H$_2$-), 29.0 (-*C*H$_2$-), 28.9 (-*C*H$_2$-), 28.6 (-*C*H$_2$-), 26.8 (-*C*H$_2$-), 26.7 (-*C*H$_2$-), 24.7 (-*C*H$_2$-) and 24.5 (-*C*H$_2$-); HRMS (FAB, NBA matrix) Calcd. for C$_{82}$H$_{93}$N$_8$O$_8$ [(M+H)$^+$] 1317.71164. Found: 1317.70829.

(*Z*),*N*-{12-[3-(2,2-Diphenyl-ethylcarbamoyl)-acryloylamino]-dodecyl}-succinamic acid 2,2-diphenylethyl ester, *Z*-5.
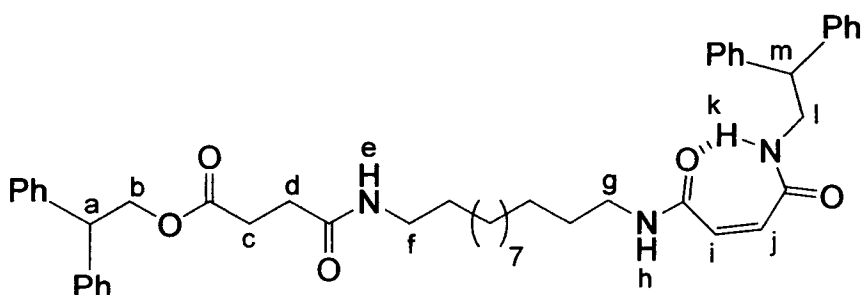
To a stirred solution of **S10** (0.25 g, 0.43 mmol) in anydrous CHCl$_3$ (30 mL) was added TFA (5 mL) and the solution stirred for 2 h. The solution was reduced in volume and the excess of TFA removed *in vacuo* over 16 h. The resulting oil was taken up in anydrous CHCl$_3$ (200 mL) and Et$_3$N (1 mL), **S8** (0.14 g, 0.47 mmol) and EDCI·HCl (0.10 g, 0.51 mmol) added sequentially under cooling with an ice bath. After 16 h the solution was reduced in volume and the resulting oil taken up with CHCl$_3$ and washed with 0.5N HCl (3 x 100 mL). The organic layer was dried over anhydrous MgSO$_4$, filtered and the

filtrate reduced in volume to give a colourless solid that was purified by column chromatography CHCl₃/MeOH (90/10) (Z-5, 0.23 g, 70%).

Compound Z-5 has been also obtained using the general procedure for the photo-isomerization from the thread E-5 (57% by ^{1}H NMR). m.p. 54-56 °C; ^{1}H NMR (400 MHz, CDCl₃): δ = 8.45 (br t, ^3J(H,H) = 5.7 Hz, 1H, NH$_h$), 7.91 (br t, ^3J(H,H) = 5.7 Hz, 1H, NH$_k$), 7.28-7.08 (m, 20H, ArCH), 5.90 (d, ^3J(H,H) = 13.4 Hz, 1H, CH$_i$ or CH$_j$), 5.82 (d, ^3J(H,H) = 13.4 Hz, 1H, CH$_i$ or CH$_j$), 5.53 (br t, ^3J(H,H) = 5.7 Hz, 1H, NH$_e$), 4.55 (d, ^3J(H,H) = 7.7 Hz, 2H, CH$_b$), 4.27 (t, ^3J(H,H) = 7.7 Hz, 1H, CH$_a$), 4.17 (t, ^3J(H,H) = 8.0 Hz, 1H, CH$_m$), 3.87 (dd, ^3J(H,H) = 8.0 Hz, ^3J(H,H) = 5.7 Hz, 2H, CH$_l$), 3.16 (td, ^3J(H,H) = 7.0 Hz, ^3J(H,H) = 5.7 Hz, 2H, CH$_g$), 3.08 (td, ^3J(H,H) = 7.0 Hz, ^3J(H,H) = 5.7 Hz, 2H, CH$_f$), 2.48 (t, ^3J(H,H) = 7.0 Hz, 2H, CH$_c$), 2.24 (t, ^3J(H,H) = 7.0 Hz, 2H, CH$_d$), 1.51-1.40 (m, 2H, CH₂-CH$_g$), 1.40-1.31 (m, 2H, CH₂-CH$_f$), 1.30-1.12 (m, 16H, -CH₂-, (alkyl chain)); ^{13}C NMR (100 MHz, CDCl₃): δ = 173.3 (CH$_c$-CO-O), 171.6 (CO-NH$_e$), 165.4 (CO maleic), 165.0 (CO maleic), 142.2 (ArC- (ipso)), 141.4 (ArC- (ipso)), 133.9 (CH$_i$ or CH$_j$), 131.7 (CH$_i$ or CH$_j$), 129.1 (ArCH- (meta)), 129.0 (ArCH- (meta)), 128.6 (ArCH-(ortho)), 128.4 (ArCH- (ortho)), 127.2 (ArCH- (para)), 67.3 (CH$_b$), 50.7 (CH$_a$), 50.2 (CH$_m$), 44.6 (CH$_l$), 40.2 (CH$_g$ or CH$_f$), 40.0 (CH$_g$ or CH$_f$), 31.4 (CH$_d$ or CH$_c$), 30.1 (CH$_d$ or CH$_c$), 29.9 (-CH₂-), 29.8-29.7 (-CH₂-), 29.6 (-CH₂-), 29.5 (-CH₂-), 27.4 (-CH₂-) and 27.3 (-CH₂-); MS(FAB): m/z = 758 [(M+H)$^+$]; Anal. Calcd. for C₄₈H₅₉N₃O₅: C 76.06, H 7.85, N 5.54. Found: C 76.09, H 8.11, N 5.63.

(Z)-But-2-enedioic   acid   **2,2-diphenylethylamide**   **{12-[3-(2,2-diphenylethylcarbamoyl)-propionylamino]-dodecyl}-amide**, *Z*-6.
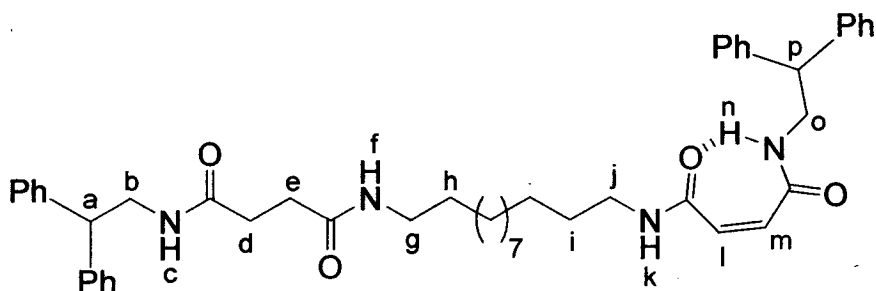
To a stirred solution of **S14** (0.50 g, 1.04 mmol) in anhydrous $CHCl_3$ (50 mL) at 0 °C was added **S8** (0.34 g, 1.15 mmol), 4-DMAP (0.15 g, 1.25 mmol) and EDCI·HCl (0.24 g, 1.25 mmol) and the resulting reaction mixture stirred for 16 h at rt. The solution was then washed with a solution of 1N NaOH (3 x 100 mL), 1N HCl (3 x 100 mL) and H_2O (1 x 100 mL). The organic layer was dried over anhydrous $MgSO_4$, filtered and the solvent removed under reduced pressure to obtain a colourless solid that was subjected to column cromatography using a solvent gradient of CH_2Cl_2 to CH_2Cl_2/MeOH (95/5) (*Z*-6, 0.63 g, 70%). m.p. 68-69 °C; ^{1}H NMR (400 MHz, $CDCl_3$): δ = 8.40 (br t, ^3J(H,H) = 5.7 Hz, 1H, NH_k), 7.80 (br t, ^3J(H,H) = 5.7 Hz, 1H, NH_n), 7.25-7.09 (m, 20H, ArCH), 5.91-6.00 (br m, 2H, NH_c and NH_f), 5.92 (d, ^3J(H,H) = 13.3 Hz, 1H, CH_l or CH_m), 5.83 (d, *J* = 13.3 Hz, 1H, CH_l or CH_m), 4.18 (t, ^3J(H,H) = 8.0 Hz, 1H, CH_p), 4.09 (t, ^3J(H,H) = 8.0 Hz, 1H, CH_a), 3.87 (dd, ^3J(H,H) = 8.0 Hz, ^3J(H,H) = 5.7 Hz, 2H, CH_o), 3.79 (dd, ^3J(H,H) = 8.0 Hz, ^3J(H,H) = 5.7 Hz, 2H, CH_b), 3.16 (td, ^3J(H,H) = 7.0 Hz, ^3J(H,H) = 5.7 Hz, 2H, CH_j), 3.08 (td, ^3J(H,H) = 7.0 Hz, ^3J(H,H) = 5.7 Hz, 2H, CH_g), 2.29 (s, 4H, CH_d and CH_e), 1.45 (m, 2H, CH_i), 1.37 (m, 2H, CH_h) and 1.12-1.29 (m, 16H, -CH_2- (alkyl chain)); ^{13}C NMR (100 MHz, $CDCl_3$): δ = 172.6 (*C*O succinic), 172.4 (*C*O succinic), 165.4 (*C*O maleic), 164.9 (*C*O maleic), 142.2 (Ar*C*- (ipso)), 142.1 (Ar*C*- (ipso)), 133.9 (*C*H_l or *C*H_m), 131.6 (*C*H_l or *C*H_m), 129.1 (Ar*C*H (meta)), 128.4 (Ar*C*H (ortho)), 127.2

(ArC*H* (para)), 51.0 (*C*H$_p$), 50.7 (*C*H$_a$), 44.6 (*C*H$_o$), 44.2 (*C*H$_b$), 40.2 (*C*H$_j$ or *C*H$_g$), 40.0 (*C*H$_g$ or *C*H$_j$), 32.2 (*C*H$_d$ or *C*H$_e$), 32.1 (*C*H$_d$ or *C*H$_e$), 29.9-29.8 (-*C*H$_2$- (alkyl chain)), 29.6-29.5 (-*C*H$_2$- (alkyl chain)), 27.3 (-*C*H$_2$- (alkyl chain)) and 27.2 (-*C*H$_2$- (alkyl chain)); MS (FAB): *m/z* = 757 [(M+H)$^+$]; Anal. Calcd. for C$_{48}$H$_{60}$N$_4$O$_4$: C 76.16, H 7.99, N 7.40. Found: C 75.98, H 8.10, N 7.45.
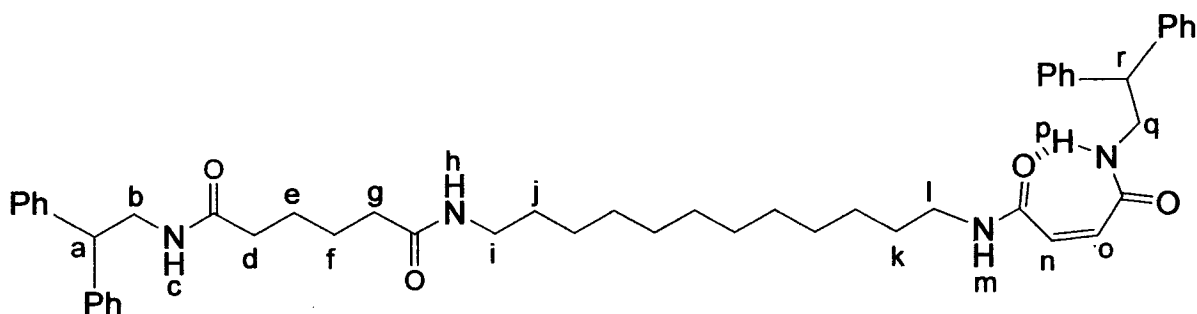
(*Z*)-Hexanedioic acid 2,2-diphenylethylamide{12-[3-(2,2–diphenylethylcarbamoyl)-acryloylamino]-dodecyl}-amide, *Z*-7.

A solution of **S8** (0.16 g, 0.54 mmol), **S18** (0.3 g, 0.59 mmol) and 4-DMAP (0.07 g, 0.54 mmol) in CHCl$_3$ (10 mL) was stirred at 0 °C for 10 mins followed by addition of EDCI·HCl (0.10 g, 0.537 mmol). The reaction mixture was stirred for 16 h at rt. The solution was diluted with CHCl$_3$ (10 mL) and the combined organic phase washed with 1N HCl (3 x 10 mL), saturated NaHCO$_3$ (3 x 10 mL) and brine (1 x 10 mL). The organic layer was dried over anhydrous MgSO$_4$, filtered and the filtrate concentrated to give the product as a colourless solid (*Z*-7, 0.35 g, 83%). ^{1}H NMR (400 MHz, CDCl$_3$): δ = 8.45 (br t, ^3J(H,H) = 5.7 Hz, 1H, N*H*$_m$), 7.88 (br t, ^3J(H,H) = 5.7 Hz, 1H, N*H*$_p$), 7.33-7.20 (m, 20H, ArC*H*), 6.02 (d, ^3J(H,H) = 13.3 Hz, 1H, C*H*$_n$ or C*H*$_o$), 5.92 (d, ^3J(H,H) = 13.3 Hz, 1H, C*H*$_n$ or C*H*$_o$), 5.72 (br m, 2H, N*H*$_c$ and N*H*$_h$), 4.26 (t, ^3J(H,H) = 8.0 Hz, 1H, C*H*$_r$), 4.20 (t, ^3J(H,H) = 8.0 Hz, 1H, C*H*$_a$), 3.96 (dd, ^3J(H,H) = 8.0 Hz, ^3J(H,H) = 5.7 Hz, 2H,

C*H*$_q$), 3.89 (dd, ^3J(H,H) =8.0 Hz, ^3J(H,H) = 5.7 Hz, 2H, C*H*$_b$), 3.23 (m, 4H, C*H*$_i$ and C*H*$_l$), 2.10 (t, ^3J(H,H) = 7.3 Hz, 2H, C*H*$_d$ or C*H*$_g$), 2.07 (t, ^3J(H,H) = 7.3 Hz, 2H, C*H*$_d$ or C*H*$_g$), 1.55-1.47 (m, 8H, C*H*$_e$, C*H*$_f$, C*H*$_j$ and C*H*$_k$), 1.32-1.27 (m, 16H, -C*H*$_2$- (alkyl chain)); ^{13}C NMR (100 MHz, CDCl$_3$): δ = 172.8 (*C*O adipamide), 172.6 (*C*O adipamide), 165.0 (*C*O maleic), 164.6 (*C*O maleic), 141.9 (Ar*C*- (ipso)), 141.8 (Ar*C*-(ipso)), 133.4 (*C*H$_n$ or *C*H$_o$), 131.4 (*C*H$_n$ or *C*H$_o$), 128.7 (Ar*C*H (meta)), 128.6 (Ar*C*H (meta)), 128.0 (Ar*C*H (ortho)), 126.8 (Ar*C*H (para)), 50.6 (*C*H$_r$), 50.3 (*C*H$_a$), 44.2 (*C*H$_q$), 43.8 (*C*H$_b$), 39.8 (*C*H$_l$), 39.5 (*C*H$_i$), 36.2 (*C*H$_d$ or *C*H$_g$), 36.1 (*C*H$_d$ or *C*H$_g$), 29.5 (-*C*H$_2$-), 29.3 (-*C*H$_2$-), 29.1 (-*C*H$_2$-), 29.0 (-*C*H$_2$-), 26.9 (-*C*H$_2$-), 26.8 (-*C*H$_2$-) and 24.9 (-*C*H$_2$-). HRMS (FAB, NBA matrix) Calcd. for C$_{50}$H$_{65}$N$_4$O$_4$ [(M+H)$^+$] 785.50058. Found: 785.49929.

N,N'-bis-(2,2-Diphenylethyl)-succinamide, S1.
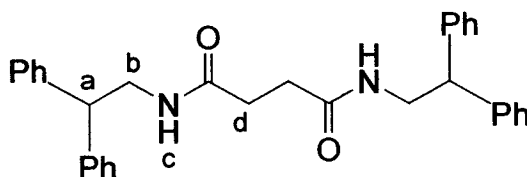
To a stirred solution of 2,2-diphenylethylamine (0.50 g, 2.54 mmol) and Et$_3$N (0.26 g, 2.54 mmol) in CH$_2$Cl$_2$ (20 mL) at 0 °C was added dropwise a solution of succinyl dichloride (0.2 g, 1.27 mmol) in CH$_2$Cl$_2$. The obtained solution was allowed to stir for 3 h and then washed with 1N HCl (2 x 20 mL), 1N NaOH (2 x 20 mL) and H$_2$O (1 x 20 mL). The organic layer was dried over anhydrous MgSO$_4$, filtered and the solvent removed under reduced pressure to obtain a solid that was recrystallized from acetone to give colourless needles (S1, 0.59 g, 97%). m.p. 168-169 °C; ^{1}H NMR (400 MHz, CDCl$_3$): δ = 7.34-7.18 (m, 20H, ArC*H*), 5.84 (br t, ^3J(H,H) = 5.7 Hz, 2H, N*H*$_c$), 4.14 (t, ^3J(H,H) = 8.0 Hz, 2H, C*H*$_a$), 3.83 (dd, ^3J(H,H) = 8.0 Hz, ^3J(H,H) = 5.7 Hz, 4H, C*H*$_b$),

2.28 (s, 4H, CH_d); ^{13}C NMR (100 MHz, CDCl$_3$): δ = 172.0 (CO), 141.8 (ArC-CH-(ipso)), 128.9 (ArCH (meta)), 128.0 (ArCH (ortho)), 126.8 (ArCH (para)), 50.5 (CH$_a$), 43.8 (CH$_b$) and 31.6 (CH$_d$); MS(FAB): m/z = 477 [(M+H)$^+$]; Anal. Calcd. for C$_{32}$H$_{32}$N$_2$O$_2$: C 80.64, H 6.77, N 5.88. Found: C 81.03, H 6.92, N 6.09.

[2]-(1,7,14,20–Tetraaza–2,6,15,19–tetraoxo–3,5,9,12,16,18,22,25– tetrabenzocyclohexacosane)-(_N,N'-bis_-(2,2-diphenyl-ethyl)-succinamide)-rotaxane, S2.
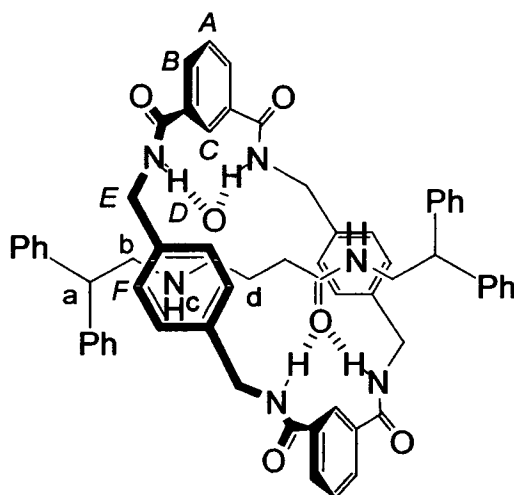
Rotaxane **S2** was obtained using the general procedure for the preparation of benzylic amide macrocycle containing [2]rotaxane from the thread **S1** (0.50 g, 1.05 mmol). The crude obtained was subjected to column cromatography on silica gel [CH$_3$Cl/MeOH (5/95)] to obtain a colourless solid (**S2**, 0.55 g, 52%). m.p. 230-232 °C; ^{1}H NMR (400 MHz, CDCl$_3$): δ = 8.31 (br t, ^4J(H$_C$,H$_B$) = 1.3 Hz, 2H, ArCH$_C$), 8.19 (dd, ^4J(H$_B$,H$_C$) = 1.3 Hz, ^3J(H$_B$,H$_A$) = 7.7 Hz, 4H, ArCH$_B$), 7.62 (t, ^3J(H$_A$,H$_B$) = 7.7 Hz, 2H, ArCH$_A$), 7.47 (br t, ^3J(H,H) = 5.4 Hz, 4H, NH$_D$), 7.30-7.15 (m, 12H, ArCH (para and meta thread)), 7.12 (d, ^3J(H,H) = 7.1 Hz, 8H, ArCH (ortho thread)), 6.85 (s, 8H, ArCH$_F$), 5.87 (br t, ^3J(H,H) = 5.6 Hz, 2H, NH$_c$), 4.43 (d, ^3J(H,H) = 5.4 Hz, 8H, CH$_E$), 4.04 (t, ^3J(H,H) = 7.8

Hz, 2H, CH_a), 3.65 (dd, ^3J(H,H) = 7.8 Hz, ^3J(H,H) = 5.6 Hz, 4H, CH_b) and 0.89 (s, 4H, CH_d); ^{13}C NMR (100 MHz, CDCl$_3$): δ = 172.8 (CO thread), 166.5 (CO macrocycle), 141.4 (ArC-CH- (ipso thread)), 137.6 (ArC-CH$_E$), 134.0 (ArC-CO-), 130.8 (ArCH$_B$), 129.3 (ArCH$_F$), 129.0 (ArCH$_A$), 128.9 (ArCH (meta)), 127.8 (ArCH (ortho)), 127.2 (ArCH (para)), 125.4 (ArCH$_C$), 49.4 (CH$_a$), 44.3 (CH$_b$), 43.9 (CH$_E$) and 28.4 (CH$_d$); MS(FAB): m/z = 1009 [(M+H)$^+$]; Anal. Calcd. for C$_{64}$H$_{60}$N$_6$O$_6$: C 76.17, H 5.99, N 8.33. Found: C 76.28, H 5.85, N 8.16.

X-ray crystallographic data for compound S2.

C$_{76}$H$_{88}$N$_{10}$O$_{10}$, M = 1301.56, crystal size 0.24 × 0.06 × 0.06mm, triclinic P-1, a = 9.8887(5), b = 13.1481(6), c = 15.3131(7) Å, α = 108.0300(10), β = 106.0530(10), γ = 101.9480(10) °, V = 1723.58(14) A^3, Z = 1, ρ_{calcd} = 1.254 Mg m^{-3}; Mo$_{Ka}$ radiation (graphite monochromator, λ = 0.71073 Å), μ = 0.084 mm^{-1}, T = 293(2) K. 8463 data (4770 unique, R_{int} = 0.0628, 1.50 < θ < 23.31°), were collected on a Siemens SMART CCD diffractometer using narrow frames (0.3° in ω), and were corrected semi-empirically for absorption and incident beam decay (transmission 1.00–0.70). The structure was solved by direct methods and refined by full-matrix least-squares on F^2 values of all data (G.M.Sheldrick, SHELXTL manual, Siemens Analytical X-ray Instruments, Madison WI, USA, 1994, version 5) to give wR = $\{\Sigma[w(F_o^2-F_c^2)^2]/\Sigma[w(F_o^2)^2]\}^{1/2}$ = 0.2659, conventional R = 0.0866 for F values of 4770 reflections with $F_o^2 > 2\sigma(F_o^2)$, S = 1.027 for 446 parameters. Residual electron density extremes were 0.356 and –0.250 eÅ^{-3}. Amide hydrogen atoms were refined isotropically with the remainder constrained; anisotropic displacement parameters were used for all non-hydrogen atoms.

Hexanedioic acid *bis*-[2,2-diphenylethylamide], S3.
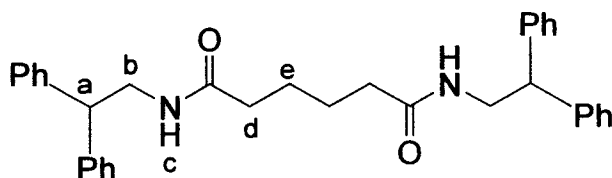
To a solution of 2,2-diphenylethylamine (0.42 g, 2.1 mmol) in CH$_2$Cl$_2$ (10 mL) was added Et$_3$N (0.25 g, 2.5 mmol) followed by dropwise addition of hexanedionyl dichloride (0.18 g, 1 mmol) in CH$_2$Cl$_2$ (5 mL) over 10 min at 0 °C. The reaction mixture was allowed to stir for 16 h at rt and then washed with 1N HCl (2 x 10 mL), saturated aqueous NaHCO$_3$ (2 x 10 mL) and brine (10 mL). The organic layer was dried over anhydrous MgSO$_4$, filtered and the solution concentrated under reduced pressure to give a colourless solid that was recrystallized in CH$_2$Cl$_2$/MeOH to afford colourless needles (S3, 0.40 g, 79%). m.p. 183 °C; ^{1}H NMR (400 MHz, CDCl$_3$): δ = 7.35-7.22 (m, 20H, Ar*CH*), 5.60 (br t, ^3J(H,H) = 5.7 Hz, 2H, N*H*$_c$), 4.21 (t, ^3J(H,H) = 8.0 Hz, 2H, C*H*$_a$), 3.91 (dd, ^3J(H,H) = 8.0 Hz, ^3J(H,H) = 5.7 Hz, 4H, C*H*$_b$), 2.03 (m, 4H, C*H*$_d$) and 1.47 (m, 4H, C*H*$_e$); ^{13}C NMR (100 MHz, CDCl$_3$): δ = 172.6 (*C*O), 141.9 (Ar*C*-CH- (ipso)), 128.7 (Ar*C*H (meta)), 128.0 (Ar*C*H (ortho)), 126.8 (Ar*C*H (para)), 50.6 (*C*H$_a$), 43.7 (*C*H$_b$), 36.1 (*C*H$_d$) and 24.7 (*C*H$_e$); HRMS (FAB, THIOG matrix) Calcd. for C$_{34}$H$_{37}$N$_2$O$_2$ [(M+H)$^+$] 505.28695. Found: 505.28550.

[2]-(1,7,14,20-Tetraaza-2,6,15,19-tetraoxo-3,5,9,12,16,18,22,25 tetrabenzocyclohexacosane)-(hexanedioic acid *bis*-[2,2-diphenylethylamide])-rotaxane, S4.
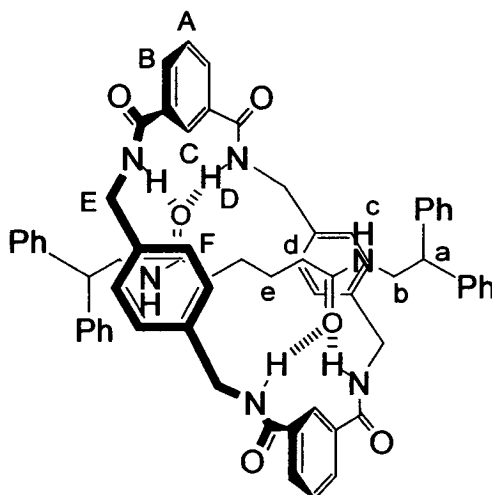
Rotaxane **S4** was prepared from thread **S3** (0.50 g, 0.99 mmol) according to the general procedure for the preparation of benzylic amide macrocycle containing [2]rotaxane. The crude product was purified by column chromatography (CHCl$_3$/MeOH (97/3)) to give the desidered compound as a colourless solid (**S4**, 0.08 g, 8%). m.p. 264 °C; ^{1}H NMR (400 MHz, CDCl$_3$): δ = 8.16 (br t, 4H, ArCH$_B$), 8.14 (br s, 2H, ArCH$_C$), 7.59 (t, ^3J(H,H) = 7.8 Hz, 2H, ArCH$_A$), 7.49 (br t, 4H, NH$_D$), 7.40-7.25 (m, 20H, ArCH (thread)), 7.06 (s, 8H, ArCH$_F$), 5.99 (br t, 2H, NH$_c$), 4.55 (d, ^3J(H,H) = 5.6 Hz, 8H, CH$_E$), 4.12 (t, ^3J(H,H) = 7.8 Hz, 2H, CH$_a$), 3.65 (dd, ^3J(H,H) = 7.8 Hz, 4H, CH$_b$), 0.91 (m, 4H, CH$_d$) and 0.50 (m, 4H, CH$_e$); ^{13}C NMR (100 MHz, CDCl$_3$): δ = 173.5 (*C*O thread), 166.5 (*C*O macrocycle), 142.0 (Ar*C*-CH (ipso thread)), 137.8 (Ar*C*-CH$_E$), 134.1 (Ar*C*-CO), 131.1 (ArCH$_B$), 129.3 (ArCH$_A$), 128.8 (ArCH$_F$), 128.7 (ArCH (meta thread)), 128.0 (ArCH (ortho thread)), 126.9 (ArCH (para thread)), 124.5 (ArCH$_C$), 50.2 (*C*H$_a$), 44.2 (*C*H$_b$), 43.8 (*C*H$_E$), 34.7 (*C*H$_d$) and 23.8 (*C*H$_e$); HRMS (FAB, THIOG matrix) Calcd. for C$_{66}$H$_{65}$N$_6$O$_6$ [(M+H)$^+$] 1037.49395. Found: 1037.49656.

X-ray crystallographic data for compound S4.

Crystals of rotaxane grown in CHCl₃/MeOH: $C_{68}H_{72}N_6O_6$, M = 1101.32, crystal size 0.10 × 0.06 × 0.05 mm, monoclinic, $C2/c$, a = 30.939(6), b = 11.3129(18), c = 18.568(3) Å, β = 118.147(17)°, V = 5730.5(17) Å³, Z = 4, ρ_{calcd} = 1.277 Mg m⁻³; synchrotron radiation (CCLRC Daresbury Laboratory Station 9.8, silicon monochromator, λ = 0.69230 Å), μ = 0.084 mm⁻¹, T = 150(2) K. 18920 data (7604 unique, R_{int} = 0.0348, 2.42 < θ < 29.30 °), were collected on a Siemens SMART CCD diffractometer using narrow frames (0.3° in ω), and were corrected semi-empirically for absorption and incident beam decay (transmission 1.00–0.60). The structure was solved by direct methods and refined by full-matrix least-squares on F^2 values of all data (G.M.Sheldrick, SHELXTL manual, Siemens Analytical X-ray Instruments, Madison WI, USA, 1994, version 5) to give wR = $\{\Sigma[w(F_o^2-F_c^2)^2]/\Sigma[w(F_o^2)^2]\}^{1/2}$ = 0.1361, conventional R = 0.0541 for F values of 7604 reflections with $F_o^2 > 2\sigma(F_o^2)$, S = 1.070 for 384 parameters. Residual electron density extremes were 0.429 and –0.411 eÅ⁻³. Amide hydrogen atoms were refined isotropically with the remainder constrained; anisotropic displacement parameters were used for all non-hydrogen atoms.

2,2-Diphenylethyl succinic acid mono ester, S5.
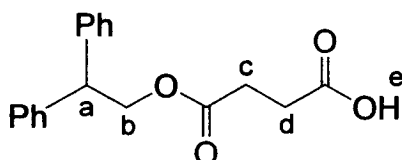
To a stirred solution of 2,2-diphenylethanol (3.00 g, 15.0 mmol) in CH_2Cl_2 (150 mL) was added one drop of Et_3N and a solution of succinic anhydride (1.66 g, 16.7 mmol) in CH_2Cl_2 (25 mL) added slowly over 30 mins. After 16 h the solution was reduced in

volume and recrystallized from CH_2Cl_2 (10 mL) to obtain a colourless solid (S5, 4.00 g, 90%). m.p. 103-104 °C; ^1H NMR (400 MHz, d_6-DMSO): δ = 7.38-7.21 (m, 10H, ArCH), 4.61 (d, ^3J(H,H) = 7.7 Hz, 2H, CH_b), 4.35 (t, ^3J(H,H) = 7.7 Hz, 1H, CH_a) and 2.40 (m, 4H, CH_c and CH_d); ^{13}C NMR (100 MHz, d_6-DMSO): δ = 173.9 (CO), 172.4 (CO), 141.8 (ArC-CH- (ipso)), 128.8 (ArCH (meta)), 128.3 (ArCH (ortho)), 127.0 (ArCH (para)), 66.5 (CH$_b$), 49.6 (CH$_a$), 29.1 (CH$_c$ or CH$_d$) and 28.9 (CH$_c$ or CH$_d$); MS (FAB): m/z = 299 [(M+H)$^+$]; Anal. Calcd. for $C_{18}H_{18}O_4$: C 72.47, H 6.08. Found: C 73.01, H 6.22.

N-(2,2-Diphenylethyl)-succinamic acid 2,2-diphenyl-ethyl ester, S6.
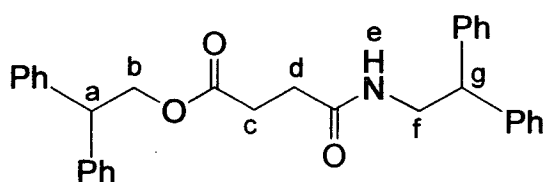
To a stirred solution of S5 (1.0 g, 3.40 mmol), 2,2-diphenylethylamine (0.66 g, 3.40 mmol) and 4-DMAP (0.49 g, 4 mmol) in CH_2Cl_2 (350 mL) cooled in an ice bath was added EDCI.HCl (0.71 g, 3.68 mmol) and the solution allowed to stir for 16 h. The reaction mixture was washed with a saturated solution of citric acid (3 x 50 mL) and H_2O (3 x 50 mL). The organic layer was dried over anhydrous $MgSO_4$, filtrated and the filtrate reduced in volume and the resulting solid purified by chromatography on silica gel using a gradient of CH_2Cl_2 to CH_2Cl_2/EtOAc (80/20) to obtain the desired compound as a colourless powder (S6, 1.16 g, 71%). m.p. 150-153 °C; ^1H NMR (400 MHz, CDCl$_3$): δ = 7.42-7.22 (m, 20H, ArCH), 5.60 (br, 1H, NH_e), 4.64 (d, ^3J(H,H) = 7.8 Hz, 2H, CH_b), 4.38 (t, ^3J(H,H) = 7.8 Hz, 1H, CH_a), 4.21 (t, ^3J(H,H) = 8.0 Hz, 1H, CH_g), 3.90 (dt, ^3J(H,H) = 8.0 Hz, 1H, CH_f), 2.55 (t, ^3J(H,H) = 7.0 Hz, 2H, CH_c) and 2.27 (t, ^3J(H,H) = 7.0 Hz, 2H, CH_d); ^{13}C NMR (100 MHz, CDCl$_3$): δ = 173.1 (CH$_c$-CO-O), 171.6 (-CO-

NH$_e$), 142.3 (ArC-CH (ipso)), 141.5 (ArC-CH (ipso)), 129.2 (ArCH (meta)), 129.0 (ArCH (meta)), 128.6 (ArCH (ortho)), 128.5 (ArCH (ortho)), 127.3 (ArCH (para)), 67.3 (CH$_b$), 51.0 (CH$_a$), 50.0 (CH$_g$), 44.3 (CH$_f$), 31.3 (CH$_c$) and 29.9 (CH$_d$); FABMS: m/z 478 [M+H]$^+$; Anal. Calcd. for C$_{32}$H$_{31}$NO$_3$: C 80.48, H 6.54, N 2.93. Found: C 80.70, H 6.68, N 3.02.

[2]-(1,7,14,20-Tetraaza-2,6,15,19-tetraoxo-3,5,9,12,16,18,22,25-tetrabenzocyclohexacosane)-(N-(2,2-diphenylethyl)-succinamic acid 2,2-diphenylethyl ester)-rotaxane, S7.
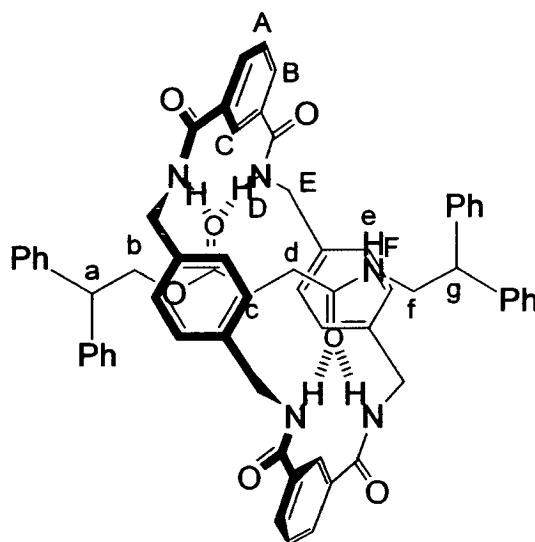
Rotaxane **S7** was obtained using the general procedure for the preparation of benzylic amide macrocycle containing [2]rotaxane from thread **S6** (1.16 g, 2.4 mmol). The solid crude was subjected to column chromatography on silica gel using CH$_2$Cl$_2$/EtOAc (75/15) as eluent to obtain the desired compound as a colourless powder (**S7**, 95 mg, 4%). m.p. 204-205 °C. ^{1}H NMR (400 MHz, CDCl$_3$): δ = 8.21 (dd, ^4J(H$_B$,H$_C$) = 1.5 Hz, ^3J(H$_B$,H$_A$) = 7.8 Hz, 4H, ArCH$_B$), 8.17 (br t, ^4J(H$_C$,H$_B$) = 1.5 Hz, 2H, ArCH$_C$), 7.66 (t, ^3J(H$_A$,H$_B$) = 7.8 Hz, 2H, ArCH$_A$), 7.31-7.08 (m, 24H, ArCH(thread) and NH$_D$), 6.84 (s,

8H, ArCH$_F$), 7.33 (br t, ^3J(H,H) = 5.6 Hz, 1H, NH$_e$), 4.46 (dd, ^2J(H$_E$,H'$_E$) = 14.4 Hz, ^3J(H$_E$,H$_D$) = 5.6 Hz, 4H, CHH'$_E$), 4.40 (dd, ^2J(H$_E$,H'$_E$) = 14.4 Hz, ^3J(H'$_E$,H$_D$) = 5.3 Hz, 4H, CHH'$_E$), 4.34 (d, ^3J(H,H) = 7.3 Hz, 2H, CH$_b$), 4.14 (t, ^3J(H,H) = 7.3 Hz, 1H, CH$_a$), 4.05 (t, ^3J(H,H) = 7.8 Hz, 1H, CH$_g$), 3.57 (dd, ^3J(H,H) = 7.8 Hz, ^3J(H,H) = 5.6 Hz, 2H, CH$_f$), 1.26 (br t, ^3J(H,H) = 7.5 Hz, 2H, CH$_c$) and 0.86 (br t, ^3J(H,H) = 7.5 Hz, 2H, CH$_d$); ^{13}C NMR (100 MHz, d_6-DMSO): δ = 173.1 (CH$_c$-CO-O), 171.9 (-CO-NH$_e$), 166.1 (CO macrocycle), 143.2 (ArC-CH (ipso thread)), 141.6 (ArC-CH (ipso thread)), 137.6 (ArC-CH$_E$), 134.9 (ArC-CO-), 130.7 (ArCH$_B$) , 129.1 (ArCH$_A$), 128.8 (ArCH$_F$), 128.7 (ArCH (meta thread)), 128.0 (ArCH (ortho thread)), 126.9 (ArCH (para thread)), 126.7 (ArCH (para thread)), 125.8 (ArCH$_C$), 66.3 (CH$_b$), 50.4 (CH$_a$ or CH$_g$), 49.3 (CH$_a$ or CH$_g$), 43.6 (CH$_f$), 43.5 (CH$_E$), 28.8 (CH$_c$ or CH$_d$) and 28.1 (CH$_c$ or CH$_d$); MS (FAB): m/z = 1010 [M+H]$^+$; Anal. Calcd. for C$_{64}$H$_{59}$N$_5$O$_7$: C 76.09, H 5.89, N 6.93. Found C 76.31, H 5.78, N 6.79.

X-ray crystallographic data for compound S7.

C$_{72}$H$_{82}$N$_5$O$_{11}$S$_4$, M = 1321.67, crystal size 0.15 × 0.10 × 0.08mm, triclinic P-1, a = 9.9959(4), b = 12.8280(4), c = 15.1241(6) Å, α = 107.0330(10), β = 105.5420(10), γ = 99.0490(10)°, V = 1726.95(11) A^3, Z = 1, ρ_{calcd} = 1.271 Mg m^{-3}; Mo$_{Ka}$ radiation (graphite monochromator, λ = 0.71073 Å), μ = 0.201 mm^{-1}, T = 180(2) K. 11064 data (7963 unique, R_{int} = 0.0510, 1.72 < θ < 28.97 °), were collected on a Siemens SMART CCD diffractometer using narrow frames (0.3° in ω), and were corrected semi-empirically for absorption and incident beam decay (transmission 1.00–0.45). The structure was solved by direct methods and refined by full-matrix least-squares on F^2 values of all data (G.M.Sheldrick, SHELXTL manual, Siemens Analytical *X*-ray Instruments, Madison WI, USA, 1994, version 5) to give wR = $\{\Sigma[w(F_o^2-F_c^2)^2]/\Sigma[w(F_o^2)^2]\}^{1/2}$ = 0.2697, conventional R = 0.0963 for F values of 7963 reflections with $F_o^2 > 2\sigma(F_o^2)$, S = 0.873 for 438 parameters. Residual electron density extremes were 0.998 and −0.719 eÅ^{-3}.

Amide hydrogen atoms were refined isotropically with the remainder constrained; anisotropic displacement parameters were used for all non-hydrogen atoms.

N-(2,2-Diphenylethyl)-maleamide acid, S8.
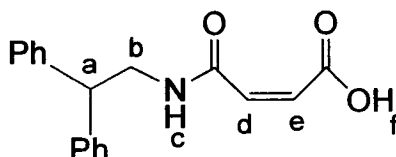
To a stirred solution of 2,2-diphenylethylamine (5.00 g, 25.3 mmol) in anhydrous THF (25 mL) at 0 °C, was added dropwise a solution of maleic anhydride (2.50 g, 25.5 mmol) in anhydrous THF (10 mL). The mixture obtained was allowed to stir at rt for 16 h and then reduced in volume and the resulting oil taken up with $CHCl_3$ (50 mL) and washed with a solution of 1N NaOH (3 x 20 mL) and H_2O (1 x 20 mL). The organic layer was dried over anhydrous $MgSO_4$, filtered and the solvent removed under reduced pressure to obtain a colourless solid which was recrystallized from CH_2Cl_2 (S8, 5.62 g, 75%). m.p. 209 °C; ^1H NMR (400 MHz, $CDCl_3$): δ = 7.29-7.23 (m, 4H, ArCH (meta)), 7.20-7.14 (m, 6H, ArCH (ortho and para)), 6.43 (br t, ^3J(H,H) = 5.7 Hz, 1H, NH_c), 6.19 (d, ^3J(H,H) = 12.6 Hz, 1H, CH_e), 6.02 (d, ^3J(H,H) = 12.6 Hz, 1H, CH_d), 4.18 (t, ^3J(H,H) = 8.0 Hz, 1H, CH_a) and 3.95 (dd, ^3J(H,H) = 8.0 Hz, ^3J(H,H) = 5.7 Hz, 2H, CH_b); ^{13}C NMR (100 MHz, $CDCl_3$): δ = 166.0 (-CO-OH), 164.5 (-CO-NH$_c$), 140.7 (ArC-CH (ipso)), 137.1 (CH$_e$), 130.2 (CH$_d$), 129.0 (ArCH (meta)), 127.9 (ArCH (ortho)), 127.4 (ArCH (para)), 50.0 (CH$_a$) and 44.6 (CH$_b$); HRMS (FAB, THIOG matrix): m/z = 262.12884 [(M+H)$^+$] (Anal. Calcd. for $C_{18}H_{18}NO_3$: m/z = 296.12867). Anal. Calcd. for $C_{18}H_{17}NO_3$: C 73.20, H 5.80, N 4.74. Found: C 73.13, H 5.85, N 4.61.

12-Aminododecylcarbamic acid *tert*-butyl ester, S9.
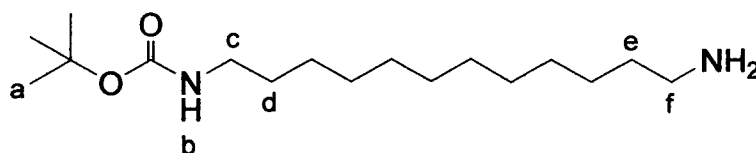
To a stirred solution of 1,12-diaminododecane (20.00 g, 100 mmol) in CHCl$_3$ (500 mL) was added di-*tert*-butyl dicarbonate (11 g, 50 mmol). The reaction was allowed to stir for 16 h at rt after which time the solvent was removed under reduced pressure and the residual oil subjected to column cromatography using a solvent gradient of CHCl$_3$/MeOH (95/5) to CHCl$_3$/MeOH/NH$_4$OH (89/10/1) to obtain a colourless solid (**S9**, 9 g, 60%). m.p. 96-97 °C. ^{1}H NMR (400 MHz, CDCl$_3$): δ = 4.50 (br t, ^3J(H,H) = 5.7 Hz, 1H, N*H*$_b$), 3.10 (td, ^3J(H,H) = 7.0 Hz, ^3J(H,H) = 5.7 Hz, 2H, C*H*$_c$), 2.67 (t, ^3J(H,H) = 7.0 Hz, 2H, C*H*$_f$), 1.49-1.36 (br, 13H, C*H*$_a$, C*H*$_e$ and C*H*$_d$) and 1.33-1.20 (br, 16H, -C*H*$_2$- (alkyl chain)); ^{13}C NMR (100 MHz, CDCl$_3$): δ = 156.3 (*C*O), 79.2 (*C*(CH$_3$)$_3$), 42.6 (*C*H$_c$), 40.9 (*C*H$_f$), 34.2 (-*C*H$_2$-), 30.4 (-*C*H$_2$-), 30.0 (-*C*H$_2$-), 29.9 (-*C*H$_2$-), 29.7 (-*C*H$_2$-), 29.6 (-*C*H$_2$-), 29.2 (-*C*H$_2$-), 28.9 (-*C*H$_2$-), 28.8 (*C*H$_a$), 27.2 (-*C*H$_2$-) and 27.1 (-*C*H$_2$-); HRMS (FAB, THIOG matrix): *m/z* = 301.28491 [(M+H)$^+$] (Anal. Calcd. for C$_{17}$H$_{37}$N$_2$O$_2$: *m/z* = 301.28550). Anal. Calcd. for C$_{17}$H$_{36}$N$_2$O$_2$: C 67.95, H 12.08, N 9.32. Found: C 67.73, H 11.94, N 9.31.

N-(12-*tert*-Butoxycarbonylaminododecyl)-succinamic acid 2,2-diphenylethyl ester, **S10**.
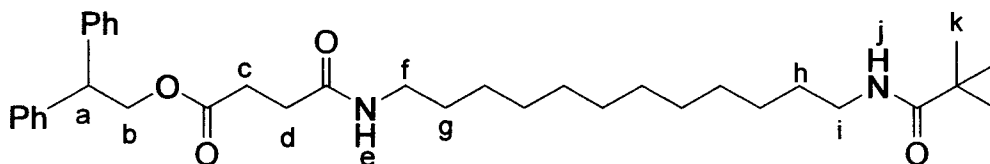
To a stirred solution of **S5** (0.40 g, 1.30 mmol), **S9** (0.40 g, 1.30 mmol) and 4-DMAP (0.20 g, 1.60 mmol) in anhydrous CH_2Cl_2 (200 mL) cooled on an ice bath, was added EDCI·HCl (0.28 g, 1.50 mmol) and the reaction allowed to to stir for 48 h at rt. The solution was washed with a saturated solution of citric acid (2 x 50 mL) and H_2O (2 x 50 mL) and the organic layer dried over anhydrous $MgSO_4$, filtered and the filtrate reduced in volume. The solid obtained was subjected to column cromatography using a solvent gradient of CH_3Cl to $CH_3Cl/MeOH$ (90/10) to obtain a colourless solid (**S10**, 0.52 g, 68%). m.p. 88-89 °C; ^1H NMR (400 MHz, $CDCl_3$): δ = 7.22-7.18 (m, 4H, ArCH (meta)) 7.17-7.09 (m, 6H, ArCH (ortho and para)), 5.52 (t br, ^3J(H,H) = 5.7 Hz, 1H, NH_e), 4.56 (d, ^3J(H,H) = 7.7 Hz, 2H, CH_b), 4.47 (br, 1H, NH_j), 4.28 (t, ^3J(H,H) = 7.7 Hz, 1H, CH_a), 3.10 (td, ^3J(H,H) = 7.0 Hz, ^3J(H,H) = 5.7 Hz, 2H, CH_f), 3.02 (br, 2H, CH_i), 2.50 (t, ^3J(H,H) = 7.0 Hz, 2H, CH_c), 2.25 (t, ^3J(H,H) = 7.0 Hz, 2H, CH_d), 1.42-1.30 (m, 13H, CH_k, CH_g and CH_h) and 1.25-1.13 (m, 16H, -CH_2- (alkyl chain)); ^{13}C NMR (100 MHz, $CDCl_3$): δ = 173.2 (CH_c-CO-O), 171.6 (CO-NH_e), 156.3 (CO), 141.4 (ArC- (ipso)), 128.9 (ArCH (meta)), 128.6 (ArCH (ortho)), 127.2 (ArCH (para)), 79.4 ($C(CH_3)_3$), 67.3 (CH_b), 50.2 (CH_a), 41.0 (CH_i), 40.0 (CH_f), 32.4 (CH_c), 31.0 (CH_d), 30.4 (-CH_2-), 30.1 (-CH_2-), 30.0-29.9 (-CH_2-), 29.6 (-CH_2-), 29.5 (-CH_2-), 29.4 (-CH_2-), 28.8 (CH_k), 27.3 (-CH_2-) and 27.2 (-CH_2-); MS (FAB): m/z = 581 [(M + H)$^+$]; Anal. Calcd. for $C_{35}H_{52}N_2O_5$: C 72.38, H 9.02, N 4.82. Found: C 72.62, H 9.40, N 5.02.

N-(2,2-Diphenylethyl)-fumaric acid ethyl ester, S11.
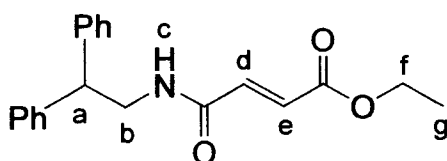
To a stirred solution of 2,2-diphenylethylamine (0.50 g, 2.50 mmol), fumaric acid monoethylester (0.37 g, 2.50 mmol) and 4-DMAP (0.33 g, 2.70 mmol) in anhydrous

CH_2Cl_2 (200 mL) cooled on an ice bath was added EDCI·HCl (0.52 g, 2.7 mmol). After 24 h the solution was washed with a saturated solution of citric acid (3 x 50 mL) and H_2O (3 x 50 mL) and the organic layer dried over anhydrous $MgSO_4$, filtered and the filtrate reduced in volume to obtain a colourless solid that was recrystallized from EtOAc (**S11**, 0.70 g, 85%). m.p. 112-113 °C. ^1H NMR (400 MHz, $CDCl_3$): δ = 7.34-7.27 (m, 4H, ArH (meta)), 7.26-7.19 (m, 6H, ArH (ortho and para)), 6.77 (d, $^3J(H,H)$ = 14.4 Hz, 1H, CH_e), 6.72 (d, $^3J(H,H)$ = 14.4 Hz, 1H, CH_d), 5.90 (br t, $^3J(H,H)$ = 5.7 Hz, 1H, NH_c), 4.25-4.15 (m, 3H, CH_a and CH_f), 3.98 (dd, $^3J(H,H)$ = 8.0 Hz, $^3J(H,H)$ = 5.7 Hz, 2H, CH_b) and 1.28 (t, $^3J(H,H)$ = 7.0 Hz, 3H, CH_g); ^{13}C NMR (100 MHz, $CDCl_3$): δ = 165.6 (-CO-OEt), 163.6 (-CO-NH), 141.5 (ArC- (ipso)), 136.0 (CH$_e$), 130.6 (CH$_d$), 128.9 (ArCH (meta)), 128.1 (ArCH (ortho)), 127.0 (ArCH (para)), 61.2 (CH$_f$), 50.3 (CH$_a$), 44.1 (CH$_b$) and 14.1 (CH$_g$); MS (FAB): m/z = 324 [(M+H)$^+$]; Anal. Calcd. for $C_{20}H_{21}NO_3$: C 74.28, H 6.55, N 4.33. Found: C 74.83, H 6.91, N 4.38.

N-(2,2-Diphenylethyl)-fumaramide acid, S12.
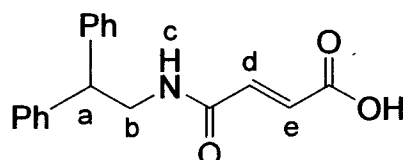
To a stirred solution of **S11** (0.70 g, 2.20 mmol) in EtOH (50 mL) was added dropwise a solution of NaOH (0.10 g, 2.40 mmol) in H_2O (2.5 mL). After 16 h the solution was reduced in volume and washed several times with Et_2O to obtain a colourless powder that was recrystallized from $CHCl_3$ (**S12**, 0.58 g, 91%). m.p. >270 °C (decomp). ^1H NMR (400 MHz, d_6-DMSO): δ = 12.83 (br s, 1H, -COOH), 8.57 (br t, $^3J(H,H)$ = 5.7 Hz, 1H, NH_c), 7.33-7.15 (m, 10H, ArCH), 6.87 (d, $^3J(H,H)$ = 15.4 Hz, 1H, CH_e), 6.47 (d, $^3J(H,H)$ = 15.4 Hz, 1H, CH_d), 4.22 (t, $^3J(H,H)$ = 8.0 Hz, 1H, CH_a) and 3.81 (dd, $^3J(H,H)$ = 8.0 Hz, $^3J(H,H)$ = 5.7 Hz, 2H, CH_b); ^{13}C NMR (100 MHz, d_6-DMSO) δ 168.0 (CO-

OH), 164.5 (CO-NH$_c$), 143.1 (ArC- (ipso)), 134.3 (CH$_e$), 134.0 (CH$_d$), 128.8 (ArCH (meta)), 128.2 (ArCH (ortho)), 126.7 (ArCH (para)), 50.3 (CH$_a$) and 43.7 (CH$_b$); MS (FAB): m/z = 296 [(M+H)$^+$]; Anal. Calcd. for C$_{18}$H$_{17}$NO$_3$: C 73.20, H 5.80, N 4.70. Found: C 73.10, H 5.20, N 4.73.

N-(2,2-Diphenylethyl)-succinamic acid, S13.
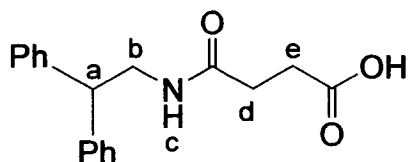
To a stirred solution of succinic anhydride (2.53 g, 25.3 mmol) in anhydrous THF (25 mL) was added at rt dropwise a solution of 2,2-diphenylethylamine (5.00 g, 25.3 mmol) in anhydrous THF (25 mL). After 16 h the sovent was removed under reduced pressure and the resulting oil recrystallized in CH$_2$Cl$_2$ to obtain a colourless solid (**S13**, 7.16 g, 95%). m.p. 153-154 °C; ^{1}H NMR (400 MHz, CDCl$_3$): δ = 7.34-7.28 (m, 4H, ArCH (meta)), 7.26-7.19 (m, 6H, ArCH (ortho and para)), 5.63 (br t, ^3J(H,H) = 5.7 Hz, 1H, NH_c), 4.18 (t, ^3J(H,H) = 8.0 Hz, 1H, CH_a), 3.90 (dd, ^3J(H,H) = 8.0 Hz, ^3J(H,H) = 5.7 Hz, 2H, CH_b), 2.63 (t, ^3J(H,H) = 6.5 Hz, 2H, CH_e) and 2.39 (t, ^3J(H,H) = 6.5 Hz, 2H, CH_d); ^{13}C NMR (100 MHz, CDCl$_3$): δ = 176.2 (CO-OH), 172.1 (CO-NH$_c$), 141.5 (ArC-(ipso)), 128.8 (ArCH (meta)), 128.0 (ArCH (ortho)), 127.0 (ArCH (para)), 50.4 (CH$_a$), 44.0 (CH$_b$), 30.6 (CH$_e$) and 29.6 (CH$_d$); MS (FAB): m/z = 298 [(M+H)$^+$]; Anal. Calcd. for C$_{18}$H$_{19}$NO$_3$: C 72.71, H 6.44, N 4.71. Found: C 72.83, H 6.57, N 4.80.

N-(12-Aminododecyl)-N'-(2,2-diphenylethyl)-succinamide, S14.
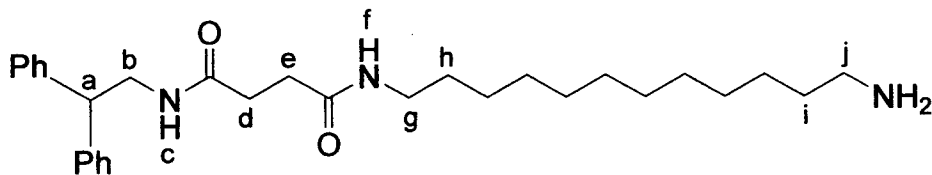
To a stirred solution of **S13** (0.50 g, 1.68 mmol) in CH_2Cl_2 was added thionyl chloride (0.12 mL, 1.68 mmol). The solution was heated until complete dissolution of **S13** and the resulting solution added dropwise to a solution of 1,12-diaminododecane (1.68 g, 8.40 mmol) and Et_3N (0.17 g, 1.68 mmol) in CH_2Cl_2 at 0 °C. After 30 min the reaction mixture was washed with 1N NaOH (1 x 100 mL) and H_2O (1 x 100 mL). The organic layer was dried over anhydrous $MgSO_4$, filtered and the filtrate reduced in volume to obtain a solid that was subjected to column cromatography using a solvent gradient of $CHCl_3$ to $CHCl_3/MeOH$ (90/10) to obtain a colourless solid (**S14**, 0.28 g, 35%). m.p. 78-79 °C. ^1H NMR (400 MHz, $CDCl_3$): δ = 7.36-7.29 (m, 4H, Ar*H* (meta)), 7.28-7.21 (m, 6H, Ar*H* (ortho and para)), 6.14 (br t, $^3J(H,H)$ = 5.7 Hz, 1H, N*H*$_c$), 6.09 (br t, $^3J(H,H)$ = 5.7 Hz, 1H, N*H*$_f$), 4.19 (t, $^3J(H,H)$ = 8,0 Hz, 1H, C*H*$_a$), 3.89 (dd, $^3J(H,H)$ = 8.0 Hz, $^3J(H,H)$ = 5.7 Hz, 2H, C*H*$_b$), 3.19 (td, $^3J(H,H)$ = 7.0 Hz, $^3J(H,H)$ = 5.7 Hz, 2H, C*H*$_g$), 2.69 (t, $^3J(H,H)$ = 7.0 Hz, 2H, C*H*$_j$), 2.41 (m, 4H, C*H*$_d$ and C*H*$_e$), 1.40-1.54 (m, 4H, C*H*$_h$ and C*H*$_i$) and 1.20-1.40 (m, 16H, -C*H*$_2$- (alkyl chain)); ^{13}C NMR (100 MHz, $CDCl_3$): δ = 172.6 (*C*O), 172.3 (*C*O), 142.3 (Ar*C*- (ipso)), 129.1 (Ar*C*H (meta)), 128.4 (Ar*C*H (ortho)), 127.2 (Ar*C*H (para)), 51.0 (*C*H$_a$), 44.2 (*C*H$_b$), 42.7 (*C*H$_j$), 40.0 (*C*H$_g$), 34.3 (*C*H$_i$), 32.2 (*C*H$_d$ or *C*H$_e$), 32.1 (*C*H$_d$ or *C*H$_e$), 30.0 (-*C*H$_2$-), 29.9 (-*C*H$_2$-), 29.8 (-*C*H$_2$-), 29.7 (-*C*H$_2$-), 27.3 (-*C*H$_2$-) and 27.2 (-*C*H$_2$-); MS (FAB): m/z = 480 [(M+H)$^+$]; Anal. Calcd. for $C_{30}H_{45}N_3O_2$: C 75.11, H 9.46, N 8.76. Found: C 75.23, H 9.65, N 8.87.

5-(2,2-Diphenylethylcarbamoyl)-pentanoic acid ethyl ester, S15.
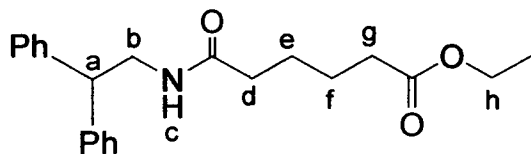
A solution of adiptic acid monoethyl ester (4.01 g, 23 mmol), 2,2-diphenylethylamine (5.00 g, 25 mmol) and 4-DMAP (2.81 g, 23 mmol) in CH_2Cl_2 (250 mL) was stirred at 0 °C for 10 min followed by addition of EDCI·HCl (4.42 g, 23 mmol). After 16 h the organic phase was washed with 1N HCl (3 x 70 mL), saturated aqueous $NaHCO_3$ (3 x 70 mL) and brine (1 x 70 mL). The organic layer was dried over anhydrous $MgSO_4$, filtered and the filtrate concentrated to give the product as a colourless solid (S15, 7.03 g, 86%). m.p. 44 °C; ^1H NMR (400 MHz, $CDCl_3$): δ = 7.34-7.21 (m, 10H, ArCH,), 5.70 (br t, ^3J(H,H) = 5.7 Hz, 1H, NH_c), 4.23 (t, ^3J(H,H) = 8.0 Hz, 1H, CH_a), 4.13 (q, ^3J(H,H) = 7.0 Hz, 2H, CH_h), 3.91 (dd, ^3J(H,H) = 8.0 Hz, ^3J(H,H) = 5.7 Hz, 2H, CH_b), 2.26 (t, ^3J(H,H) = 7.0 Hz, 2H, CH_d or CH_g), 2.09 (t, ^3J(H,H) = 7.0 Hz, 2H, CH_d or CH_g), 1.56 (m, 4H, CH_e and CH_f), 1.27 (t, ^3J(H,H) = 7.0 Hz, 3H, CH_i); ^{13}C NMR (100 MHz, $CDCl_3$): δ = 173.8 (CO-OEt), 172.9 (CO-NH$_c$), 142.3 (ArC- (ipso)), 129.1 (ArCH (meta)), 128.5 (ArCH (ortho)), 127.2 (ArCH (para)), 60.7 (CH$_h$), 51.0 (CH$_a$), 44.2 (CH$_b$), 36.6 (CH$_d$ or CH$_g$), 34.3 (CH$_d$ or CH$_g$), 25.4 (CH$_e$ or CH$_f$), 24.7 (CH$_e$ or CH$_f$) and 14.7 (CH$_i$); HRMS (FAB, THIOG matrix) Calcd. for $C_{22}H_{28}NO_3$ [(M+H)$^+$] 354.20692. Found: 354.20660.

5-(2,2-Diphenylethylcarbamoyl)-pentanoic acid, S16.
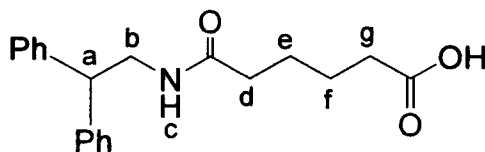
To a solution of **S15** (7.03 g, 19.9 mmol) in EtOH (50 mL) was added aqueous KOH (5.58 g in 9 mL of H_2O, 99.4 mmol) and the resulting solution stirred for 2 h at 78 °C. The yellow solution was cooled to rt, poured into water and acidified with dropwise addition of concentrated HCl resulting in a colourless precipitate that was filtered and dried *in vacuo* to give the product as a colourless solid (**S16**, 6.12 g, 95%). m.p. 124 °C; ^{1}H NMR (400 MHz, $CDCl_3$): δ = 7.36-7.23 (m, 10H, ArCH), 5.55 (br t, ^3J(H,H) = 5.7 Hz, 1H, NH_c), 4.21 (t, ^3J(H,H) = 8.0 Hz, 1H, CH_a), 3.92 (dd, ^3J(H,H) = 8.0 Hz, ^3J(H,H) = 5.7 Hz, 2H, CH_b), 2.33 (t, ^3J(H,H) = 7.0 Hz, 2H, CH_g), 2.12 (t, ^3J(H,H) = 7.0 Hz, 2H, CH_d), 1.59 (m, 4H, CH_e and CH_f); ^{13}C NMR (100 MHz, $CDCl_3$): δ = 178.2 (-CO-OH), 172.8 (-CO-NH), 141.7 (ArC- (ipso)), 128.7 (ArC- (meta)), 128.0 (ArC- (ortho)), 126.9 (ArC- (para)), 50.6 (CH$_a$), 43.8 (CH$_b$), 36.2 (CH$_g$), 33.5 (CH$_d$), 24.9 (CH$_e$ or CH$_f$) and 24.0 (CH$_e$ or CH$_f$); HRMS (FAB, THIOG matrix) Calcd. for $C_{20}H_{24}NO_3$ [(M+H)$^+$] 326.17562. Found: 326.17637.

(12-[5-(2,2-Diphenylethylcarbamoyl)-pentanoylamino]-dodecyl}-carbamic acid *tert*-butyl ester, S17.
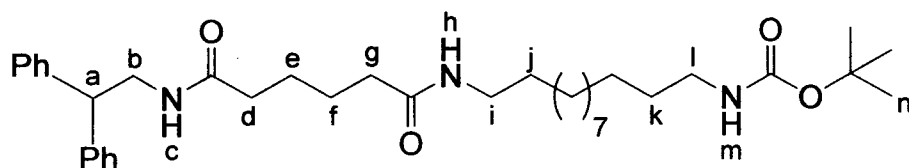
A solution of **S16** (0.50 g, 1.54 mmol), **S9** (0.51 g, 1.69 mmol) and 4-DMAP (0.19 g, 1.54 mmol) in $CHCl_3$ (20 mL) was stirred at 0 °C for 10 min followed by addition of EDCI·HCl (0.29 g, 1.54 mmol). After 16 h the reaction mixture diluted with $CHCl_3$ (10 mL) and the organic phase washed with 1N HCl (3 x 10 mL), saturated $NaHCO_3$ (3 x 10 mL) and brine (1 x 10 mL). The organic layer was dried over anhydrous $MgSO_4$, filtered and the filtrate concentrated to give the product as a colourless solid (**S17**, 0.85 g, 92%).

m.p. 114 °C; ^{1}H NMR (400 MHz, CDCl$_3$): δ = 7.33-7.20 (m, 10H, ArCH), 5.84 (br t, ^3J(H,H) = 5.7 Hz, 1H, NH_h), 5.79, (br t, ^3J(H,H) = 5.7 Hz, 1H, NH_c), 4.57 (br t, ^3J(H,H) = 5.7 Hz, 1H, NH_m), 4.22 (t, ^3J(H,H) = 8.0 Hz, 1H, CH_a), 3.90 (dd, ^3J(H,H) = 8.0 Hz, ^3J(H,H) = 5.7 Hz, 2H, CH_b), 3.23 (td, ^3J(H,H) = 7.0 Hz, ^3J(H,H) = 5.7 Hz, Hz, 2H, CH_i), 3.11 (m, 2H, CH_l), 2.11 (t, ^3J(H,H) = 7.3 Hz, 2H, CH_d or CH_g), 2.09 (t, ^3J(H,H) = 7.3 Hz, 2H, CH_d or CH_g), 1.56 (m, 4H, CH_e and CH_f), 1.46 (s, 13H, CH_j, CH_k and CH_n), 1.27 (br s, 16H, -CH_2- (alkyl chain)); ^{13}C NMR (100 MHz, CDCl$_3$): δ = 172.7 (CO), 172.5 (CO), 157.6 (NH$_m$-CO-O), 141.9 (ArC- (ipso)), 128.7 (ArCH (meta)), 128.0 (ArCH (ortho)), 126.8 (ArCH (para)), 79.4 (C(CH$_3$)$_3$), 50.6 (CH$_a$), 43.7 (CH$_b$), 40.6 (CH$_i$), 39.6 (CH$_l$), 36.2 (CH$_d$ or CH$_g$), 36.1 (CH$_d$ or CH$_g$), 30.0 (-CH$_2$-), 29.6 (-CH$_2$-), 29.5 (-CH$_2$-), 29.3 (-CH$_2$-), 28.4 (-CH$_2$-), 26.9 (-CH$_2$-), 26.8 (-CH$_2$-), 24.9 (-CH$_2$-) and 24.8 (-CH$_2$-); MS(FAB): m/z = 608 [(M + H)$^+$]; HRMS (FAB, THIOG matrix) Calcd. for C$_{37}$H$_{58}$N$_3$O$_4$ [(M+H)$^+$] 608.44273. Found: 608.44148.

Hexanedioic acid (12-aminododecyl)-amide (2,2-diphenylethyl)-amide, S18.
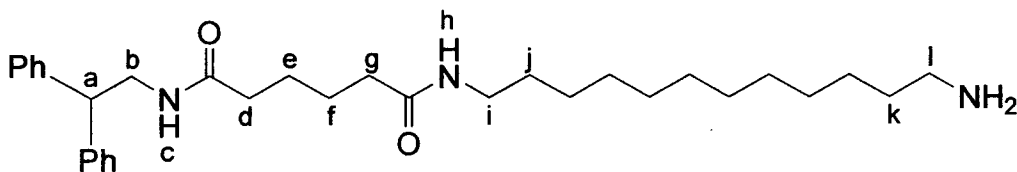
A solution of **S17** (0.4 g, 6.58 mmol) in TFA (15 mL) was stirred at rt for 30 min. The reaction mixture was concentrated under reduced pressure and CH$_2$Cl$_2$ (20 mL) added. The organic phase was washed with 1N NaOH (2 x 10 mL), brine (1 x 10 mL), dried over anhydrous MgSO$_4$, filtered and the filtrate concentrated to give the product as a colourless solid (**S18**, 0.22 g, 66%). m.p. 91 °C; ^{1}H NMR (400 MHz, CDCl$_3$): δ = 7.35-7.22 (m, 10H, ArCH), 5.77 (br t, ^3J(H,H) = 5.7 Hz, 1H, NH_c or NH_h), 5.75 (br t, ^3J(H,H) = 5.7 Hz, 1H, NH_c or NH_h), 4.22 (t, ^3J(H,H) = 8.0 Hz, 1H, CH_a), 3.91 (dd, ^3J(H,H) = 8.0

Hz, ^3J(H,H) = 5.7 Hz, 2H, CH_b), 3.24 (td, ^3J(H,H) = 7.0 Hz, ^3J(H,H) = 5.7 Hz, 2H, CH_i), 2.69 (m, 2H, CH_k), 2.11 (t, ^3J(H,H) = 7.3 Hz, 2H, CH_d or CH_g), 2.09 (t, ^3J(H,H) = 7.3 Hz, 2H, CH_d or CH_g), 1.58 (m, 4H, CH_e and CH_f), 1.51 (m, 2H, CH_j), 1.45 (m, 2H, CH_i), 1.28 (brs, 16H, -CH_2-, alkyl); ^{13}C NMR (100 MHz, CDCl$_3$): δ = 172.7 (CO), 172.6 (CO), 141.9 (ArC- (ipso)), 128.7 (ArCH (meta)), 128.0 (ArCH (ortho)), 126.8 (ArCH (para)), 50.6 (CH$_a$), 43.7 (CH$_b$), 42.2 (CH$_i$), 39.5 (CH$_l$), 36.2 (CH$_d$ or CH$_g$), 36.1 (CH$_d$ or CH$_g$), 33.7 (-CH$_2$-), 29.6-29.5 (-CH$_2$-), 29.4 (-CH$_2$-), 29.2 (-CH$_2$-), 26.9 (-CH$_2$-), 26.8 (-CH$_2$-), 24.9 (-CH$_2$-) and 24.8 (-CH$_2$-); HRMS (FAB, THIOG matrix) Calcd. for C$_{32}$H$_{50}$N$_3$O$_2$ [(M+H)$^+$] 508.39030. Found: 508.39143.

4.3.4 Details of X-Ray Crystal Structure Determination

Crystallographic data for E-4, S2, S4 and S7 (excluding structure factors) have been deposited with the Cambridge Crystallographic Data Centre as supplementary publication numbers CCDC-157383, 157381, 199285 and 199286 respectively. Copies of the data can be obtained free of charge on application to The Director, CCDC, 12 Union Road, Cambridge CB2 1EZ, UK (fax: +44-1223-336-033; e-mail: teched@chemcrys.cam.ac.uk).

4.4 References

1. For recent reviews see a) V. Balzani, A. Credi, F. M. Raymo, J. F. Stoddart, *Angew. Chem.* **2000**, *112*, 3484-3530; *Angew. Chem. Int. Ed.* **2000**, *39*, 3349-3391. b) Special issue on *Molecular Machines*, *Acc. Chem. Res.* **2001**, *34*, 409-522. c) Special issue on *Molecular Machines and Motors*. Structure and Bonding *Vol. 99* (Ed.: J.-P. Sauvage), Springer, Berlin, **2001**.

2. A. C. Benniston, A. Harriman, *Angew. Chem.* **1993**, *105*, 1553-1555; *Angew. Chem. Int. Ed. Engl.* **1993**, *32*, 1459-1461.

3. A. C. Benniston, A. Harriman, V. M. Lynch, *J. Am. Chem. Soc.* **1995**, *117*, 5275-5291.

4. A. C. Benniston, *Chem. Soc. Rev.* **1996**, *25*, 427-436.

5. H. Murakami, A. Kawabuchi, K. Kotoo, M. Kunitake, N. Nakashima, *J. Am. Chem. Soc.* **1997**, *119*, 7605-7606.

6. P. R. Ashton, R. Ballardini, V. Balzani, A. Credi, K. R. Dress, E. Ishow, C. J. Kleverlaan, O. Kocian, J. A. Preece, N. Spencer, J. F. Stoddart, M. Venturi, S. Wenger, *Chem. Eur. J.* **2000**, *6*, 3558-3574.

7. N. Armaroli, V. Balzani, J. P. Collin, P. Gavina, J. P. Sauvage, B. Ventura, *J. Am. Chem. Soc.* **1999**, *121*, 4397-4408.

8. A. M. Brouwer, C. Frochot, F. G. Gatti, D. A. Leigh, L. Mottier, F. Paolucci, S. Roffia, G. W. H. Wurpel, *Science* **2001**, *291*, 2124-2128.

9. G. W. H. Wurpel, A. M. Brouwer, I. H. M. van Stokkum, A. Farran, D. A. Leigh, *J. Am. Chem. Soc.* **2001**, *123*, 11327-11328.

10. C. A. Stanier, S. J. Alderman, T. D. W. Claridge, H. L. Anderson, *Angew. Chem.* **2002**, *114*, 1847-1850; *Angew. Chem. Int. Ed.* **2002**, *41*, 1769-1772.

11. For examples featuring the use of stimuli other than light to induce shuttling in rotaxanes see a) R. A. Bissell, E. Cordova, A. E. Kaifer, J. F. Stoddart, *Nature* **1994**, *369*, 133-137. b) J. P. Collin, P. Gavina, J. P. Sauvage, *New J. Chem.* **1997**, *21*, 525-

528. c) C. Gong, H. W. Gibson, *Angew. Chem.* **1997**, *109*, 2426-2428; *Angew. Chem. Int. Ed. Engl.* **1997**, *36*, 2331-2333. d) A. S. Lane, D. A. Leigh, A. Murphy, *J. Am. Chem. Soc.* **1997**, *119*, 11092-11093. e) C. P. Collier, E. W. Wong, M. Belohradsky, F. M. Raymo, J. F. Stoddart, P. J. Kuekes, R. S. Williams, J. R. Heath, *Science* **1999**, *285*, 391-394. f) H. Shigekawa, K. Miyake, J. Sumaoka, A. Harada, M. Komiyama, *J. Am. Chem. Soc.* **2000**, *122*, 5411-5412. g) M. C. Jimenez-Molero, C. Dietrich-Buchecker, J. P. Sauvage, *Chem. Eur. J.* **2002**, *8*, 1456-1466. h) Y. Luo, C. P. Collier, J. O. Jeppesen, K. A. Nielsen, E. Delonno, G. Ho, J. Perkins, H. R. Tseng, T. Yamamoto, J. F. Stoddart, J. R. Heath, *ChemPhysChem* **2002**, *3*, 519-525.

12. G. Campari, M. Fagnoni, M. Mella, A. Albini, *Tetrahedron Asym.* **2000**, *11*, 1891-1906.

13. F. G. Gatti, D. A. Leigh, S. A. Nepogodiev, A. M. Z. Slawin, S. J. Teat, J. K. Y. Wong, *J. Am. Chem. Soc.* **2001**, *123*, 5983-5989.

14. The wavelength for the reaction has not yet been optimised [F. G. Gatti, S. León, J. K. Y. Wong, G. Bottari, A. Altieri, A. M. Farran Morales, S. J. Teat, C. Frochot, D. A. Leigh, A. M. Brouwer, F. Zerbetto, *Proc. Natl. Acad. Sci. U.S.A.* **2003**, *100*, 10-14].

15. ^{1}H NMR experiments show that the macrocycle spins $>10^6$ times faster in the *Z*-form of the rotaxane than the *E*-form in CD_2Cl_2 at 233K.

16. G. Brancato, F. Coutrot, D. A. Leigh, A. Murphy, J. K. Y. Wong, F. Zerbetto, *Proc. Natl. Acad. Sci. U. S. A.* **2002**, *99*, 4967-4971.

17. V. Bermudez, N. Capron, T. Gase, F. G. Gatti, F. Kajzar, D. A. Leigh, F. Zerbetto, S. W. Zhang, *Nature* **2000**, *406*, 608-611.

18. D A Leigh and J K Y Wong, unpublished results

19. Unlike rotaxanes with dipeptide stations separated by alkyl chains[ref 11d], *E*-1-3 do not behave as solvent-switchable shuttles; even in d_6-DMSO the fumaramide station is still occupied by the macrocycle ~85% of the time.

20. The yield of the adipamide-maleamide rotaxane Z-3 (20%) is reproducibly higher than that of the model single site adipamide rotaxane shown in Figure 2 (8%). The significant differences in yield (and the anomalously poor binding of the adipamide unit to the macrocycle in Z-3) may indicate that the intramolecularly hydrogen bonded 9 membered ring [S. H. Gellman, G. P. Dado, G.-B. Liang, B. R. Adams, _J. Am. Chem. Soc._ **1991**, _113_, 1164-1173] has differing stabilities in the one- and two-station adipamide threads and rotaxane Z-3.

21. N. L. Allinger, Y. H. Yuh, J. H. Lii, _J. Am. Chem. Soc._ **1989**, _111_, 8551-8582.

22. J. W. Ponder, F. Richards, _J. Comput. Chem._ **1987**, _8_, 1016-1024.

23. F. Biscarini, M. Cavallini, D. A. Leigh, S. Leon, S. J. Teat, J. K. Y. Wong, F. Zerbetto, _J. Am. Chem. Soc._ **2002**, _124_, 225-233.

24. In analogy to the MM3 H-bonding of (C)H atoms connected to sp^2 carbons, we introduced a term to reproduce weak H-bonding of the acidic succinic methylene groups (well-depth 0.22 kcal mol^{-1}; equilibrium H-bonding distance 2.78 Å).

A Temperature-Responsive Hydrogen Bonded Molecular Shuttle

Chapter Five - Synopsis

In this chapter the unexpected behaviour of a molecular shuttle in response to changes in the temperature is reported. The rotaxane E-1 consists of an endo pyridyl macrocycle locked onto a thread containing two hydrogen bonding sites, namely a photoactive fumaramide (green) and a succinic amide-ester (orange) stations, separated by a C_{12} lipophilic chain (purple) (Scheme 1). ^1H NMR experiments (298K) prove that in E-1 the macrocycle is positioned almost exclusively over the fumaramide unit, similarly to its isophthaloyl analogous seen in chapter four. The discrimination of the ring for the photoactive unit is maintained even by lowering the temperature (258K). Isomerisation at 254 nm of E-1 gives the maleamide containing rotaxane Z-1 therefore inducing the shuttling of the macrocycle over the amide-ester station as confirmed by ^1H NMR spectroscopy at 308K (co-conformer Z-1a). Interestingly enough low temperature ^1H NMR experiments (258K) on Z-1 suggest that the Z-rotaxane adopts a co-conformation resulting in the positioning of the pyridyl macrocycle over the alkyl chain with the thread disposed in a "S" shape conformation (co-conformer Z-1b).
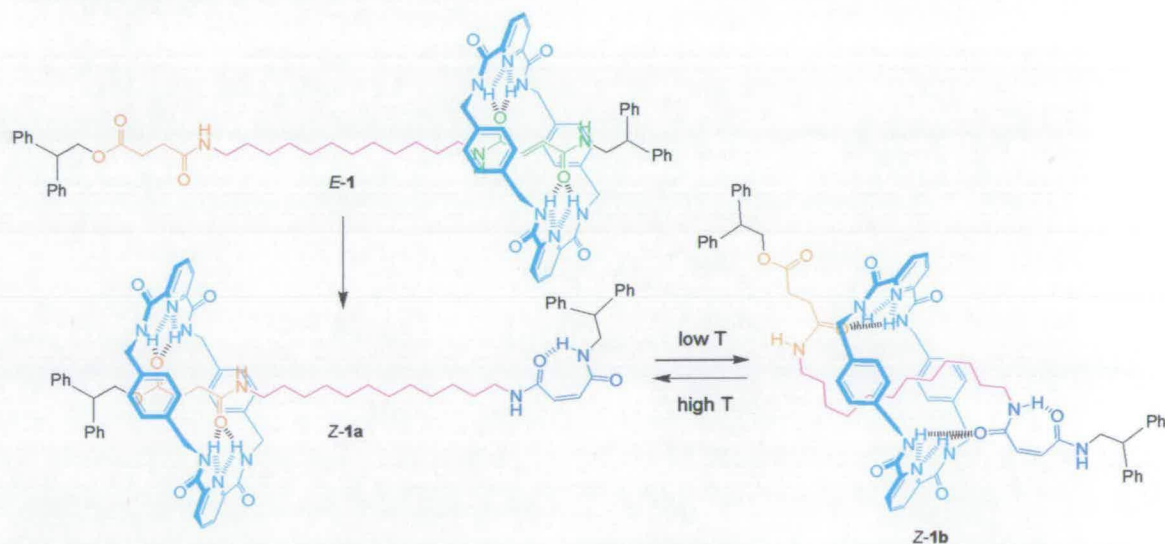
Scheme 1 *An example of tri-stable rotaxane. The interconversions between the two co-conformers Z-1a and Z-1b are the entropy-driven processes*

The temperature-driven co-conformational changes are possible in virtue of the different enthalpic and entropic stabilisation that the two co-conformers have. In Z-

1b the high entropic cost paid by the system in order to organise the thread in an "S" shape conformation is paid back by a better enthalpic stabilisation (formation of strong amide-amide hydrogen bonds). In **Z-1a** the situation is reversed with the poorer enthalpic stabilisation (formation of weak amide-ester hydrogen bonds) compensated by the lower entropic term associated with this co-conformation. Being the $\Delta G_{binding} = \Delta H_{binding} - T\Delta S_{binding}$ if the $\Delta S_{binding}$ terms of the two co-conformations are sufficiently different then the relative binding affinity of the macrocycle for the two stations can be reversed increasing or decreasing the temperature, as it happen in this rotaxane; the first example of entropy-driven molecular shuttle!

5.1 Introduction

Stimuli-responsive molecular "shuttles" are mechanically interlocked molecules in which a macrocycle can reside on stations of different binding affinities (Figure 5.1a).[1] In response to an external stimulus one of the stations is chemically changed and the relative binding affinity of the macrocycle for the stations altered, resulting in a "shuttling" of the ring by biased Brownian motion (Figure 5.1b).
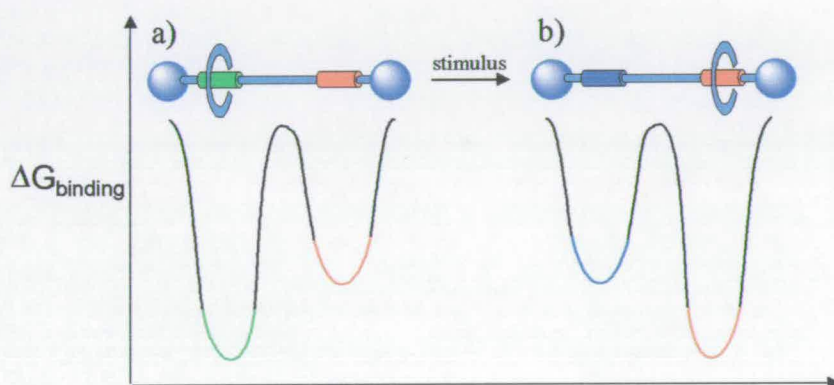
Figure 5.1 A stimuli-responsive molecular shuttle.

Although many external stimuli have been used to induce shuttling (*e.g.* pH,[2] light,[3] electrons[4] etc.), a temperature change is not one of them (except when it brings about a chemical change in one of the stations, as already seen in chapter four) because changing the temperature will normally not change the relative binding affinity of the stations for the macrocycle, only the degree of discrimination that the macrocycle has for the two stations. However, in principle, a change of relative binding affinity with temperature *is* possible because $\Delta G_{binding} = \Delta H_{binding} - T\Delta S_{binding}$. If the $\Delta S_{binding}$ terms of the two stations are sufficiently different then the relative binding affinity of the macrocycle for the two stations can be reversed by increasing or lowering the temperature.

Here we describe the first example of this phenomenon in the form of a molecular shuttle where the ring moves between two different portions of the thread with high

fidelity in response to changes in the temperature. During this shuttling processes there is no change to the covalent structure of the molecule or the environment (except for the temperature change). The rotaxane in question is, in fact, a tri-stable shuttle in which interconversion between three forms is achieved by photo and thermal stimuli (Figure 5.2). Switching between two of the three forms is the entropy-driven process.
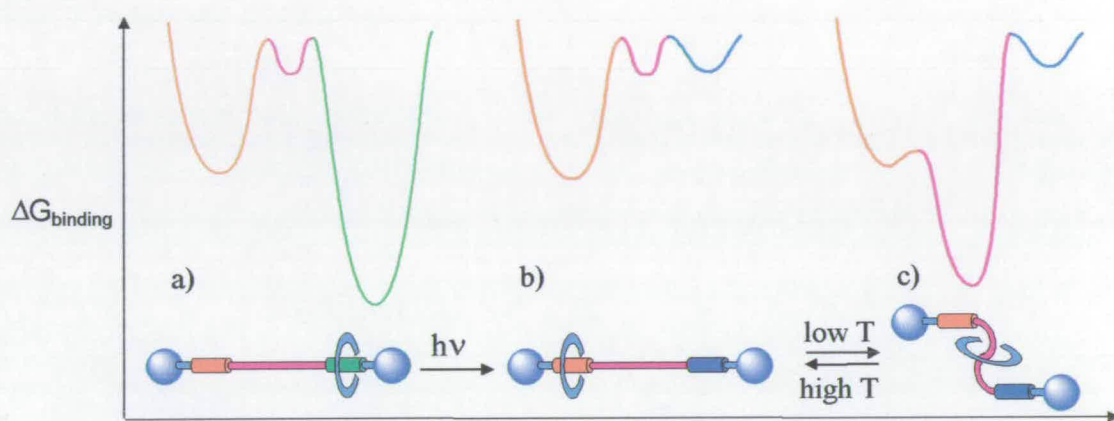
Figure 5.2 Macrocycle translocation in a tri-stable photo- and thermally- responsive molecular shuttle.

5.2 Result and Discussion

The rotaxane *E*-**1**, synthesised in a 32% yield from the thread *E*-**2**, contains two hydrogen bonding sites for the endo pyridyl tetraamide macrocycle, namely a photoactive fumaramide (green) and a succinic amide-ester (orange) units, separated by a C_{12} lipophilic chain (purple) and can be considered, as we will see later, a three station shuttle – the fumaramide/maleamide, the succinic amide-ester and the alkyl chain (Scheme 5.1).

Since the xylylene units of the macrocycle shield the encapsulated regions of the thread, the position of the ring in *E*-**1** could be determined by ^{1}H NMR spectroscopy by comparing the chemical shift of the protons in the rotaxane with those of the corresponding thread.
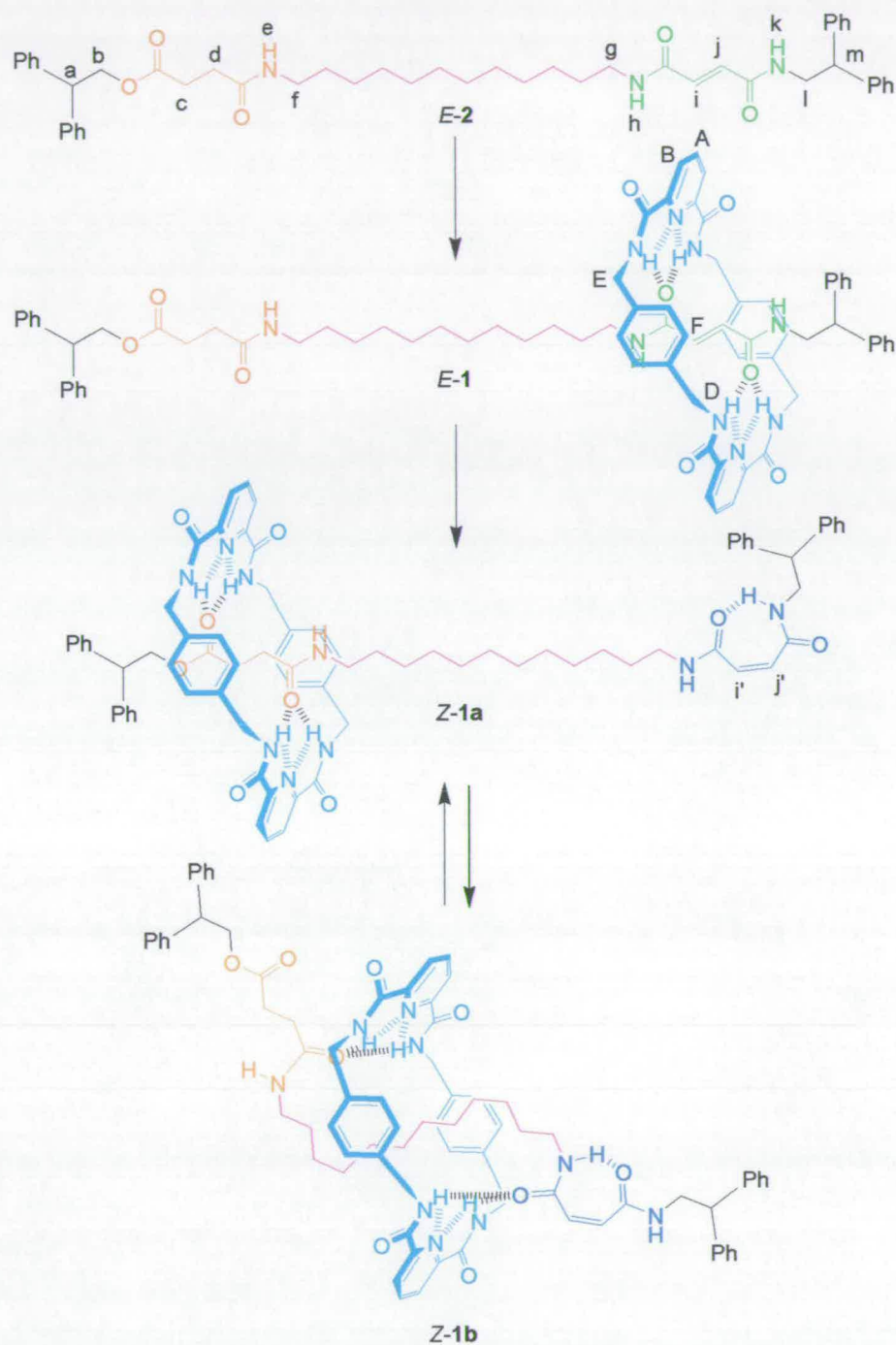
Scheme 5.1 Synthesis of tri-stable molecular shuttles *E*/*Z*-**1**. (i) isophthaloyl dichloride, *p*-xylylenediamine, Et₃N, CHCl₃, *E*-**1**, 32%; (ii) hν at 254 nm for 15 mins in CH₂Cl₂, *Z*-**1**, 48%. Full experimental procedures can be found in the Experimental Section.

As seen for to the two-station fumaramide-containing rotaxanes of the previous chapter, in E-**1** the *trans*-olefin *bis*-amide unit presents a better binding affinity for the macrocycle compared to the succinic amide-ester station (Figure 5.2a). The ^{1}H NMR spectra (400 MHz, 298K) of E-**1** and the linear component E-**2** in CDCl$_3$ show in fact the E-alkene protons H$_i$ and H$_j$ shielded by more that 1.5 ppm in the rotaxane E-**1** compared to the thread E-**2**, whereas the chemical shifts of the succinic amide-ester protons H$_c$ and H$_d$ are unchanged (Figure 5.3).
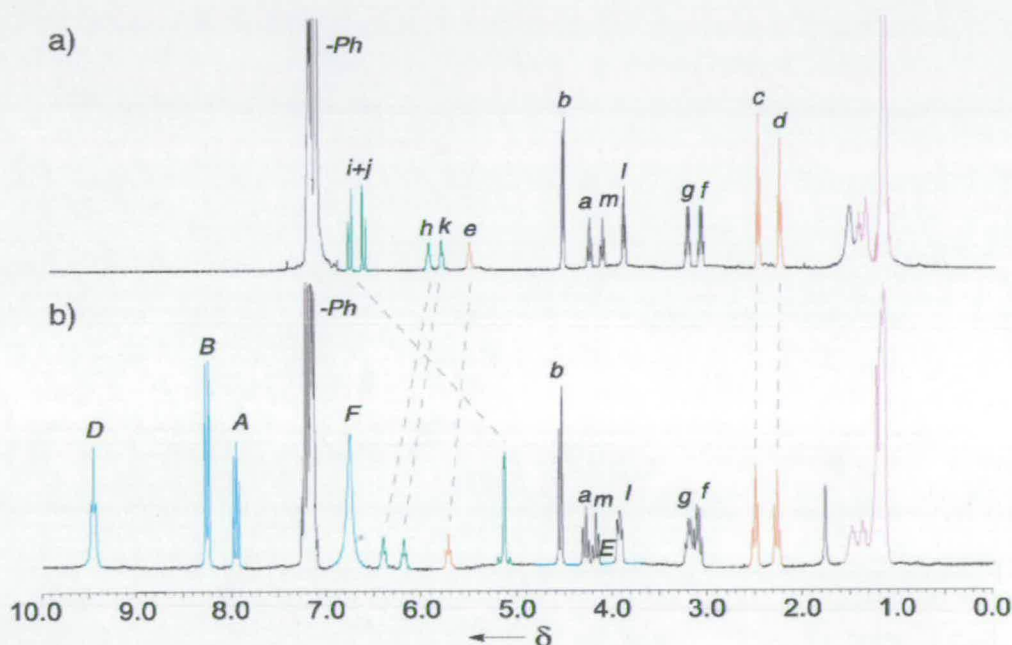
Figure 5.3 400 MHz ^{1}H NMR spectra of (a) thread E-**2** and (b) rotaxane E-**1** in CDCl$_3$ at 298K. The assignments correspond to the lettering shown in Scheme 5.1

It is interesting to notice from the spectrum of E-**1** at room temperature how the restricted rotamerisation of the benzylic amides of the macrocycle, imposed by the formation of intracomponent hydrogen bonds between the amide hydrogens and the pyridine nitrogens, ultimately results in a "dampening" of the circumrotation of the ring. This is indicated by the coalescence of the diastereotopic benzylic protons H$_E$ (for a

detailed explanation of the circumrotation process in hydrogen-bonded rotaxanes see chapter three).

Low temperature ^{1}H NMR experiment (258K) of E-1 showed the same chemical shifts for the fumaric and succinic amide-ester protons as seen at 298K, only resulting in the resolution of the benzylic protons H_E as consequence of the slowed circumrotation, thus proving that at this temperature, as at room temperature, the co-conformer bearing the macrocycle over the fumaric station is by far the major one (>95%).

Isomerisation of the fumaramide-containing rotaxane E-1 at 254 nm afforded the corresponding cis-rotaxane isomer Z-1 in a 48% yield. In Z-1 the excellent fumaramide template has been converted into a poor one (*i.e.* maleamide unit). To our surprise, the ^{1}H NMR spectra of this rotaxane proved highly temperature dependent, in contrast to E-1 and the isophthalamide analogue of Z-1 seen in the previous chapter.

At 308K, ^{1}H NMR spectra (400 MHz) in CDCl$_3$ of the rotaxane Z-1 and the maleamide thread show identical chemical shifts for the maleamide protons Hi' and Hj' whereas the succinic amide-ester ones H_c and H_d are shifted upfield by ~1.2 ppm (Figure 5.4a and b), thus confirming the positioning of the ring over the succinic amide-ester unit at this temperature (co-conformer Z-1a, Figure 5.2b).

The low temperature ^{1}H NMR spectrum (258K) of Z-1 shows an increased complexity (Figure 5.4c). Remarkably, at this temperature the succinic amide-ester protons H_c and H_d occur at the same chemical shifts as in the uninterlocked maleamide thread, as do the maleamide protons $H_{i'}$ and $H_{j'}$. However the alkyl protons of the C_{12} chain experience dramatic upfield shift (up to 1 ppm). Moreover a splitting is observed in the chemical shifts of the protons of the macrocycle suggesting that the two halves of the ring are experiencing magnetically different environments.
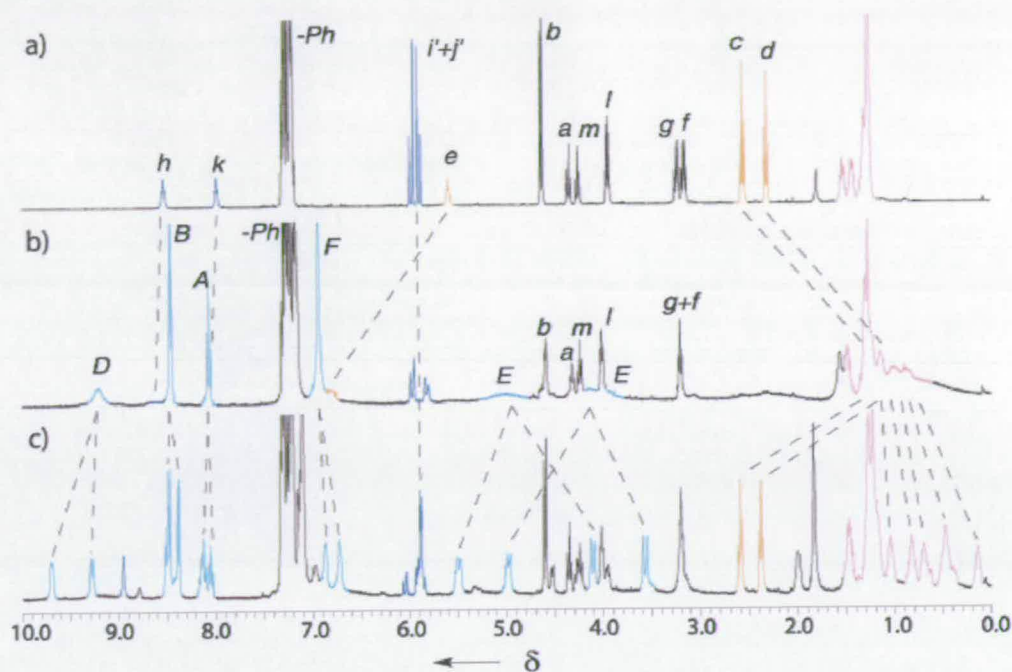
Figure 5.4 400 MHz ^{1}H NMR spectra in CDCl$_3$ of (a) maleamide isomer of *E-2* at 308K, (b) rotaxane *Z-1* at 308K and (c) rotaxane *Z-1* at 258K. The assignments correspond to the lettering shown in Scheme 5.1

Although these are preliminary data and more experiments (NOESY, TOCSY) and calculations (molecular modelling) need to be done, it seems that at this temperature the Z-rotaxane adopts a co-conformation resulting in positioning of the pyridine macrocycle over the lipophilic region of the thread. The two "uncovered" stations of the thread probably act as hydrogen bond acceptors towards the amide hydrogens of the macrocycle forcing the alkyl chain to adopt a "S" shape conformation (co-conformer *Z-1b*, Figure 5.2c).

Interestingly the "S" shape conformation of the thread that we assume to be present for the co-conformer *Z-1b* at low temperature is observed in the solid state structure of an isophthalamide rotaxane containing two amide units separated by a C$_{12}$ lipophilic chain (Figure 5.5). It is worth noting that at room temperature in a non-polar solvent such as CDCl$_3$ in this rotaxane the isophthalamide macrocycle shuttles along the linear component displaying no discrimination for any particular portion of the thread!
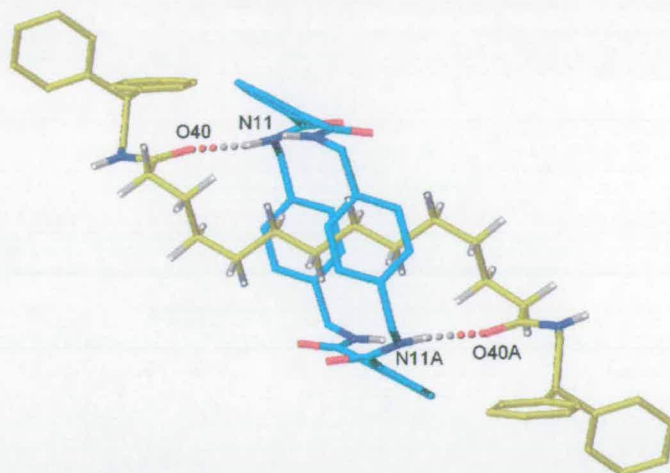
Figure 5.5 *X*-Ray crystal structure of an isophthaloyl-based rotaxane in which the two amide are separated by a C_{12} alkyl chain. The carbon atoms of the macrocycles are shown in blue, carbon atoms of the threads in yellow, oxygen atoms in red and nitrogen atoms in dark blue. The amide and the C_{12} alkyl hydrogen atoms are shown in white while all others are removed for clarity. Intramolecular hydrogen bond distances and angles are the following: O40-HN11/O40A-HN11A 1.92 Å, 156.4°.

To summarise, at higher temperature (308K) the macrocycle of rotaxane *Z*-**1** resides predominantly (>95%) on the succinic amide-ester station, whereas at lower temperature (258K) it shuttles to spend >95% encapsulating the alkyl chain! The reversal of the binding affinity of the macrocycle for the succinic amide-ester and the alkyl chain at different temperatures can <u>only</u> occur by the TΔS term reversing the relative $\Delta G_{binding}$ of these two stations (Figure 5.2b and c).

5.3 Conclusions

Why does the *Z*-rotaxane behave in such a way whereas *E*-**1** and the isophthalamide analogue of *Z*-**1** seen in the previous chapter do not? Clearly the endo pyridyl nitrogen atoms play a crucial role. The amide hydrogens of the macrocycle are in fact partially self-satisfied by the formation of intracomponent hydrogen bonds with the pyridine atoms and hydrogen bonding to the thread is therefore relatively weak.

In the co-conformer Z-**1a** two of the amide hydrogens of the macrocycle bind to the ester carbonyl (a significantly weaker hydrogen bond acceptor than the amide - estimated of ~1 kcal mol^{-1} in related rotaxane systems) whereas in the co-conformer Z-**1b** all the hydrogen bonds are formed to amide carbonyls which gives a better enthalpic stabilisation for that co-conformation but obviously requires considerable organisation of the alkyl chain into the "S" shape.

In Z-**1b** the entropic cost paid by the thread in order to restrict its numerous degrees of freedom and assume an "S" shape conformation (a C_{12} chain has more than 500000 (3^{12}) possible C-C rotamers between the amide carbonyls!) is paid back by the enthalpic stabilisation derived from the formation of the stronger amide-amide hydrogen bonds. The raising of the temperature results in an increase of the entropic term of the co-conformer Z-**1b** so that the Z-rotaxane predominantly adopts the enthalpically less favourable but ultimately entropically preferred Z-**1a** co-conformation.

5.4 Experimental Section

The synthesis and the spectroscopic data of the linear components of the rotaxanes E-1 and Z-1 have been reported in the Experimental Section of chapter four.

[2]-(1,4,7,14,17,20-Hexaaza-2,6,15,19-tetraoxo-3,5,9,12,16,18,22,25 – tetrabenzocyclohexacosane)-((E)-N-{12-[3-(2,2-diphenylethylcarbamoyl)-acryloylamino]-dodecyl}-succinamic acid 2,2-diphenylethyl ester)-rotaxane, E-1.
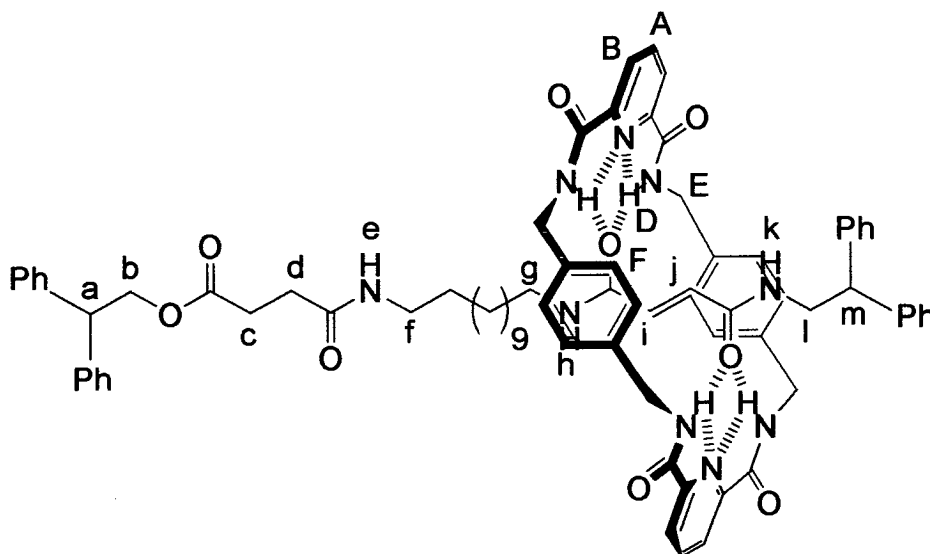
Rotaxane E-1 has been synthesized using the general procedure for the preparation of benzilyc amide macrocycle containing [2]rotaxane from the thread E-1 (0.19 g, 0.25 mmol). The crude was subjected to column cromatography on silica gel using a gradient of CH_2Cl_2 to CH_2Cl_2/EtOAc (80/20) as eluent to obtain the desired compound as a colourless powder (E-1, 0.10 g, 32%). ^{1}H NMR (400 MHz, CDCl$_3$, 298K): δ = 9.47 (m, 4H, NH_D), 8.36 (d, ^3J(H,H) = 7.6 Hz, 4H, CH_B), 8.04 (t, ^3J(H,H) = 7.7 Hz, 2H, CH_A), 7.33-7.17 (m, 20H, ArCH), 6.82 (br s, 8H, ArCH_F), 6.12 (br s, 1H, NH_k), 6.05 (br s, 1H, NH_h), 5.73 (t, ^3J(H,H) = 5.3 Hz, 1H, NH_e), 5.22 (d, ^3J(H,H) = 14.5 Hz, 1H, C$H_{i\,or\,j}$), 5.16

(d, ^3J(H,H) = 14.5 Hz, 1H, C$H_{i \text{ or } j}$), 4.80-3.70 (br m, 8H, CH_E), 4.63 (d, ^3J(H,H) = 7.6 Hz, 2H, CH_b), 4.34 (t, ^3J(H,H) = 7.6 Hz, 2H, CH_a), 4.22 (t, ^3J(H,H) = 8.0 Hz, 1H, CH_m), 3.97 (m, 2H, CH_l), 3.25 (dt, 2H, CH_g), 3.16 (dt, 2H, CH_f), 2.56 (t, ^3J(H,H) = 6.8 Hz, 2H, CH_c), 2.32 (t, ^3J(H,H) = 6.8 Hz, 2H, CH_d), 1.55 (m, 2H, -CH_2-CH$_f$), 1.44 (m, 2H, -CH_2-CH$_g$), 1.35-1.17 (m, 16H, -CH_2-); ^{13}C NMR (100 MHz, CDCl$_3$,): δ = 172.8 (CO succinic), 171.1 (CO succinic), 165.2 (CO fumaric), 164.9 (CO fumaric), 163.6 (CO macrocycle), 149.1, 141.4, 141.0, 138.7 (CH$_A$), 137.9, 129.0, 128.6 (CH$_F$), 128.2, 127.8, 127.3, 126.8, 124.9 (CH$_B$), 66.9 (CH$_b$), 50.3 (CH$_m$), 49.8 (CH$_a$), 44.7 (CH$_l$), 40.2 (CH$_g$), 39.6 (CH$_f$), 31.0 (CH$_d$), 29.7 (CH$_c$), 29.5, 29.4, 29.3, 29.2, 29.1, 27.0, 26.8; HRMS (FAB) Calcd. for C$_{78}$H$_{86}$N$_9$O$_9$ [M+H]$^+$ 1292.65485. Found 1292.65598.

[2]-(1,4,7,14,17,20-Hexaaza-2,6,15,19-tetraoxo-3,5,9,12,16,18,22,25 – tetrabenzocyclohexacosane)-((Z)-N-{12-[3-(2,2-diphenylethylcarbamoyl)-acryloylamino]-dodecyl}-succinamic acid 2,2-diphenylethyl ester)-rotaxane, Z-1.
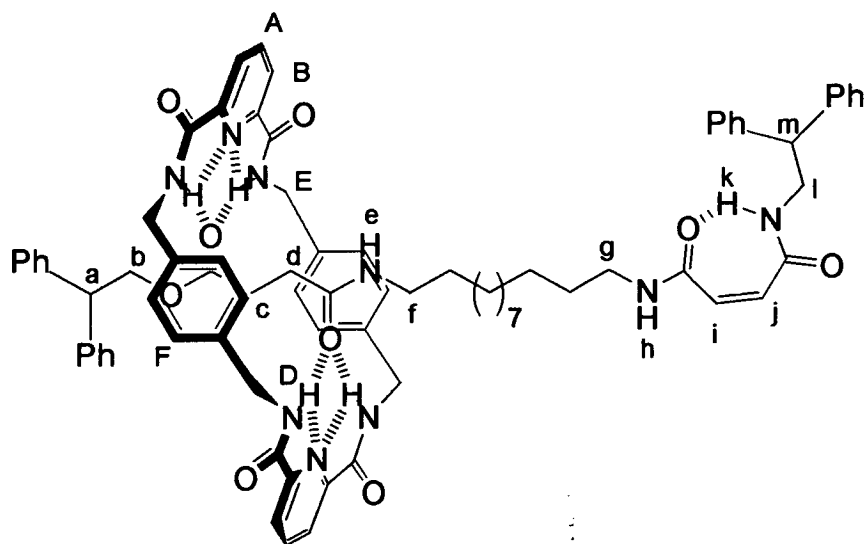
Rotaxane Z-1 was obtained by photochemical isomerisation at 254 nm of E-1 (0.05 g, 0.04 mmol) in CH$_2$Cl$_2$ for 15 mins. The solution was then concentrated and columned on silica gel using a gradient of CHCl$_3$/EtOAc 3/1 to obtain the desired compound as a

colourless solid (*Z*-**1**, 0.02 g, 48%). ^{1}H NMR (400 MHz, CDCl$_3$, 308K): δ = 9.21 (s, 4H, NH_D), 8.64 (br s, 1H, NH_h), 8.47 (d, ^3J(H,H) = 7.8 Hz, 4H, CH_B), 8.09 (br s, 1H, NH_k), 8.07 (t, ^3J(H,H) = 7.7 Hz, 2H, CH_A), 7.35-7.12 (m, 20H, ArCH), 6.94 (br s, 8H, ArCH_F), 6.88 (br s, 1H, NH_e), 5.97 (d, ^3J(H,H) = 13.4 Hz, 1H, C$H_{i'\ or\ j'}$), 5.83 (d, ^3J(H,H) = 13.4 Hz, 1H, C$H_{i'\ or\ j'}$), 5.25-4.79 (br m, 4H, CH_E), 4.59 (d, ^3J(H,H) = 7.1 Hz, 2H, CH_b), 4.39-3.88 (br m, 4H, CH_E), 4.31 (t, ^3J(H,H) = 7.1 Hz, 1H, CH_a), 4.24 (t, ^3J(H,H) = 8.0 Hz, 1H, CH_m), 4.01 (br dd, 2H, CH_l), 3.21 (br m, CH_g+ CH_f), 1.52-0.45 (br m, -CH_2- + CH_c + CH_d); ^{13}C NMR (100 MHz, CDCl$_3$): δ = 174.2 (*C*O), 171.9 (*C*O), 163.5 (*C*O), 158.1 (*C*O), 149.1 (*C*O), 141.0, 138.7, 129.0, 128.8, 128.6, 128.1, 127.7, 127.3, 126.9, 125.4, 60.4, 50.9, 49.7, 42.9, 39.7, 29.7, 29.5, 29.4, 29.2, 29.2, 26.8; HRMS (FAB) Calcd. for C$_{78}$H$_{86}$N$_9$O$_9$ [M+H]$^+$ 1292.65485. Found 1292.65564.

5.5 References

1. For recent reviews see a) V. Balzani, A. Credi, F. M. Raymo, J. F. Stoddart, *Angew. Chem.* **2000**, *112*, 3484-3530; *Angew. Chem. Int. Ed.* **2000**, *39*, 3349-3391. b) Special issue on *Molecular Machines, Acc. Chem. Res.* **2001**, *34*, 409-522. c) Special issue on *Molecular Machines and Motors.* Structure and Bonding *Vol. 99* (Ed.: J.-P. Sauvage), Springer, Berlin, **2001**.

2. P. R. Ashton, R. Ballardini, V. Balzani, I. Baxter, A. Credi, M. C. T. Fyfe, M. T. Gandolfi, M. Gómez-López, M.-V. Martínez-Díaz, A. Piersanti, N. Spencer, J. F. Stoddart, M. Venturi, A. J. P. White, D. J. Williams, *J. Am. Chem. Soc.* **1998**, *120*, 11932-11942.

3. a) P. R. Ashton, R. Ballardini, V. Balzani, A. Credi, K.R. Dress, E. Ishow, C. J. Kleverlaan, O. Kocian, J. A. Preece, N. Spencer, , J. F. Stoddart, M. Venturi, S. Wenger, *Chem. Eur. J.* **2000**, *6*, 3558-3574. b) A. M. Brouwer, C. Frochot, F. G. Gatti, D. A. Leigh, L. Mottier, F. Paolucci, S. Roffia, G. W. H. Wurpel, *Science*, **2001**, *291*, 2124-2128. c) G. W. H. Wurpel, A. M. Brouwer, I. H. M. van Stokkum, A. Farran, D. A. Leigh, *J. Am. Chem. Soc.* **2001**, *123*, 11327-11328. d) H. Murakami, A. Kawabuchi, K, Kotoo, M. Kunitake, N. Nakashima, *J. Am. Chem. Soc.* **1997**, *119*, 7605-7606.

4. a) N. Armaroli, V. Balzani, J.-P. Collin, P. Gaviña, J.-P. Sauvage, B. Ventura, *J. Am. Chem. Soc.* **1999**, *121*, 4397-4408. b) R. Ballardini, V. Balzani, W. Dehaen, A. E. Dell'Erba, F. M. Raymo, J. F. Stoddart, M. Venturi, *Eur. J. Org. Chem.* **2000**, 591-602. c) C. P. Collier, J. O. Jeppesen, Y. Luo, J. Perkins, E. W. Wong, J. R. Heath, J. F. Stoddart, *J. Am. Chem. Soc.* **2001**, *123*, 12632-12641.

Control of the Expression of Chirality in Hydrogen Bonded [2]Rotaxanes

Prepared as a communication to Journal of American Chemical Society as:

"Switching "On" and "Off" the Expression of Chirality in Bistable, Light and Heat-Switchable, Hydrogen Bonded Molecular Shuttles"

Bottari, G.; Leigh, D. A.

In this Chapter we describe a chiral [2]rotaxane (E-1, Scheme 1) in which stimuli-induced translocation of the macrocycle between the two stations of a thread causes remarkable changes in the circular dichroism (CD) absorption. The molecule E-1 consists of a benzylic amide macrocycle mechanically interlocked onto a thread containing a photoisomerisable fumaramide station (green) and a chiral, non-photoactive, glycyl-(L)-leucine dipeptide station (orange).
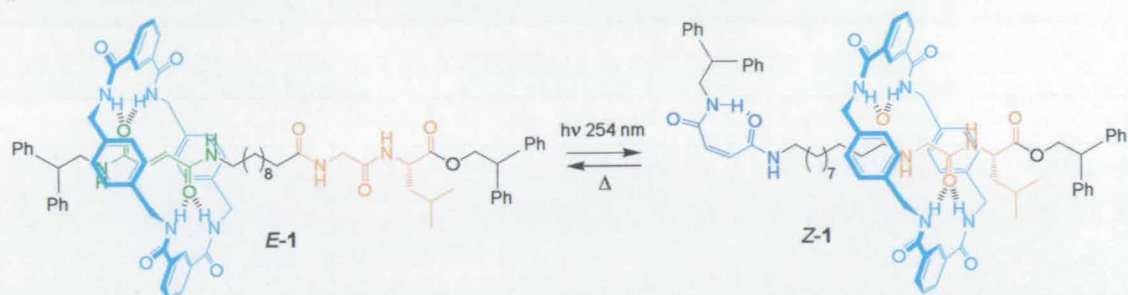
Scheme 1 *An example of photo- and thermal- induced stimuli-responsive molecular shuttle in which the submolecular motion of the ring is accompanied by changes in the CD absorption spectrum.*

Similarly to the stimuli-responsive fumaramide containing two-station [2]rotaxanes seen in the previous two chapters, also in E-1 at room temperature the macrocycle resides preferentially over the fumaramide template as confirmed by ^1H NMR spectroscopy. E→Z photochemical isomerisation is then used to convert the fumaramide unit into the poor maleamide template thus resulting in the translocation of the ring over the dipeptide portion as confirmed by ^1H NMR spectroscopy (Z-1). The photochemical isomerisation process can be reversed by subjecting Z-1 to a thermal stimulus, as already seen in the previous chapters, thus re-obtaining the rotaxane isomer E-1. CD spectra of dilute chloroform solutions of E/Z-1 and their respective uninterlocked linear components were recorded in the aromatic excitation region between 235-320 nm. The CD spectra shows that in rotaxane Z-1, where the macrocycle is positioned over the dipeptide portion, the absorption is more that four fold of magnitude bigger than in E-1 and the other two uninterlocked linear components. The phenomenon, already reported for simpler "one station" dipeptide rotaxanes, is related to the possibility of transmitting chirality from the amino acid asymmetric center on the thread via the macrocycle to the C-terminal stopper of the rotaxane.

6.1 Introduction

A rotaxane[1] is a molecule consisting of a macrocycle trapped onto a dumbbell-shaped component by two bulky stoppers. The unique architecture of rotaxanes give rise, in some cases, to remarkable changes in the physical properties of the mechanically interlocked molecule with respect to its separate, uninterlocked constituents.[2]

Moreover rotaxanes are a class of compounds well-suited for exploring switching phenomena. Control of the translocation of the macrocycle from one portion of the thread to another, a so-called "molecular shuttle", is a key feature for the realisation of such switchable molecules, the forerunners of artificial molecular machines.[3] To date several systems have been developed in which the shuttling movement is promoted by the use of different external stimuli such as light, electrons, pH and the nature of the environment.[4]

6.2 Results and Discussion

Here we describe the first examples of bistable hydrogen bonded rotaxanes (*E/Z*-**1**) in which the expression of the chirality can be switched "on" and "off" through large amplitude translational motion of the macrocycle over the stoppered thread in response to photonic or thermic stimuli.

It has been shown how chiral peptide units induce an asymmetric response in the optical absorption band of achiral partners (ICD) in rotaxane architectures.[2e] The phenomenon is related to the transmission of chirality from the amino acid asymmetric center *via* the macrocycle to the C-terminal aromatic stoppers of the rotaxane as consequence of the tight fitting of the intrinsically achiral ring onto the chiral dipeptide. The magnitude and sign of this absorption can be altered either thermally or by changes in the nature of the environment. By incorporating a chiral dipeptide unit in a bistable rotaxane we reasoned that it might be possible to obtain the same switching phenomenon through the controlled shuttling movement of the cyclic unit.

The chiral peptido[2]rotaxane E-1, containing two distinct and separated (~1.5 nm) binding stations for the benzylic tetra-amide macrocycle, namely a fumaric diamide and a glycyl-(L)-leucine, was synthesized from E-2 in 58% yield (Scheme 6.1).
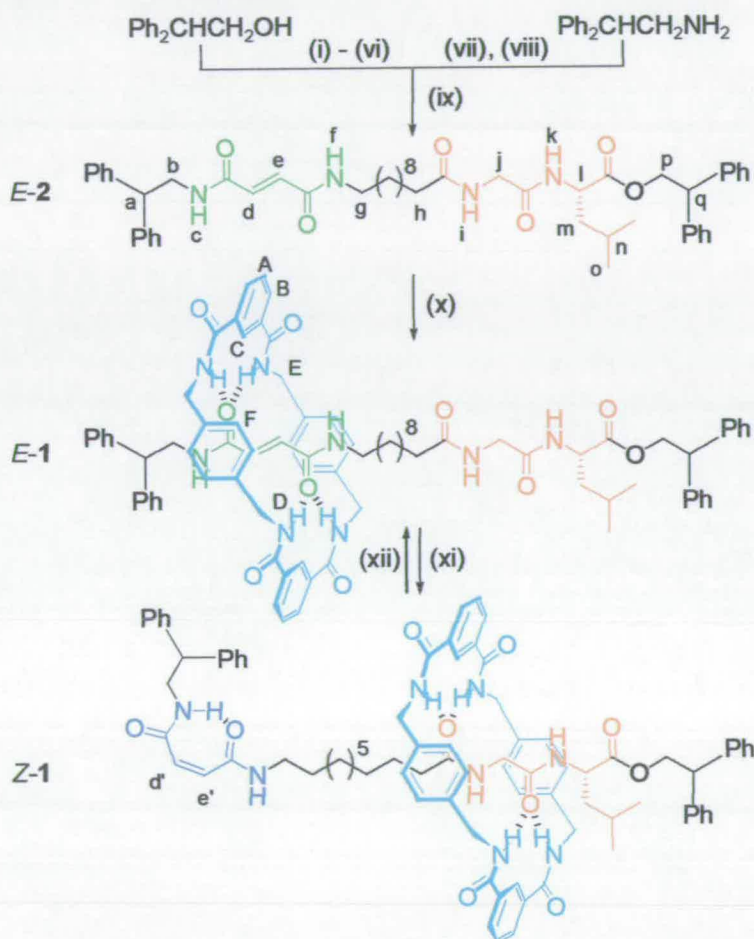
Scheme 6.1 Synthesis of bistable molecular shuttles E/Z-1; i) N-(*tert*-butoxycarbonyl)-L-leucine monohydrate, 4-dimethylaminopyridine (4-DMAP), 1-(3-dimethylaminopropyl)-3-ethyl-carbodiimide hydrochloride (EDCI), CHCl$_3$, 94%. ii) trifluoroacetic acid (TFA), CHCl$_3$, quantitative. iii) N-(*tert*-butoxycarbonyl)-glycine, 4-DMAP, EDCI, CHCl$_3$, 91%. iv) TFA, CHCl$_3$, quantitative. v) N-(*tert*-butoxycarbonyl)-11-undecanoic acid, 4-DMAP, EDCI, CHCl$_3$, 82%. vi) TFA, CHCl$_3$, quantitative. vii) fumaric acid monoethylester, 4-DMAP, EDCI, CHCl$_3$, 85%. viii) EtOH, NaOH, 91%. ix) 4-DMAP, EDCI, DMF, 74%. x) *para*-xylylenediamine, isophthaloyl dichloride, Et$_3$N, CHCl$_3$, 58%. xi) CH$_2$Cl$_2$/MeOH, 20 mins, 254 nm, 42%. xii) C$_2$H$_2$Cl$_4$ at 130°C, 6 days, 95%. Full experimental procedures can be found in the Experimental Section.

The ^{1}H NMR spectrum of this rotaxane shows remarkable positional discrimination of the macrocycle *in virtu* of its different binding affinity towards the two diamide stations.

In fact where the peptidic protons are only slightly affected by the aromatic shielding effect of the molecular ring thus occurring at almost identical chemical shifts to that of the thread (*e.g.* j ~0.2 ppm), instead the *E*-olefin protons are shifted upfield (*i.e.* d and e ~1.2 ppm). This suggests that the co-conformer having the macrocycle over the fumaramide portion is the major isomer on the NMR timescale (Figure 6.1a and 6.1b).
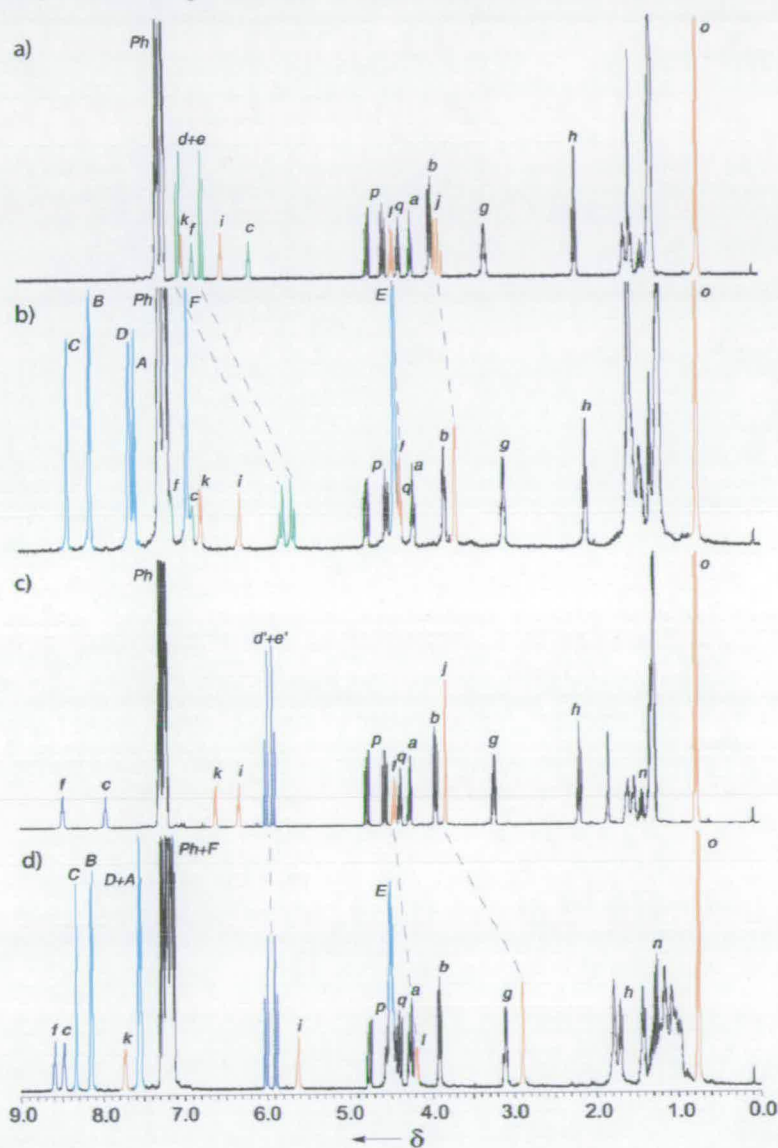
Figure 6.1. 400 MHz ¹H NMR spectra in CDCl₃ at 298K of a) thread *E*-2, b) rotaxane *E*-1, c) maleamide isomer of *E*-2, d) rotaxane *Z*-1. The assignments correspond to the lettering shown in Scheme 6.1.

Light-driven $E \rightarrow Z$ isomerization is then used to reverse the binding affinity order of the macrocycle for the two stations, and consequentially its preferred position shifts from the fumaramide station to the peptidic portion.[5] The ^{1}H NMR spectra in Figure 6.1c and 6.1d show that the position of the macrocycle on the thread is completely reversed in the maleamide isomer Z-1. The Z-olefin protons $H_{d'}$ and $H_{e'}$ are almost isochronous in the rotaxane and the thread, whereas the glycine methylene protons are now shielded by 0.9 ppm, suggesting that the macrocycle is situated preferentially over the peptide. By heating a solution of Z-1 in $C_2H_2Cl_4$ at 130 °C for 6 days the fumaramide isomer E-1 is obtained in a 95% yield. Circular dichroism (CD) measurements in the wavelength region of the aromatic excitation (235-320 nm) were carried out on dilute (0.1 mM) solutions of the two rotaxanes E/Z-1 and their respective linear uninterlocked components in CHCl$_3$ at 10 °C (Figure 6.2). Of the four dipeptide molecules only rotaxane Z-1 presented a strong (13k deg cm^2 dmol^{-1}) negative induced CD (θ) value in the scanned region whereas for rotaxane E-1 and the two uninterlocked threads the elliptical polarization fell close to zero. The result is in perfect agreement with both our understanding about the mechanism of the generation of the CD response in chiral peptide rotaxanes and the positional discrimination of the macrocycle in rotaxanes E/Z-1 deduced by ^{1}H NMR.
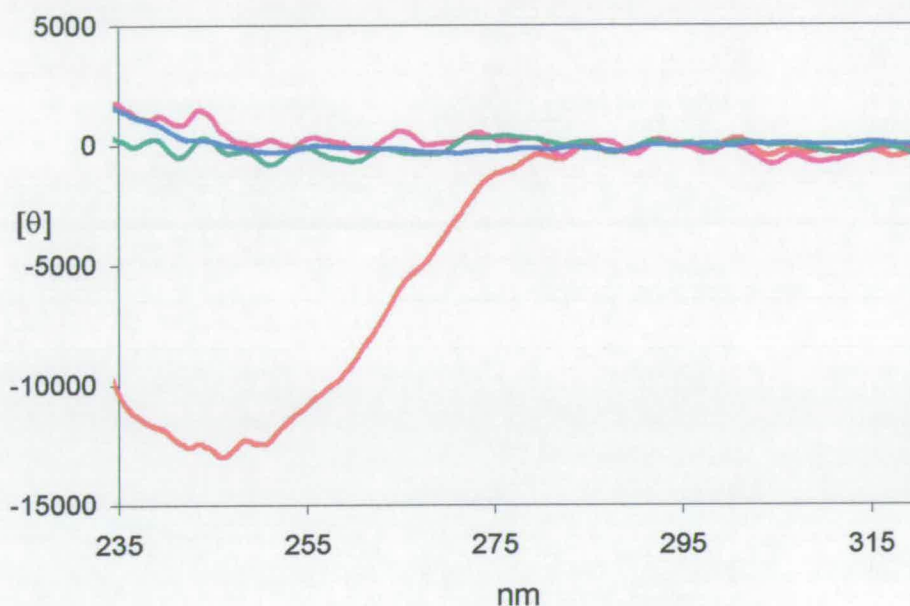
Figure 6.2. CD spectra (0.1 mM) in CHCl₃ at 283K of rotaxane *Z*-**1** (red), *E*-**1** (purple), *E*-**2** (green) and maleamide isomer of *E*-**2** (blu).

In rotaxane *Z*-**1** in fact the macrocycle is preferentially situated over the peptide unit in close proximity to the C- terminal phenyl stoppers, the aromatic units considered responsible for the CD absorption, whereas in the *E*-**1** isomer this proximity is drastically diminished and consequentially the CD absorption extinguished.

6.3 Conclusions

It has been shown how control of the positioning of submolecular units in rotaxane architectures can be used to alter the CD absorption. Control of the expression of the chirality in switchable interlocked systems using light and heat stimuli through hiding or revealing chiral units could have important application in areas where chiral transmission from one chemical entity to another underpins a physical or chemical response, such as the seeding of supertwisted nematic liquid crystalline phase or asymmetric synthesis.

6.4 Experimental Section

(2S)-*tert*-Butoxycarbonylamino-4-methyl-pentanoic acid 2,2-diphenyl-ethyl ester, S1
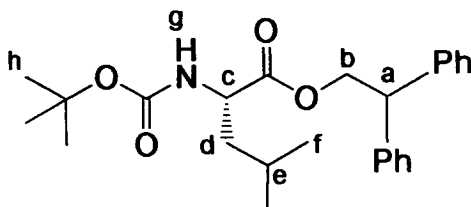
To a stirred solution of *N*-(*tert*-butoxycarbonyl)-L-leucine monohydrate (3 g, 12 mmol) in anhydrous CHCl$_3$ (150 mL) at 0 °C were simultaneously added under argon 4-DMAP (1.76 g, 14.4 mmol) and EDCI·HCl (2.65 g, 13.8 mmol). After 5 min 2,2-diphenylethylamine (2.38 g, 12 mmol) was added and the reaction mixture allowed to stir for 16 h under inert atmosphere. The solution was then washed with 1N HCl (3 x 100 mL) and the organic layer dried over anhydrous MgSO$_4$ and filtered. The filtrate was then evaporated under reduced pressure to obtain a colourless oil that was purified by column chromatography (petroleum ether:diethyl ether 12:1) to afford the desired compound as a colourless oil (S1, 4.65 g, 94%). $[\alpha]^{25}_D$ = -28° (c = 0.5, MeOH); ^{1}H NMR (400 MHz, CDCl$_3$) δ 7.38-7.29 (m, 4H, ArC*H* (meta)), 7.28-7.20 (m, 6H, ArC*H* (ortho and para)), 4.82 (br m, 2H, C*H*H'$_b$ and N*H*$_g$), 4.62 (br m, 1H, CH*H*'$_b$), 4.42 (br dd, 1H, C*H*$_a$), 4.23 (m, 1H, C*H*$_c$), 1.48-1.40 (m, 10H, C*H*$_e$ and C*H*$_h$), 1.33-1.21 (m, 2H, C*H*$_d$), 0.82 (d, ^3J(H,H) = 6.3 Hz, 3H, C*H*$_f$), 0.79 (d, ^3J(H,H) = 6.5 Hz, 3H, C*H*$_f$); ^{13}C NMR (100 MHz, CDCl$_3$) δ 173.3 (CH$_c$-*C*O-O), 155.3 (NH$_g$-*C*O-O), 140.9 (Ar*C*- (ipso)), 140.7 (Ar*C*- (ipso)), 128.6 (Ar*C*H (meta)), 128.2 (Ar*C*H (ortho)), 128.1 (Ar*C*H (ortho)), 126.9 (Ar*C*H (para)), 79.7 (*C*(CH$_3$)$_3$), 67.2 (*C*H$_b$), 52.0 (*C*H$_a$), 49.8 (*C*H$_c$), 41.7 (*C*H$_d$), 28.3 (*C*H$_h$), 24.6 (*C*H$_e$), 22.5 (*C*H$_f$), 21.9 (*C*H$_f$); MS (FAB): *m/z* = 412 [(M+H)$^+$]; Anal. Calcd. for C$_{25}$H$_{33}$N$_1$O$_4$: C 72.96, H 8.08, N 3.40. Found: C 72.49, H 8.29, N 3.69.

(2S)-(2-*tert*-Butoxycarbonylamino-acetylamino)-4-methyl-pentanoic **acid** **2,2-diphenyl-ethyl ester, S2**
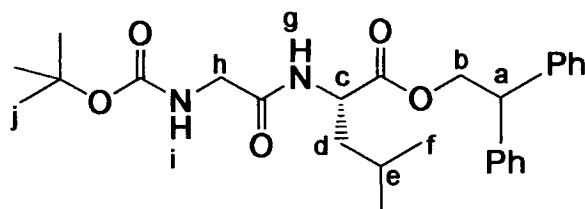
To a stirred solution of **S1** (2.30 g, 5.6 mmol) in anydrous $CHCl_3$ (30 mL) was added TFA (7 mL). After 2 h the solution was reduced in volume and the remained TFA removed *in vacuo*. The resulting oil was taken up in anhydrous $CHCl_3$ (100 mL) and *N*-(*tert*-butoxycarbonyl)-glycine (0.98 g, 5.6 mmol), 4-DMAP (0.82 g, 6.7 mmol) and EDCI·HCl (1.18 g, 6.2 mmol) added sequentially under argon at 0°C whilst stirring. After 16 h the solution was washed with 0.5N HCl (3 x 100 mL) and the organic layer was dried over anhydrous $MgSO_4$, filtered and the filtrate reduced in volume to obtain a yellow oil that was purified by column chromatography (CH_2Cl_2/EtOAc) (**S2**, 2.42 g, 91.2%). $[\alpha]^{25}_D$ = -23° (c = 0.5, MeOH); ^{1}H NMR (400 MHz, $CDCl_3$) δ 7.36-7.29 (m, 4H, ArC*H* (meta)), 7.28-7.22 (m, 6H, ArC*H* (ortho and para)), 6.38 (d, ^3J(H,H) = 8.1 Hz, 1H, N*H*$_g$), 5.05 (br, 1H, N*H*$_i$), 4.80 (dd, ^2J(H,H) = 10.6 Hz, ^3J(H,H) = 8.3 Hz, 1H, C*H*H'$_b$), 4.59 (dd, ^2J(H,H) = 10.6 Hz, ^3J(H,H) = 7.3 Hz, 1H, CH*H*'$_b$), 4.53 (m, 1H, C*H*$_c$), 4.40 (br dd, 1H, C*H*$_a$), 3.73 (m, 2H, C*H*$_h$), 1.50-1.38 (m, 10H, C*H*$_e$ and C*H*$_j$), 1.34 (m, 2H, C*H*$_d$), 0.81 (d, ^3J(H,H) = 6.3 Hz, 3H, C*H*$_f$), 0.78 (d, ^3J(H,H) = 6.6 Hz, 3H, C*H*$_{f'}$); ^{13}C NMR (100 MHz, $CDCl_3$) δ 172.4 (CH$_c$-*C*O-O), 169.1 (NH$_g$-*C*O), 155.2 (NH$_i$-*C*O-O), 140.7 (Ar*C*- (ipso)), 140.5 (Ar*C*- (ipso)), 128.6 (Ar*C*H (meta)), 128.2 (Ar*C*H (ortho)), 128.1 (Ar*C*H (ortho)), 126.9 (Ar*C*H (para)), 79.7 (*C*(CH$_3$)$_3$), 67.3 (*C*H$_b$), 50.7 (*C*H$_a$), 49.8 (*C*H$_c$), 44.2 (*C*H$_h$), 41.3 (*C*H$_d$), 28.2 (*C*H$_j$), 24.6 (*C*H$_e$), 22.6 (*C*H$_f$), 21.8 (*C*H$_{f'}$); MS (FAB): *m/z* = 469 [(M+H)$^+$]; Anal. Calcd for $C_{27}H_{36}N_2O_5$: C 69.21, H 7.74, N 5.98. Found: C 69.84, H 7.52, N 6.42.

11-*tert*-Butoxycarbonylamino-undecanoic acid, S3
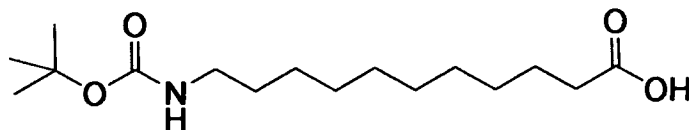
To a stirred solution of 11-aminoundecanoic acid (5 g, 24.8 mmol) in a mixture THF/H$_2$O (130 mL/130 mL) was added NaOH (2.18 g, 54.5 mmol). After 10 min di-*tert*-butyl dicarbonate was added and the reaction mixture let to stir for 20 h. The solution was reduced in volume, taken up with CHCl$_3$ (150 mL) and washed with 1N HCl (3 x 100 mL). The organic layer was then dried over MgSO$_4$, filtered and the filtrate reduced in volume to obtain a colourless powder that was recrystalized from hexane (S3, 7.15 g, 96%). m.p. 68 °C; ^{1}H NMR (400 MHz, CDCl$_3$) δ 4.55 (br, 1H, N*H*), 3.12 (br, 1H, NH-C*H$_2$*), 2.37 (t, ^3J(H,H) = 7.5 Hz, 2H, C*H$_2$*-CO), 1.66 (m, 2H, C*H$_2$*-CH$_2$-CO), 1.54-1.41 (m, 11H, C(C*H$_3$*)$_3$ and C*H$_2$*), 1.40-1.24 (m, 12H, C*H$_2$*); ^{13}C NMR (100 MHz, CDCl$_3$) δ 179.1 (*C*O-OH), 155.7 (NH-*C*O-O), 79.1 (*C*(CH$_3$)$_3$), 40.6, 34.0, 30.0, 29.4, 29.2, 29.1, 29.0, 28.9, 28.4 (C(*C*H$_3$)$_3$), 26.7, 24.7; MS (FAB): *m/z* = 302 [(M+H)$^+$]; Anal. Calcd. for C$_{16}$H$_{31}$NO$_4$: C 63.75, H 10.37, N 4.65. Found: C 63.28, H 10.08, N 4.62.

(2S)-[2-(11-*tert*-Butoxycarbonylamino-undecanoylamino)-acetylamino]-4-methyl-pentanoic acid 2,2-diphenyl-ethyl ester, S4
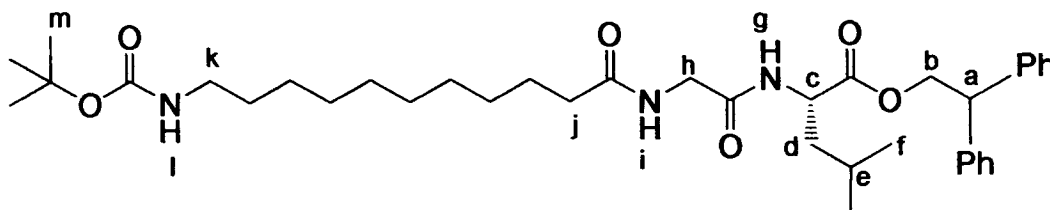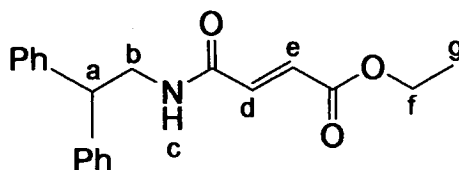
To a stirred solution of **S2** (2.62 g, 5.6 mmol) in anydrous $CHCl_3$ (30 mL) was added TFA (6 mL). After 2 h the solution was reduced in volume and the remained TFA removed *in vacuo*. The resulting oil was taken up in anhydrous $CHCl_3$ (100 mL) and **S3** (1.69 g, 5.6 mmol), 4-DMAP (0.82 g, 6.7 mmol) and EDCI·HCl (1.18 g, 6.2 mmol) added sequentially under argon at 0°C whilst stirring. After 16 h the solution was washed with 0.5N HCl (3 x 100 mL) and the organic layer was dried over anhydrous $MgSO_4$, filtered and the filtrate reduced in volume to obtain a colourless oil that was purified by column chromatography (CH_2Cl_2/EtOAc) (**S4**, 3 g, 82%). $[\alpha]^{25}_D = -18°$ (c = 0.5, MeOH); ^{1}H NMR (400 MHz, $CDCl_3$) δ 7.34-7.26 (m, 4H, ArCH (meta)), 7.25-7.20 (m, 6H, ArCH (ortho and para)), 6.62 (d, ^3J(H,H) = 7.8 Hz, 1H, NH_g), 6.34 (t, ^3J(H,H) = 5.0 Hz, 1H, NH_i), 4.78 (dd, ^2J(H,H) = 11.1 Hz, ^3J(H,H) = 8.6 Hz, 1H, CHH'$_b$), 4.56 (dd, ^2J(H,H) = 11.1 Hz, ^3J(H,H) = 7.3 Hz, 2H, CHH'$_b$ and NH_l), 4.45 (dd, ^3J(H,H) = 7.8 Hz, ^3J(H,H) = 7.0 Hz, 1H, CH_c), 4.38 (br dd, 1H, CH_a), 3.87 (d, ^3J(H,H) = 5.0 Hz, 2H, CH_h), 3.09 (m, 2H, CH_k), 2.20 (t, ^3J(H,H) = 7.7 Hz, 2H, CH_j), 1.62 (m, 2H, CH_2-CH$_j$), 1.50-1.39 (m, 10H, CH_e and CH_m), 1.35-1.24 (m, 16H, CH_2 and CH_d), 0.78 (d, ^3J(H,H) = 6.6 Hz, 3H, CH_f), 0.76 (d, ^3J(H,H) = 6.6 Hz, 3H, C$H_{f'}$); ^{13}C NMR (100 MHz, $CDCl_3$) δ 173.7 (NH$_i$-CO), 172.3 (CH$_c$-CO-O), 168.9 (NH$_g$-CO), 157.9 (NH$_l$-CO-O), 140.7 (ArC-(ipso)), 140.5 (ArC- (ipso)), 128.6 (ArCH (meta)), 128.2 (ArCH (ortho)), 128.1 (ArCH (ortho)), 126.9 (ArCH (para)), 79.0 (C(CH$_3$)$_3$), 67.3 (CH$_b$), 51.0 (CH$_a$), 49.8 (CH$_c$), 43.0 (CH$_h$), 41.0 (CH$_d$), 40.6, 36.3, 33.9, 30.0, 29.4, 29.3, 29.2, 29.1, 28.4 (CH$_m$), 26.8, 25.6, 24.6 (CH$_e$), 22.5 (CH$_f$), 21.8 (CH$_{f'}$); MS (FAB): m/z = 652 [(M+H)$^+$]; Anal. Calcd. for $C_{38}H_{57}N_3O_6$: C 70.01, H 8.81, N 6.45. Found: C 70.21, H 9.11, N 6.97.

N-(2,2-Diphenylethyl)-fumaric acid ethyl ester, S5

To a stirred solution of 2,2-diphenylethylamine (0.50 g, 2.50 mmol), fumaric acid monoethylester (0.37 g, 2.50 mmol) and 4-DMAP (0.33 g, 2.70 mmol) in anhydrous CH_2Cl_2 (200 mL) at 0 °C was added EDCI·HCl (0.52 g, 2.7 mmol). After 24 h the solution was washed with a saturated solution of citric acid (3 x 50 mL) and H_2O (3 x 50 mL) and the organic layer dried over anhydrous $MgSO_4$, filtered and the filtrate reduced in volume to obtain a colourless solid that was recrystallized from EtOAc (S5, 0.70 g, 85%). m.p. 112-113 °C. ^{1}H NMR (400 MHz, $CDCl_3$): δ = 7.34-7.27 (m, 4H, ArCH (meta)), 7.26-7.19 (m, 6H, ArCH (ortho and para)), 6.77 (d, ^3J(H,H) = 14.4 Hz, 1H, CH_d or e), 6.72 (d, ^3J(H,H) = 14.4 Hz, 1H, CH_d or e), 5.90 (t, ^3J(H,H) = 5.7 Hz, 1H, NH_c), 4.25-4.15 (m, 3H, CH_a and CH_f), 3.98 (dd, ^3J(H,H) = 8.0 Hz, ^3J(H,H) = 5.7 Hz, 2H, CH_b), 1.28 (t, ^3J(H,H) = 7.0 Hz, 3H, CH_g); ^{13}C NMR (100 MHz, $CDCl_3$): δ = 165.6 (CH_e-CO-O), 163.6 (CO-NH$_c$), 141.5 (ArC- (ipso)), 136.0 (CH_d or e), 130.6 (CH_d or e), 128.9 (ArCH (meta)), 128.1 (ArCH (ortho)), 127.0 (ArCH (para)), 61.2 (CH_f), 50.3 (CH_a), 44.1 (CH_b), 14.1 (CH_g); MS (FAB): m/z = 324 [(M+H)$^+$]; Anal. Calcd. for $C_{20}H_{21}NO_3$: C 74.28, H 6.55, N 4.33. Found: C 74.83, H 6.91, N 4.38.

N-(2,2-Diphenylethyl)-fumaramide acid, S6
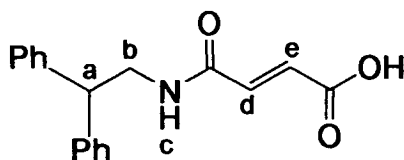
To a stirred solution of S5 (0.70 g, 2.20 mmol) in EtOH (50 mL) was added dropwise a solution of NaOH (0.10 g, 2.40 mmol) in H_2O (2.5 mL). After 16 h the solution was reduced in volume and washed several times with Et_2O to obtain a colourless powder which was recrystallized from $CHCl_3$ (S6, 0.58 g, 91%). m.p. >270 °C (decomp); ^1H NMR (400 MHz, d_6-DMSO): δ = 12.83 (br s, 1H, OH), 8.57 (t, ^3J(H,H) = 5.7 Hz, 1H, NH_c), 7.33-7.15 (m, 10H, ArCH), 6.87 (d, ^3J(H,H) = 15.4 Hz, 1H, C$H_{d \, or \, e}$), 6.47 (d, ^3J(H,H) = 15.4 Hz, 1H, C$H_{d \, or \, e}$), 4.22 (t, ^3J(H,H) = 8.0 Hz, 1H, CH_a), (dd, ^3J(H,H) = 8.0 Hz, ^3J(H,H) = 5.7 Hz, 2H, CH_b); ^{13}C NMR (100 MHz, d_6-DMSO) δ 168.0 (CO-OH), 164.5 (CO-NH_c), 143.1 (ArC- (ipso)), 134.3 (C$H_{d \, or \, e}$), 134.0 (C$H_{d \, or \, e}$), 128.8 (ArCH (meta)), 128.2 (ArCH (ortho)), 126.7 (ArCH (para)), 50.3 (CH_a), 43.7 (CH_b); MS (FAB): m/z = 296 [(M+H)$^+$]; Anal. Calcd. for $C_{18}H_{17}NO_3$: C 73.20, H 5.80, N 4.70. Found: C 73.10, H 5.20, N 4.73.

(2S)-(2-{11-[3-(2,2-Diphenyl-ethylcarbamoyl)-(E)-acryloylamino]-undecanoylamino}-acetylamino)-4-methyl-pentanoic acid 2,2-diphenyl-ethyl ester, E-2
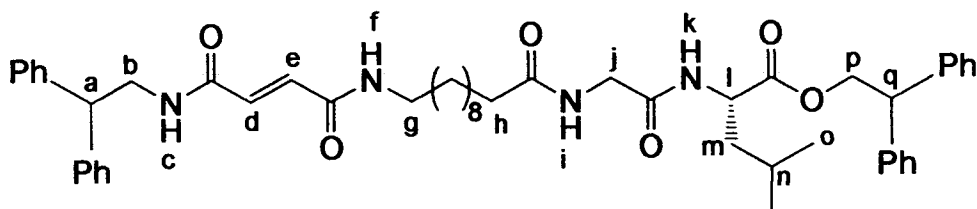
To a stirred solution of S4 (0.90 g, 1.38 mmol) in anydrous $CHCl_3$ (20 mL) was added TFA (2 mL). After 2 h the solution was reduced in volume and the remained TFA removed *in vacuo*. The resulting oil was taken up in anhydrous DMF (80 mL) and S6 (0.56 g, 1.88 mmol), 4-DMAP (0.31 g, 2.56 mmol) and EDCI·HCl (0.60 g, 3 mmol) added sequentially under argon at 0°C whilst stirring. After 16 h the solution was reduced in volume, taken up in $CHCl_3$ (150 mL) and washed with 0.5N HCl (3 x 100

mL). The organic layer was dried over anhydrous MgSO$_4$, filtered and the filtrate reduced in volume to obtain a colourless compound that was purified by column chromatography (CHCl$_3$/MeOH) (*E*-2, 0.85 g, 74%). m.p. 132°C; ^{1}H NMR (400 MHz, CDCl$_3$) δ 7.33-7.26 (m, 4H, ArC*H* (meta)), 7.26-7.19 (m, 6H, ArC*H* (ortho and para)), 7.04 (d, ^3J(H,H) = 14.9 Hz, 1H, C*H*$_{d \text{ or } e}$), 7.00 (d, ^3J(H,H) = 7.4 Hz, 1H, N*H*$_k$), 6.87 (t, ^3J(H,H) = 5.9 Hz, 1H, N*H*$_f$), 6.75 (d, ^3J(H,H) = 14.9 Hz, 1H, C*H*$_{d \text{ or } e}$), 6.54 (t, ^3J(H,H) = 5.2 Hz, 1H, N*H*$_i$), 6.18 (t, ^3J(H,H) = 5.4 Hz, 1H, N*H*$_c$), 4.74 (dd, ^2J(H,H) = 11.1 Hz, ^3J(H,H) = 8.6 Hz, 1H, C*H*H'$_p$), 4.55 (dd, ^2J(H,H) = 11.1 Hz, ^3J(H,H) = 7.3 Hz, 1H, CH*H*'$_p$), 4.55 (dd, ^3J(H,H) = 7.8 Hz, ^3J(H,H) = 7.4 Hz, 1H, C*H*$_l$), 4.37 (br dd, 1H, C*H*$_q$), 4.22 (t, ^3J(H,H) = 7.8 Hz, 1H, C*H*$_a$), 3.99 (d, ^3J(H,H) = 7.8 Hz, ^3J(H,H) = 5.4 Hz, 1H, C*H*$_b$), 3.91 (t, ^3J(H,H) = 5.2 Hz, 2H, C*H*$_j$), 3.32 (m, 2H, C*H*$_g$), 2.22 (t, ^3J(H,H) = 7.3 Hz, 2H, C*H*$_h$), 1.63 (m, 2H, C*H*$_2$-CH$_h$), 1.55 (m, 2H, C*H*$_2$-CH$_g$), 1.43 (m, 1H, C*H*$_n$), 1.36-1.26 (m, 14H, C*H*$_2$ and C*H*$_m$), 0.75 (d, ^3J(H,H) = 6.6 Hz, 3H, C*H*$_o$), 0.74 (d, ^3J(H,H) = 6.3 Hz, 3H, C*H*$_o'$); ^{13}C NMR (100 MHz, CDCl$_3$) δ 173.9 (CH$_h$-*C*O), 172.4 (CH$_l$-*C*O-O), 169.3 (CH$_j$-*C*O), 165.0 (*C*O fumaric), 164.8 (*C*O fumaric), 142.0 (Ar*C*-CH$_a$ (ipso)), 140.8 (Ar*C*-CH$_q$ (ipso)), 140.6 (Ar*C*-CH$_q$ (ipso)), 133.7 (*C*H$_{d \text{ or } e}$), 132.5 (*C*H$_{d \text{ or } e}$), 128.7 (Ar*C*H (meta)), 128.6 (Ar*C*H (meta)), 128.5 (Ar*C*H (meta)), 128.2 (Ar*C*H (ortho)), 128.1 (Ar*C*H (ortho)), 128.0 (Ar*C*H (ortho)), 126.9 (Ar*C*H (para)), 126.9 (Ar*C*H (para)), 126.8 (Ar*C*H (para)), 67.2 (*C*H$_p$), 51.0 (*C*H$_q$), 50.2 (*C*H$_a$), 49.8 (*C*H$_l$), 44.4 (*C*H$_b$), 43.2 (*C*H$_j$), 40.8 (*C*H$_m$), 39.9 (*C*H$_h$), 36.1, 29.3, 29.2, 29.1, 29.0, 28.9, 26.9, 25.6, 24.6 (*C*H$_n$), 22.6 (*C*H$_o$), 21.8 (*C*H$_o$); HRMS (FAB) Calcd. for C$_{51}$H$_{65}$N$_4$O$_6$ [M+H]$^+$ 829.49041. Found: 829.48997.

[2](1,7,14,20-Tetraaza-2,6,15,19-tetraoxo-3,5,9,12,16,18,22,25-tetrabenzocyclohexacosane)-(2S)-(2-{11-[3-(2,2-diphenyl-ethylcarbamoyl)-(E)-acryloylamino]-undecanoylamino}-acetylamino)-4-methyl-pentanoic acid 2,2-diphenyl-ethyl ester)-rotaxane, E-1
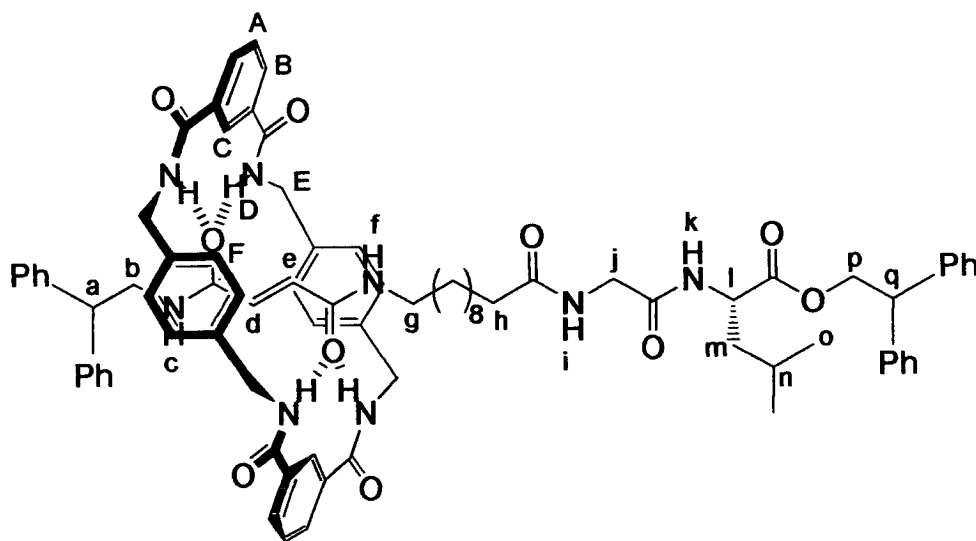

To a stirred solution of *E*-2 (0.40 g, 0.48 mmol) in anhydrous CHCl₃ (100 mL) was added simultaneously solutions of *para*-xylylenediamine (0.78 g, 5.76 mmol) and Et₃N (1.16 g, 11.5 mmol) in CHCl₃ (40 mL), and isophthaloyl dichloride (1.17 g, 5.76 mmol) in CHCl₃ (40 mL) over a period of 2 h using motor-driven syringe pumps. After a further 2 h the resulting suspension was filtered and the filtrate concentrated under reduced pressure to afford the crude product that was purified by column chromatography on silica gel using a gradient of CHCl₃ to CHCl₃/acetonitrile (1/1) as eluent to obtain the desired compound as a colourless powder (*E*-1, 0.38 g, 58%); Rotaxane *E*-1 can also be obtained by thermal-isomerisation of its isomer *Z*-1 at 130°C in C₂D₂Cl₄ for 6 days (*E*-1, 95%). m.p. 194 °C; ¹H NMR (400 MHz, CDCl₃) δ 8.42 (s, 2H, ArCH_C), 8.15 (d, ³*J*(H,H) = 7.3 Hz, 4H, ArCH_B), 7.67 (s br, 4H, NH_D), 7.60 (t, ³*J*(H,H) = 7.3 Hz, 2H, ArCH_A), 7.34-7.25 (m, 8H, ArCH (meta)), 7.25-7.16 (m, 12H,

ArCH (ortho and para)), 7.15 (br t, 1H, NH_f), 6.96 (s, 8H, ArCH_F), 6.90 (br t, 1H, NH_c), 6.79 (d, ^3J(H,H) = 7.6 Hz, 1H, NH_k), 6.32 (t, ^3J(H,H) = 4.9 Hz, 1H, NH_i), 5.81 (d, ^3J(H,H) = 15.2 Hz, 1H, C$H_{d\ or\ e}$), 5.68 (d, ^3J(H,H) = 15.2 Hz, 1H, C$H_{d\ or\ e}$), 4.78 (dd, ^2J(H,H) = 10.9 Hz, ^3J(H,H) = 8.3 Hz, 1H, CHH'$_p$), 4.54 (dd, ^2J(H,H) = 10.9 Hz, ^3J(H,H) = 7.3 Hz, 1H, CHH'_p), 4.48-4.41 (br d, 9H, CH_E and CH_l), 4.38 (m, 1H, CH_q), 4.21 (t, ^3J(H,H) = 7.7 Hz, 1H, CH_a), 3.84 (br t, 2H, CH_b), 3.71 (d, ^3J(H,H) = 4.9 Hz, 2H, CH_j), 3.12 (m, 2H, CH_g), 2.12 (t, ^3J(H,H) = 7.5 Hz, 2H, CH_h), 1.54 (m, 2H, CH_2-CH_h), 1.46 (m, 3H, CH_2-CH_g and CH_n), 1.29-1.17 (m, 14H, CH_2 and CH_m), 0.78 (d, ^3J(H,H) = 5.3 Hz, 3H, CH_o), 0.76 (d, ^3J(H,H) = 5.5 Hz, 3H, C$H_{o'}$); ^{13}C NMR (100 MHz, CDCl$_3$) δ 173.7 (CH_h-CO), 172.3 (CH_l-CO-O), 168.7 (CH_j-CO), 166.7 (CO macrocycle), 165.3 (CO fumaric), 165.0 (CO fumaric), 141.4 (ArC-CH_a (ipso)), 140.7 (ArC-CH_q (ipso)), 140.5 (ArC-CH_q (ipso)), 137.1 (ArC-CH_E (ipso)), 133.8 (ArC-CO-NH_D (ipso)), 131.3 (ArCH_B), 130.5 (C$H_{d\ or\ e}$), 129.8 (C$H_{d\ or\ e}$), 129.1, 129.0, 128.9, 128.6 (ArCH (meta)), 128.5 (ArCH (meta)), 128.1 (ArCH (ortho)), 128.0 (ArCH (ortho)), 127.8 (ArCH (para)), 127.1, 127.0, 124.5 (ArCH_C), 67.4 (CH_p), 51.0 (CH_q), 50.3 (CH_a), 49.8 (CH_l), 44.7 (CH_b), 44.1 (CH_E), 42.9 (CH_j), 41.0 (CH_m), 40.1 (CH_h), 36.0, 29.1, 29.0, 28.7, 26.8, 25.5, 24.6 (CH_n), 22.5 (CH_o), 21.9 (C$H_{o'}$); HRMS (FAB) Calcd. for C$_{83}$H$_{93}$N$_8$O$_{10}$ [M+H]$^+$ 1361.70147. Found: 1361.70093.

(2S)-(2-{11-[3-(2,2-diphenyl-ethylcarbamoyl)-(Z)-acryloylamino]-undecanoylamino}-acetylamino)-4-methyl-pentanoic acid 2,2-diphenyl-ethyl ester), Z-2
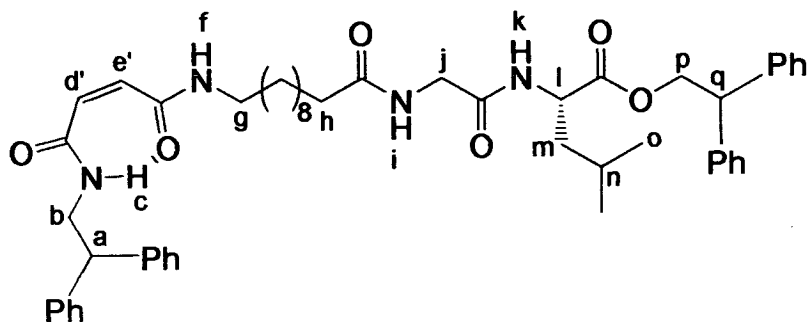
A CH_2Cl_2 solution (20 mL) of E-2 (0.10 g, 0.12 mmol) in a quartz vessel was directly irradiated for 40 min at 254 nm using a multilamp photo-reactor. The reaction mixture was concentrated under reduced pressure to afford the crude product that was subjected to column chromatography on silica gel using a gradient of $CHCl_3$ to $CHCl_3$/EtOAc (1/3) as eluent to obtain the desired compound as a colourless powder (Z-2, 0.05 g, 54%). m.p. 121 °C; ^{1}H NMR (400 MHz, $CDCl_3$) δ 8.49 (t, ^3J(H,H) = 5.8 Hz, 1H, NH_f), 7.97 (t, ^3J(H,H) = 5.3 Hz, 1H, NH_c), 7.35-7.18 (m, 20H, ArCH), 6.62 (d, ^3J(H,H) = 7.8 Hz, 1H, NH_k), 6.33 (t, ^3J(H,H) = 5.2 Hz, 1H, NH_i), 6.00 (d, ^3J(H,H) = 13.1 Hz, 1H, $CH_{d'}$ or e'), 5.92 (d, ^3J(H,H) = 13.1 Hz, 1H, $CH_{d'}$ or e'), 4.78 (dd, ^2J(H,H) = 11.1 Hz, ^3J(H,H) = 8.3 Hz, 1H, CHH'$_p$), 4.56 (dd, ^2J(H,H) = 11.1 Hz, ^3J(H,H) = 7.3 Hz, 1H, CHH'_p), 4.45 (m, 1H, CH_l), 4.38 (d, ^3J(H,H) = 8.0 Hz, 1H, CH_q), 4.26 (d, ^3J(H,H) = 8.0 Hz, 1H, CH_a), 3.95 (dd, ^3J(H,H) = 8.0 Hz, ^3J(H,H) = 5.8 Hz, 2H, CH_b), 3.83 (d, ^3J(H,H) = 5.2 Hz, 2H, CH_j), 3.24 (br dt, 2H, CH_g), 2.20 (t, ^3J(H,H) = 7.6 Hz, 2H, CH_h), 1.61 (m, 2H, CH_2-CH_h), 1.53 (m, 2H, CH_2-CH_g), 1.44 (m, 1H, CH_n), 1.36-1.27 (m, 14H, CH_2 and CH_m), 0.79 (d, ^3J(H,H) = 6.6 Hz, 3H, CH_o), 0.77 (d, ^3J(H,H) = 6.6 Hz, 3H, CH_o); ^{13}C NMR (100 MHz, $CDCl_3$) δ 173.7 (CH_h-CO), 172.3 (CH_l-CO-O), 168.8 (CH_j-CO), 165.1 (CO maleic), 164.6 (CO maleic), 141.8 (ArC-CH_a (ipso)), 140.7 (ArC-CH_q (ipso)), 140.6 7 (ArC-CH_q (ipso)), 133.4 ($CH_{d'}$ or e'), 131.3 ($CH_{d'}$ or e'), 128.7 (ArCH (meta)), 128.6 (ArCH (meta)), 128.5 (ArCH (meta)), 128.2 (ArCH (ortho)), 128.1 (ArCH (ortho)), 128.0 (ArCH (ortho)), 127.0 (ArCH (para)), 126.9 (ArCH (para)), 126.8 (ArCH (para)), 67.3 (CH_p), 51.0 (CH_q), 50.3 (CH_l), 49.8 (CH_a), 44.2 (CH_b), 43.0 (CH_j), 41.0 (CH_m), 39.8 (CH_g), 36.3, 29.3, 29.2, 29.1, 29.0, 28.9, 26.9, 25.5, 24.7 (CH_n), 22.5 (CH_o), 21.8 (CH_o); HRMS (FAB) Calcd. for $C_{51}H_{65}N_4O_6$ $[M+H]^+$ 829.49041. Found: 829.49082.

**[2](1,7,14,20-Tetraaza-2,6,15,19-tetraoxo-3,5,9,12,16,18,22,25-tetrabenzocyclohexacosane)-(2S-(2-{11-[3-(2,2-diphenyl-ethylcarbamoyl)-(Z)-acryloylamino]-undecanoylamino}-acetylamino)-4-methyl-pentanoic acid 2,2-diphenyl-ethyl ester)-rotaxane, Z-1**
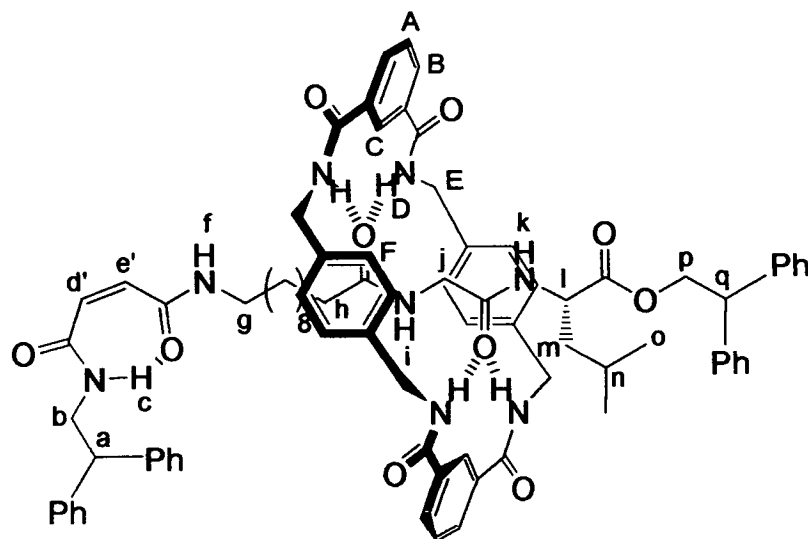
A CH_2Cl_2/MeOH (20 mL, 9/1 v/v) solution of *E*-1 (0.26 g, 0.19 mmol) in a quartz vessel was directly irradiated for 20 mins at 254 nm using a multilamp photo-reactor. The reaction mixture was concentrated under reduced pressure to afford the crude product that was subjected to column chromatography on silica gel using a gradient of $CHCl_3$ to $CHCl_3$/EtOAc (1/1.5) as eluent to obtain the desired compound as a colourless powder (*Z*-1, 0.11 g, 42%). m.p. 169 °C; ^{1}H NMR (400 MHz, $CDCl_3$) δ 8.60 (t, $^3J(H,H)$ = 5.2 Hz, 1H, NH_f), 8.48 (t, $^3J(H,H)$ = 5.3 Hz, 1H, NH_c), 8.34 (s, 2H, ArCH_C), 8.15 (d, $^3J(H,H)$ = 7.8 Hz, 4H, ArCH_B), 7.74 (d, $^3J(H,H)$ = 7.3 Hz, 1H, NH_k), 7.56 (t, $^3J(H,H)$ = 7.8 Hz, 2H, ArCH_A), 7.55 (br s, 4H, NH_D), 7.31-7.12 (m, 28H, ArCH and ArCH_F), 6.01 (d, $^3J(H,H)$ = 13.4 Hz, 1H, C$H_{d' or e'}$), 5.89 (d, $^3J(H,H)$ = 13.4 Hz, 1H, C$H_{d' or e'}$), 5.63 (d, $^3J(H,H)$ = 3.8 Hz, 1H, NH_i), 4.76 (dd, $^2J(H,H)$ = 11.1 Hz, $^3J(H,H)$ = 8.6 Hz, 1H, CHH'$_p$), 4.58-4.43 (m, 8H, CH_E), 4.40 (dd, $^2J(H,H)$ = 11.1 Hz, $^3J(H,H)$ = 7.3 Hz, 1H,

CHH'_p), 4.28 (br dd, 1H, CH_q), 4.25 (t, ^3J(H,H) = 8.0 Hz, 1H, CH_a), 4.19 (m, 1H, CH_l), 3.92 (dd, ^3J(H,H) = 8.0 Hz, ^3J(H,H) = 5.8 Hz, 2H, CH_b), 3.11 (m, 2H, CH_g), 2.90 (d, ^3J(H,H) = 3.8 Hz, 2H, CH_j), 1.71 (t, ^3J(H,H) = 8.0 Hz, 2H, CH_h), 1.48-1.37 (m, 3H, CH_2-CH$_g$ and CH_n), 1.35-0.95 (m, 16H, CH_2 and CH_m), 0.77 (d, ^3J(H,H) = 6.8 Hz, 3H, CH_o), 0.75 (d, ^3J(H,H) = 6.8 Hz, 3H, C$H_{o'}$); ^{13}C NMR (100 MHz, CDCl$_3$) δ 173.7 (CH$_h$-CO), 172.1 (CH$_l$-CO-O), 169.6 (CH$_j$-CO), 166.4 (CO macrocycle), 166.3 (CO macrocycle), 165.1 (CO maleic), 164.7 (CO maleic), 141.8 (ArC-CH$_a$ (ipso)), 140.5 (ArC-CH$_q$ (ipso)), 140.2 (ArC-CH$_q$ (ipso)), 137.5 (ArC-CH$_E$ (ipso)), 137.3 (ArC-CH$_E$ (ipso)), 133.7 (ArC-CO-NH$_D$ (ipso)), 133.0 (CH$_{d'\ or\ e'}$), 131.7 (CH$_{d'\ or\ e'}$), 131.6 (ArCH$_B$), 131.5 (ArCH$_B$), 129.3, 129.2, 129.0, 128.7 (ArCH (meta)), 128.6 (ArCH (meta)), 128.1 (ArCH (ortho)), 128.0 (ArCH (ortho)), 127.9 (ArCH (ortho)), 127.1 (ArCH (para)), 127.0 (ArCH (para)), 126.8 (ArCH (para)), 123.8 (ArCH$_C$), 67.5 (CH$_p$), 51.4 (CH$_q$), 50.3 (CH$_a$), 49.8 (CH$_l$), 44.3 (CH$_b$), 44.1 (CH$_E$), 42.0 (CH$_j$), 40.5 (CH$_m$), 40.0 (CH$_h$), 36.0, 29.1, 29.0, 28.9, 28.8, 26.7, 24.9, 24.7 (CH$_n$), 22.5 (CH$_o$), 21.7 (CH$_{o'}$); HRMS (FAB) Calcd. for C$_{83}$H$_{93}$N$_8$O$_{10}$ [M+H]$^+$ 1361.70147. Found: 1361.69808.

6.5 References

1. (a) G. Schill, *Catenanes, Rotaxanes and Knots*, Academic Press: New York, 1971. (b) J.-P. Sauvage, C. Dietrich-Buchecker, Eds. *Molecular Catenanes, Rotaxanes and Knots*; Wiley-VCH: Weiheim, **1999**.

2. (a) A. G. Johnston, D. A. Leigh, A. Murphy, J. P. Smart, M. D. Deegan, *J. Am. Chem. Soc.* **1996**, *118*, 10662-10663. (b) S. Anderson, R. T. Aplin, T. D. W. Claridge, T. Goodson, A. C. Maciel, G. Rumbles, J. F. Ryan, H. L. Anderson, *J. Chem. Soc.- Perkin Trans.* **1998**, *1*, 2383-2397. (c) E. Cordova, R. A. Bissell, A. E. Kaifer, *J. Org. Chem.* **1995**, *60*, 1033-1038. (d) V. Bermudez, N. Capron, T. Gase, F. G. Gatti, F. Kajzar, D. A. Leigh, F. Zerbetto, S. Zhang, *Nature*, **2000**, *406*, 608-611. (e) M. Asakawa, G. Brancato, M. Fanti, D. A. Leigh, T. Shimizu, A. M. Z. Slawin, J. K. Y. Wong, F. Zerbetto, S. Zhang, *J. Am. Chem. Soc.* **2002**, *124*, 2939-2950.

3. For recent reviews see (a) V. Balzani, A. Credi, F. M. Raymo, J. F. Stoddart, *Angew. Chem.* **2000**, *112*, 3484-3530; *Angew. Chem. Int. Ed.* 2000, *39*, 3349-3391. (b) Special issue on *Molecular Machines, Acc. Chem. Res.* **2001**, *34*, 409-522. (c) Special issue on *Molecular Machines and Motors.* Structure and Bonding *Vol. 99* (Ed.: J.-P. Sauvage), Springer, Berlin, **2001**.

4. (a) R. A. Bissell, E. Cordova, A. E. Kaifer, J. F. Stoddart, *Nature* **1994**, *369*, 133-137. (b) A. S. Lane, D. A. Leigh, A. Murphy, *J. Am. Chem. Soc.* **1997**, *119*, 11092-11093. (c) A. M. Brouwer, C. Frochot, F. G. Gatti, D. A. Leigh, L. Mottier, F. Paolucci, S. Roffia, G. W. H. Wurpel, *Science* **2001**, *291*, 2124-2128. (d) G. W. H. Wurpel, A. M. Brouwer, I. H. M. van Stokkum, A. Farran, D. A. Leigh, *J. Am. Chem. Soc.* **2001**, *123*, 11327-11328. (e) C. P. Collier, E. W. Wong, M. Belohradsky, F. M. Raymo, J. F. Stoddart, P. J. Kuekes, R. S. Williams, J. R. Heath, *Science* **1999**, *285*, 391-394.

5. A. Altieri, G. Bottari, F. Dehez, D. A. Leigh, J. K. Y. Wong, F. Zerbetto, accepted for publication in Angew. Chem.

Publications arising from my PhD Studies

(2000-2003)

Solid-State Fingerprints of Molecular Threading Detected by Inelastic Neutron Scattering

Giovanni Bottari, Roberto Caciuffo, Marianna Fanti, David A. Leigh,
Stewart F. Parker, Francesco Zerbetto

Solid-State Fingerprints of Molecular Threading Detected by Inelastic Neutron Scattering

Giovanni Bottari,[a] Roberto Caciuffo,[c] Marianna Fanti,[b] David A. Leigh,*[a] Stewart F. Parker,[d] and Francesco Zerbetto*[b]

KEYWORDS:

inelastic neutron scattering · macrocycles · molecular modeling · noncovalent interactions · rotaxanes

Recently, it has been shown that the rate of spinning of a macrocycle mechanically locked onto a dumbbell thread, a [2]rotaxane, can be tuned in solution by an external AC electric field.[1] As a solid, such large-amplitude motions are reduced, or forbidden, by the presence of nearby molecules. In general, some effects of molecular interlocking still exist, however, and may give rise to important properties.[2] To date, solid-state vibrational spectroscopy has not been able to find direct evidence of the presence of the large amplitude intercomponent motions introduced by the mechanically interlocked architectures present in catenanes and rotaxanes.[3] Identification of vibrational band(s) that are caused by the respective motions of the noncovalently linked components becomes of fundamental and applied interest.

In this work, we measure the inelastic neutron scattering (INS) of rotaxane 2 and of the thread 1 that results from the removal of a benzylic amide macrocycle. INS spectroscopy is not subject to the restrictions of optical selection rules present in infrared or Raman spectroscopies. This permits the observation of all the motions present in a system (proportional to the contribution of

the hydrogen atoms). An impressive example of such ability was provided by Hudson and collaborators[4] for dodecahedrane, where 19 of its 30 modes are both infrared- and Raman-silent.

The case of 1 and 2 is perhaps unique for a spectroscopic investigation: In fact, the addition of the macrocycle to 1 does not introduce any new functional groups, or types of vibrations, in addition to those already present (both macrocycle and thread contain only phenyl and amide groups). No new types of vibration and bands are therefore expected when comparing the spectra of 1 and 2. However, comparison of the spectra showed that the region between 350 and 400 cm^{-1} is markedly different (see Figure 1). This difference was not anticipated, but can be readily ascribed to the effect of interlocking on the molecular motions of the rotaxane. The aim of this work is therefore to understand qualitatively the origin of this spectral difference. To achieve this goal, molecular dynamics (MD) simulations based on molecular mechanics (MM) are well suited. The model satisfies several basic requisites:
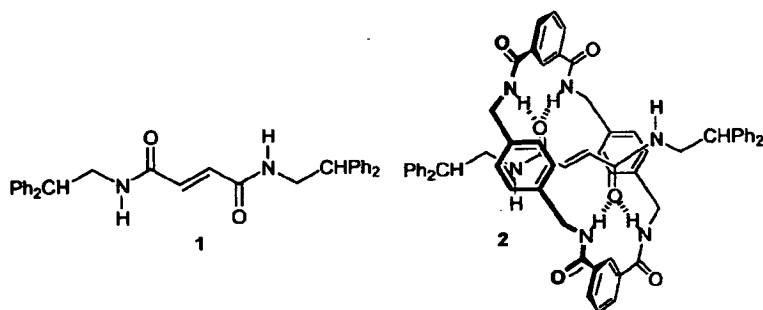
- MM has been used in the past to study the potential energy surfaces and the dynamics of this[1] and related systems,[5] and was able to locate the multiple minima that arise from the non- or weakly bonding interaction that govern the dynamics of these molecules;
- MM can be used both in the isolated molecule approximation and in the solid phase;
- The combination of MM and MD includes anharmonic effects, which are important when large amplitude motions are investigated.

[a] Prof. D. A. Leigh, G. Bottari
Department of Chemistry
University of Edinburgh
The King's Buildings
West Mains Road, Edinburgh EH9 3 JJ (UK)
Fax: (+44) 131-667-9085
E-mail: david.leigh@ed.ac.uk

[b] Prof. F. Zerbetto, Dr. M. Fanti
Dipartimento di Chimica "G. Ciamician"
Università degli Studi di Bologna
V. F. Selmi 2, 40126 Bologna (Italy)
Fax: (+39) 051-209-9456
E-mail: gatto@ciam.unibo.it

[c] Prof. R. Caciuffo
Istituto Nazionale per la Fisica della Materia e
Dipartimento di Fisica ed Ingegneria dei Materiali
Università di Ancona
Via Brecce Bianche, 60131 Ancona (Italy)

[d] Dr. S. F. Parker
ISIS Facility
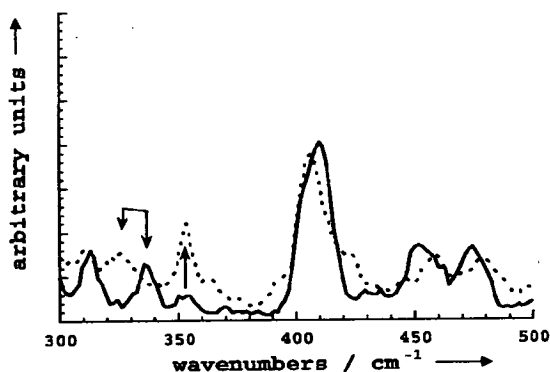Rutherford Appleton Laboratory
Chilton, Didcot OX11 0QX (UK)

Figure 1. The spectral region of most pronounced difference for the INS spectra of 1 (——) and 2 (- - - -). The arrows are used to assist the eye in matching the bands.

The first point can be further elaborated. The conclusion of previous work on the interlocked dimer of the benzylic amide macrocycle and a variation of it[5e] was that the model proved to be sufficiently accurate to distinguish between vibrations that give large contributions to the INS response. Moreover, the comparison of the results for simulations performed in the isolated molecule approximation and the solid-state approach showed the superiority of the latter, which was taken as a further validation of the various features of the model. Finally, the validation of the MD calculations through their accurate simulation of the INS spectrum justified their further analysis to extract the information that are contained in the INS spectra. Because of the similarity of the structures of the systems treated here and those modeled previously, one is therefore justified in using the same approach. Differences in frequencies can be expected, but the dynamics of the system should be delivered by the model.

Figure 2 compares the experimental and calculated spectra of **1**. While there are some shifts in the positions of the bands, their number and shape are well reproduced. Analogously, Figure 3 compares the experimental and calculated spectra of **2**; the experimental extra line of the spectrum of **2** is present in the calculations although somewhat broader and shifted to higher wavenumbers by 15–20 cm⁻¹. Notice that the calculations were performed using periodic boundary conditions that mimic the
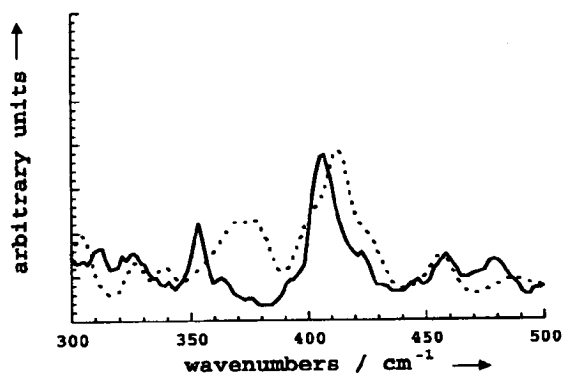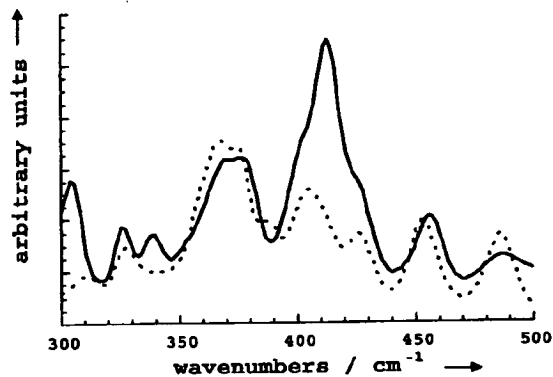
Figure 4. Calculated spectra of 2 in the solid phase (———) and as a free molecule (– – – –).

solid phase present in the experiments. Importantly, the system of bands between 350 and 400 cm⁻¹ of Figure 1 can now be assigned. The sharp feature present in the experimental spectrum of the rotaxane **2**, slightly above 350 cm⁻¹, is the enhancement of the very weak band of **1**. This band is therefore taken as a fingerprint of molecular threading.

In order to determine the nature of the 350 cm⁻¹ rotaxane band, and those of the bands located nearby, three types of simulations were performed for **2**.

In the first set of calculations (Figure 4) the INS spectrum was obtained in the isolated molecule approximation: Upon removal of the periodic boundary condition, some pronounced changes are observed above 400 cm⁻¹ where the most prominent band is not reproduced by the calculations. The results therefore support the notion that it is the combination of molecular threading and solid-state interactions that introduces a molecular motion, detected by INS spectroscopy, absent in the unthreaded dumbbell and in the isolated rotaxane molecule.

In the second set of calculations, the contributions of the different hydrogen atoms were selectively set to zero and the spectrum recalculated (Figure 5). The hydrogen atoms were divided into five sets:

- Set I was formed by the hydrogen atoms of the terminal groups of the dumbbell;
- Set II was formed by the p-xylylene hydrogen atoms of the macrocycle;
- Set III was formed by the isophthaloyl hydrogen atoms of the macrocycle;
- Set IV were the amide atoms;
- Set V included the atoms of the central C=C bond of the fumaric motif at the center of the dumbbell. Removal of Set IV and V atoms hardly modified the spectrum (not shown here).

Sets I to III contribute to the spectral region of the rotaxane fingerprints, however, in quantitative terms the major contribution is given by the isophthaloyl hydrogen atoms of the ring.

In the third set of calculations, a vibrational analysis of the region of the rotaxane fingerprints was performed. The local contributions to the 15 vibrations located between 360 and 380 cm⁻¹ were examined individually. Three types of motions were found to be mainly present: Scissoring of the phenyl stopper impeded by the presence of the macrocycle, chair-to-
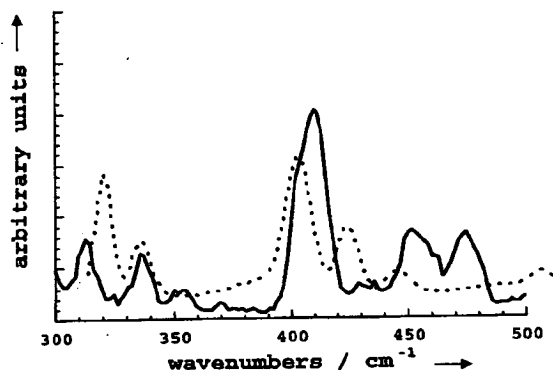

Figure 2. Experimental (———) and calculated (– – – –) spectra of 1.

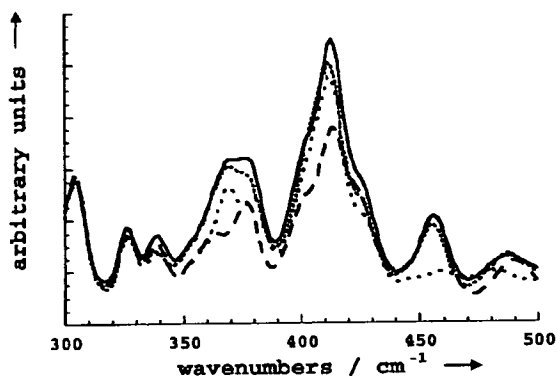*Figure 3. Experimental (———) and calculated (– – – –) spectra of 2.*

Figure 5. Spectra of 2 in the solid phase (——) and three calculated ones upon removal of the hydrogen atoms of the stoppers (- - - -), upon removal of the hydrogen atoms of the p-xylyl groups (- - - -), and upon removal of the hydrogen atoms of the isophthaloyl groups (. . . .).

boat interconversion of the threaded macrocycle, and rocking of the whole macrocycle hindered by the presence of a terminal group of the dumbbell. Examples of the motions are shown in Figure 6. The contemporaneous presence of the three motions in the same vibrations confirms that they interact and both the value of frequency and the shape of the motions are affected by interlocking, which is therefore ultimately responsible for the fingerprint region of the rotaxane.

While this is the first time that a spectroscopic signature of molecular threading is found, it is not the first time that some important properties of rotaxanes containing a benzylic amide macrocycle were determined by the interaction between thread and macrocycle. A recent study of the induced circular dichroism, in a series of dipeptide rotaxanes,[6] showed that chiral information is passed from the chiral center of the thread to the stoppers via the macrocycle through long-range spatial interactions. Future work will have to develop molecular dynamics models able to simulate the region below 100 cm⁻¹ where other intermoiety motions of interlocked systems are located. Here we have shown that a fundamental spectroscopic technique, whose use is continuously increasing, can detect the first solid-state evidence of molecular threading, a feature that had not previously emerged.

Experimental Section

The neutron experiment was performed using the indirect geometry time-of-flight spectrometer TOSCA at the ISIS pulsed spallation neutron source of the Rutherford Appleton Laboratory (UK). A combination of graphite crystal analyzers and cooled beryllium filters is used as a narrow bandpass filter to select the energy of neutrons scattered at a fixed angle of 135° ($E_f = 4$ meV). The spectrometer is optimal in the energy transfer range from 0 to 500 meV (0 – 4000 cm⁻¹), with the best results below 250 meV. The energy transfer resolution is of about 2% over the whole range. Polycrystalline samples (≈ 2 g) were synthesized[7] and checked to be entirely solvent-free. For the neutron experiment, a 1 mm thick sample was wrapped in aluminum foil, attached to the centrestick of a closed cycle refrigerator and cooled to 20 K.

The theory of incoherent neutron scattering by vibrating molecules has been discussed by several authors[8, 9] The contributions to the neutron cross-section for an initial energy E_i, final energy E_f, and solid angle Ω can be written as Equation (1), where a is the scattering length, that can be incoherent or coherent, $S(Q,\omega)$ is the dynamic structure factor, ω is the vibrational frequency, $Q = k_i - k_f$ is the scattering vector, and k is the wave vector for which the well-known relationship of Equation (2) holds (m is the mass of a neutron).

$$\frac{d^2\sigma}{d\Omega\,d\omega} = \left(\frac{E_f}{E_i}[a_{inc}^2\, S_{inc}(Q,\omega) + a_{coh}^2\, S_{coh}(Q,\omega)]^{0.5}\right) \tag{1}$$

$$\frac{h}{2\pi}\omega = E_f - E_i = \frac{h^2}{8\pi^2 m}(k_f^2 - k_i^2)$$

$$\frac{h}{2\pi}Q = \frac{h}{2\pi}(k_f - k_i) \tag{2}$$

Most atoms give comparable coherent and incoherent scattering. Hydrogen is, however, an exception because of its very large incoherent scattering length that makes it dominate the INS response of organic molecules. The incoherent scattering cross-section is the space- and time-Fourier transform of the self-correlation function and can be expressed as Equation (3),[5e, 10] where W is the Debye – Waller factor, which can be considered to be a constant for a given temperature, and the + sign corresponds to creation of a vibrational quantum in the material whilst – corresponds to the annhilation of a quantum.

$$S_{inc}(Q,\omega) \propto \exp(-2W)\frac{g(\omega)}{\omega}\left[\coth\left(\frac{h\omega}{4\pi k_B T}\right) \pm 1\right] \tag{3}$$
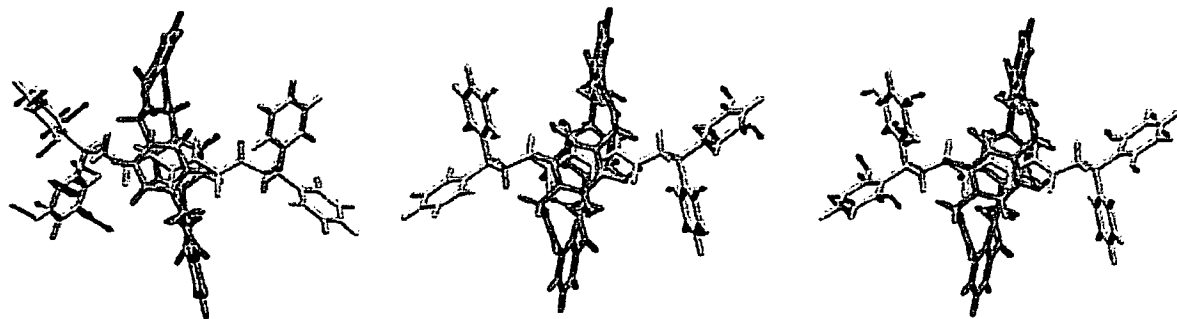

Figure 6. Illustrative examples of the vibrational motions located between 360 – 380 cm⁻¹. The arrows are proportional to the atomic displacements.

At the low temperatures of the experiments, only the first process (Stokes or down scattering) occurs.

The density of states $g(\omega)$ was here obtained as the Fourier transform of the velocity (v) autocorrelation function of the N hydrogen atoms according to Equation (4).

$$g(\omega) = \frac{1}{N}\sum_{atoms}\frac{1}{2\pi}\int_{-\infty}^{\infty}\exp(i\omega t)\langle v_a(0)\cdot v_a(t)\rangle dt \qquad (4)$$

The atom velocities were obtained by molecular dynamics calculations performed at constant energy (NVE ensemble) after equilibrating the system at 20 K. The time step was set to 0.2 fs and velocities were collected for 25 ps.

All the calculations were performed with the Tinker program[11] and the MM3 force field.[12] This approach has found wide application in our laboratories for the investigation of similar systems and related problems.[1, 5] Molecular dynamics were run both on isolated systems and applying boundary conditions to reproduce the crystal structure. The $g(\omega)$ calculations were performed in the NVE ensemble rather than the NVT where the constant temperature introduces spikes in the velocities and therefore in their Fourier transform.

[1] V. Bermudez, N. Capron, T. Gase, F. G. Gatti, F. Kajzar, D. A. Leigh, F. Zerbetto, S. Zhang, Nature 2000, 406, 608–611.
[2] a) C. P. Collier, E. W. Wong, M. Belohradsky, F. M. Raymo, J. F. Stoddart, P. J. Kuekes, R. S. Williams, J. R. Heath, Science 1999, 285, 391–394; b) C. P. Collier, G. Mattersteig, E. W. Wong, Y. Luo, K. Beverly, J. Sampaio, F. M. Raymo, J. F. Stoddart, J. R. Heath, Science 2000, 289, 1172–1175.
[3] a) M. Fanti, C.-A. Fustin, D. A. Leigh, A. Murphy, P. Rudolf, R. Caudano, R. Zamboni, F. Zerbetto, J. Phys. Chem. A 1998, 102, 5782; b) C. A. Fustin, P. Rudolf, A. F. Taminiaux, F. Zerbetto, D. A. Leigh, R. Caudano, Thin Solid Films 1998, 329, 321–325; c) C.-A. Fustin, D. A. Leigh, P. Rudolf, D. Timpel, F. Zerbetto, ChemPhysChem 2000, 1, 97–100.
[4] B. S. Hudson, D. A. Braden, S. F. Parker, H. Prinzbach, Angew. Chem. Int. Ed. 2000, 39, 514–516.
[5] a) D. A. Leigh, A. Murphy, J. P. Smart, M. S. Deleuze, F. Zerbetto, J. Am. Chem. Soc. 1998, 120, 6458; b) M. S. Deleuze, D. A. Leigh, F. Zerbetto, J. Am. Chem. Soc. 1999, 121, 2364; c) M. Cavallini, R. Lazzaroni, R. Zamboni, F. Biscarini, D. Timpel, F. Zerbetto, G. J. Clarkson, D. A. Leigh, J. Phys. Chem. B, 2001, 105, 10826–10830; d) F. Biscarini, C. Cavallini, D. A. Leigh, S. León, S. J. Teat, J. K. W. Wong, F. Zerbetto, J. Am. Chem. Soc. 2002, 124, 225–233; e) D. A. Leigh, S. F. Parker, D. Timpel, F. Zerbetto, J. Chem. Phys. 2001, 114, 5006–5011.
[6] M. Asakawa, G. Brancato, M. Fanti, D. A. Leigh, T. Shimizu, A. M. Z. Slawin, J. K. Y. Wong, F. Zerbetto, S. Zhang, J. Am. Chem. Soc. 2002, 124, 2939–2950.
[7] F. G. Gatti, D. A. Leigh, S. A. Nepogodiev, A. M. Z. Slawin, S. J. Teat, J. K. Y. Wong, J. Am. Chem. Soc. 2001, 123, 5983–5989.
[8] A. C. Zemach, J. Glauber, Phys. Rev. 1956, 101, 118; W. Marshal, S. W. Lovesey, Theory of Thermal Neutron Scattering, Oxford University, Oxford, 1971; M. W. Thomas, R. E. Ghosh, Mol. Phys. 1975, 29, 1489; A. Griffin, H. Jobic, J. Chem. Phys. 1981, 75, 5940; J. Howard, B. C. Boland, J. T. Tomkinson, J. Chem. Phys. 1983, 77, 145; Chemical Applications of Thermal Neutron Scattering (Ed.: B. T. M. Willis) Oxford University Press, Oxford, 1973.
[9] B. S. Hudson, J. Phys. Chem. A 2001, 105, 3949–3960; G. J. Kearley, Chem. Soc. Faraday Trans. 2 1986, 82, 41; G. J. Kearley, Spectrochim. Acta 1992,
48A, 349; A. Degli Esposti, O. Moze, C. Taliani, J. T. Tomkinson, R. Zamboni, F. Zerbetto, J. Chem. Phys. 1996, 104, 9704; A. Degli Esposti, F. Zerbetto, J. Phys. Chem. A 1997, 101, 7283.
[10] A. J. Ramirez-Cuesta, P. C. H. Mitchell, S. Parker, P. M. Rodger, Phys. Chem. Chem. Phys. 1999, 1, 5711; A. J. Ramirez-Cuesta, P. C. H. Mitchell, A. P. Wilkinson, S. F. Parker, P. M. Rodger, Chem. Commun. 1998, 653.
[11] J. Ponder, F. Richards, J. Comput. Chem. 1987, 8, 1016; C. Kundrot, J. Ponder, F. Richards, J. Comput. Chem. 1991, 12, 402; M. J. Dudek, J. Ponder, J. Comput. Chem. 1995, 16, 791.
[12] N. L. Allinger, Y. H. Yuh, J.-H. Lii, J. Am. Chem. Soc. 1989, 111, 8551; J.-H. Lii, N. L. Allinger, J. Am. Chem. Soc. 1989, 111, 8566; J.-H. Lii, N. L. Allinger, J. Am. Chem. Soc. 1989, 111, 8576.

Two-Dimensional Self-Assembly of Liquid-Crystalline Perylene Diimide Derivatives at the Air/Water Interface

Guodong Sui,[a] Jhony Orbulescu,[a] Mustapha Mabrouki,[a] Roger M. Leblanc,*[a] Shenggao Liu,[b] and Brian A. Gregg*[b]

Liquid crystalline (LC) perylene diimide derivatives such as PPEEB and PPMEEM are potentially promising agents for organic photovoltaic solar cells, not only because of their electrical properties but also because of their self-assembly properties in

PPEEB

PPMEEM
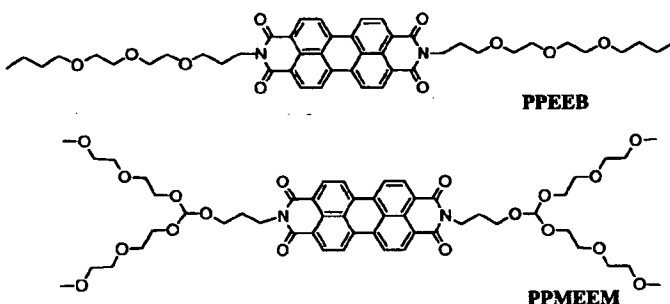
[a] Prof. Dr. R. M. Leblanc, Dr. G. Sui, J. Orbulescu, Dr. M. Mabrouki
Department of Chemistry
University of Miami, 1301 Memorial Drive
Coral Gables, FL 33124
Fax: (+1) 305-284-6367

[b] Dr. B. A. Gregg, Dr. S. Liu
National Renewable Energy Laboratory
1617 Cole Boulevard, Golden, Colorado 80401
E-mail: rml@miami.edu

Photoisomerization of a Rotaxane Hydrogen Bonding Template: Light-Induced Acceleration of a Large Amplitude Rotational Motion

Francesco G. Gatti, Salvator León, Jenny K. Y. Wong, Giovanni Bottari, Andrea Altieri,
M. Angeles Farran Morales, Simon J. Teat, Céline Frochot, David A. Leigh,
Albert M. Brouwer, Francesco Zerbetto

Photoisomerization of a rotaxane hydrogen bonding template: Light-induced acceleration of a large amplitude rotational motion

Francesco G. Gatti*, Salvador León[†], Jenny K. Y. Wong*, Giovanni Bottari*, Andrea Altieri*, M. Angeles Farran Morales*, Simon J. Teat[‡], Céline Frochot[§], David A. Leigh*[¶], Albert M. Brouwer[§¶], and Francesco Zerbetto[†¶]

*School of Chemistry, University of Edinburgh, The King's Buildings, West Mains Road, Edinburgh EH9 3JJ, United Kingdom; [†]Dipartimento di Chimica "G. Ciamician," Università degli Studi di Bologna, V. F. Selmi 2, 40126, Bologna, Italy; [‡]Central Laboratory of the Research Councils Daresbury Laboratory, Warrington WA4 4AD, United Kingdom; and [§]Laboratory of Organic Chemistry, University of Amsterdam, Nieuwe Achtergracht 129, NL-1018 WS Amsterdam, The Netherlands

Establishing methods for controlling aspects of large amplitude submolecular movements is a prerequisite for the development of artificial devices that function through rotary motion at the molecular level. Here we demonstrate that the rate of rotation of the interlocked components of fumaramide-derived [2]rotaxanes can be accelerated, by >6 orders of magnitude, by isomerizing them to the corresponding maleamide [2]rotaxanes by using light.

molecular machines | dynamics

Large amplitude internal rotations that resemble to some extent processes found in authentic machinery have recently inspired analogic molecular versions of gears (1), turnstiles (2), brakes (3), ratchets (4, 5), rotors (6), and unidirectional spinning motors (7–10) and are an inherent characteristic of many catenanes and rotaxanes (11–13). Establishing methods for controlling aspects of such movements is a prerequisite for the development of artificial devices that function through rotary motion at the molecular level.[∥] In this regard, we recently reported the unexpected discovery that the rate of rotation of the interlocked components of benzylic amide macrocycle-containing nitrone and fumaramide [2]rotaxanes can be slowed ("dampened") by 2–3 orders of magnitude by applying a modest ($\approx$1 V·cm^{-1}) external oscillating electric field (14). Here we demonstrate that the rate of rotation of the interlocked components of the olefin-based rotaxanes can also be accelerated, by >6 orders of magnitude, using another broadly useful stimulus, light.

Fumaramide threads template the assembly of benzylic amide macrocycles around them to form rotaxanes in high yields (15). This cheap and simple preparative procedure (suitable threads are prepared in a single step from fumaryl chloride and a bulky primary or secondary amine) is particularly efficient because the trans-olefin fixes the two hydrogen bond-accepting groups of the thread in an arrangement that is complementary to the geometry of the hydrogen bond-donating sites of the forming macrocycle. However, the feature of the fumaramide unit that makes it such an effective template also provides an opportunity to enforce a geometrical change in the thread after rotaxane formation, thus altering the nature and strength of the interactions between the interlocked components. Isomerization of the olefin from E- to Z- must necessarily disrupt the near-ideal hydrogen bonding motif between macrocycle and thread and therefore also change any internal dynamics governed by those interactions.

To test this idea, the photochemical isomerization of three fumaramide-based threads (E-1–3) and rotaxanes (E-4–6) was investigated. The synthesis of rotaxanes E-4 and E-6 has been described (15), and E-5 was prepared in analogous fashion from the corresponding thread, E-2, isophthaloyl

dichloride and p-xylylene diamine (Scheme 1).** Under the same reaction conditions the cis-olefin (maleamide) threads, Z-1–3, did not give detectable quantities of the corresponding Z-rotaxanes.

Experimental Procedures

General Method for the Photoisomerization of Fumaramide [2]Rotaxanes. The rotaxanes E-4–6 (0.60 g) were dissolved in CH$_2$Cl$_2$ [except for solubility reasons E-6, MeOH/CHCl$_3$ (1/9)] in a quartz vessel. The solutions were directly irradiated at 254 nm by using a multilamp photoreactor model MLU18 manufactured by Photochemical Reactors (Reading, U.K.). The progress of photoisomerization was monitored by TLC (silica, CHCl$_3$/EtOAc 4:1) or ¹H NMR. The different photostationary states were reached in a range of times not exceeding 30 min after which the reaction mixture was concentrated under reduced pressure to afford the crude products (Z-4–6). The unconverted trans isomers were isolated by triturating the solids with PhMe/CH$_2$Cl$_2$ (1:1, $\approx$20 ml) and, because the photoisomerization process produces few byproducts, could be recycled, eventually leading to >90% conversion of each rotaxane to the corresponding cis-isomer. The solutions were then passed through a pad of silica (CHCl$_3$/EtOAc, 4:1) to afford the cis isomers Z-4–6 in 50%, 47%, and 45% yields, respectively, from a single photoisomerization experiment.

Other Procedures. Experimental procedures for the synthesis of Z-5, x-ray crystallography of E-5 and Z-5, and selected charac-

[∥]Speculation over the possible utility of submolecular rotation in synthetic molecular structures ranges from "gearing" systems, where controlled motion in one part of a molecule brings about changes in conformation in another (e.g., to generate catalysts with rotating binding sites, in analogy to F$_1$-ATPase, etc.), to systems that rotate functional groups on surfaces, or in the bulk, to bring about changes in local or macroscopic characteristics (11, 23). Indeed, for wonderful examples of the use of submolecular rotational motion to bring about property changes in materials, see refs. 24 and 25. Examples of specifically controlling the frequency of large amplitude internal rotary motions include the redox-mediated acceleration/deceleration of the spinning of porphyrin ligands in cerium and zirconium sandwich complexes (26), the environment-dependant rate of circumrotation in hydrogen bonded [2]catenanes (27), and the electrochemically induced pirouetting of a macrocycle in a rotaxane (28).

**The modest yield (33%) of E-5 is probably a consequence of the {E,E}- and/or {E,Z}-tertiary amide rotamers being sterically mismatched with the forming macrocycle. Interestingly, a small amount (2%) of rotaxane E-6, presumably arising from p-xylylene diamine-catalyzed isomerization of the thread, was isolated from the reaction of pristine Z-3, again exemplifying the extraordinary efficiency of the E-3 template for rotaxane formation.

E-1 $R^1 = R^2 = CH_2CO_2CH_2Ph$ Z-1
E-2 $R^1 = Me. R^2 = CH_2CHPh_2$ Z-2
E-3 $R^1 = H. R^2 = CH_2CHPh_2$ Z-3

hʋ 254 nm
Δ

E-4 $R^1 = R^2 = CH_2CO_2CH_2Ph$ Z-4
E-5 $R^1 = Me. R^2 = CH_2CHPh_2$ Z-5
E-6 $R^1 = H. R^2 = CH_2CHPh_2$ Z-6
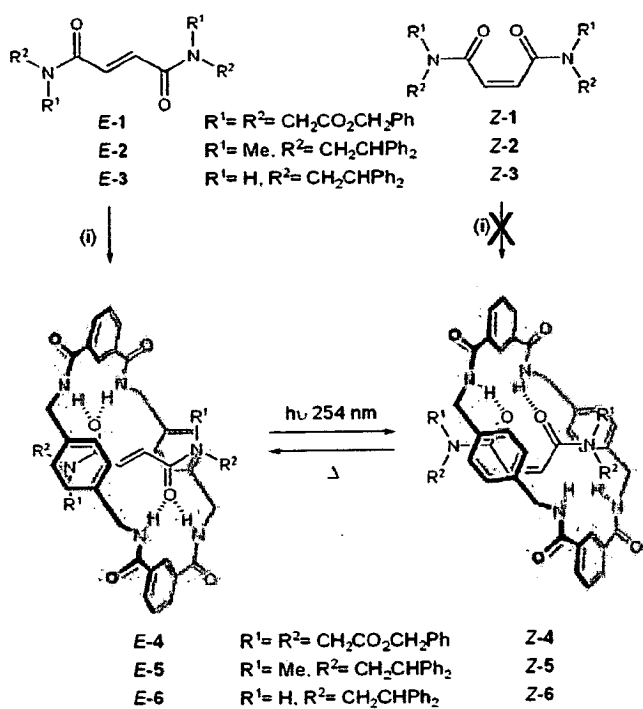
Scheme 1. Synthesis of [2]rotaxanes E/Z-4-6. (i) Four equivalents isophthaloyl dichloride, four equivalents p-xylylene diamine, Et₃N, 4 h, high dilution; CHCl₃ for E-4 (67%) and E-5 (33%), 1/9 MeCN/CHCl₃ for E-6 (97%). Direct irradiation (254 nm, 30 min)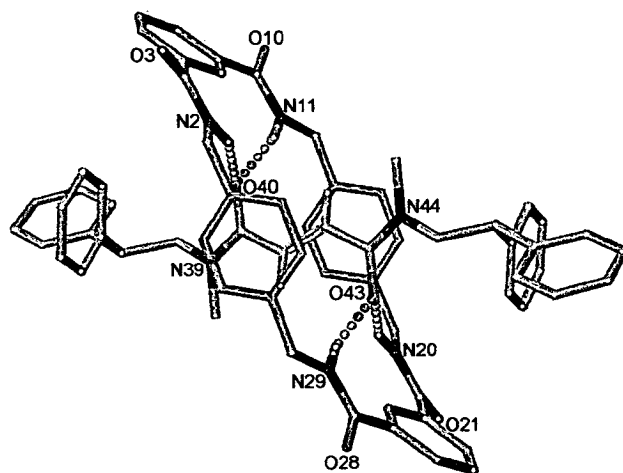 of a solution of an E-rotaxane (0.1 M, room temperature, CH₂Cl₂ [1:9 MeOH/CHCl₃ for E-6]) yields the "accelerated" Z-isomer (45–50% single experiment; >90% from four successive cycles). Heating a 0.02 M solution of a Z-rotaxane at 400 K reforms the "dampened" E-isomer (E-6: C₂D₂Cl₄, 7 days, 84% or d₆-DMSO, 4 days, 100%).

terization data for Z-5 and E-4–6 are provided as *Supporting Text*, which is published as supporting information on the PNAS web site, www.pnas.org.

Results and Discussion

Single crystals suitable for investigation by x-ray crystallography were obtained for each of the three E-rotaxanes. In each case the solid-state structure shows two sets of bifurcated hydrogen bonds between the amide groups of the macrocycle and the carbonyl groups of the fumaramide system (15). The crystal structure of E-5 is typical (Fig. 1) and shows the macrocycle in a chair conformation forming short, close-to-linear, hydrogen bonds orthogonal to the lone pairs of the fumaramide carbonyl groups. Of the three different tertiary amide rotamers present in solution (as observed by NMR) only the {ZZ}amide rotamer of E-5 is found in the crystal.

All three fumaramide threads E-1–3 and rotaxanes E-4–6 smoothly undergo photoisomerization (16, 17) (254 nm; 0.1 M solution in CH₂Cl₂ or, for solubility reasons in the case of E-6, 1:9 MeOH/CHCl₃; 30 min) to the corresponding maleamide (Z-olefin) systems. The yields for the rotaxanes, 45–50%, are remarkably good considering the confined cavity that the molecular rearrangement has to occur in and that the intercomponent hydrogen bonding between the thread and macrocycle is complementary to the positions of the amide groups only in the E-olefin. Unanticipated enhanced solubility of the Z-rotaxanes in nonpolar solvents allowed the separation of the E/Z photochemical reaction mixtures into the individual isomers by simple trituration (PhMe/CH₂Cl₂, 1:1). The photoisomerization reaction produces few byproducts so E-rotaxanes recovered in this


Fig. 1. X-ray crystal structure of [2]rotaxane E-5 (for clarity, carbon atoms of the macrocycle are shown in blue and the carbon atoms of the thread in yellow; oxygen atoms are depicted in red, nitrogen atoms are dark blue, and selected hydrogen atoms are white). Intramolecular hydrogen bond distances (Å): O40–HN2/O43–HN20 = 2.22, O40–HN11/O43–HN29 = 1.94.

way could be recycled, leading to >90% overall conversion to the Z-isomer from a series of irradiation experiments.
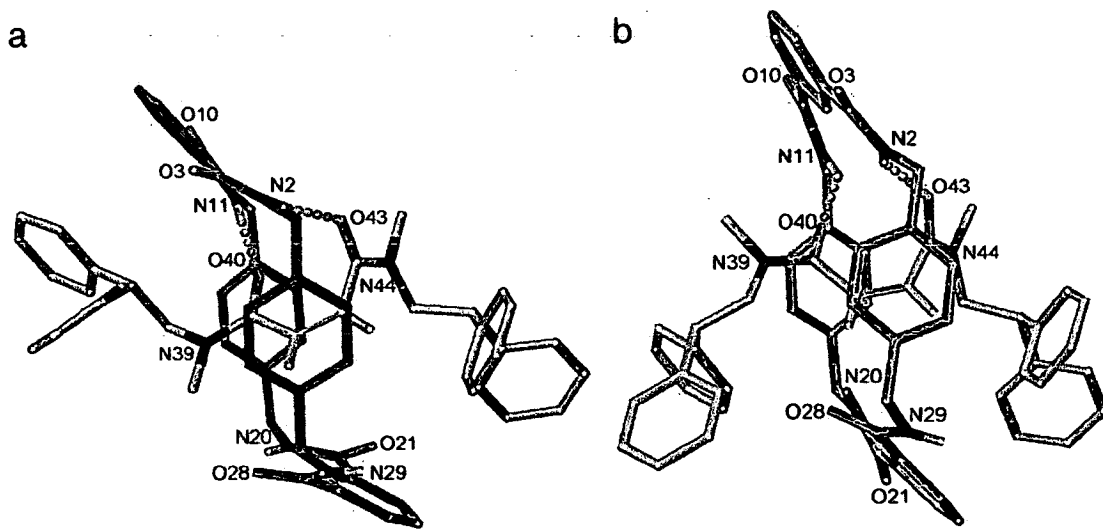
The ¹H NMR spectra of each pair of E- and Z-olefin rotaxanes gives insight regarding their structure and relative dynamic properties in nonpolar solvents. The trends are similar in all cases but the clearest information is provided by E/Z-4.[††]

The variable temperature ¹H NMR spectra of E-4 and Z-4 in CD₂Cl₂ (223–273 K) and C₂D₂Cl₄ (339–393 K) are shown in Fig. 2 (the wide temperature range involved meant different nonhydrogen bond-disrupting solvents were required to monitor the dynamic processes at high and low temperatures). Pirouetting, a 180° rotation of the macrocycle about the axis of the arrow plus formal chair–chair flip of the macrocycle, is the simplest process that must occur to translate the equatorial macrocycle methylene protons, H_{E2}, onto the axial, H_{E1}, sites. In the fumaramide system the H_E protons coalesce at 273 K and are fully resolved into the H_{E1} and H_{E2} resonances at 223 K (Fig. 2a). The coupling constants confirm the axial and equatorial assignments of H_{E1} and H_{E2}. Spin polarization transfer by selective inversion recovery experiments provided a direct measure of the rate of the exchange process I (i.e., half circumrotation of the macrocycle) at 298 K corresponding to an energy barrier $\Delta G^{\ddagger} = 13.4 \pm 0.1$ kcal·mol⁻¹, which extrapolates to a rate of macrocycle rotation of ≈1 s⁻¹ at 223 K (15). In contrast, the macrocycle methylene protons (H_E) in Z-4 remain sharp and well resolved throughout this temperature range and only begin to broaden significantly at 223 K (Fig. 2b); remarkably, the broadening of H_E in Z-4 at 223 K is comparable to that in E-4 at 359 K, a 136° temperature difference between the two rotaxane isomers! Exchange is so fast in Z-4 that it is not possible to resolve the signals and prove unequivocally by experiment that the process responsible for the broadening at this temperature is, in fact, macrocycle

---

[††]The spectra of Z-6 are complicated because intracomponent hydrogen bonding of the maleamide group desymmetrizes the rotaxane (the macrocycle methylene groups appear as an ABX system because the two faces of the macrocycle experience different environments). Similarly, the temperature-dependent equilibrium between the populations of the different amide rotamers present in the methylated rotaxanes E/Z-5 makes their study nontrivial, whereas the symmetrical tertiary amides means E/Z-4 suffers no such complication. For a discussion of the effect of the different strengths of intercomponent hydrogen bonding in E-4 and Z-4 on the dynamics of amide rotamerization, see *Supporting Text*.
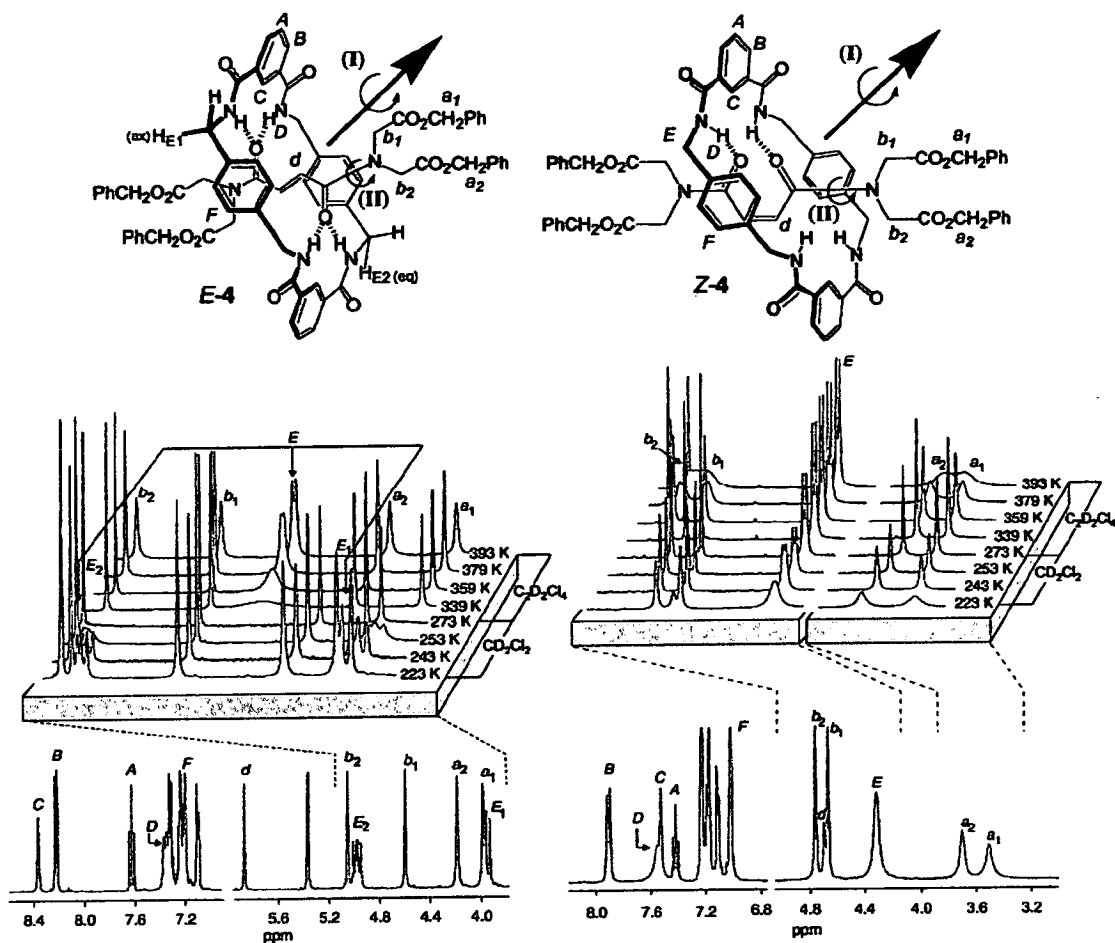
Fig. 2. Variable temperature ^{1}H NMR spectra (400 MHz) of *E*-4 (*a*) and *Z*-4 (*b*) in CD_2Cl_2 at 223 K (main traces) and 223–273 K (stackplot expansions) and $C_2D_2Cl_4$ at 339–393 K (stackplot expansions). Lettering corresponds to selected nonequivalent proton environments. A 180° rotation of the macrocycle about the axis of the arrow, plus chair–chair flipping of the macrocycle, translates the H_{E2} (equatorial) protons onto the H_{E1} (axial) sites. The NMR spectra in *a* reveal slow pirouetting of the macrocycle about the thread in *E*-4 (H_{E1} and H_{E2} coalesce at 273 K, $\Delta G^{\ddagger} = 13.4 \pm 0.1$ kcal·mol^{-1}; process I) and slow rotation of the thread tertiary amide bonds (H_{a1} and H_{a2}/H_{b1} and H_{b2} fully resolved even at 393 K, $\Delta G^{\ddagger} = 21.1 \pm 0.1$ kcal·mol^{-1}; process II). The NMR spectra in *b* show that process I is much lower in energy for *Z*-4 ($\Delta G^{\ddagger} = 6.8 \pm 0.8$ kcal·mol^{-1}) than *E*-4 and that process II is also more facile (H_{a1} and H_{a2}/H_{b1} and H_{b2} broadening at higher temperatures, $\Delta G^{\ddagger} = 20.0 \pm 0.1$ kcal·mol^{-1}) (30).

Fig. 3. X-ray crystal structures of {*ZE*} (*a*) and {*EE*} (*b*) rotamers of *N,N'*-dimethylmaleamide [2]rotaxane *Z*-5. Intramolecular hydrogen bond distances (Å): (*a*) O40-HN11 = 2.08, O43-HN2 = 2.05; (*b*) O40-HN11 = 1.76, O43-HN2 = 2.08.
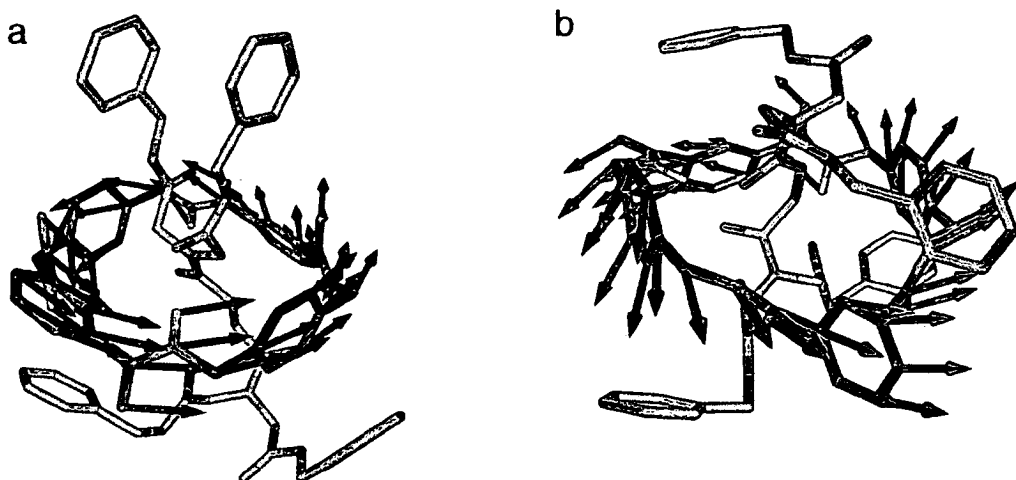
Fig. 4. Calculated transition-state structures for the macrocycle ring motions for rotaxanes Z-4 (a) and E-4 (b). Green arrows represent the corresponding atomic motion vectors connecting the transition states to their minima.

pirouetting (it could be occurring at even lower temperatures). However, making the assumption (see below) that this is the process responsible for broadening, line shape analysis gives an energy barrier of 6.8 ± 0.8 kcal·mol^{-1}, i.e., a macrocycle spinning rate >1.2 × 10^6 s^{-1} at 223 K.

Remarkably, it was possible to obtain an x-ray crystal structure of one of the rotaxanes with a "switched off" recognition motif. Small crystals of Z-5 suitable for investigation with a synchrotron source were grown from slow evaporation of a saturated solution in CHCl$_3$/MeOH. In contrast to the crystal structure of E-5, two of the three tertiary amide rotamers, i.e., {ZE} and {EE} rotamers, are present in the unit cell of Z-5 (Fig. 3 a and b, respectively). Both forms are consistent with the dramatic increase in the rate of rotation in solution for the cis-rotaxanes observed experimentally by ^{1}H NMR spectroscopy; the consequence of isomerizing the double bond is that the amide groups of the thread are held in positions such that they can hydrogen-bond to only one of the two isophthalamide groups of the macrocycle. It is interesting to note that the energy barrier for the trans-rotaxane with four intercomponent hydrogen bonds (13.4 kcal·mol^{-1}) is almost exactly twice the value for the cis-rotaxane with two intercomponent hydrogen bonds ($\approx$6.8 kcal·mol^{-1}).

To obtain a more detailed understanding of the dynamic properties of these systems and, in particular, to confirm that the low energy dynamic process measured by NMR in the maleam-

ide rotaxane was circumrotation, we carried out simulations of the dynamic processes present in both E-4 and Z-4.

Using a computational procedure that uses the MM3 forcefield (18) and the TINKER program (19) and has proved successful in describing the circumrotation pathway in catenanes (20), macrocycle pirouetting in rotaxanes (13), and other properties in mechanically interlocked molecules (21, 22), it was possible to locate the saddle points for macrocycle circumrotation in E-4 and Z-4. Fig. 4 shows the transition states, the arrows indicating the initial motion that the macrocycle would undergo away from the saddle point (arrows showing the movement of the thread are not shown for clarity). The calculated activation energies (13.51 kcal·mol^{-1} for E-4 and 6.53 kcal·mol^{-1} for Z-4) compare well with the NMR-determined ΔGs of 13.4 ± 0.1 and 6.8 ± 0.8 kcal·mol^{-1}, respectively, and thus confirm that macrocycle pirouetting is probably a major contributor to the broadening of resonances observed in the low-temperature NMR spectra of Z-4. The good agreement of calculations and experiments also allows one to take a closer look at the contributions of various kinds of interactions to the dynamic process of pirouetting. Table 1 shows the different energy contributions to the E-4 and Z-4 minima and transition states. Interestingly, from the calculations the $\approx$7 kcal·mol^{-1} difference between the activation barriers of circumrotation in the two molecules can be ascribed to contributions from all the energy components, not just H bonding.

Preliminary studies show that it is possible to reverse the photoisomerization process thermally. Heating each of Z-4–6 (C$_2$D$_2$Cl$_4$ or d$_6$-DMSO, 400 K, 4–7 days) resulted in reconversion to the more thermodynamically stable E-rotaxanes in good-to-excellent (80–100%) yields. Other simple cis-trans olefin interconversion reactions are currently being investigated.$^{++}$

The post-assembly photoconversion of a precise hydrogenbonding, rotaxane-forming template to a motif that does not template the formation of mechanical bonds is unprecedented. The resulting mismatch in recognition sites between macrocycle and thread dramatically reduces the energy barrier to macrocycle pirouetting in the rotaxane. Such control could be useful for the future construction of synthetic molecular machines that use large amplitude internal rotary motions.

Table 1. Calculated contributions to the rotaxane energy minima and transition states

	E$_v$	E$_{H\text{-bonding}}$	E$_{\pi\text{-stacking}}$	E$_{vdW}$
E-4*	29.18	−20.14	−15.36	−24.91
E-4†	33.09 (3.91)	−13.75 (6.39)	−12.65 (2.71)	−24.40 (0.51)
Z-4*	38.11	−16.84	−14.89	−30.97
Z-4†	44.66 (6.55)	−15.99 (0.85)	−16.73 (−1.84)	−29.99 (0.98)

Molecular energy contributions (kcal·mol^{-1}) divided into four components: a valence term, E$_v$, which includes stretchings and in-plane and out-of-plane bendings; a hydrogen bond contribution, E$_{H\text{-bonding}}$; π-π stacking energy, E$_{\pi\text{-stacking}}$; and the remaining van der Waals components, E$_{vdW}$. The energy differences between the minima and the transition states are given in parentheses.
*Energy minimum.
†Transition state energy.

1. Iwamura, H. & Mislow, K. (1988) *Acc. Chem. Res.* **21**, 175–182.
2. Bedard, T. C. & Moore, J. S. (1995) *J. Am. Chem. Soc.* **117**, 10662–10671.
3. Kelly, T. R., Bowyer, M. C., Bhaskar, K. V., Bebbington, D., Garcia, A., Lang, F., Kim, M. H. & Jette, M. P. (1994) *J. Am. Chem. Soc.* **116**, 3657–3658.
4. Kelly, T. R., Tellitu, I. & Sestelo, J. P. (1997) *Angew. Chem. Int. Ed. Engl.* **36**, 1866–1868.
5. Kelly, T. R., Sestelo, J. P. & Tellitu, I. (1998) *J. Org. Chem.* **63**, 3655–3665.
6. Schoevaars, A. M., Kruizinga, W., Zijlstra, R. W. J., Veldman, N., Spek, A. L. & Feringa, B. L. (1997) *J. Org. Chem.* **62**, 4943–4948.
7. Kelly, T. R., De Silva, H. & Silva, R. A. (1999) *Nature* **401**, 150–152.
8. Koumura, N., Zijlstra, R. W. J., van Delden, R. A., Harada, N. & Feringa, B. L. (1999) *Nature* **401**, 152–155.
9. Kelly, T. R., Silva, R. A., De Silva, H., Jasmin, S. & Zhao, Y. (2000) *J. Am. Chem. Soc.* **122**, 6935–6949.
10. Koumura, N. L., Geertsema, E. M., van Gelder, M. B., Meetsma, A. & Feringa, B. L. (2002) *J. Am. Chem. Soc.* **124**, 5037–5051.
11. Balzani, V., Credi, A., Raymo, F. M. & Stoddart, J. F. (2000) *Angew. Chem. Int. Ed.* **39**, 3348–3391.
12. Stoddart, J. F., ed. (2001) *Acc. Chem. Res.* **34**, 409–522.
13. Sauvage, J.-P., ed. (2001) *Molecular Machines and Motors: Structure and Bonding* (Springer, Berlin), Vol. 99.
14. Bermudez, V., Capron, N., Gase, T., Gatti, F. G., Kajzar, F., Leigh, D. A., Zerbetto, F. & Zhang, S. (2000) *Nature* **406**, 608–611.
15. Gatti, F. G., Leigh, D. A., Nepogodiev, S. A., Slawin, A. M. Z., Teat, S. J. & Wong, J. K. Y. (2001) *J. Am. Chem. Soc.* **123**, 5983–5989.
16. Campari, G., Fagnoni, M., Mella, M. & Albini, A. (2000) *Tetrahedron Asym.* **11**, 1891–1906.
17. Frkanec, L., Jokic, M., Makarevic, J., Wolsperger, K. & Zinic, M. (2002) *J. Am. Chem. Soc.* **124**, 9716–9717.
18. Allinger, N. L., Yuh, Y. H. & Lii, J.-H. (1989) *J. Am. Chem. Soc.* **111**, 8551–8556.
19. Dudek, M. J. & Ponder, J. (1995) *J. Comput. Chem.* **16**, 791–816.
20. Deleuze, M. S., Leigh, D. A. & Zerbetto, F. (1999) *J. Am. Chem. Soc.* **121**, 2364–2379.
21. Biscarini, F., Cavallini, C., Leigh, D. A., León, S., Teat, S. J., Wong, J. K. W. & Zerbetto, F. (2002) *J. Am. Chem. Soc.* **124**, 225–233.
22. Fustin, C.-A., Leigh, D. A., Rudolf, P., Timpel, D. & Zerbetto, F. (2000) *ChemPhysChem* **1**, 97–100.
23. Vacek, J. & Michl, J. (1997) *New J. Chem.* **21**, 1259–1268.
24. van Delden, R. A., Koumura, N., Harada, N. & Feringa, B. L. (2002) *Proc. Natl. Acad. Sci. USA* **99**, 4945–4949.
25. Collier, C. P., Mattersteig, G., Wong, E. W., Luo, Y., Beverly, K., Sampaio, J., Raymo, F. M., Stoddart, J. F. & Heath, J. R. (2000) *Science* **289**, 1172–1175.
26. Tashiro, K., Konishi, K. & Aida, T. (2000) *J. Am. Chem. Soc.* **122**, 7921–7926.
27. Leigh, D. A., Murphy, A., Smart, J. P., Deleuze, M. S. & Zerbetto, F. (1998) *J. Am. Chem. Soc.* **120**, 6458–6467.
28. Raehm, L., Kern, J.-M. & Sauvage, J.-P. (1999) *Chem. Eur. J.* **5**, 3310–3317.
29. Chatterjee, S., Pedireddi, V. R. & Rao, C. N. R. (1998) *Tetrahedron Lett.* **39**, 2843–2846.
30. Clegg, W., Gimenez-Saiz, C., Leigh, D. A., Murphy, A., Slawin, A. M. Z. & Teat, S. J. (1999) *J. Am. Chem. Soc.* **121**, 4124–4129.

Information Storage Using Supramolecular Surface Patterns

Massimiliano Cavallini, Fabio Biscarini, Salvator León, Francesco Zerbetto,
Giovanni Bottari, David A. Leigh

BREVIA

CHEMISTRY

Information Storage Using Supramolecular Surface Patterns

Massimiliano Cavallini,[1] Fabio Biscarini,[1] Salvador León,[2] Francesco Zerbetto,[2] Giovanni Bottari,[3] David A. Leigh[3]

Novel strategies for information storage technology rely upon multistable systems that can be controllably switched between different configurations of comparable free energy. Multistability is present in many molecular and supramolecular systems through a variety of properties (conformations, redox and spin states, shape and dimensionality) that can be influenced by external stimuli. In the solid state, however, it is difficult to amplify the effects of molecular switching to higher length scales in order to relay the response to the outside world.

Rotaxanes (1) are molecules in which a macrocycle is mechanically locked onto a "thread" by two bulky "stoppers." Their architecture, analogous to that of an abacus, suggests that they could be used as switchable components for artificial machines (2) that function through mechanical motion at the molecular level (3, 4). Controlling such motion in the solid state could be used to store information.

Thin films (3- to 35-nm thickness) of each of three amide-based rotaxanes (1 to 3, Scheme 1) (5) were grown by drop casting and postthermal annealing onto graphite and mica. The films can be imaged by atomic force microscopy (AFM) in contact mode with a set point force below a threshold value of 2 nN. They exhibit a homogeneous morphology over a cm² area and are stable over a period of several months.

An increase in the load force to just above the 2-nN threshold results in a mechanical perturbation whose effect is localized at the contact area of the tip. When the tip is continuously scanned along a line, a string of regularly spaced dots appears. The dots emerge upon repeating the line scan a number of times (between 4 and 20) depend-

ing on the scan rate (typically 1 to 2 Hz). Scanning a series of lines results in a regular array of dots of uniform width, height, and pitch (Fig. 1A). The number of dots is proportional to the length of each line scan (Fig. 1B), so that any predetermined number of dots can be reliably fabricated on the surface. The film thickness controls the dot size and the spacing and hence the density of dots per unit line; the thinner the film, the denser and smaller the dots are. The transformation can be induced over a large area (Fig. 1C), and it produces robust features even in the presence of surface steps and terraces. The linear dependence on the scan length allows one to write information as strings of bits (Fig. 1D).

The effect of the mechanical perturbation on the film appears during line scans as a roughening of the topographical profile, with the position of the dots fixed at early stages. The transformation can be interrupted and restarted by turning off and on the perturbation. No sign of scraping or wear of the film is observed, ruling out plowing with the AFM tip, which instead occurs as the set point force exceeds 3 to 4 nN.

The transformation takes place only with the rotaxanes, not the component threads or macrocycles alone, and is thus intrinsically related to the mechanically interlocked architecture. Molecular modeling of the solid state rotaxane structure (4) shows the existence of two nearly degenerate surfaces, (100) and (101), which can be switched with a relatively low activation energy (200.4 kJ mol⁻¹) by circumrotation of the macrocycles. The collective fabrication of dots arises from coupled nucleation recrystallization favored by the ease of intercomponent mobility in the solid state. The scanning AFM tip gives the energy to the molecules along the line to reorganize into nuclei. As nuclei coarsen by ripening, a characteristic distance emerges. Finally, stable nuclei grow by incorporation

of the mobile molecules to form the dots.

Information storage by writing individual dots with a scanning probe has previously been demonstrated (6, 7). Our approach enables the writing of multiple dots simultaneously. This could make it suitable for scaling up to a lithography based on multiple sources of perturbation, for instance by using a stamp. With such an approach, information storage on a thin film could reach densities of 10 to 100 Gbit/in².
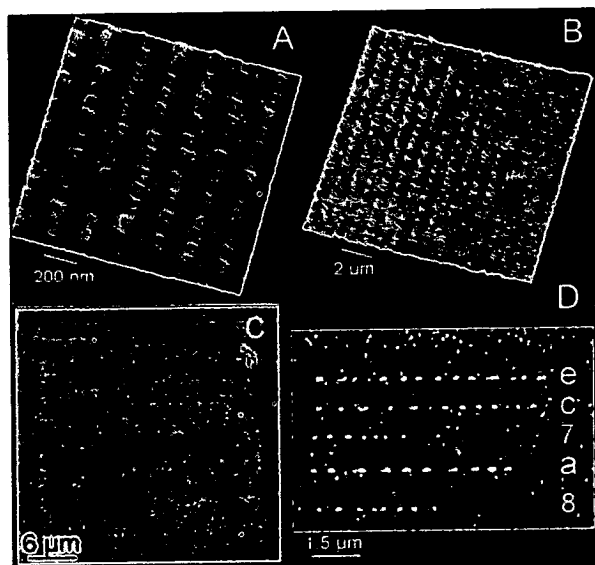

Fig. 1. (A) Array of dots fabricated of 1 by individual line scans of the AFM tip on a 5-nm-thick film of 1 deposited on highly oriented pyrolitic graphite. (B) For a given thickness (here 20 nm), the number of dots is linearly proportional to the scan length. The number of dots can be determined with an accuracy of at least 2%. Film thickness controls the characteristic size. Varying the film thickness in the range between 3 and 35 nm, interdot distance increases from 100 to 500 nm, the dot full-width-half-maximum from 40 to 250 nm, and the dot height from 1 to 20 nm, with a dispersion of 10 to 20%. (C) Pattern made of 31 lines with 45 dots each on an ≈30 by 30 μm² area on a thicker film. (D) Proof-of-concept for information storage. The sequence "e c 7 a 8" in the hexadecimal base corresponds to the number 968616.
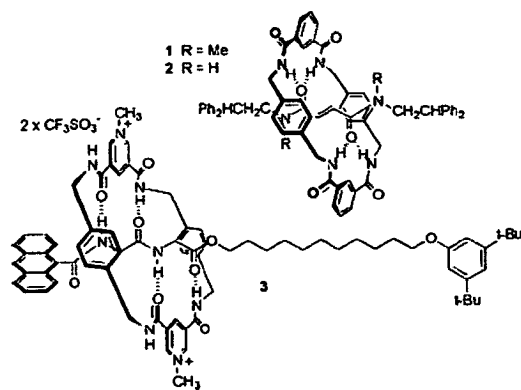
References and Notes

1. J.-P. Sauvage, C. Dietrich-Buchecker, Eds. *Molecular Catenanes, Rotaxanes and Knots* (Wiley-VCH, Weiheim, Germany, 1999).
2. Molecular Machines Special Issue, J. F. Stoddart ed., *Acc. Chem. Res.* 34, 410 (2001).
3. C. P. Collier et al., *Science* 285, 391 (1999).
4. F. Biscarini et al., *J. Am. Chem. Soc.* 124, 225 (2002).
5. F. G. Gatti et al., *J. Am. Chem. Soc.* 123, 5983 (2001).
6. R. García et al., *J. Appl. Phys.* 86, 1898 (1999).
7. G. Binnig et al., *Appl. Phys. Lett.* 74, 1329 (1999).

[1] Consiglio Nazionale delle Ricerche–ISMN, Sezione di Bologna, Via P. Gobetti 101, I-40129 Bologna, Italy. [2] Dipartimento di Chimica "G. Ciamician," Università degli Studi di Bologna, Via F. Selmi 2, I-40126 Bologna, Italy. [3] School of Chemistry, University of Edinburgh, The King's Buildings, West Mains Road, Edinburgh EH9 3JJ UK.

1 R = Me
2 R = H

2 x CF₃SO₃⁻

Scheme 1.